



The Recruitment Mechanisms and Beneficial Roles of Haematopoietic Stem Cells in Murine Acute Kidney Injury

by
REBECCA LUCY WHITE

A thesis submitted to the University of Birmingham
for the degree of DOCTOR OF PHILOSOPHY

College of Medical and Dental Sciences
School of Clinical and Experimental Medicine
The University of Birmingham
September 2013

UNIVERSITY OF
BIRMINGHAM

University of Birmingham Research Archive

e-theses repository

This unpublished thesis/dissertation is copyright of the author and/or third parties. The intellectual property rights of the author or third parties in respect of this work are as defined by The Copyright Designs and Patents Act 1988 or as modified by any successor legislation.

Any use made of information contained in this thesis/dissertation must be in accordance with that legislation and must be properly acknowledged. Further distribution or reproduction in any format is prohibited without the permission of the copyright holder.

ABSTRACT

Haematopoietic stem cells (HSCs) can migrate to the injured kidney and aid in tissue repair, however clinical success remains poor and is partially attributed to limited HSC recruitment. This study determined the molecular mechanisms governing HSC recruitment to the ischaemia-reperfusion (IR) injured kidney, whether this recruitment could be enhanced and also any immuno-modulatory effects HSCs may be having on surrounding injured microvasculature. HSC adhesion was significantly enhanced to the IR injured kidney compared to sham; this recruitment was governed by CD49d/VCAM-1 and CD44/HA. KC or SDF-1 α pre-treatment enhanced HSC adhesion to the IR kidney. KC and SDF-1 α also increased CD44 and CD49d surface clusters on HSCs respectively, and therefore increased HSC adhesion to HA and VCAM-1. Following injection into IR injured mice, HSCs improved blood flow and kidney function in the injured kidney compared to sham. This may be related to inflammatory modulation, as neutrophil recruitment and number of platelet microthrombi were reduced following HSC administration. This is the first study to show that pre-treatment of HSCs increases their recruitment to the site of injury, and that recruitment of HSCs can reduce inflammatory cell infiltration following injury.

ACKNOWLEDGEMENTS

There are a number of people who have significantly contributed to my time during my PhD. Firstly, I would like to say thank you to my supervisors Dr. Neena Kalia and Professor Caroline Savage for providing me with the opportunity to work within both of their laboratories for the last four years. The career opportunities that have opened up due to this experience are invaluable. I would also like to thank the Medical Research Council for funding this work.

There are many people on the first floor to whom I am grateful. Huge thanks have to go to DJ Dean Kavanagh (my PhD dad) for giving me a great deal of support throughout the last four years. Work would have most definitely not been the same without you: the 'dark and sinister' music sessions, Team America sing-a-longs, and many animal videos have made four long years of IVM experiments entertaining. Thanks also to Joe for his amazing animal stories, dead-pan humour and co-teasing Dean, Yemm for making sure my statistical ability and competitive nature were tested, and last, but definitely not least, to Craig for showing me the secret dark room. When lab days are dark and dreary these four, along with Stevie T, Kate and Brendizzle have made the hours more enjoyable. I honestly could not have wished for better people to work alongside.

Outside of the lab, my friends, especially Duckling, Penel and Smith, have kept me sane over the years and supplied me with coffee, prosecco and lent me their ears! Ultimately my greatest thanks go to my family. Their continued love, support and encouragement over the many, *many* years of studying has been infallible and without it I surely would have never have got this far. To Paul, over the last few years you have listened, made me relax, laugh and have kept me going even when I thought I couldn't. From the bottom of my heart, thank you to you all. So now onto pastures new, you can all finally breathe a sigh of relief that I will not be moaning about mice and feeding the stem cells anymore!

PUBLICATIONS ARISING FROM THIS THESIS

Papers:

White RL, Nash G., Kavanagh DPJ., Savage COS., Kalia N. (2013).

Modulating the Adhesion of Haematopoietic Stem Cells with Chemokines to Enhance Their Recruitment to the Ischaemically Injured Murine Kidney. *PLoS ONE*.

Oral Presentations:

62nd Meeting of the British Microcirculation Society, University of Oxford, Oxford, UK

White RL, Savage COS., Kalia N.

"CD49d and CD44 Enhance Stem Cell Adhesion to the Injured Kidney"

61st Meeting of the British Microcirculation Society, Barts & The London School of Medicine and Dentistry, London, UK

White RL, Kavanagh DPJ., Savage COS., Kalia N.

"CD49d, CD44 and Chemokines SDF-1 α Govern HSC Adhesion Within Ischaemically Injured Kidney"

GlaxoSmithKline Clinical Science Meeting

White RL, Kavanagh DPJ., Savage COS., Kalia N.

"Mechanisms governing haematopoietic stem cell recruitment to the murine IR injured kidney"

60th Meeting of the British Microcirculation Society, Peninsula Medical School, Exeter, UK

White RL, Mann J., Kavanagh DPJ., Savage COS., Kalia N.

"Modulating adhesion of hematopoietic stem cells to ischemia-reperfusion injured kidney sections"

Poster Presentations:

13th International Union of Physiological Sciences, Birmingham, UK

White RL, Kavanagh DPJ., Savage COS., Kalia N.

“Recruitment Mechanisms and Vasculoprotective Effects of Haematopoietic Stem Cells in vivo in the Murine Injured Kidney”

Understanding Impact, University of Nottingham, Oxford, UK

White RL, Nash G., Kavanagh DPJ., Savage COS., Kalia N.

“New Insights into Haematopoietic Stem Cell Recruitment to the Injured Kidney”

9th World Congress for Microcirculation, Paris, UK

White RL, Mann J., Kavanagh DPJ., Savage COS., Kalia N.

“Modulating adhesion of hematopoietic stem cells to ischemia-reperfusion injured kidney”

British Renal Society / Renal Association, Manchester Central Convention Complex, UK

White RL, Mann J., Kavanagh DPJ., Savage COS., Kalia N.

“Modulating the adhesion of haematopoietic stem cells (HSCs) to ischaemia-reperfusion (IR) injured kidney sections and identification of molecular mechanisms governing their adhesion”

CONTENTS

1	General Introduction	2
1.1	<i>Kidney disease and dysfunction.....</i>	2
1.1.1	Acute Kidney Injury.....	2
1.1.2	Ischaemic Acute Kidney Injury.....	3
1.2	<i>Inflammatory Cell Types at the Ischaemia-Reperfusion Injury Interface</i>	12
1.2.1	Inflammatory Response.....	12
1.2.2	Different Leukocyte Populations Contribute at Different Time Points in IR Injury	13
1.3	<i>Leukocyte-Endothelial Adhesion Cascade</i>	14
1.3.1	Rolling Phase Governed by Selectins.....	15
1.3.2	Activation of Rolling Leukocytes Governed by Chemoattractants.....	18
1.3.3	Firm Adhesion Governed by Integrins	21
1.3.4	Non-Integrin CD44 Based Leukocyte Adhesion.....	23
1.3.5	Transmigration.....	24
1.3.6	Platelets	24
1.4	<i>Injury Diagnosis, Renal Repair and Current Treatments</i>	26
1.4.1	Injury Diagnosis.....	26
1.4.2	Renal Repair Following Ischaemia-Reperfusion Injury.....	27
1.4.3	Existing Treatment Options	27
1.5	<i>Stem Cells as a Source for Regenerative Medicine</i>	29
1.5.1	The Different Progenitor Cells of the Bone Marrow	29
1.5.2	Mesenchymal Stem Cells.....	30
1.5.3	Haematopoietic Stem Cells.....	31
1.5.4	HSC Regeneration by Differentiation, Cell Fusion and Paracrine Mechanisms.....	34
1.5.5	HSC Recruitment to Adult Peripheral Tissues	35
1.5.6	HSCs in the Injured Kidney.....	38
1.6	<i>Summary</i>	41

1.7	<i>Aims and Hypotheses</i>	42
2	Materials and Methods	45
2.1	<i>Materials</i>	45
2.1.1	Antibodies	45
2.1.2	Common Materials	46
2.2	<i>Cell Culture, Cell Isolation and Cell and Supernatant Preparation</i>	46
2.2.1	Cell Counting	46
2.2.2	Haematopoietic Progenitor Cell-5 and -7 (HPC-5 and HPC-7).....	47
2.2.3	Culture of Immortalised Murine Renal Endothelium	48
2.2.4	CFSE- Labelling of Cells	49
2.2.5	Cell Adhesion Molecule Blocking.....	49
2.2.6	HPC-7 and Kidney Pre-treatments with Inflammatory Factors.....	50
2.3	<i>Monitoring HSC Trafficking in vivo using Intravital Microscopy</i>	51
2.3.1	Animals	51
2.3.2	Surgical Preparation	52
2.3.3	Induction of Renal Ischaemia-Reperfusion Injury	53
2.3.4	Intravital Microscopy Kidney Preparation to Understand HSC Trafficking	53
2.3.5	Quantification of Cell Trafficking <i>in vivo</i>	56
2.3.6	Quantification of HSC Recruitment in Major Organs <i>ex vivo</i>	57
2.3.7	Blood Flow Measurements.....	57
2.4	<i>Monitoring Inflammatory Cells using Confocal Intravital Microscopy</i>	58
2.4.1	Intravital Preparations	58
2.4.2	Surgical Preparation	58
2.5	<i>Quantification of Injury</i>	61
2.5.1	FITC-BSA.....	61
2.5.2	Creatinine and Urea Levels.....	61
2.6	<i>Techniques to Quantify Cell Adhesion in vitro</i>	62
2.6.1	Frozen Tissue Stamper-Woodruff Assay	62

2.6.2	Immobilised Counter-Ligand Adhesion Assay	63
2.6.3	Renal Endothelial Cell Static Adhesion Assay	64
2.6.4	Immunohistochemistry on 6 hour Reperfused Tissue Sections	64
2.7	<i>In vitro Techniques to Dissect the Effects of Injury and Cytokines on HPC-7 Adhesion and Free-Flowing Numbers</i>	65
2.7.1	Conditioned Media Preparation from Injured and Sham Kidneys	65
2.7.2	Determination of Protein Content within Conditioned Media	66
2.7.3	Adhesion Molecule Clustering	67
2.7.4	Micropipette Assay	67
2.8	<i>FACS-Based Studies</i>	68
2.8.1	HPC-7 Cell Surface	68
2.9	<i>Statistics</i>	69
3	Recruitment of HSCs by Ischaemia-Reperfusion Injury	71
3.1	<i>Introduction and Hypotheses</i>	71
3.1.1	Introduction	71
3.1.2	Aims and Hypotheses	72
3.2	<i>Methods</i>	72
3.3	<i>Results</i>	73
3.3.1	HPC-5 adhesion is not increased to IR injured kidney tissue sections <i>in vitro</i>	73
3.3.2	HPC-7 adhesion is increased to IR injured kidney tissue sections <i>in vitro</i>	74
3.3.3	Adherent and free-flowing HPC-5 numbers <i>in vivo</i> do not change in IR injured animals	77
3.3.4	Adherent and free-flowing HPC-7 numbers <i>in vivo</i> are significantly increased in the renal IR injured model	77
3.3.5	The number of adherent HPC-7 <i>in vivo</i> is significantly increased to the injured kidney with the new kidney intravital preparation	80
3.3.6	Free-flowing HPC-7 numbers <i>in vivo</i> are significantly increased at the point of cell infusion	80
3.4	<i>Major Findings for Chapter 3</i>	84
3.5	<i>Discussion</i>	85

4 Mechanisms of Haematopoietic Stem Cell Recruitment to the IR Injured Kidney ...91

4.1	<i>Introduction and Hypotheses</i>	91
4.1.1	Introduction	91
4.1.2	Aims and Hypotheses	93
4.2	<i>Methods</i>	94
4.3	<i>Results</i>	95
4.3.1	Blocking HSC surface expression of CD18 does not have a role in HPC-7 adhesion to the injured kidney	95
4.3.2	CD49d has an important role in HPC-7 adhesion to the injured kidney	96
4.3.3	HPC-7 adhesion is significantly reduced by <i>in vivo</i> blockade of VCAM-1	99
4.3.4	CD44 also has an important role in HPC-7 adhesion to the injured kidney	99
4.3.5	HA is the counter-ligand for CD44 and helps HPC-7 adhere to the injured kidney	102
4.3.6	The chemokines receptors CXCR2 and CXCR4 are expressed on HPC-7	105
4.3.7	The chemokines KC and SDF-1 α are involved in HPC-7 homing to the kidney	105
4.3.8	Both KC and SDF-1 α topical treatments cause decreases in free-flowing HPC-7	108
4.3.9	A direct role of CXCR2 and CXCR4 in HPC-7 recruitment was confirmed <i>in vivo</i>	112
4.4	<i>Major Findings of Chapter 4</i>	115
4.5	<i>Discussion</i>	116

5 Methods of Enhancing Haematopoietic Stem Cell Adhesion to the IR Injured Kidney124

5.1	<i>Introduction and Hypotheses</i>	124
5.1.1	Introduction	124
5.1.2	Aims and Hypotheses	125
5.2	<i>Methods</i>	126

5.3	Results.....	128
5.3.1	Media conditioned by the injured kidney can enhance HPC-7 recruitment <i>in vitro</i>	128
5.3.2	Increased levels of small molecular weight proteins are within the IR injured kidneys.....	130
5.3.3	Pre-treating HPC-7 with low doses of SDF-1 α enhances HPC-7 adhesion <i>in vitro</i>	132
5.3.4	SDF-1 α pre-treatment is the only cytokine to enhance HPC-7 adhesion using the Stamper-Woodruff assay	132
5.3.5	KC and SDF-1 α HPC-7 pre-treatments enhance adhesion to TNF- α treated renal endothelium	136
5.3.6	IL-1 β pre-treatment does not enhance HPC-7 adhesion to the IR injured kidney <i>in vivo</i>	136
5.3.7	KC pre-treatment enhances HPC-7 adhesion to the IR injured kidney <i>in vivo</i>	137
5.3.8	SDF-1 α pre-treatment enhances HPC-7 adhesion to the IR injured kidney <i>in vivo</i>	137
5.3.9	TNF- α pre-treatment enhances HPC-7 adhesion to the IR injured kidney <i>in vivo</i>	137
5.3.10	Dual HPC-7 pre-treatment with KC and SDF-1 α does not further enhance HPC-7 adhesion.....	144
5.3.11	Hydrogen peroxide increases HPC-7 adhesion to activated renal endothelium only.....	146
5.3.12	Cytokines, especially SDF-1 α , significantly increase HPC-7 deformability	148
5.3.13	KC or SDF-1 α HPC-7 pre-treatments do not alter adhesion molecule expression.....	152
5.3.14	KC and SDF-1 α pre-treatments enhances HPC-7 adhesion to both VCAM-1 and HA <i>in vitro</i>	152
5.3.15	KC and SDF-1 α pre-treatments alter CD44 and CD49d adhesion molecule distribution on the HPC-7 cell surface	153
5.4	Major Findings of Chapter 5	157
5.5	Discussion.....	158
6	Beneficial Effects of Haematopoietic Stem Cells within the Injured Renal Microvasculature.....	166

6.1	<i>Introduction and Hypotheses</i>	166
6.1.1	Introduction	166
6.1.2	Aims and Hypotheses	168
6.2	<i>Methods</i>	168
6.3	<i>Results</i>	169
6.3.1	HPC-7 reduce neutrophil numbers in a murine model of renal IR injury <i>in vivo</i>	169
6.3.2	HPC-7 also reduce the number of platelet microthrombi in the IR injured microvasculature <i>in vivo</i>	170
6.3.3	Platelet microthrombi decrease in size after HPC-7 administration <i>in vivo</i>	175
6.3.4	Fluorescent immunohistochemistry of frozen renal sections further confirms the <i>in vivo</i> observations that HPC-7 can reduce platelet microthrombi after IR injury	175
6.3.5	Vascular albumin leakage is improved after HPC-7 administration	179
6.3.6	Using the Chandler loop, administration of HPC-7 reduces blood clot weigh	179
6.3.7	Blood flow in IR injured kidneys is improved after HPC-7 administration	182
6.3.8	Urea and creatinine levels are reduced, thereby function improves, after HPC-7 administration	182
6.4	<i>Major Findings for Chapter 6</i>	185
6.5	<i>Discussion</i>	186
7	General Discussion	194
7.1	<i>Summary of Main Findings</i>	194
7.2	<i>Future Work</i>	204
7.3	<i>Concluding Remarks</i>	207
8	References	209

Abbreviation	Meaning
AChR	Acetylcholine receptor
AKI	Acute kidney injury
ATP	Adenosine tri-phosphate
AUC	Area under the curve
BMPC	Bone marrow progenitor cell
BUN	Blood urea nitrogen
CKD	Chronic kidney disease
CL	Contralateral
COX2	Cyclooxygenase-2
CPF	Cells per field
EC	Endothelial cell
ELISA	Enzyme-linked immunosorbent assay
eNOS	Endothelial nitric oxide synthase
FITC	Fluorescein isothiocyanate
GAG	Glycoaminoglycan
GFR	Glomerular filtration rate
HA	Hyaluronan
HPC-7	Haematopoietic progenitor cell-7
HSC	Haematopoietic stem cell
HSPC	Haematopoietic stem / progenitor cell
ICAM-1	Intercellular cell adhesion molecule-1
ICM	Injured conditioned media
IL-1 β	Interleukin-1 beta
IMCD	Inner medullary collecting duct
IPC	Ischaemic pre-conditioning
IR	Ischaemia-reperfusion
IVM	Intravital microscopy
KC	Keratinocyte-derived chemoattractant
KSL	c-kit ⁺ Sca1 ⁺ Lin ⁻ cells

LE-AF	Low-endotoxin axide-free
MSC	Mesenchymal stem cell
NO	Nitric oxide
PAF	Platelet activating factor
PE	Phycoerythrin
PGI ₂	Prostacyclin
RBC	Red blood cell
rm	Recombinant murine
ROS	Reactive oxygen species
RT	Room temperature
SC	Stem cell
SCM	Sham conditioned media
SDF-1 α	Stromal derived factor-1 alpha
TNF- α	Tumour necrosis factor-alpha
VCAM-1	Vascular cell adhesion molecule-1
VLA-4	Very late antigen-4
WT	Wildtype

Chapter 1



General Introduction

1 General Introduction

1.1 Kidney disease and dysfunction

1.1.1 Acute Kidney Injury

Acute kidney injury (AKI) is common and arises from multiple initiating insults including ischaemia-reperfusion (IR) injury, glomerulonephritis, cardiovascular surgery, shock and sepsis. It is characterised as a sudden and prolonged decline in glomerular filtration rate (GFR), which leads to an inability to remove metabolic waste, sustain fluid balance and electrolyte homeostasis (Devarajan 2006). AKI affects 5% of all hospitalised patients and if untreated can develop into end-stage renal disease, therefore requiring dialysis or renal transplantation (Winterberg and Lu 2012). Although a common condition, prognosis is poor and has not changed much over the past 40 years due to very few successful therapies being developed. Evidence suggests AKI predisposes a person to accelerated chronic kidney disease (CKD) (Basile 2007). Although the kidney has regenerative capacity, these mechanisms become overwhelmed during sustained periods of renal injury. The lack of an effective pharmacological therapeutic intervention has led to AKI becoming a major emerging healthcare problem, particularly in an ageing population. An increased hospital stay is associated with severe AKI, especially if renal replacement therapy is required (Chertow *et al.* 2005). This clearly has a huge economic impact on healthcare resources.

1.1.2 Ischaemic Acute Kidney Injury

The kidneys receive almost a quarter of cardiac output and it is disproportionately distributed to aid good urinary concentration; however, this does make kidney function particularly susceptible to changes in blood flow. The kidney is made up of many tiny filtration units (nephrons) that act to sieve the blood (**Figure 1.1**). As previously stated, IR injury is one of the main causes of AKI and it develops following a sudden transient drop in total or regional blood flow to the kidney. It occurs in clinical practice in association with sepsis, shock, severe trauma and major cardiovascular surgery, which leads to a range of clinical manifestations (Stroo *et al.* 2009). Patients with diabetes, congestive heart failure, liver cirrhosis or chronic renal failure are most at risk from ischaemic AKI. Once developed, ischaemic AKI therapy is predominantly supportive and continues to be associated with significant morbidity and mortality (Thadhani *et al.* 1996; Song and Humes 2009). Studies in rats have shown that after weeks or months, surviving animals develop CKD and renal failure, as marked by increased tubulointerstitial fibrosis (Forbes *et al.* 2000; Basile *et al.* 2001). AKI causes many changes to renal structure and function; this has been documented by most published groups as a substantial decrease in GFR shown by a 7-10 fold increase in serum creatinine. This is one of the most serious functional changes in ischaemic renal injury, as even small changes are associated with increased mortality (Coca *et al.* 2007).

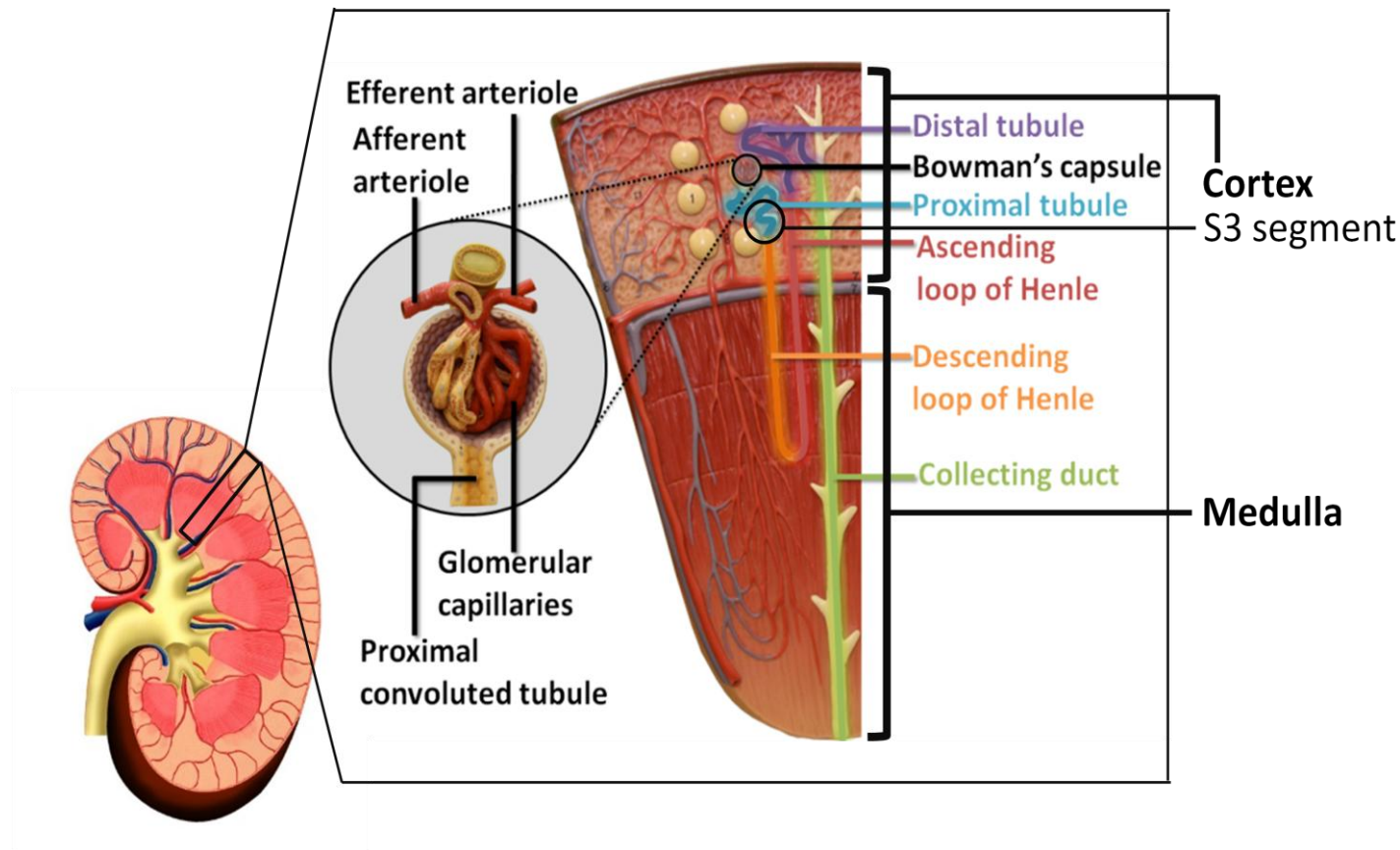


Figure 1.1. The kidney is made up of many functional units known as nephrons. The nephron is made up of three distinct parts: 1) the central filtration unit, the glomerulus; 2) a tubule that runs through the proximal, distal and intermediate segments of the kidney, that reabsorbs and secretes solutes to modify the passing filtrate; and finally 3) a duct that carries the urine into the collecting duct system prior to the bladder. There are up to a million nephron units per fully-functional human kidney. During AKI, the latter part of the proximal tubule, known as the S3 segment, is most affected by the hypoxic environment. This diagram was adapted from images published by the Algonquin College, Canada.

Clinically, ischaemic AKI is split into four different stages: 1) the initiation phase; 2) the activation phase; 3) the extension phase and 4) the maintenance stage.

1. During the “initiation phase”, injury is first caused by the restricted oxygen and nutrient supply during ischaemia (Greek. *isch-* restriction, *haema-* blood). Due to the decrease in blood flow, tissue metabolism is reduced and therefore restricts the resynthesis of energy-rich phosphates, e.g. adenosine 5'-triphosphate (ATP) and phosphocreatine. As cellular levels of ATP fall, hypoxanthine accumulates in ischaemic tissue. High levels of hypoxanthine react with the oxygen, via the enzyme xanthine oxidase, producing reactive oxygen species (ROS) (**Figure 1.2**). These molecules cause local endothelial damage.
2. The “activation stage” swiftly follows and corresponds with the increased ROS numbers; this propagates renal inflammation by increasing adhesion molecule expression and enhances pro-inflammatory cytokine release from the vasculature (Eltzschig and Collard 2004).
3. The third stage of ischaemic AKI is known as the “extension phase”. Although blood flow returns during this phase, it is paradoxically the phase where most tissue injury occurs. Red blood cells (RBCs), platelets and leukocytes adhere to the impaired area once blood flow is resumed (Eltzschig and Collard 2004). Large numbers of adherent pro-inflammatory cell types severely reduce blood flow, thus cell death continues to rise, particularly in the susceptible corticomedullary

region. Furthermore, post-resumption of blood flow, neutrophils in the vasculature become activated and produce higher levels of ROS, causing further oxidative stress (Tapuria *et al.* 2008).

4. Lastly the “maintenance stage” is where cells undergo repair and re-establish cellular and tubular integrity if possible; however during longer periods of ischaemia these innate processes are not powerful enough to fully reverse cellular injury and require external treatment options.

Endothelial dysfunction plays a central role in ischaemic AKI and is a common feature observed in other ischaemic organs, such as the heart, brain and liver (Patel *et al.* 2001; Nadar *et al.* 2005; Kavanagh *et al.* 2010). Early on in AKI, the swelling of endothelial cells (ECs) in the renal vasculature leads to the narrowing of the vessel lumen, contributing to the “no-reflow” hypothesis. Flores and colleagues were the first to demonstrate that endothelial swelling was an important part of ischaemic AKI, as reducing the lumen size hinders microvascular clearance (Flores *et al.* 1972).

Further contributing to the smaller lumen size, the renal endothelium attenuates its release of endothelial nitric oxide synthase (eNOS) after an ischaemic insult, thereby reducing the generation of nitric oxide (NO), which is a potent vasodilator (Yamasowa *et al.* 2005). It has been argued that continued constriction in the afferent arterioles feeding the glomerulus is central to the impaired GFR seen in AKI (Oken 1984).

NO can also inhibit platelet aggregation and this, plus other anti-coagulant substances, that act to reduce fibrin formation are released by the resting endothelium; however after ischaemia their production is halted, promoting a pro-coagulant phenotype post-IR injury. Therefore clot formation is increased due to the increased deposition of fibrin, as seen in renal IR injury (Enestrom *et al.* 1988), contributing to a reduced blood perfusion, particularly at the corticomedullary junction. Continued arteriole constriction, along with clot formation and the accumulation of platelets, leukocytes and red blood cells within the microvasculature, clogs and further compresses the peritubular capillaries, reducing blood flow.

Blood flow within the kidney is differentially distributed (**Figure 1.3**) and during IR injury, blood flow from medullary regions is redirected to the cortex, which contains the glomeruli, to preserve their blood flow and function (Badr and Ichikawa 1988). This redirection of blood flow reduces the oxygen partial pressure to 10% of its normal levels (Yamamoto *et al.* 1984). Therefore, the most affected areas during ischaemic AKI are the outer medullary and corticomedullary regions, especially the lower descending part the proximal tubule, the S3 segment. When blood flow to the tissue is resumed, it returns to 40-50% of the normal range due to vascular congestion, resulting in prolonged cellular injury (Molitoris and Sutton 2004). These alterations in blood flow contribute significantly to the continual worsening of kidney function over the following 24-48 hours (Regner and Roman 2012). Permanent damage and even loss of peritubular capillaries

has also been recorded after ischaemia, which has been associated with development of tubulointerstitial fibrosis and increased blood pressure (Basile *et al.* 2001).

Collective evidence therefore demonstrates that damage to the microcirculation is a major target of IR injury (**Figure 1.4**). It follows that the development of new strategies to treat ischaemic AKI must involve approaches that improve renal microcirculatory haemodynamics, reduce pro-inflammatory cell recruitment and focus on endothelial repair.

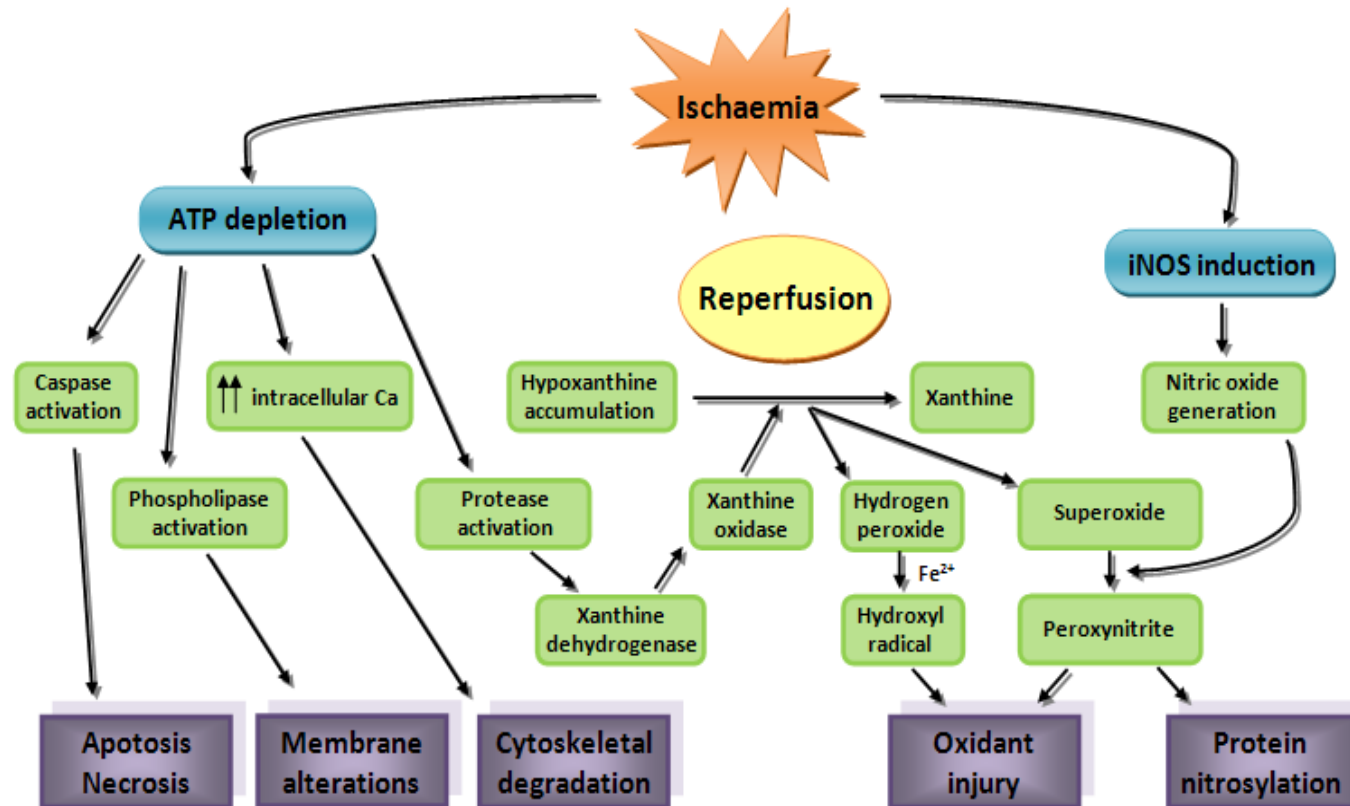


Figure 1.2. Alterations in the cellular metabolism after ischaemia-reperfusion injury. The ischaemic period is predominated by a large reduction in ATP synthesis; this propels the cell into pro-apoptotic and oxidative phenotypes, leading to a complex series of events including the disruption of the cytoskeleton and cellular ionic homeostasis (Bonventre and Weinberg 2003). Reperfusion causes the conversion of accumulated hypoxanthine into ROS, resulting in DNA damage and more specifically repressing protective gene products. Large amounts of oxidative damage to endothelium occur, resulting in an upregulation of cytokines that help recruit and activate other cell types to exacerbate injury. Diagram adapted from 'Update on Mechanisms of Acute Kidney Injury' (Devarajan 2006).

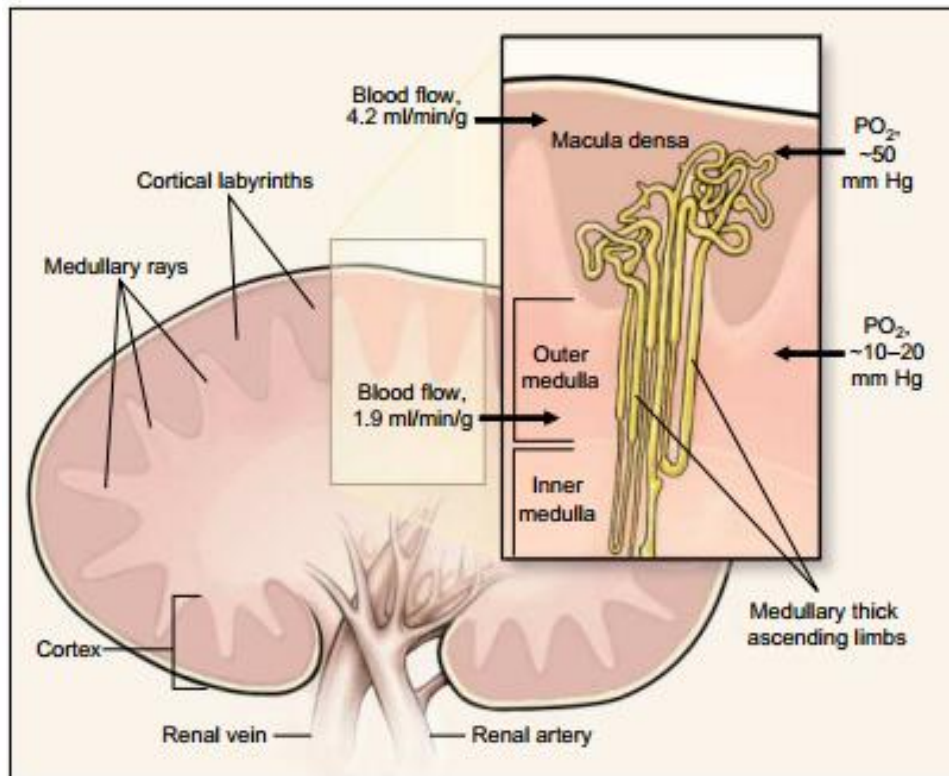


Figure 1.3. Different areas of oxygenation within the kidney. The effects of an ischaemic insult vary in the different regions of the kidney. This is because the normal ranges of oxygen partial pressures differ between the outer renal cortex and the inner medulla. The outer cortex receives the majority of the blood flow that the kidney receives, therefore exposing the endothelium here to more oxygen. The outer medulla receives a relatively small proportion of blood flow, which explains the lower partial pressure of oxygen seen here. During IR injury, a reduction in total blood flow can be reduced to 40-50% of normal figures, further reducing the decreased flow seen in the medulla (Lieberthal 1997). Diagram taken from 'Hypoxia of the renal medulla – its implications for disease' (Brezis and Rosen 1995).

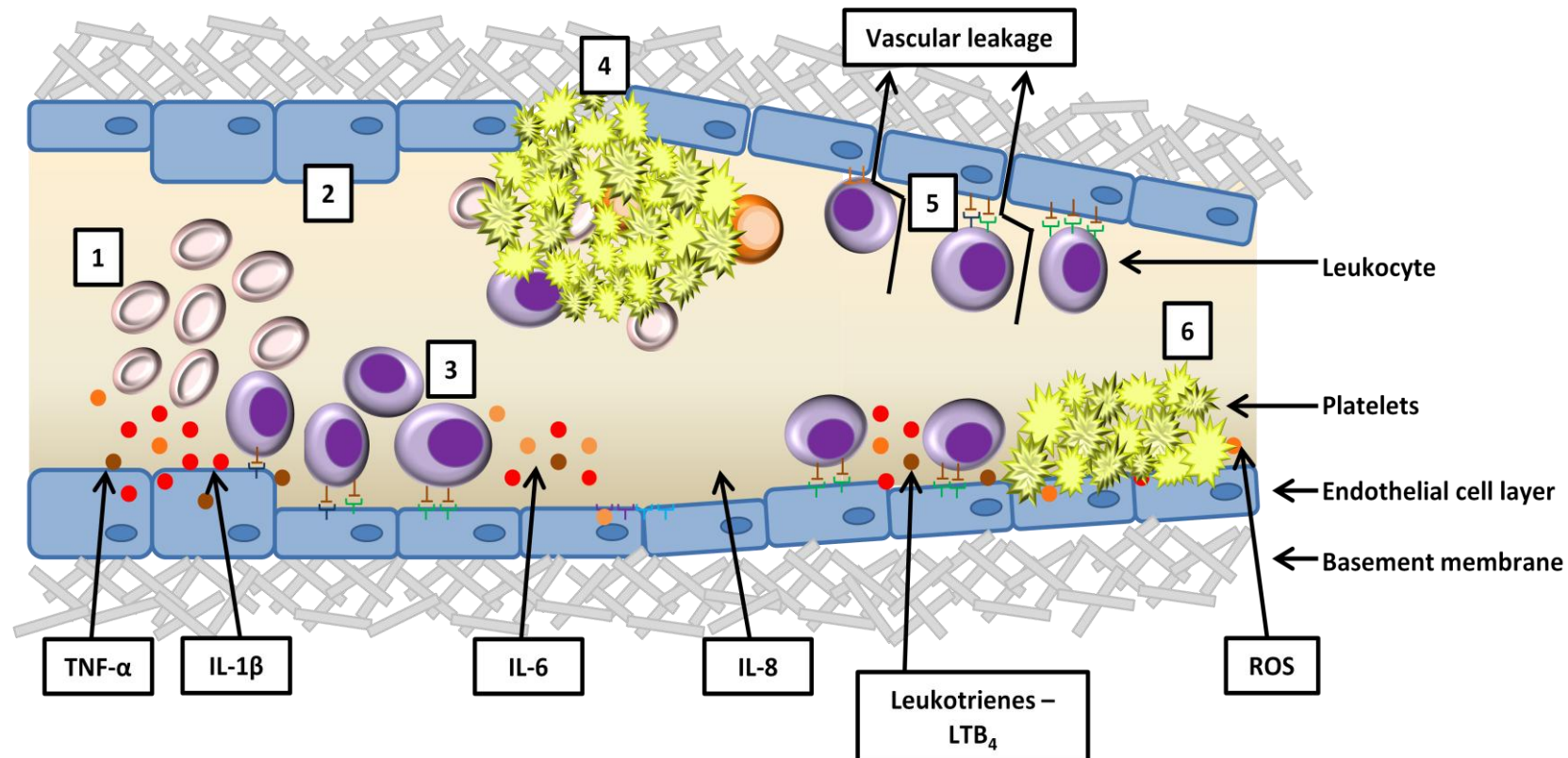


Figure 1.4. Effects of IR injury on the microvasculature. Cytokines, leukotrienes and ROS are released from the activated endothelium and cells during IR injury. Many of these released chemical mediators enhance neutrophil adhesion, which are the major exacerbators of IR injury. There are many effects of IR injury on the surrounding microenvironment and some of these are outlined above. 1. vascular congestion from RBC, leukocytes and other cell types; 2. endothelial cell swelling; 3. leukocyte adhesion; 4. thrombosis formation; 5. upregulation of adhesion molecules, e.g. VCAM-1 and ICAM-1; 6. vasodilatation due to perturbed eNOS activity. All these effects cause a decrease in renal perfusion, which causes significant surrounding tissue hypoxia (Singbartl *et al.* 2001). This phenomenon has been described in both animal models of ischaemic AKI and in the human condition (Sutton *et al.* 2002).

1.2 Inflammatory Cell Types at the Ischaemia-Reperfusion Injury Interface

1.2.1 Inflammatory Response

IR injury initiates an inflammatory reaction. Inflammation is a localised protective reaction to a source of irritation, injury or infection and is mediated by the immune system. Depending on the situation, the immune system has either the innate or adaptive response. The innate response is the first line of defence and plays an important role in ischaemic AKI. It requires no prior exposure to the insult and is activated by toll-like receptors (TLRs). These are a large family of transmembrane proteins that serve to recognise a wide range of pathogen-specific molecular structures (Akira *et al.* 2006). When infection or tissue damage occurs, TLRs on resident parenchymal cells are activated and then secrete chemoattractants, causing rapid leukocyte recruitment to the site of injury. Once these leukocytes (mainly neutrophils and macrophages) are recruited, they can clear pathogens, invading microorganisms and any damaged cells by engulfment. To complement the innate immune response, the body has an adaptive immune response, which includes the other leukocyte sub-sets, mainly T- and B-cells. The adaptive immune response occurs up to 10 days post-injury/infection. B-cells produce specific antibodies against a particular pathogen and have immunological memory; therefore, if there is another exposure to the same pathogen, a specific immune response will be more rapid. The efficiency of the inflammatory response is dependent on the highly orchestrated movement and actions of many different inflammatory cell types.

1.2.2 Different Leukocyte Populations Contribute at Different Time Points in IR Injury

During renal IR injury, there is an influx of inflammatory cells in response to the original insult. Cytokines and chemokines are released from the injured kidney; these are small secreted molecules that act to activate and attract cells and will be further discussed in section 1.3.2. When circulating leukocytes are activated by these factors, they become more rigid and subsequent firm adhesion to the injured endothelium occurs, contributing to the vascular congestion. (Akca *et al.* 2009). Different subtypes of leukocytes may contribute different effects to IR injury (Linas *et al.* 1988; Klausner *et al.* 1989).

1.2.2.1 Neutrophils Govern Early Stages of Renal IR Injury

Neutrophil influx and adhesion is now considered a hallmark of substantial IR injury, including that of the kidney (Linas *et al.* 1988; Kelly *et al.* 1994; Linas *et al.* 1995; Rabb *et al.* 1995; Kelly *et al.* 1996). Soon after the ischaemic insult, several studies have shown that adherent post-ischaemic neutrophils are mainly located in the medullary regions, which is not surprising as these are the areas of most injury (Willinger *et al.* 1992). After adherence and chemotaxis into the tissue, infiltrating neutrophils can release ROS that damage the surrounding areas (Linas *et al.* 1988). To further support this, creatinine levels have been shown to be positively correlated with the number of neutrophils at the time of ischaemia. Blocking the neutrophil adhesion receptor, E-selectin, or using anti-neutrophil serum *in vivo*, improves injury scores and kidney function (Singbartl and Ley 2000). Other studies have shown that by reducing neutrophil infiltration, tissue injury is

ameliorated (Paller 1989; Kelly *et al.* 1994). Although there are many studies like these showing that neutrophils are involved in the progression of AKI, injury is still seen in patients who are neutropenic, which suggests that neutrophil depletion alone is not sufficient to protect against AKI (Franca *et al.* 2013).

1.2.2.2 Later Stages of AKI are Characterised by Macrophage and T-lymphocyte

Infiltration

Later stages of renal IR injury are characterised by macrophages and T-lymphocytes, which predominate over neutrophils (Klausner *et al.* 1989; Takada *et al.* 1997). Macrophages are a source of pro-inflammatory molecules such as TNF- α , IL-1 β , and iNOS, all of which have been shown to propagate renal disease (Nikolic-Paterson and Atkins 2001). Macrophage-mediated effects on the renal medulla after IR injury have been noted in both mouse and rat models (De Greef *et al.* 2001; Jo *et al.* 2006). Regarding T lymphocytes, one study demonstrated that mice that lacked both CD4⁺ and CD8⁺ T-cells were protected from renal IR injury. When naïve CD4⁺ and CD8⁺ T cells were injected back into the IR animal, renal damage occurred; this data suggests a role for T cells in ischaemic injuries (Rabb *et al.* 2000). Similar results were also seen in a cisplatin model of AKI (Liu *et al.* 2006).

1.3 Leukocyte-Endothelial Adhesion Cascade

Leukocyte adhesion to endothelial cells is a main contributor of IR injury, as their presence determines the duration of damage (Buras and Reenstra 2007). Leukocytes

arresting from flow was initially proposed by Cohnheim over 135 years ago (Cohnheim 1877). Since then, our understanding of leukocyte recruitment has improved. The leukocyte-endothelial adhesion cascade, which was initially proposed by Butcher (1991), involves four main steps: tethering, rolling, firm adhesion and transmigration; an overview of this is illustrated in **Figure 1.5**.

1.3.1 Rolling Phase Governed by Selectins

Capture and slow rolling of passing leukocytes is essential if these cells are to stably adhere to the injured endothelium. Slow rolling largely mediated by a cell-surface glycoprotein family called selectins. These are categorised into E-selectin, P-selectin and L-selectin (Rosen and Bertozzi 1996). The only ligand known to interact with all three selectins is P-selectin glycoprotein 1 (PGSL-1) (Katayama *et al.* 2003; Sperandio *et al.* 2003).

Under baseline conditions, E-selectin expression is negligible; however after injury, E-selectin expression by the inflamed endothelium increases, taking several hours to reach maximal expression (McEver 1991). E-selectin can also bind to glycosylated CD44 and E-selectin ligand 1 (ESL1) (Steegmaier *et al.* 1995; Dimitroff *et al.* 2001).

P-selectin is stored in the Weibel-Palade bodies of endothelial cells and in the membranes of platelet α -granules. After renal IR injury, P-selectin is quickly upregulated (< 10 minutes) on the endothelial surface and can interact with PGSL-1 on passing

leukocytes; this interaction is of low affinity and therefore cannot support stable adhesion, but rather allows leukocytes to roll on the endothelium (Norman *et al.* 1995). Both E-selectin and P-selectin are up-regulated on the endothelial surface during renal ischaemia (Eppihimer *et al.* 1997; Molitoris and Marrs 1999). Reduction of E- and P-selectin using mutant animals and function-blocking antibodies in models of ischaemic AKI have reduced injury; most likely due to decreased leukocyte adhesion (Singbartl *et al.* 2000; Singbartl and Ley 2000).

L-selectin is not expressed on endothelial cells, but on all monocytes, neutrophils, lymphocytes and haematopoietic progenitor cells (Sackstein 1997). The main role of L-selectin is to govern naïve T cell homing into lymphoid tissues (Gallatin *et al.* 1983) and has been shown to functionally interact with E- and P-selectins (Lawrence *et al.* 1994). Redundancy in selectin roles has been proposed in certain situations, which may explain why, following IR-induced AKI in L-selectin ^{-/-} mice, no changes in adherent leukocytes or renal injury levels were reported (Rabb *et al.* 1996).

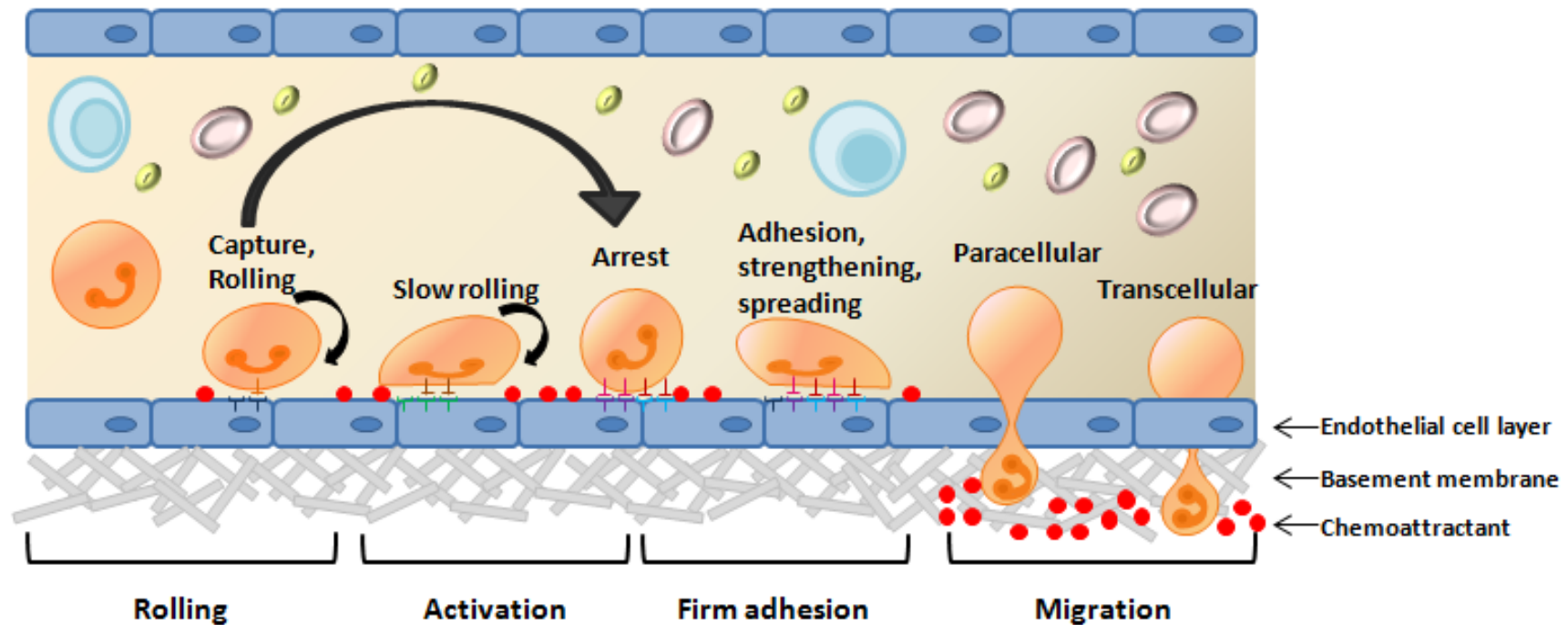


Figure 1.5. The leukocyte-endothelial adhesion cascade. This multi-step adhesive cascade was characterised by 4 main stages: rolling; activation; firm adhesion; and lastly migration (Butcher 1991). The start of this cascade involves the selectin family to firstly cause the slowing of the leukocytes from the circulation and initiate their rolling on the endothelium; secondly, the increases in chemokine concentrations trigger leukocyte activation and they subsequently flatten; activated leukocytes then make strong connections with the endothelium through integrin receptors, such as immunoglobulin cell adhesion molecules, ICAM-1 and VCAM-1; and lastly once firm adhesion takes place, these flattened cells can migrate towards cell junctions and transmigrate through the endothelial layer into the tissue using a variety of EC adhesion molecules. Further insights into this mechanism have been dissected by using *in vitro* flow models and *in vivo* intravital techniques; there is thought to be sub-steps within this process including slow rolling, adhesion strengthening, intraluminal crawling and migration through basement membrane. Diagram adapted from Ley and Tedder (Ley and Tedder 1995).

1.3.2 Activation of Rolling Leukocytes Governed by Chemoattractants

Selectin-mediated rolling allows the leukocyte to 'sample' the surrounding environment and transmit those signals through G-protein-coupled receptors (GPCRs) (Alon and Ley 2008). In the context of inflammation, cytokines are produced by the activated endothelium and they interact with their corresponding receptor on target cells, including neutrophils or stem cells (SCs). Cytokines are small 7-30 kDa secreted proteins that principally act to regulate immune and haematopoietic cell proliferation and activity. Cytokines can be grouped broadly into interleukins (IL), colony-stimulating factors, interferons, chemokines and growth factors. Secreted chemokines are extracellular signalling molecules that create a chemotactic gradient for surrounding cells and can also modulating all areas of the adhesion cascade by causing changes in integrin affinity and avidity (Ley *et al.* 2007). The cytokine family targets cells over a range of distances and can further activate the cells which secreted them. Following GPCR activation by a cytokine, rapid inside-out signalling results in almost instantaneous integrin activation (Shamri *et al.* 2005). Several cytokines and chemokines are involved in this process but within this study we looked only at IL-1 β , KC (murine IL-8), SDF1 α and TNF- α .

1.3.2.1 Interleukin-1 β

Interleukins (IL) were the first shown cytokines to be released from leukocytes. Local production of IL-1 β and/or TNF- α by polymorphonuclear neutrophils increases E- and P-selectin expression on endothelium. This increases leukocyte binding and infiltration into injured tissues, therefore promoting further injury (Rice and Bevilacqua 1989; Weller *et*

al. 1992). More recently, injured endothelium has shown elevated IL-1 β gene expression and been shown to release IL-1 β into the circulation 4 hours post-reperfusion (Jo *et al.* 2006). Upon endothelial activation, IL-1 β is released in its inactive form and is cleaved by the pro-inflammatory enzyme, caspase-1. After cisplatin induced AKI, IL-1 β plasma concentrations were increased in WT mice, but by using caspase-1^{-/-} mice, IL-1 β levels were reduced (Faubel *et al.* 2007). However, direct blocking of its receptor IL-1R does not affect injury markers (Haq *et al.* 1998), thereby questioning the involvement of IL-1 β in AKI.

1.3.2.2 Keratinocyte-derived Chemokine

Keratinocyte-derived chemokine (KC; CXCL1; murine functional homologue of human IL-8) is a strong leukocyte chemoattractant and is released by a variety of cells, including leukocytes and endothelial cells (Yoshimura *et al.* 1987; Schroder and Christophers 1989). KC production can be increased by pre-treating with IL-1 or TNF- α (Detmers *et al.* 1990). KC acts to recruit both neutrophils and T-lymphocytes to the site of inflammation (Frangogiannis 2007) and has also been shown to trigger monocyte arrest on atherosclerotic endothelium (Huo *et al.* 2001). The main chemokine receptor for KC is CXCR2, but it can also interact with CXCR1. When a CXCR2 inhibitor, repertaxin, is used in a model of rat renal transplantation, neutrophil infiltration is reduced and renal function is preserved (Cugini *et al.* 2005). Intravital microscopy shows that leukocyte rolling in CXCR2^{-/-} murine cremaster venules have an increased velocity compared to WT mice (Morgan *et al.* 1997), implicating this receptor in the slow rolling stage of the leukocyte adhesion cascade. KC levels are increased in serum readings 2 hours after AKI (Molls *et*

al. 2006). This could be useful as an early biomarker for AKI, so that patients could be subjected to treatment before any substantial or irreversible damage is done.

1.3.2.3 Stromal Cell Derived Factor-1 α

Stromal cell derived factor-1 α (SDF-1 α ; CXCL12) is a chemokine that has been extensively studied with regards to its role in the regulation of cell migration and inflammation. Its receptor, CXCR4, is present on all immune cells and those of the central nervous system. CXCR4-deficient mouse embryos have several lethal defects, including the bone marrow being devoid of progenitor cells (Ratajczak *et al.* 2006). SDF-1 α was originally purified from bone marrow (BM) stromal cell releasate, which established a high chemokine concentration in the BM (Sweeney *et al.* 2002). Surratt and colleagues (2004) have shown that this high concentration of SDF-1 α acts to retain CXCR4⁺ neutrophils in the BM under normal conditions. SDF-1 α is upregulated during many tissue injuries, including kidney IR (Togel *et al.* 2005) and disrupts the BM concentration gradient, consequently causing neutrophil and progenitor cell egress (Hattori *et al.* 2001). Until recently, CXCR4 was thought to be the sole receptor of SDF-1 α , but CXCR7 has also been identified and shown to dimerise with CXCR4 to regulate its activity (Sierro *et al.* 2007).

1.3.2.4 Tumour Necrosis Factor- α

Tumour necrosis factor- α (TNF- α) is released from infiltrating leukocytes and can activate the endothelium and stimulate the production of many other cytokines and chemokines, including KC and IL-1 β (Detmers *et al.* 1990). It is involved in the acute phase of

inflammation and is deregulated in many diseases, including cancer (Charles *et al.* 2009). Raised levels of TNF- α are shown in chronic end-stage renal disease patients on haemodialysis and they correlate with their life-expectancy (Balakrishnan *et al.* 2004). Elevated levels were also seen in patients with AKI, but at a lower extent to those of a chronic nature (Ficek *et al.* 2006). Reducing circulating TNF- α concentration causes decreased leukocyte rolling, adhesion and vascular leakage in ocular inflammation (Koizumi *et al.* 2003). TNF- α has been shown to be increased after myocardial IR injury and further exacerbates damage by producing ROS leading to coronary endothelial dysfunction (Zhang *et al.* 2006).

1.3.3 Firm Adhesion Governed by Integrins

Integrins are a superfamily of cell adhesion transmembrane receptors. They are made up of an α - and a β -chain and can bind to extracellular matrix (ECM) components, cell-surface ligands and some soluble molecules. There are eighteen α -integrins and eight β -integrins that can dimerise to form 24 distinct heterodimer integrins. These receptors can switch between low- and high-affinity states according to the state of the local environment, i.e. cytokine concentrations, to mediate stable adhesion to their endothelial counter-ligands (Hynes 2002). The functions of the $\alpha_4\beta_1$ integrin VLA-4 (very late antigen-4) and the β_2 integrins have been widely investigated and are discussed below.

1.3.3.1 CD49d

CD49d is the $\alpha 4$ chain which can bind to the $\beta 1$ chain, CD29 to form the integrin, VLA-4 ($\alpha 4\beta 1$). This integrin is found on most leukocytes and mainly interacts with vascular cell adhesion molecule-1 (VCAM-1) on endothelial cells or fibronectin within the ECM. This integrin is best known for its role in lymphocyte adhesion to its counter-ligand VCAM-1 on the inflamed endothelium (Elices *et al.* 1990). Studies have shown that VLA-4/VCAM-1 is essential for the release of neutrophils from the BM into the periphery and this process is regulated by the SDF-1 α /CXCR4 pathway. SDF-1 α enhances neutrophil binding to VCAM-1 coated plates and injecting antibodies against both CXCR4 and VCAM-1 further enhanced neutrophil mobilisation compared to that seen when each antibody is administered separately (Petty *et al.* 2009). This is most likely due to SDF-1 α initiating the clustering of VLA-4 via GPCR signalling (inside-out signalling), as previously seen in lymphocytes (Grabovsky *et al.* 2000). These results show the importance of crosstalk between chemokines and adhesion molecules. Similar crosstalk has also been shown regarding human SC adhesion and transmigration (Peled *et al.* 2000).

1.3.3.2 CD18

CD18 is the β_2 subunit for three separate integrins, associating with αL (CD11a), αM (CD11b) or αX (CD11c) to form Mac-1, LFA-1 and integrin $\alpha X\beta 2$ respectively (Chakravorty *et al.* 1999). Inflammatory mediators, such as platelet activating factor (PAF) and leukotrienes, can induce CD18 expression on neutrophils within 2 minutes, which allows rapid adhesion of neutrophils to the endothelium (Granger and Kubes 1994). β_2 integrins

on mature leukocytes can bind to ICAM-1 (intercellular adhesion molecule-1) expressed on the endothelium (Springer 1994). Expression of renal ICAM-1 is increased on the endothelium in response to ischaemic injury (Ichikawa *et al.* 1997). ICAM-1 deficient mice are protected from acute renal IR injury (Kelly *et al.* 1996), implicating the role of ICAM-1 in worsening acute tubular necrosis. This protective effect of blocking ICAM-1 was also seen by Rabb *et al.* (1995), as administering monoclonal ICAM-1 blocking antibodies up to 2 hours post-ischaemia can reduce injury.

1.3.4 Non-Integrin CD44 Based Leukocyte Adhesion

CD44 is a type I transmembrane glycoprotein expressed on a variety of cell types, including leukocytes and endothelial cells. It is encoded by a single gene with multiple splice sites, resulting in the expression of various spliciforms. All spliciforms have a hyaluronan (HA) and osteopontin binding site, which are the major ligands for CD44. Also, interactions with VLA-4 can enhance firm adhesive endothelial contact (Nandi *et al.*, 2004). CD44 is involved in leukocyte activation, haematopoiesis, and SC migration when modified. Under normal conditions, CD44 is minimally expressed in the kidney but after renal inflammation expression is markedly increased, especially on glomerular cells (Burne *et al.* 2001). Rouschop *et al.* (2005) discovered that endothelial CD44 governs neutrophil trafficking in their renal IR injury model; blockade or deficiency of endothelial CD44 caused a decrease in the number of infiltrating neutrophils into the ischaemic kidney tissue, improved renal function and reduced renal fibrosis.

1.3.5 Transmigration

Following firm adhesion, leukocytes must migrate through the endothelium and into the underlying inflamed tissue stroma with minimal disruption to the vessel wall. Transendothelial migration (TEM) is known as the point of no return regarding inflammation, as all previous steps in the leukocyte-endothelial cascade can be reversed. Paracellular transmigration is a well-described process involving cell movements through cellular junctions in the endothelium monolayer; this is the most common way cells cross the endothelial barrier. It has been shown that neutrophils can migrate through an endothelial cell, but this event is rare (Feng *et al.* 1998).

1.3.6 Platelets

Another cell type that plays a role in IR injury is the platelet. They are discoid-shaped cells, with their diameter measuring between 0.5 - 3µm. In mammals, platelets are anucleated cells that originate from BM-derived megakaryocytes and circulate within the body, ready to respond to losses in vessel integrity. For years it was thought that platelets could only adhere to the exposed subendothelial collagen matrix, but now it is understood that under high shear stress inflammatory conditions, such as IR injury, GPIb on the platelet surface can interact with von Willebrand factor (vWF) on intact but activated endothelium early after reperfusion (Chintala *et al.* 1994; Clemetson and Clemetson 2008).

During IR injury, endothelial cells synthesize tissue factor and bind soluble fibrinogen. This, along with platelet inhibition by endothelial NOS and PGI₂ production being perturbed, promotes platelet aggregation (Frenette *et al.* 1998; Yamasawa *et al.* 2005). Platelet accumulation is inversely proportional to blood flow (Laws *et al.* 1983). Once attached to the activated endothelium through P-selectin (Massberg *et al.* 1998), platelets release IL-1 β and soluble CD40-ligand, which acts upon the endothelium to support further platelet adhesion and maintain the stability of the developing thrombus (Massberg *et al.* 2002; Theilmeier *et al.* 2002). Also, when thrombin-activated platelets were co-incubated with human intestinal endothelial cells (EC), the ECs became activated and released more IL-8 coupled with an upregulation of ICAM-1 and VCAM-1 expression, all of which promotes leukocyte-endothelium adhesion (Danese *et al.* 2004).

Therefore, it is not surprising that platelets have been shown to be involved in the pathogenesis of IR injury. Platelet adhesion has been shown to increase with increasing reperfusion times whereas, without injury, platelet adhesion is negligible (Carvalho *et al.* 1974). When platelets are depleted in a coronary artery occlusion-reperfusion rabbit model, there was a reduced infarct size and improved heart function (Golino *et al.* 1987). Platelets can also bind to leukocytes, via P-selectin and P-selectin glycoprotein ligand-1 (PGSL-1), to form heterotypic aggregates in the circulation and in microvascular beds (Weyrich *et al.* 2003). Activated platelets help to recruit neutrophils to sites of inflammation in experimental models of AKI (Singbartl *et al.* 2000). Platelets also release a concoction of inflammatory mediators, such as PAF, SDF-1 α and various cytokines, which all promote a pro-inflammatory environment.

1.4 Injury Diagnosis, Renal Repair and Current Treatments

1.4.1 Injury Diagnosis

Despite our increased understanding of AKI over the last decade, diagnosis of this condition is still poor. This is mainly due to very few sensitive early biomarkers of injury, the heterogeneity of the disease and not being able to detect the severity to give the most suitable treatment (Tsagalis 2011). The kidney receives 25% of cardiac output and facilitates the high GFR required for regulating the body's fluid and electrolyte balance. After renal IR injury, there is a drop in blood flow and consequently a fall in GFR, which produces an increase in nitrogenous waste products in the blood, such as urea and creatinine (Thadhani *et al.* 1996). Currently, serum creatinine is the most common indicator of kidney function that is used clinically: it has been suggested that creatinine should be used to differentiate between different degrees of kidney damage so that the appropriate treatment can be given accordingly (Bellomo *et al.* 2004). There is now an increased recognition that even relatively small rises in serum creatinine are associated with poor prognosis, with high rates of morbidity and mortality (Chertow *et al.* 2005; Ostermann *et al.* 2008).

1.4.2 Renal Repair Following Ischaemia-Reperfusion Injury

The kidney is a highly complex organ made up of many cell types. Even though the cell turnover rate of the kidney is much lower than other organs, such as the gut and skin, the kidney still has auto-regenerative capacity (Iwatani and Imai 2010) and can recover from short periods of kidney damage. Due to the large transport demands and the architectural arrangement of the kidney, cells of the kidney are likely to experience toxic insults and ischaemia. Proximal tubules in particular can be susceptible to such damage but have been shown to undergo repair after short periods of ischaemic damage; the apoptotic epithelial cells generate signals that initiate the repair response (Toback 1992). Some groups have shown that in both human and animal models of AKI, the tubular cells which surround the injury start to change their phenotype and begin to proliferate more quickly than usual (Witzgall *et al.* 1993; Abbate *et al.* 1999). However when injury is more substantial the kidney cannot repair itself, which results in persistent tubulointerstitial inflammation and fibroblast proliferation; both of which cause fibrosis to develop. Due to the kidneys innate repair processes being overwhelmed, external assistance is required.

1.4.3 Existing Treatment Options

Once AKI develops, supportive measures aside, there is no treatment available to effectively treat or prevent it. Severity differs between patients who have AKI, but in critically ill patients mortality rates are as high as 50% (Karsou *et al.* 2000). Patients who experience AKI require dialysis or subsequently progress to CKD. The number of people suffering from AKI and CKD is increasing and in 2006, \$23 billion was spent on their

medical care, as calculated by the U.S. Renal Data System. Available therapies at the moment cannot enhance kidney repair or regeneration. Renal replacement therapies such as dialysis are used, but this only helps the excretory function of the kidney and although it is life sustaining, it is an extremely exhausting and invasive procedure that dramatically reduces average life-expectancy (Owen *et al.* 1993). Therefore, there is an urgent need for better renal replacement therapies.

Using animal models, drugs such as mannitol, loop diuretics, dopamine and calcium channel blockers have been partially successful in promoting diuresis, as urine production is altered due to increases in endothelial permeability, but results have not been replicated in humans (Agmon and Brezis 1993). Human AKI is a very heterogeneous in its functional changes therefore therapies affecting more than one pathway are of particular interest. Something that has been used in an attempt to reduce the risk of ischaemic AKI is ischaemic preconditioning (IPC). IPC refers to causing non-lethal tissue ischaemia for a very short period of time to protect against a future prolonged ischaemic insult: this was first tested in mice and had extremely positive results with a decreased number of infiltrating neutrophils and macrophages in the kidney (Kinsey *et al.* 2010). Cross-clamping of the common iliac artery to induce remote ischaemic preconditioning (RIPC) in patients undergoing abdominal aortic aneurysm repair has been investigated: the incidence of AKI was reduced by 23%, determined by creatinine serum concentrations (Ali *et al.* 2007). Similar beneficial effects have also been seen in patients undergoing multivessel coronary artery bypass graft surgery who received RIPC in the form of three 5-minute cycles of ischaemia by use of a blood pressure cuff (Zhou *et al.* 2010). The ideal

therapy for kidney disease would be something that would target the heart of the problem therefore removing all of the secondary effects.

1.5 Stem Cells as a Source for Regenerative Medicine

1.5.1 The Different Progenitor Cells of the Bone Marrow

Given the poor prognosis of AKI, SC -based therapy has been heralded as a favourable option for the management of renal disease progression; this is mainly due to many reports showing the plasticity of SCs, thus making them a promising aid to regeneration and organ recovery. SCs are defined by having the dual-capacity to self-renew and also to produce a more mature differentiated daughter progeny. SCs drive normal development and as this progresses, lineage-restricted progenitor cells create the tissues and organs of the body. During late embryonic development, SCs migrate from the foetal liver to the BM (Christensen *et al.* 2004). During adulthood, SCs still play a role in the maintenance of tissue and organ homeostasis: the BM is responsible for maintaining haematopoiesis and contains a mixture of immature and maturing cells. The immature cells include mesenchymal stem cells (MSCs); endothelial progenitor cells (EPCs); and haematopoietic stem cells (HSCs). Several studies have shown that BM-derived SCs (BMSCs) can be beneficial in several organ injuries, including the heart, kidney, brain, liver and gut (Orlic *et al.* 2001; Kale *et al.* 2003; Deng *et al.* 2005; Kavanagh *et al.* 2010; Kavanagh *et al.* 2013). Furthermore, using BMSCs to treat AKI is encouraging due to the adaptable

nature of these cells according to their environment (Bussolati *et al.* 2009). Most studies investigating SCs in organ repair have looked at MSC and HSC BM- subsets.

1.5.2 Mesenchymal Stem Cells

The term 'mesenchymal stem cells' was first coined by Caplan (1991) for the ability of these BM-derived cells to differentiate along several mesenchymal lineages. These cells are less abundant than their haematopoietic counter-part and are not easy to define due to the lack of specific marker proteins; this has been the main hindrance in completely understanding MSCs full potential. Currently, the most popular way to define them is by their capability of differentiating into specialised mesenchymal cells, such as osteocytes, chondrocytes and adipocytes, and also by their ability to adhere to plastic (Meirelles Lda *et al.* 2009). As well as being able to differentiate into these different types of cells, MSCs can provide stromal support for HSCs within the BM (Bensidhoum *et al.* 2004) and are capable of differentiating into glomerular and tubular epithelium and interstitial cells when in the presence of the embryonic kidney (Yokoo *et al.* 2005).

Regarding their regenerative potential, MSC benefits are not wholly dependent on MSC differentiation into tissue parenchyma. There has been much speculation about MSCs having paracrine effects on the surrounding tissue; Togel and colleagues (2007) observed that after MSC infusion into a rat model of renal IR injury, there was an improvement in renal function after 24 hours. This effect was not due to differentiation into epithelium or endothelium but due to an altered expression in inflammatory mediators, such as

VEGF, IGF-1 and HGF. Also, injecting MSCs overexpressing the Akt1 survival gene into the myocardium following an acute myocardial infarction improved cardiac function in less than 72 hours post-MSC injection (Gnecchi *et al.* 2005). Due to differentiation and fusion events being uncommon, it was proposed that this improvement was due to paracrine protective factors being released (Gnecchi *et al.* 2006).

1.5.3 Haematopoietic Stem Cells

HSCs were first identified by Till and McCulloch in the early 1960s as 'colony forming units' and were defined as being able to form within the spleen of irradiated mice and differentiate into several blood lineages (Till *et al.* 1964). HSCs are multipotent SCs that are self-renewing and can differentiate to produce myeloid and lymphoid adult blood cells (**Figure 1.6**). Krause and colleagues (1994) have shown that by transplanting a single male HSC into a lethally-irradiated female mouse replenished all of the blood cells. HSCs are a relatively rare population of cells, constituting 1 in 10^5 cells in the BM and can be identified and purified by isolating c-kit⁺ Sca1⁺ Lin⁻ (KSL) populations from the BM. In humans, HSCs are most commonly identified by being CD34⁺ (Civin *et al.* 1984), however roughly 90% of mouse HSCs do not express this marker making it unfeasible to use CD34 for isolating murine HSCs (Osawa *et al.* 1996). Although in adult life, HSCs reside in the bone marrow, they can migrate out of the BM and circulate in the blood, trafficking to different organs during homeostasis and trauma (Wright *et al.* 2001; Massberg *et al.* 2007; Si *et al.* 2010). It has been proposed that <400 HSCs circulate in the mouse circulation and are important for homeostatic maintenance (Wright *et al.* 2001).

HSCs have received a great deal of attention with regard to their regenerative capacity, as they are not confined to producing cells of just the haematopoietic lineage. Numerous laboratories have shown that HSCs can differentiate into cells of a non-haematopoietic origin, therefore replenishing lost cell types in different injured organs (Lagasse *et al.* 2000; Graf 2002; Sata *et al.* 2002; Kale *et al.* 2003; Lin *et al.* 2003; Bailey *et al.* 2004). However, the mechanism is still under investigation.

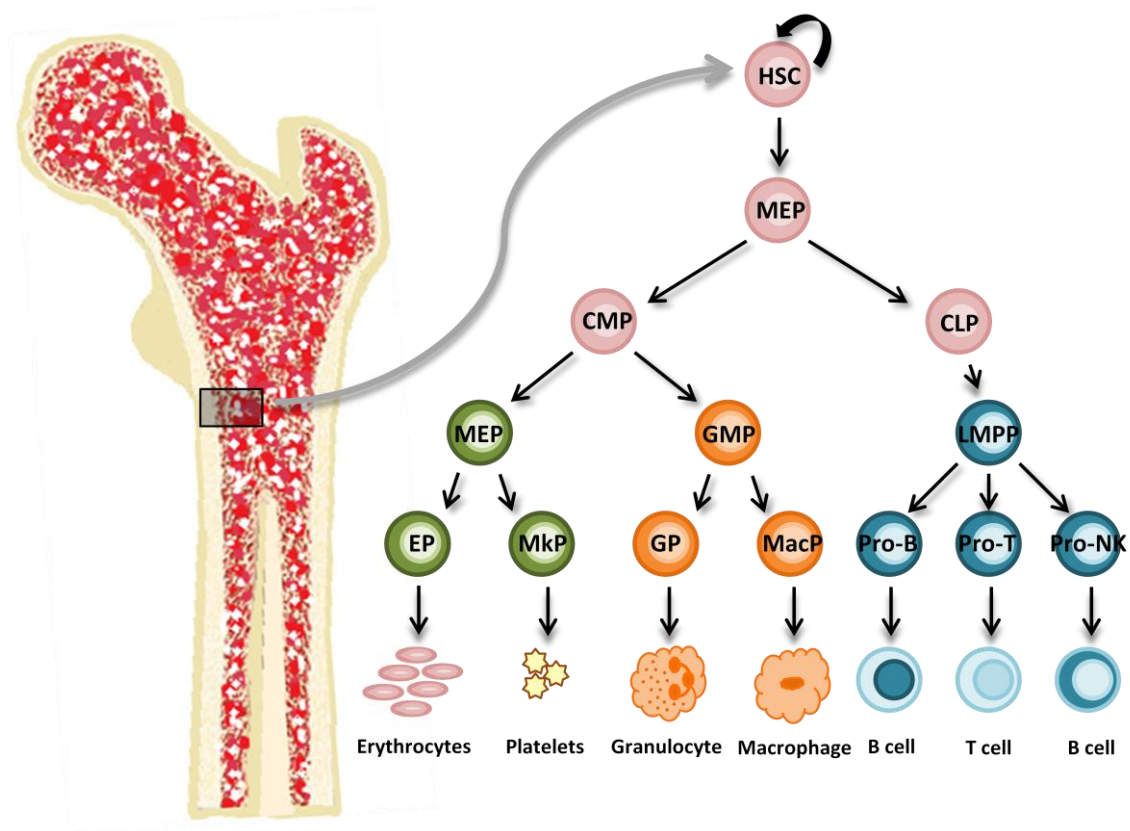


Figure 1.6. The haematopoietic system. HSC differentiation begins in the bone medulla and each stage is governed by a variety of signals. HSCs can produce all cells that make up the blood and the process into a terminally differentiated cell is outlined above. CMP: common myeloid progenitor; CLP: common lymphoid progenitor; MEP, megakaryocyte–erythrocyte progenitor; GMP: granulocyte-macrophage progenitor; LMPP: lymphoid primed multipotent progenitor; EP: erythrocyte progenitor; MkpP: megakaryocyte progenitor; GP: granulocyte progenitor; MacP, macrophage progenitor; Pro-B: progenitor B cell; Pro-T: progenitor T cell; Pro-NK: progenitor natural killer.

1.5.4 HSC Regeneration by Differentiation, Cell Fusion and Paracrine Mechanisms

Once at the injury site, there are three main theories to explain how HSCs produce an effect: differentiation; fusion; or via paracrine mechanisms. Differentiation was initially the most common theory and has stemmed from the studies of sex-mismatched transplantations in humans: female kidneys were transplanted into male recipients and later in life developed acute tubular necrosis (ATN), kidney biopsies were taken and cells containing the Y chromosome were found (Gupta *et al.* 2002). Poulsom and colleagues (2001) also showed similar results in their human gender mis-matched experiments. In a CKD model, which uses male mice deficient in fumarylacetoacetate hydrolase (Fah) to produce a build up of acid causing chronic proximal tubule damage, it was found that nine months post female Fah⁺ bone marrow transplantation there were 25-50% renal tubule cells that were positive for Fah (Held *et al.* 2006). This showed that engraftment of BM cells to improve kidney function can occur. Researchers have also explored the possibility that these progenitor cells may be fusing with other surrounding cells. Terada *et al.* (2002) was the first to hypothesise that BM cells and embryonic stem (ES) cells could spontaneously fuse *in vitro*, as the BM cells adopt a more ES cell phenotype. However, the Sca1⁺Lin⁻ fraction did not increase fusion events, suggesting that HSCs do not undergo such occurrences. Some studies have demonstrated fusion events in the first week or the first month after folic acid or IR kidney injuries (Fang *et al.* 2005; Li *et al.* 2007), although fusion occurred in very small percentages.

Ever-increasing evidence suggests HSCs are able to contribute to tissue repair via paracrine anti-inflammatory mechanisms. In our lab, the HPC-7 HSC cell line has shown

to reduce the number of leukocytes in a murine model of liver IR injury and also intestinal IR injury (Kavanagh *et al.* 2013). Biziuleviciene and colleagues (2007) have shown reduced oedema and TNF- α release after HSC administration into a paw oedema model of mouse inflammation.

Investigations that have used HSCs in renal IR injury have had a poor recruitment of cells (Lin *et al.* 2003; Li *et al.* 2010), which may be the reason for poor renal recovery following injury. Therefore, ways in which to enhance such recruitment would most likely lead to enhanced beneficial results.

1.5.5 HSC Recruitment to Adult Peripheral Tissues

Jia and colleagues stated that the movement of SCs is critical for repair in adulthood (Jia *et al.* 2012). Certain techniques have been employed to understand HSC trafficking; intravital microscopy (IVM) has been one of the main ones, as it allows the direct visualisation of a single cell's movement in a particular organ of an anaesthetised animal (Furlani *et al.* 2009; Kavanagh *et al.* 2010; Lo Celso *et al.* 2011; Kavanagh *et al.* 2012). Although SC homing to the BM has been extensively studied (Frenette *et al.* 1998; Lapidot and Petit 2002; Avigdor *et al.* 2004), SC homing to injured sites is still in its infancy. This is mainly due to low endogenous HSC numbers. Therefore many studies have used exogenously-derived HSCs to understand such trafficking, for example Massberg and colleagues (2006) infused 1.5×10^5 HSC into a murine thrombosis model. It has been hypothesised that the way in which BM-derived SCs adhere to the injured

endothelium is similar to that of differentiated BM cells (Lapidot and Petit 2002); therefore many studies have been conducted on that premise.

It was primary studies by Tavassoli and Hardy (1990) that first suggested that membrane lectin-carbohydrate interactions were involved between circulating HSCs and endothelium. A few years later, haematopoietic progenitor cells were shown to exhibit a similar repertoire of surface adhesion molecules to leukocytes, expressing $\beta 1$ and $\beta 2$ integrins which could bind to their endothelial counter-ligands, VCAM-1 and ICAM-1 respectively (Turner *et al.* 1995) and their adhesion can be regulated by cytokines (Kinashi and Springer 1994).

Studies have shown that without the $\beta 1$ integrin, haematopoietic cell migration to the foetal liver is impaired in pre-natal stages (Hirsch *et al.* 1996). Also, HSCs home to sites of new vessel growth to promote angiogenesis, and this recruitment is dependent on the $\alpha_4\beta_1$ /VCAM-1 pathway (Jin *et al.* 2006). Similar interactions also mediate HSC recruitment to BM: there is a 50% reduction in HSC numbers within the BM after inhibiting VCAM-1 or α_4 subunits, thus implicating an important role for this integrin in HSC homing (Papayannopoulou *et al.* 1995). During periods of ischaemia, fusion events between HSCs and murine cardiomyocytes occur through $\alpha_4\beta_1$ /VCAM-1 interactions (Zhang *et al.* 2007) and work from our group demonstrated a critical role for the CD49d (α_4 subunit of $\alpha_4\beta_1$ integrin) / VCAM-1 interaction in mediating HSC recruitment to injured murine liver *in vivo* (Kavanagh *et al.* 2010). It is not known whether CD49d is

universally responsible for retaining HSCs in all injured vascular beds, including the kidney.

In IR injured mouse gut, HSC recruitment has shown to be independent of $\alpha 4\beta 1$ activity but dependent upon the $\beta 2$ integrin CD18. Interestingly, in an IR injured cremaster muscle, both CD49d and CD18 have a role in facilitating HSC adhesion to the injured vasculature (Kavanagh *et al.* 2013). The non-integrin cell-surface glycoprotein molecule CD44 has been implicated in HSC homing to the BM (Dimitroff *et al.* 2001). In our previous IR-injury models, we have not found a role of the non-integrin cell-surface glycoprotein molecule CD44 in assisting HSC adhesion.

Many of the factors responsible for maintaining HSCs within the BM are also used by peripheral organs to recruit HSCs. One of the most potent candidates responsible for retaining HSCs within the BM is the extensively studied G-protein coupled chemokine receptor CXCR4 and its ligand SDF-1 α . Osteoblasts are a local source of this HSC-attracting chemokine (Jung *et al.* 2006). SDF-1 α gradients are incredibly important with regard to the recruitment and localisation of HSCs: hypoxic conditions upregulated local SDF-1 α expression through the increased actions of hypoxia inducible factor-1 α (HIF- α) (Ceradini *et al.* 2004). When there is an altered oxygen tension, such as in ischaemic injuries, there is an increase in SDF-1 α release from the damaged endothelium and CXCR4⁺ HSCs egress from the BM and home to the injured tissue (Togel *et al.* 2005). Another rich source of SDF-1 α is activated platelets. Platelets adhere to inflamed

vasculature and release SDF-1 α which then induces the accumulation of human CD34⁺ progenitor cells (Stellos *et al.* 2008). Blocking platelet adhesion or platelet-secreted SDF-1 α in a murine arterial thrombosis model eradicated almost all HSC adhesion *in vivo* (Massberg *et al.* 2006). The endothelial surface presents SDF-1 α to the local environments and it can act to coordinate the actions of many adhesion molecule receptors, including VLA-4, LFA-1 and CD44 (Peled *et al.* 2000). Avigdor and colleagues (2004) have shown that human CD44⁺ HSCs cooperate with SDF-1 α and this improves transendothelial migration in the BM. Blocking its receptor inhibits progenitor cell homing and engraftment in NOD/SCID mice (Peled *et al.* 1999).

1.5.6 HSCs in the Injured Kidney.

SCs need to be able to localise to the injured kidney if they are to have a beneficial effect in repairing AKI. Both Park and Akashi and colleagues (Park *et al.* 2002; Akashi *et al.* 2003) stated that their isolated HSCs could retain their developmental plasticity and that their gene expression was different to less primitive BM-derived cells, which may govern the pluripotent nature of HSCs. Data from the same lab produced the first report showing that a pure population of HSCs could differentiate into renal tubule cells thus contributing to kidney regeneration after IR injury (Lin *et al.* 2003). In these experiments, the renal artery was clamped for 15 minutes which produced tubule damage including epithelial cell detachment from basement membrane, loss of proximal tubule (PT) brush border and an increase in tubular cell death as assessed by increases in BrdU staining. 2000 LacZ⁺ HSCs were transplanted into the female recipient 2 hours post-reperfusion and 4-12 weeks later the injured animals that received HSCs had a stripe of LacZ⁺ cells in

the S3 segment of the proximal tubule, where most damage occurs post-IR injury. Some of the LacZ⁺ cells in this area expressed a sodium/phosphate cotransporter type 2, which is located in the brush border of the proximal tubule, indicating that some of the transplanted HSCs had adopted a renal phenotype. However, only very few of the transplanted HSCs actually adhered ($8.3 \pm 2.3\%$) and even fewer took on the PT phenotype. No creatinine or blood urea nitrogen (BUN) experiments were conducted to show any improvement in function and judging from the poor HSC engraftment and even poorer phenotypic changes it would be unlikely for this kidney to show any clinically relevant improvements.

Li and colleagues in 2010, administered human haematopoietic stem/progenitor cells (HSPCs) 24 hours post-renal IR injury. At day 3, HSPCs underwent a phenotypic switch to a more endothelial characteristic (Li *et al.* 2010) and at day 7, 90% of mice survived compared to 50% in the vehicle-treated group. HSPCs were primarily located in the peritubular region, as assessed by immunostaining, and these HSPCs were still evident on days 14 and 28 after IR injury (Li *et al.* 2010).

More recently, Li *et al.* (2012) showed that by treating human CD34⁺ haematopoietic stem/progenitor cells (HSPCs) with cytokines, growth factors and deacetylation inhibitors they can be induced towards a more committed renal lineage. These treated HSPCs can form tubular structures in 3-dimensional cultures, similar to the control renal inner medullary collecting duct (IMCD) differentiated cells. In these studies, sex-mismatched

BM transplanted animals received an intravenous injection of 5×10^6 treated HSPCs 2 hours after 35 minutes ischaemia, which improved renal morphology and function. However, very few tubular epithelial cells possessed the Y chromosome, indicating low HSPC engraftment from the male donor; this suggested that beneficial effects may be exerted through paracrine mechanisms. Conditioned media from these treated cells contained VEGF, IGF-1 and HGF and these alone can reduce injury markers 24 hours after renal IR injury, further supporting the paracrine theory. In agreement with this study, injection of MSCs following renal ischaemia in rats reduced injury markers and this could be reversed by selectively knocking down VEGF within the MSC (Togel *et al.* 2007; Togel *et al.* 2009). One point to mention concerning the Li *et al.* (2012) study would be that after intravenous injection of HSPCs, these cells localise to the lungs, liver and even home back to the BM thereby explaining low numbers of direct cell engraftment.

Using a mixture of BMSCs or HSCs in specifically treating renal IR injury has had mixed results: Poulsom and colleagues (2001) showed that BM-derived cells could contribute to the repair of the renal parenchyma by adopting a renal phenotype, although the exact source(s) of these cells was unknown. Within this study, changes in SC phenotype and marginal improvements in morphology were seen, although engraftment into tubules after ischaemic injury was poor. This low level of engraftment has also been seen in experiments by Lin and colleagues (2003), showing that cell engraftment/differentiation mechanisms are contributing very little to overall renal regeneration. Several other studies have shown that the BMSC role in repair is negligible (Duffield *et al.* 2005; Lin *et al.* 2005).

Discrepancies in the contribution to renal regeneration are most likely due to poor recruitment of HSCs, mainly due to the majority being lost to non-injury sites. Therefore, understanding how to increase the homing and adhesion of these SCs to the site of injury would be extremely beneficial. Currently, there are no papers describing HSC recruitment mechanisms to the IR-injured kidney.

1.6 Summary

AKI usually occurs after shock, transplantation, sepsis and vascular surgery. It is unlikely to happen in isolation and frequently occurs in critically ill patients. Published mortality rates for intensive care unit patients with AKI are between 30 and 70%. When kidney injury is extensive, its intrinsic repair programs are insufficient. As there is such a high mortality rate and financial burden coupled with limited effective treatments against AKI, the use of SC therapy to repair such an injury is an exciting alternative.

In human studies, it has been shown that extrarenal cells can participate in renal tubule regeneration (Gupta *et al.* 2002), which supports findings seen in injured livers and hearts after cell/organ transplants (Alison *et al.* 2000; Jackson *et al.* 2001; Orlic *et al.* 2001). Despite emerging clinical evidence that these SCs can improve a variety of inflammatory disorders, benefits are either minor or transitory (Lanzoni *et al.* 2008; Dai and Kloner 2011). This has been partially explained by low numbers of HSCs actually adhering within the local microcirculation of injured organs. Therefore, when delivered by the preferred

systemic route, poor homing and a subsequent low efficiency of tissue engraftment occur, processes that are essential for HSCs to mediate repair (Karp and Leng Teo 2009).

If SCs do hold promise in the context of regenerative diseases or the repair of renal injury, what is clear is that strategies to enhance, inhibit or modulate HSC migration is of utmost importance. However, there is a lack of published literature that has addressed this and the molecular adhesive events that govern their recruitment within injured non-BM sites are currently unknown. It is possible that BMSCs utilise the same classes of adhesion molecules used by mature leukocytes for recruitment to inflamed sites. As most renal repair occurs during the first week post-injury, this research therefore primarily focuses on the molecular adhesive mechanisms that govern the recruitment of HSCs to sites of renal injury immediately after HSC infusion. This study will also determine what local inflammatory factors may be responsible in mediating HSC adhesion and whether once present within the injured tissues, HSCs are beneficial for treating renal IR injury. Understanding the recruitment mechanisms and enhancing this process will hopefully prevent non-specific HSC adhesion to extrarenal organs and potentially lead to a more rapid, efficient and longer lasting tissue repair.

1.7 Aims and Hypotheses

The major hypothesis for this thesis is that HSCs home to the injured kidney after IR injury via organ specific recruitment mechanisms, and that HSC adhesion can be modulated.

More specifically, the aims and hypotheses of this research were as follows:

1. Aim: Develop a viable model of murine AKI for intravital monitoring of labelled HSC trafficking through the injured microvasculature *in vivo*
2. Hypothesis: Renal IR injury promotes HSC adhesion to the injured microvasculature *in vitro* and *in vivo*
3. Hypothesis: Blockade of adhesion molecules would decrease HSC recruitment in the injured mouse *in vivo*
4. Hypothesis: The injured kidney releases inflammatory substances that can enhance HSC adhesion both *in vitro* and *in vivo*
5. Aim: Develop an extensive model of murine AKI for visualisation of endogenously labelled platelets and neutrophils in the peritubular capillaries *in vivo*
6. Hypothesis: HSC recruitment produces anti-inflammatory effects that reduce both platelet microthrombi and neutrophil numbers and this attenuates injury

Chapter 2



Materials and Methods

2 Materials and Methods

2.1 Materials

2.1.1 Antibodies

Various antibodies were used within this study and these are outlined in the below table.

Exp ^t	Antibody	Conj	Clone	Origin	Target	Company	Conc ⁿ
Flow cytometry and Clustering	IgG control	FITC	IgG2b	Rat	Mouse	eBioscience	1:50
	IgG control	PE	IgG2b	Rat	Mouse	eBioscience	1:50
	Anti-CD18	FITC	GAME-46	Rat	Mouse	Santa Cruz	1:50
	Anti-CD44	PE	IM7	Rat	Mouse	eBioscience	1:50
	Anti-CD49d	FITC	MFR4.B	Rat	Mouse	eBioscience	1:50
	Anti-CXCR2	PE	242216	Rat	Mouse	R&D sys.	1:16
	Anti-CXCR4	FITC	2B11	Rat	Mouse	eBioscience	1:50
Immuno	LE-AF IgG control	N/A	IgG2a	Rat	Mouse	Cambridge Bioscience	1:50
	Anti-CD42b	N/A	Xia.B2	Rat	Mouse	EmFret	1:50
	IgG control	488	-	Goat	Rat	Life Tech.	1:50
HSC blocking	LE-AF IgG	N/A	IgG2b	Rat	Mouse	Cambridge Bioscience	80 µg/ml
	LE-AF Anti-CD18	N/A	GAME-46	Rat	Mouse	BD Pharm.	80 µg/ml
	LE-AF Anti-CD44	N/A	IM7	Rat	Mouse	Cambridge Bioscience	80 µg/ml
	LE-AF Anti-CD49d	N/A	R1-2	Rat	Mouse	Cambridge Bioscience	80 µg/ml
	Anti-CXCR2	N/A	242216	Rat	Mouse	R&D sys.	50 µg/ml
	Anti-CXCR4	N/A	2B11	Rat	Mouse	R&D sys.	40 µg/ml
	LE-AF IgG	N/A	IgG2b	Rat	Mouse	Cambridge Bioscience	Varies depending on treatment
In vivo blocking	Hyaluronidase	N/A	Type VI-S	Bovine	Mouse	Sigma	10mg (enzymatic activity of 3000-15000 units per mg)
	LE-AF Anti-CD44	N/A	IM7	Rat	Mouse	Cambridge Bioscience	100µg
	LE-AF Anti-CD104	N/A	429/MVCAM.A	Rat	Mouse	Cambridge Bioscience	70µg
	Anti-Ly6G	660	RB6-8C5	Rat	Mouse	eBioscience	60 µg
	Anti-CD41	N/A	MWReg30	Rat	Mouse	BD Pharm	40 µg
	IgG	488	-	Goat	Rat	Life Tech.	80 µg
	IgG	568	-	Goat	Rat	Life Tech.	80 µg
	IgG	568	-	Goat	Rat	Life Tech.	80 µg

2.1.2 Common Materials

A number of materials were used repeatedly in this thesis and these are presented in the below table for clarity.

	Abbreviation	Company	Location
Acetone	-	Fisher Scientific	Leicestershire, UK
Bovine Serum Albumin	BSA	Sigma	Poole, UK
5'6-carboxyfluorescein diacetate succinimidyl ester	CFSE	Molecular Probes (Life technologies)	Paisley, UK
D-Valine MEM	-	Promocell	UK
Dimethyl Sulfoxide	DMSO	Sigma	Poole, UK
Hanks' Balanced Salt Solution	HBSS	Sigma	Poole, UK
Heat inactivated Fetal Bovine Serum	FBS	Life Technologies	Paisley, UK
Gelatin (Type I from porcine skin)	-	Sigma	Poole, UK
Glutaraldehyde		Sigma	Poole, UK
Interleukin 1 beta	IL-1 β	Peprtech	London, UK
Keratinocyte Chemokine	KC	Peprtech	London, UK
Ketamine	-	Amersham Bioscience and Upjohn Ltd	Buckinghamshire, UK
L-Glucose	-	Sigma	Poole, UK
L-Glutamine (Glutamax™)	-	PAA Labs	Somerset, UK
Pencillin	-	PAA Labs	Somerset, UK
Phosphate Buffered Saline	PBS	Life Technologies	Paisley, UK
Propidium Iodide	PI	Sigma	Poole, UK
Sodium ethylene tetraacetic acid	Na.EDTA	Sigma	Poole, UK
Sodium Chloride	NaCl	Sigma	Poole, UK
Stem-Pro 34-SFM	-	Life Technologies	Paisley, UK
Streptomycin	-	Life Technologies	Paisley, UK
Stromal Derived Factor 1 alpha	SDF-1 α	Peprtech	London, UK
Trypsin-EDTA	-	Life Technologies	Paisley, UK
Tumour Necrosis Factor 1 alpha	TNF- α	Peprtech	London, UK
Xylazine Hydrochloride	-	Millpledge Pharmaceuticals	Nottinghamshire, UK

2.2 Cell Culture, Cell Isolation and Cell and Supernatant Preparation

2.2.1 Cell Counting

For all cell counting, a standard Neubauer haemocytometer was used and Trypan Blue (9:1) was added to exclude dead cells. 90 μ L of Trypan Blue was added to 10 μ L of cell suspension and approximately 20 μ L of the resulting suspension was viewed using a

haemocytometer under a x10 objective. The number of cells that had not taken up the blue stain (viable cells) were counted in the four grid $1 \times 1\text{mm}^2$ fields. The average count from the four grids was calculated and multiplied by 1×10^5 to yield the number of cells per ml.

2.2.2 Haematopoietic Progenitor Cell-5 and -7 (HPC-5 and HPC-7)

Intravital studies monitoring HSC trafficking to sites of injury have been limited due to difficulties in isolating sufficient numbers for detection following systemic infusion. We have found that approximately 5000 primary murine HSCs, defined as being c-Kit⁺, Sca-1⁺ and lineage negative (Lin⁻; KSL cells), can be obtained from one adult mouse. This is too low for intravital or even *in vitro* adhesion assays – pooling cells from mice would require an unacceptable number of donor mice to be culled for individual intravital or endothelial experiments. Therefore, an adult and embryonic murine HSPC line, HPC-5 and HPC-7 respectively, were used in this study (gift from Professor L Carlsson, Umea University, Sweden). HPC-5 are an immortalised adult murine SC line, created from adult BM genetic modification (Pinto do *et al.* 1998). HPC-7 are an immortalised embryonic SC line, but they were generated by transfection with the LIM-Homeobox gene, Lhx2 into a lethally irradiated mouse (Pinto do *et al.* 2001). Crucially, HSCs generated in this way are extremely similar to primary HSCs: they can fully reconstitute haematopoiesis when injected into a lethally irradiated host (Pinto do *et al.* 2002) and display many of the critical characteristics of primary HSCs, including expression of c-kit and Sca-1 on their surface and being and lineage negative. Furthermore, HPC-5 and HPC-7 express surface adhesion molecules known to be expressed on primary HSCs and we have previously

used them to model hepatic and intestinal recruitment intravitaly (Kavanagh *et al.* 2010; Kavanagh *et al.* 2012). HPC-5 and HPC-7 were maintained in Stem Pro 34 SFM supplemented with the manufacturer's supplement, L-glutamine, penicillin and streptomycin. In addition to stem cell factor (SCF), HPC-5 cells are dependent on IL-6 and were cultured in the presence of 10ng/ml murine IL-6. Both progenitor cells were maintained daily at a density of $1.0\text{-}1.2 \times 10^6$ cells/ml in Stem-Pro media with the above additives.

2.2.3 Culture of Immortalised Murine Renal Endothelium

Isolation of primary murine endothelial cells (ECs) is typically very difficult and requires elaborate time consuming purification techniques (Marelli-Berg *et al.* 2000). Therefore, immortalised murine renal ECs (a gift from Dr. J. Steven Alexander, LSU-HSC, USA) were used to conduct *in vitro* static adhesion assays. These renal ECs were maintained in growth media at 33°C: the growth media consists of D-Valine MEM supplemented with 10% FBS, 50U/ml penicillin, 50U/ml streptomycin, 2mM L-Glutamine, 1% vitamin mix and 10% interferon- γ . Once cells had grown to confluence, cells were enzymatically dissociated using Trypsin-EDTA, washed in complete media and then split 1 in 3. For static adhesion assays, a confluent flask of renal EC was enzymatically dissociated using Trypsin-EDTA, washed, and then one third resuspended in experiment medium. 1.5ml of this resulting cell suspension was then added to each well of a 24 well plate and incubated at 37°C ready for experimentation once confluent.

2.2.4 CFSE-Labeling of Cells

Cells were centrifuged (1200rpm, RT, 5 minutes) and 2ml of pre-warmed PBS with 0.1% albumin in PBS (PBSA) was added before centrifuging again. The cell pellet was resuspended in 2ml of PBSA and an additional 2ml of 10 μ M CFDA-SE solution was added, giving a final staining concentration of 5 μ M; this was then incubated for 15 minutes at 37°C in the dark. Cell labelling is achieved by using CFDA-SE, which is a non-fluorescent, cell-permeable fluorescein derivative; this is modified inside cells by endogenous esterases, which causes the molecule to become fluorescent. Modification by these intracellular enzymes also renders the modified molecule cell impermeant. Stock CFDA-SE was diluted to 10mM in DMSO and aliquoted for future use. After the 15 minute incubation, the reaction was hydrated with 6ml of the appropriate cell medium and was then washed twice by centrifugation (1200rpm, room temperature (RT), 5 minutes). Stained cells were then allowed 5 minutes to allow any non-reacted CFDA-SE to diffuse out of cells. Cells underwent a final wash in medium before being suspending at the appropriate concentration in culture medium.

2.2.5 Cell Adhesion Molecule Blocking

To identify critical surface adhesion molecules involved in the recruitment of HSCs to the kidney, HPC-7 were pre-treated with 0.1% PBSA containing 80 μ g/ml of the blocking antibody. Low endotoxin azide-free (LE-AF) antibodies, including IgG2b, anti-CD18, anti-CD44 and anti-CD49d, were used to block the corresponding adhesion molecules function on the HPC-7 surface. FACS studies have already been performed within our lab in order

to ensure 80µg/ml is an adequate dose to ensure complete blockade of the respective antigen (Kavanagh 2009). Anti-CXCR2 and anti-CXCR4 function blocking monoclonal antibodies were also used to block chemokine receptor activity on HPC-7 at concentrations of 50µg/ml and 40µg/ml respectively, as suggested by the supplier. For some studies, animals received a bolus injection of anti-CD44, anti-VCAM-1 or hyaluronidase to understand if these endothelial counter-ligands are responsible for HSC adhesion to the injured kidney *in vivo*. Hyaluronidase type VI-S from bovine testes (Sigma-Aldrich, UK) has an enzymatic activity of 3000-15000 units per mg and is relatively pure in comparison to an U.S.P standard. Control animals received an intra-arterial bolus of the corresponding dose of rat IgG or PBS. Animals were surgically prepared as described in section 2.3.2 and immediately following ischaemia, the bolus injection of antibody, enzyme or PBS in 100µl was administered via the carotid artery. *In vivo* antibody or enzyme doses were consistent with concentrations published in the literature using the same antibody or enzyme (John and Crispe 2004; Belcher *et al.* 2005; Orito *et al.* 2007).

2.2.6 HPC-7 and Kidney Pre-treatments with Inflammatory Factors

Recombinant murine IL-1β, KC, SDF-1α, TNF-α, plus a combination of KC and SDF-1α were used to pre-treat HPC-7 or the exposed sham kidney. Cytokines and chemokines were made at a stock concentration of 10µg/ml in PBS containing 0.1% BSA. Cytokines and chemokines were used experimentally at 25ng/ml, 50ng/ml and 125ng/ml for HPC-7 pre-treatments and were made up in Stem Pro medium. For topical applications, 2ml of 200ng/ml of KC or SDF-1α was used to treat a healthy kidney and was made up in PBS.

1mL of fresh 200ng/ml chemokine was added to the bath at 1 hour, 2 hour and 3 hour time points to replace the media lost by evaporation or by absorption by the kidney. H₂O₂ was also used to pre-treat HPC-7 at 100μM for 5 minutes or 1 hour; this was made up in Stem Pro medium. After HPC-7 pre-treatment with cytokines, chemokines or H₂O₂, HPC-7 were washed, centrifuged (1200rpm, RT, 5 minutes) and were resuspended in Stem Pro medium. H₂O₂ concentration of 100μM was used due to previous experimentation showing that this concentration did not cause HPC-7 apoptosis and enhanced their adhesion to the IR injured gut (Kavanagh *et al.* 2012).

2.3 Monitoring HSC Trafficking *in vivo* using Intravital Microscopy

2.3.1 Animals

Animal experiments were completed with prior approval of the local ethics committee and the United Kingdom Home Office, in accordance with the Animal Scientific Procedures Act of 1986 under Project Licence 40/3336 (Dr. Neena Kalia). Male 8-12 weeks old C57Bl/6 mice were obtained from Harlan, UK. All animals had *ad libitum* access to food and water. The 3 R's of animal research, replacement, reduction and refinement, were heavily thought of during this work: endothelial assays were utilised during preliminary investigations into HSC adhesion to replace *in vivo* work; a trusted HSPC line to understand their trafficking mechanisms replaced the use of many donor animals needed for primary HSC sorting and this in turn reduced the number of animals needed for this project; animals were closely monitored for temperature and respiration

changes in order to refine and improve the way in which the animal experimentation is carried out. Something that has been promoted very recently is the use of power calculations: these were not used in this body of work but would have been useful in the initial design of in vivo experiments. Power calculations calculate the sample size required to accept or reject the hypothesis, giving greater validity to the results that are attained; this therefore give the scientist an indication of how likely the hypothesis is to be accepted and if it is ethically sound and scientifically responsible to continue with such a hypothesis. When performed correctly, these calculations could reduce the number of animals used in experiments. I would implore scientists to investigate the use of power calculations for continued animal work.

2.3.2 Surgical Preparation

Anaesthesia was induced by intra-peritoneal administration of ketamine (100 mg/kg Vetalar) and xylazine hydrochloride (10 mg/kg) delivered in 0.9% saline. Maintenance of anaesthesia was delivered intra-peritonally as not to disrupt blood volume. These mice underwent a tracheostomy to assist breathing and carotid artery cannulation with polyethylene portex tubing (Smiths Medical, Hythe, UK) to assist breathing and to allow administration of labelled cells, antibodies or FITC-BSA. A midline laparotomy was performed by cutting along the *linea alba*, an avascular fibrous structure found between the left and right rectus abdominis muscles, to prevent any bleeding. The intestines were then exteriorised and kept moist so that the left kidney could be seen.

2.3.3 Induction of Renal Ischaemia-Reperfusion Injury

Following a midline laparotomy, unilateral ischaemia was induced by the application of an atraumatic vascular clamp to the left renal pedicle for 45 minutes. The clamp was then removed and the left kidney was allowed to reperfuse for 60 minutes, as this has been shown to produce a significant amount of damage (Mashiach *et al.* 1998). During the last 30 minutes of reperfusion the left kidney was exteriorised for intravital monitoring. To exteriorise the left kidney, a flank laparotomy was performed and a cautery was used to remove the peritoneum. The left kidney was always imaged due to the fact it is easier to exteriorise, due to no large organs (i.e. liver) causing any obstructions and it also has a longer renal pedicle due to the extended left renal vein.

2.3.4 Intravital Microscopy Kidney Preparation to Understand HSC Trafficking

This imaging modality is frequently used to visualise the microcirculation of solid organs. However, using intravital microscopy for imaging the renal microcirculation in mice is challenging and as a result, there are limited studies of this nature. This is primarily due to the difficulties associated with exteriorising the mouse kidney, minimizing the effects of respiratory movements and having the correct optics and cameras to get high resolution, dynamic, real-time images. We have established several murine renal preparations that allow continuous intravital monitoring of the renal microcirculation *in vivo*. Firstly we used an upright fluorescent intravital microscope to view HPC-7 recruitment to the kidney (**Figure 2.1.A-B**). However, the most recent preparation gives

the clearest view of the superficial peritubular capillaries with minimal respiratory movement (**Figure 2.1.C-D**). The initial intravital prep consisted of the kidney was gently teased out using a cotton bud, removing the renal capsule and being secured by its peritoneal fat onto a bed of agar. The newer prep involved making a flank incision and then using the cautery to remove peritoneum to show the kidney. The kidney was popped out using gentle manipulation, the kidney capsule was removed using forceps and then the mouse was placed on its side allowing the mouse body weight to gently press the kidney to the petri-dish creating a flat surface to image; this was the prep that was then used throughout the whole of my experiments in the rest of results chapters 3, 4 and 5. Animals undergoing sham procedures during all preps were exposed to the same surgical manipulation of the kidney except the clamp wasn't applied.

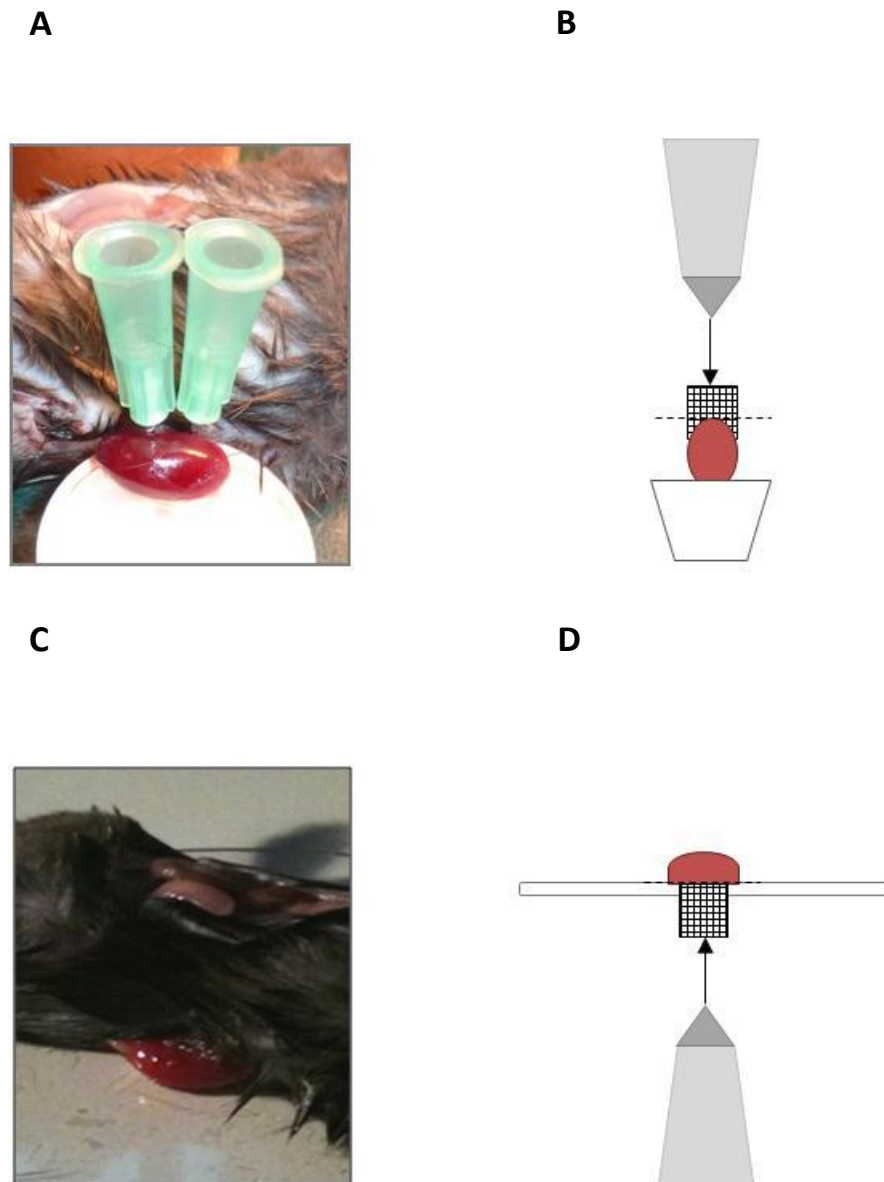


Figure 2.1. Kidney prep using the upright (A, B) and the inverted (C, D) microscope. (A) The initial prep used on the upright microscope involved visualising the left kidney due to the vessels being slightly longer on this side. After a flank incision, the kidney is manipulated outside the body and is pinned either side of the renal pedicle into a bed of agar. (B) The kidney is viewed from above and this microscope gets a clear image by focusing its field of view onto the flattest part of the kidney. However the kidney hasn't got a complete field of view that is flat so the image loses clarity towards the edges. (C) After IR/sham injury has occurred, a flank laparotomy incision is made with the cautery to expose the kidney. The kidney is then manipulated out of the hole with a cotton bud to prevent any further injury and the capsule is carefully removed. (D) The mouse is lies on its left side on a petri-dish causing the kidney to become pressed against the flat edge, giving a larger flat area to view without losing sharpness.

2.3.5 Quantification of Cell Trafficking *in vivo*

Using the x10 objective, one renal field of view ($413\mu\text{m} \times 308\mu\text{m}$) towards the renal lower pole was focussed and a 10 second digital video at 200ms was taken as a control before the administration of cells. 2×10^6 CFSE-labelled HPC-5 or HPC-7 were administered through the carotid as a $100\mu\text{l}$ bolus at 60 minute post-reperfusion. 1 minute recordings were taken from the same pre-selected field of view every 5 minutes until 120 minutes post-reperfusion and then every 10 minutes for the following 40 minutes (i.e. until 160 minutes post-reperfusion). At the end of each intravital experiment, five fields of view were taken of the left kidney to ensure the events taking place in the recorded pre-selected field of view were representative of the whole organ. All recordings were stored digitally using Slidebook software (Intelligent Imaging Innovations, Denver, US) and analysed offline. Quantification of cell trafficking using an intravital set-up has been well documented within the area of microcirculatory research (Lim *et al.* 2002; Au *et al.* 2008; Kavanagh *et al.* 2010). Rolling cells in the peritubular capillaries are extremely rare to see in the renal microcirculation and so only adherent and free flowing cells were counted. Adherent cells were those that had been still/non-moving for 30 seconds or more; free-flowing ones were non-static or static for less than 30 seconds. Cells that entered the monitored field of view after the 30 second recording were classed as free-flowing, as it couldn't be certain if they remained adherent beyond 30 seconds. Adherent cells throughout all focus planes were counted. Results are expressed as mean adherent or mean free flowing cells per field (CPF) per minute at each time point \pm SEM. The mean speed ($\mu\text{m/s}$) of cells trafficking through the renal microvasculature was also calculated using Slidebook imaging software.

2.3.6 Quantification of HSC Recruitment in Major Organs *ex vivo*

After completed intravital experiments, animals were culled and the left injured and right non-injured contralateral kidney were removed and observed *ex vivo* for labelled HSC recruitment using an Olympus IX81 inverted microscope. IR and CL kidneys were washed twice with 0.9% saline to remove traces of blood and were placed on a petri dish so that the flat vascular surface could be visualised. The initial field was blindly chosen in the bottom right hand corner of the tissue and the subsequent five fields of view were selected to give complete organ coverage (**Figure 2.2**). Fluorescent cells were counted manually using in-house blinded counting software (courtesy of Dr. Dean Kavanagh).

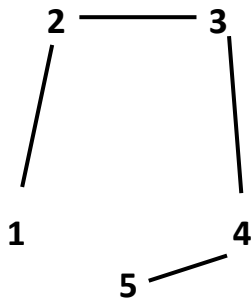


Figure 2.2. Pre-determined pattern for counting fields of view on organs. This pattern was used to count adhering cells in different organs during *ex vivo* analysis. The first point was always positioned towards the right bottom

2.3.7 Blood Flow Measurements

We combined intravital microscopy with laser speckle microscopy to calculate renal blood flow during injury and sham experiments. The Moor FLPI laser speckle camera (Moor Instruments, UK) was used to determine renal surface blood flow within exposed IR injured and sham kidneys as described previously (Holstein-Rathlou *et al.* 2011). When

the laser is targeted on the tissue it produces a speckle pattern; continued movement, like that from blood flow, produces a more intensely fluctuating pattern. High levels of flow corresponded with a white to red colour; areas of lower flow were depicted with a blue to purple colour. Recordings were made every 15 minutes throughout the ischaemic and reperfusion phases, using the same region of interest, and an arbitrary unit of flux was obtained.

2.4 Monitoring Inflammatory Cells using Confocal Intravital Microscopy

2.4.1 Intravital Preparations

To monitor endogenous inflammatory cells during IR injury, I decided to use the new confocal microscope that is connected to the upright Olympus microscope, as it has better resolution. A new prep was designed to provide a better image than the initial upright prep used during results chapter 1; this involved exteriorising the kidney through the flank incision like before, but putting the mouse on its side with the kidney resting on the petri dish creating a flat surface in which to image (**Figure 2.3.A-B**).

2.4.2 Surgical Preparation

Mice were surgically prepared as previously described. Maintenance of anaesthesia was maintained by intra-peritoneal administration of ketamine (100 mg/kg) and xylazine hydrochloride (10 mg/kg) was delivered in 0.9% saline, as not to disrupt blood volume. These mice underwent a tracheotomy to assist breathing and carotid artery cannulation

with polyethylene portex tubing (Smiths Medical, Hythe, UK). Endogenous platelets were labelled by adding 40µl Alexa Fluor 594 with 20µl rat anti-murine CD41 (GPIIb) antibody and this was made up to 100µl with saline and then injected via the carotid cannula. To visualise neutrophils *in vivo*, 30µl of pre-conjugated anti-mouse Ly-6G eFluor® 660 was made up to 100µl with saline and also injected via the carotid cannula. Antibodies circulated for 5 minutes before further surgery was performed: a midline laparotomy was performed by cutting along the *linea alba*, an avascular fibrous structure found between the left and right *rectus abdominis* muscles, to prevent any bleeding. The intestines were then exteriorised and kept moist so that the left kidney could be seen and clamped for 45 minutes like before and then allowed to reperfuse for 6 hours. HPC-7 were introduced into the IR injured animal at 1 hour reperfusion. Five fields of view were taken at 1 hour, 4 hours and 6 hours reperfusion and the number of platelet microthrombi and neutrophils, along with the size and intensity of each platelet microthrombi, were quantified using Slidebook analysis software and ImageJ.

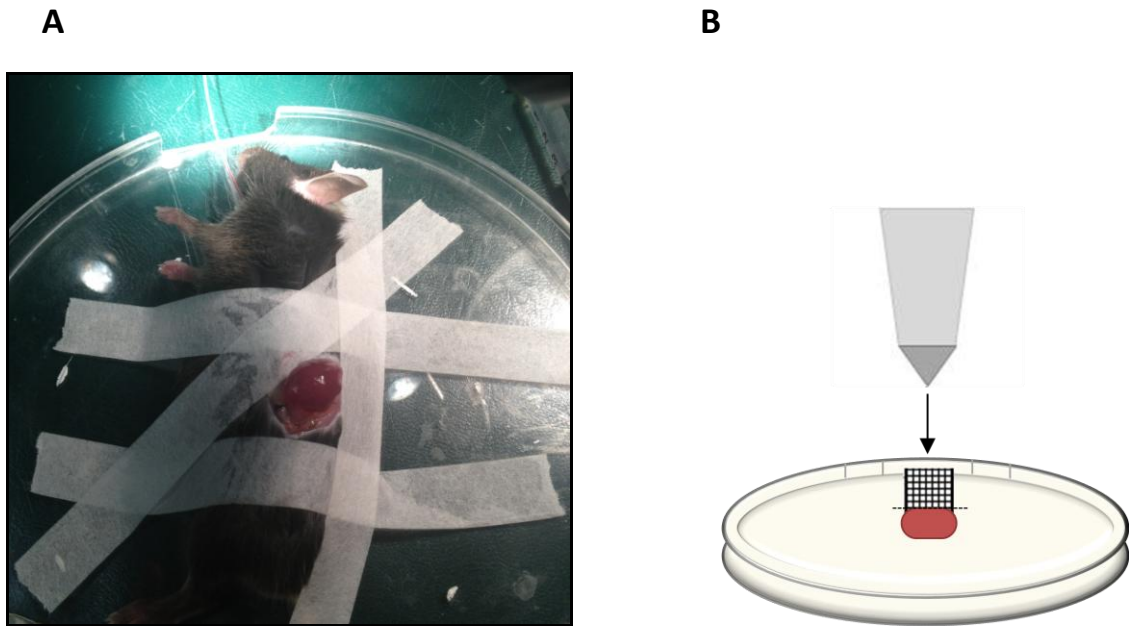


Figure 2.3. Monitoring inflammatory cell recruitment after renal IR injury using the confocal upright intravital microscope. A new kidney intravital preparation was designed for use on the confocal upright intravital microscope. This involved using a larger petri-dish with holes cut out for air holes and carotid tubing. The mouse was prepared as before on the inverted prep (**Figure 2.1.C-D**). Briefly, the trachea and carotid are cannulated to assist breathing and administration of antibodies and cells. After IR injury or sham surgery, the left kidney is exteriorised through a flank incision and the capsule is carefully removed. The mouse is placed on a large petri-dish and secured in place with surgical tape. The lid of the petri-dish is placed on top so that the kidney light touches the lid providing a flat surface in which to image (**Figure 2.3.A-B**).

2.5 Quantification of Injury

2.5.1 FITC-BSA

During IR injury the integrity of the vessel is lost therefore giving vascular leakage. Therefore to measure the integrity of the vessels, a fluorescent molecule can be introduced and this allows easy visualisation of blood flow and if any injury is present (Kalia *et al.* 2002). 200µl of FITC-conjugated bovine serum albumin (FITC-BSA) was injected intra-arterially. FITC-BSA was made by mixing 10% FITC on celite, BSA and 10ml of bicarbonate pH 9.0 buffer overnight at 4°C. Afterwards this was centrifuged (12 000 rpm, 4°C, 10 minutes) and any conjugated or unconjugated BSA was separated by dialysis (12,000MW cut off; Spectrum Laboratories, CA, USA). Prepared FITC-BSA was frozen and stored until use in 1ml eppendorfs.

2.5.2 Creatinine and Urea Levels

To biochemically confirm that renal injury has occurred, blood samples were obtained from mice subject to sham or IR procedures at 6 hours reperfusion. Urea is a waste product that is normally excreted in the urine, but during kidney malfunction and disease is it retained within the blood. Serum creatinine is a well known indirect marker of GFR and is widely used to assess kidney function. Using a 26G needle containing 100µl of acid citrate dextrose (ACD) to prevent clot formation, blood was removed via descending aorta puncture and then centrifuged (1000g, 4°C, 10 minutes). The supernatant (serum) was then aliquoted and stored at -80°C. Samples were analysed by the Pathology

department at the Queen Elizabeth hospital, Birmingham, UK, with increased levels of serum creatinine and urea being directly proportional to the extent of renal injury.

2.6 Techniques to Quantify Cell Adhesion *in vitro*

2.6.1 Frozen Tissue Stamper-Woodruff Assay

The Stamper-Woodruff static adhesion assay was used to examine HPC-5 and HPC-7 cell adhesion to snap frozen murine kidney sections (Stamper and Woodruff 1976). C57BL/6 mice were subjected to renal IR injury or sham surgery as previously described in section 2.3. Ischaemia was induced for 45 minutes and then reperfused for 120 minutes. After reperfusion, the left injured, right non-injured contralateral or sham kidneys were removed, snap frozen in liquid nitrogen, and stored at -80°C until ready for sectioning. Cryo-M-bed (Bright Instruments, Cambridge, UK) was used to embed the kidneys on a cork disc and 10µm sections were cut using a Bright Instruments cryostat and mounted on X-tra™ adhesive microscope slides (Surgipath, Peterborough, UK). These slides were then fixed for 20 minutes using acetone and then stored at -20°C until use. Two kidney sections were put onto one slide, carefully placed so that they had only touched the blade once, so it didn't affect the tissues adhesive capabilities (Mann et al., 2009). To prepare the kidney sections for the assay, slides were fixed in 100% acetone for 5 minutes, washed in PBS and sections were encircled using a wax immunology pen (Immedge; Vector Laboratories, Peterborough, UK). HPC-5 and HPC-7 were labelled with CFDA-SE as previously described. Some HPC-7 were pre-treated with IL-1β, KC, SDF-1α or

TNF- α (25ng/ml in complete Stem Pro 34 SFM) for 5 minutes or for 30 minutes with media conditioned by an injured or sham kidney. After pre-treatments, 5×10^4 CFSE-labelled HPC-7 in 100 μ l were added to each section and these slides were incubated on a humidified tray on a laboratory rocker for 20 minutes to allow any HSC adhesion to occur. Slides were then fixed for 5 minutes in 100% acetone and subsequently washed three times in PBS. Slides were dried and coverslips were applied using Gel Mount aqueous mounting medium (Sigma, UK). Once dry, slides were analysed using a Zeiss Axiovert Microscope (Carl Zeiss, Herefordshire, UK). Five fields of view were selected from each tissue sections using a set field pattern, as previously described (**Figure 2.2**). Fluorescent cells were counted manually using blinded counting software Counter.exe; this software was developed by Dr. Dean Kavanagh, Birmingham, UK. Results are expressed as mean adhesion per field \pm SEM.

2.6.2 Immobilised Counter-Ligand Adhesion Assay

96-well plates (Nunc, Rochester, USA) were coated with 50 μ l of recombinant murine (rm) ICAM-1, rmVCAM-1 or 0.5mg/ml rmHA for 1 hour. Wells were then washed, blocked using 10mg/ml heat-denatured BSA. HPC-7 were blocked with LE-AF CD16/32 function-blocking antibody for 30 minutes before pre-treating HPC-7 for 5 minutes at 37°C with 25ng/ml of IL-1 β , KC, SDF-1 α or TNF- α , made up in complete Stem Pro 34 SFM. Pre-treated HPC-7 were subsequently washed and resuspended in 100 μ l of complete Stem-Pro 34 SFM and exposed to the immobilised proteins for 20 minutes at 37°C. Wells were washed thoroughly with PBS to remove any unbound cells. Adherent HPC-7 were fixed with 2% glutaraldehyde at RT for 15 minutes. Wells were washed and 100 μ l PBS was

added for imaging adherent cells on an inverted Olympus IX81 microscope. Five fields of view were selected from each well using a set field pattern as previously described (**Figure 2.2**). HPC-7 were counted manually using blinded counting software, Counter.exe. Results are expressed as mean adhesion per field \pm SEM.

2.6.3 Renal Endothelial Cell Static Adhesion Assay

The immortalised murine renal ECs (gift from Dr. J. Steven Alexander, LSU-HSC, USA) were cultured to confluence in gelatin-coated wells in a 24 well plate (BD Biosciences). At confluence, monolayers were treated for 4 hours with 100ng/ml TNF- α . Following washing with 0.1% PBSA, 1×10^5 HPC-7 cells were added for 20 minutes. Some HPC-7 were pre-treated with IL-1 β , KC, SDF-1 α or TNF- α (25ng/ml in complete Stem Pro 34 SFM) for 5 minutes or for 30 minutes with media conditioned by an injured or sham kidney. Wells were washed with PBS and fixed with 2% glutaraldehyde in PBS for 15 minutes at RT. Five fields of view were selected from each tissue sections using a set field pattern (**Figure 2.2**) and were imaged using fluorescent microscopy (Olympus IX81; Olympus, UK). Fluorescent cells were counted manually using blinded counting software, Counter.exe. Results are expressed as mean adhesion per field \pm SEM.

2.6.4 Immunohistochemistry on 6 hour Reperfused Tissue Sections

After 6 hours reperfusion experiments, the left kidneys were removed and snap frozen in liquid nitrogen and stored at -80°C ready for sectioning. As stated above, Cryo-M-bed was used to embed the kidneys on a cork disc and 10 μ m sections were cut using a Bright

Instruments cryostat and mounted on X-tra™ adhesive microscope slides. These slides were then fixed for 20 minutes using acetone and then stored at -20°C until use. To prepare the kidney sections for the assay, slides were fixed in 100% acetone for 5 minutes, washed in PBS and sections were encircled using a wax immunology pen (Immedge; Vector Laboratories, Peterborough, UK). A primary antibody against CD42b and a control IgG antibody were applied to sections for 3 hours at 4°C. Slides were then thoroughly washed with PBS on a rocker and a secondary fluorescent antibody, Alexa 488, was applied to each section for 1 hour at 4°C. Any unbound fluorescent secondary antibody was thoroughly washed off with several PBS washes, followed by dehydration steps with acetone prior to applying coverslips using Gel Mount aqueous mounting medium (Sigma, UK). Once dry, slides were analysed using a Zeiss Axiovert Microscope (Carl Zeiss, Herefordshire, UK). Five fields of view were selected from each tissue sections using a set field pattern, as previously described (**Figure 2.2**). Fluorescent cells were counted manually using blinded counting software Counter.exe (downloaded gratis from <http://www.dephilon.com/Counter.exe>). This software was developed by Dr. Dean Kavanagh. Results are expressed as mean adhesion per field \pm SEM.

2.7 *In vitro* Techniques to Dissect the Effects of Injury and Cytokines on HPC-7

Adhesion and Free-Flowing Numbers

2.7.1 Conditioned Media Preparation from Injured and Sham Kidneys

In order to determine whether factors released from injured kidney could potentially modulate expression of adhesion molecules and therefore alter the amount of SC

adhesion. The kidney was clamped for 45 minutes and allowed to reperfuse for 60 minutes, or sham-operated, as previously described. The whole kidney was then removed and put into 2ml DMEM medium and incubated at 37°C for 24 hours from the point of reperfusion. Following incubation, the tissues were homogenised using an electronic tissue homogeniser (Power Gen 125; Fisher Scientific, Leicestershire, UK). The homogenate was then centrifuged at 1200rpm for 5min and the resulting supernatant was sterile filtered using a 0.22µm filter (Millipore, Watford, UK). This filtrate was then aliquotted and stored at -20°C until needed.

2.7.2 Determination of Protein Content within Conditioned Media

To determine whether there was a variation in the levels of proteins contained within the conditioned media from injured kidney compared to sham, a Coomassie stained gel was prepared. Conditioned media samples were removed and added to an equal volume of 2 x Laemmli sample buffer (Reducing: 20% glycerol, 10% β-mercaptoethanol, 4% SDS, 50mM tris, trace Brilliant Blue R; Non-reducing: 20% glycerol, 4% SDS, 50mM tris, trace Brilliant Blue R) for whole cell protein studies. SDS is an anionic detergent which denatures proteins and applies a negative charge to each protein in proportion to its mass. This was then boiled for 5 minutes at 100°C. Denatured proteins were separated by electrophoresis through sodium dodecyl sulphate polyacrylamide gels (10% and 15%). Pre-stained molecular weight markers (Bio-Rad, Hemel Hempstead, UK) were run alongside the samples. Following electrophoresis, the gels were stained with a Coomassie stain (10% acetic acid, 45% methanol, trace CBBR-250 stain) for 1 hour at

room temperature. This was then de-stained with several washes of de-stain (10% acetic acid, 45% methanol).

2.7.3 Adhesion Molecule Clustering

To examine the effects of KC and SDF-1 α on HPC-7 adhesion receptor clustering, HPC-7 were treated for 5 minutes with 25ng/ml KC and/or SDF-1 α at 37°C and then fixed with 2% glutaraldehyde for 15 minutes at room temperature. Following fixation, Fc receptors were blocked using CD16/32 antibody for 30 minutes. Cells were washed with warm 0.1% PBSA and centrifuged (1200rpm, RT, 5 minutes) and subsequently incubated with primary LE-AF anti-CD49d or LE-AF anti-CD44 for 1 hour on ice. Cells were washed and centrifuged again and then incubated with an Alexa Fluor® 488 goat anti-rat IgG secondary antibody for 30 minutes on ice. Cells were added to air-dried washed lysine coverslips for 1 hour. These cells were then mounted onto coverslips ready for imaging using confocal microscopy (Leica TCS-SP2) and 90 cells were imaged per treatment group. Areas of adhesion molecule clustering were identified using the “Find Maxima” plugin in ImageJ (NIH, NH, US), using a noise tolerance level of 20 to separate clusters from background.

2.7.4 Micropipette Assay

The deformability of HPC-7 following cyto/chemokine pre-treatment was assessed using a micropipette assay as previously described (Tse *et al.* 2005). HPC-7 were pre-treated with 25ng/ml of IL-1 β , LC, SDF-1 α and TNF- α for 5 minutes. Cells were then washed with

warm 0.1% PBSA and centrifuged (1200rpm, RT, 5 minutes) and fixed with 2% glutaraldehyde and were placed in a chamber made up of two coverslips separated by a U-shaped gasket and placed on a microscope stage held at 37°C. A micropipette with an internal diameter of approximately 5µm was introduced into the chamber from the open side, and a fixed aspiration pressure of 1000Pa (10cmH₂O) was applied by lowering a water reservoir connected to the pipette. Video recordings were made of HPC-7 aspirated into the pipette and the time taken to enter the pipette was measured offline. Typically 50 cells were tested in each sample.

2.8 FACS-Based Studies

2.8.1 HPC-7 Cell Surface

HPC-7 were analysed using flow cytometry to identify changes in cell surface expression of CD18, CD44, CD49d, CXCR2 and CXCR4. 1×10^6 HPC-7 were pre-treated for 5 minutes with PBS or 25ng/ml KC and/or SDF-1 α . Subsequently, cells were fixed with 5% formalin at RT for 20 minutes. HPC-7 were blocked with LE-AF CD16/32 function blocking antibody to reduce subsequent non-specific antibody binding. Cells were then incubated with fluorochrome-conjugated primary antibody for 30 minutes at 4°C. Cells were subsequently washed and resuspended in 300µl 0.1% PBSA and supplemented with 0.6µl of 0.5mg/ml propidium iodide (PI). PI is a red fluorescent nuclear and chromosome counterstain; it does not permeate live cells so can therefore be used to distinguish between live and dead cells from a general population. After cytokine and chemokines pre-treatment, the amount of F-actin was also quantified by using FITC-Phalloidin (Life

Technologies, UK). Phalloidin is isolated from the deadly *Amanita phalloides* mushroom and competes with the binding sites of F-actin, therefore giving an indication of the quantity of F-actin within a cell. Post pre-treatment, HPC-7 were washed and fixed with 5% formalin at RT for 20 minutes. Cells were washed, centrifuged (1200rpm, RT, 5 minutes) and then resuspended in 0.1% Triton X-100 in PBS for 5 minutes. After washing several times, HPC-7 were resuspended in 2 μ M of FITC-conjugated Phalloidin for 1 hour at RT and then washed and resuspended with 300 μ l 0.1% PBSA before analysis. Cells fluorescence was subsequently interrogated using flow cytometry on a BD FACSCalibur cytometer (Becton Dickinson, USA). Cell counting was terminated following the collection of 10 000 live events and data was analysed with CellQuest (Becton Dickinson, USA) by calculating the median average value from each repeat and then doing a one-tailed t-test (when only two groups) or a one-way ANOVA with Dunnett's post-tests (when more than two groups) on these values to determine any significance.

2.9 Statistics

Unpaired Student t-tests were used to make comparisons between two experimental groups for static adhesion assays, FACS data, changes in velocity and deformability. For more than two experimental groups, a one-way ANOVA followed by Dunnett's post-tests were carried out. For *in vivo* experiments, area-under-curve (AUC) calculations were performed to identify any significant differences between treatments. Analysis of free-flowing cells and blood flow data were analysed using a two-way ANOVA with Bonferroni post-tests. Values were considered significant when $p < 0.05$.

Chapter 3



Recruitment of HSCs Following IR Injury

3 Recruitment of HSCs by Ischaemia-Reperfusion Injury

3.1 Introduction and Hypotheses

3.1.1 Introduction

AKI is a common disease and with limited treatment options it continues to have a high rate of morbidity and mortality. IR injury is one of the most common causes of AKI and results in cell death, inflammation and altered cell metabolism. One of the main pathophysiological consequences post-renal IR injury is the loss of vascular endothelial cells (Molitoris and Sutton 2004). Li et al., (2010) showed that HSPCs incorporate into post-ischaemic renal tubules and begin to adopt a more endothelial phenotype; HSPCs express endothelial marker CD146 and lose expression of progenitor cell markers CD133 and CD45. Although these experiments show promising protective effects of HSCs, clinical success is poor and is partially attributed to small numbers of HSCs actually being recruited to the kidney. Experimental studies suggest that this is primarily due to non-specific entrapment of SCs within non-injured regions, such as the liver or lungs (Karp and Leng Teo 2009). The general consensus is that to improve the therapeutic efficacy of these cells, increasing their delivery to and recruitment within the injured kidney is key. Since systemic infusion of SCs is the preferred route of administration, capture of trafficking HSCs is dependent upon firm interactions with endothelial cells within the local renal microcirculation. The kinetics of HSC recruitment within the IR injured mouse kidney has not been previously investigated directly *in vivo*. This could be partly due to the difficulty associated with imaging the mouse kidney using intravital microscopy (IVM).

This chapter therefore aimed to establish an experimental model of acutely injured mouse kidney for intravital observations of HSC recruitment.

3.1.2 Aims and Hypotheses

For the work included in this chapter, the main aims and hypotheses were:

1. Aims: Establish a kidney preparation that will allow SC adhesion to be monitored using static adhesion assays *in vitro* and continuous IVM of the renal microcirculation in IR injured and sham / non-injured anaesthetised mice *in vivo*.
2. Hypothesis: HSC adhesion to snap frozen IR injured kidney sections would be significantly greater than that to snap frozen contralateral and sham non-injured kidney tissue.
3. Hypothesis: The number of HSCs adhering to the injured renal microcirculation *in vivo* will be significantly greater than that to the sham non-injured renal microvasculature.

3.2 Methods

The methods used in this chapter are described in detail in Chapter 2. Briefly, Stamper-Woodruff static adhesion assays were conducted to view the adhesion of the adult HSC line, HPC-5, and the embryonic HSC line, HPC-7, to injured renal tissue. Briefly, the left kidney was subjected to 45 minutes of ischaemia and 2 hours reperfusion. The left injured kidney, the right non-injured contralateral kidney (CL) and non-injured sham

kidneys were snap frozen in liquid nitrogen. HPC-5 and HPC-7 were stained with CFSE and then 1×10^5 cells were exposed to frozen tissue sections. For intravital *in vivo* studies, anaesthetised mice were surgically prepared by cannulation of the carotid artery and intubation of the trachea. Following laparotomy, the left renal pedicle was clamped to induce ischaemic injury as above. Thereafter, 2×10^6 CFSE labelled HPC-5 and HPC-7 were introduced via the carotid artery. Initially, the first kidney preparation was conducted on an upright IVM set-up. We subsequently utilised the inverted IVM as the exteriorised kidney was flatter, more still and subject to less manipulation; this therefore generated better quality images of circulating and adhesive labelled cells. On both the upright and inverted IVM renal preparations, one field of view was selected and monitored for 60 seconds every 5 minutes, until the final 30 minutes where the adhesion and free-flowing cells were monitored every 10 minutes. Observations were made for a total of 90 minutes. Cells were quantitated *in vivo* within the microcirculation as either adherent (static for ≤ 30 seconds) or free-flowing (visible in the field, but not adherent).

3.3 Results

3.3.1 HPC-5 adhesion is not increased to IR injured kidney tissue sections *in vitro*

Adhesion of HPC-5 did not increase to IR sections compared to tissue from sham animals. There were also no significant differences in HPC-5 adhesion between CL renal sections and the non-injured sham sections (Cells per field (CPF): IR: 7.40 ± 1.50 ; CL: 6.40 ± 1.81 ; Sham: 16.20 ± 5.29 ; **Figure 3.1.A-D**). Interestingly, less adhesion was observed on the IR and CL tissue sections in relation to sham sections.

3.3.2 HPC-7 adhesion is increased to IR injured kidney tissue sections *in vitro*

Significantly ($p < 0.05$) increased HPC-7 adhesion was observed *in vitro* to both injured and CL renal section taken from IR injured mice compared to sham tissue (CPF: IR: 42.00 ± 9.88 ; CL: 48.00 ± 4.81 ; Sham: 13.00 ± 5.00 ; **Figure 3.2.A**). Interestingly, adhesion on the IR injured kidney was very similar to that observed on the non-injured CL taken from the injured mice. Representative images of the tissue sections are shown and it's clear that the IR injured renal tissue architecture (**Figure 3.2.C**) looks more disturbed and damaged than the healthy tubular anatomy observed in the sham controls (**Figure 3.2.B**) and the non-injured contralateral kidney (**Figure 3.2.D**).

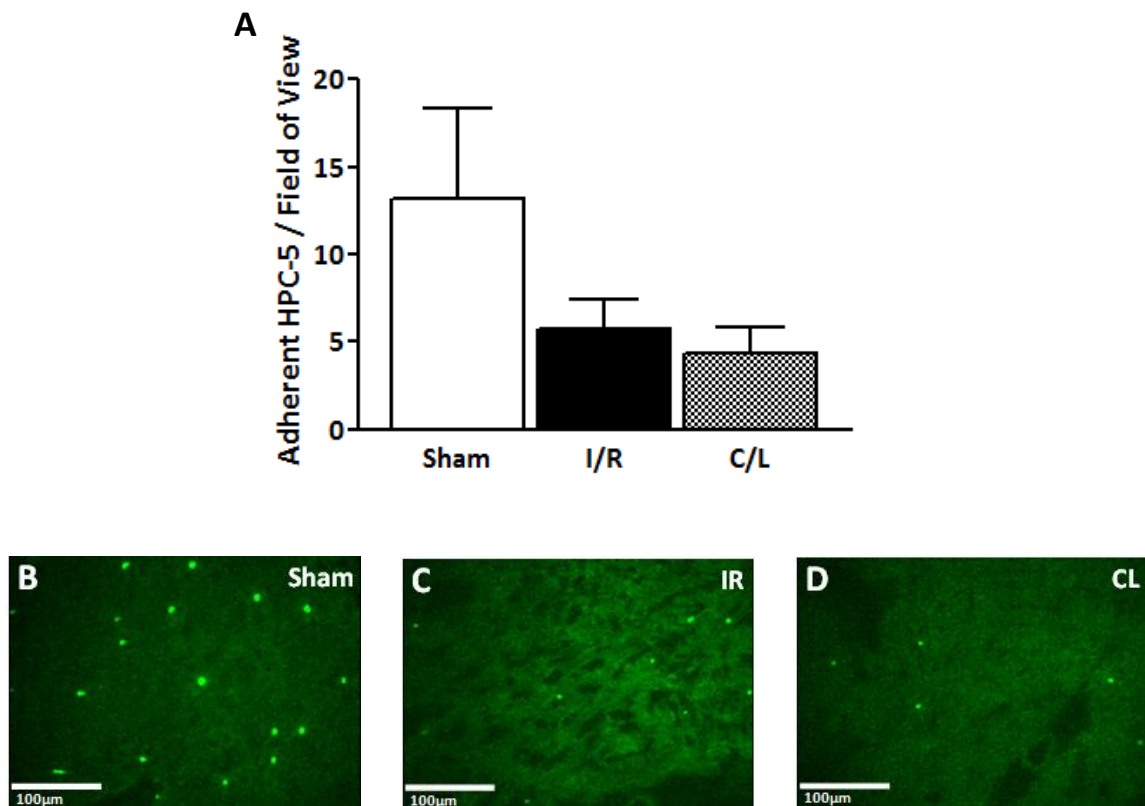


Figure 3.1. *HPC-5 do not adhere more so to IR injured kidney sections.* Kidney sections were isolated from sham and IR-treated animals and 1×10^5 CFSE-labelled HPC-5 were applied to each section for 20 minutes. HPC-5 adhesion was quantified from 5 fields of view per section using a pre-selected pattern and an average for each tissue section was calculated. There were no significant differences in HPC-5 to frozen sections of IR injured, non-injured CL tissue compared to controls. Results are shown in **panel A**. Representative images are shown of sham (**panel B**), non-injured contralateral (**panel C**) and IR injured (**panel D**) renal sections. Plots represent mean adhesion \pm SEM of at least 4 separate experiments; no significance using one-way ANOVA and Dunnett's post-test.

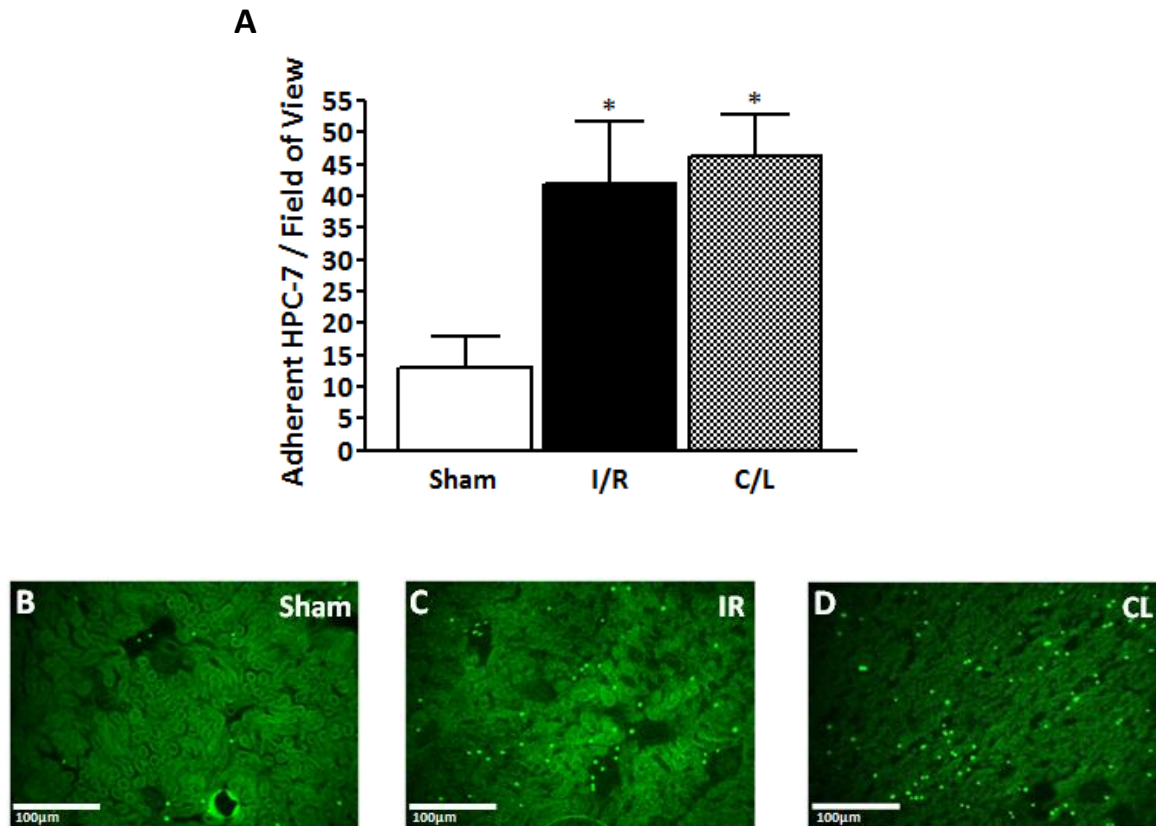


Figure 3.2. The number of adherent HPC-7 is increased to frozen IR injured kidney sections *in vitro*. Kidney sections were isolated from sham and IR-treated animals and 1×10^5 CFSE-labelled HPC-7 were applied to each section for 20 minutes. HPC-7 adhesion was quantified from 5 fields of view per section using a pre-selected pattern and an average for each tissue section was calculated. A significant increase in HPC-7 to frozen sections of IR injured and non-injured CL tissue was observed compared to controls. 223% more HPC-7 adhered to IR injured tissue compared to sham-operated kidney. Results are shown in **panel A**. Representative images are shown of sham (**panel B**), non-injured contralateral (**panel C**) and IR injured (**panel D**) renal sections. Plots represent mean adhesion \pm SEM of at least 4 separate experiments; * $p < 0.05$ (one-way ANOVA and Dunnett's post-test).

3.3.3 Adherent and free-flowing HPC-5 numbers *in vivo* do not change in IR injured animals

Initial experiments were conducted using an upright IVM set-up (**Figure 3.3.A**). No significant differences were observed in the number of adherent HPC-5 to the injured renal microvasculature compared to sham (AUC: IR: 84.67 ± 23.92 ; Sham: 134.20 ± 8.34 ; **Figure 3.3.B-D**), which is consistent with the previous SW assay results. No significant differences in the number of free-flowing HPC-5 were observed in the IR injured kidney compared to those seen in the sham controls (CPF: IR: 29.33 ± 6.17 ; Sham: 35.33 ± 7.97 ; **Figure 3.3.E**).

3.3.4 Adherent and free-flowing HPC-7 numbers *in vivo* are significantly increased in the renal IR injured model

Using the upright microscope and corresponding kidney preparation, HPC-7 adhesion was significantly ($p < 0.001$) increased within the peritubular microcirculation *in vivo* in injured animals compared to shams (AUC: Sham: 80.67 ± 17.86 ; IR: 192.00 ± 46.05 ; **Figure 3.4.A**). Free-flowing non-adherent HPC-7 trafficking in the peritubular capillaries was also monitored. Significantly ($p < 0.001$) more HPC-7 were seen homing to the kidney upon initial administration after IR injury when compared to the numbers observed in the non-injured kidney microvasculature (CPF: IR: 37.83 ± 9.94 ; Sham: 17.00 ± 6.36 ; **Figure 3.4.B**). The high numbers of free flowing HPC-7 in the kidney were only observed when first administered; thereafter, only occasional circulating cells were identified.

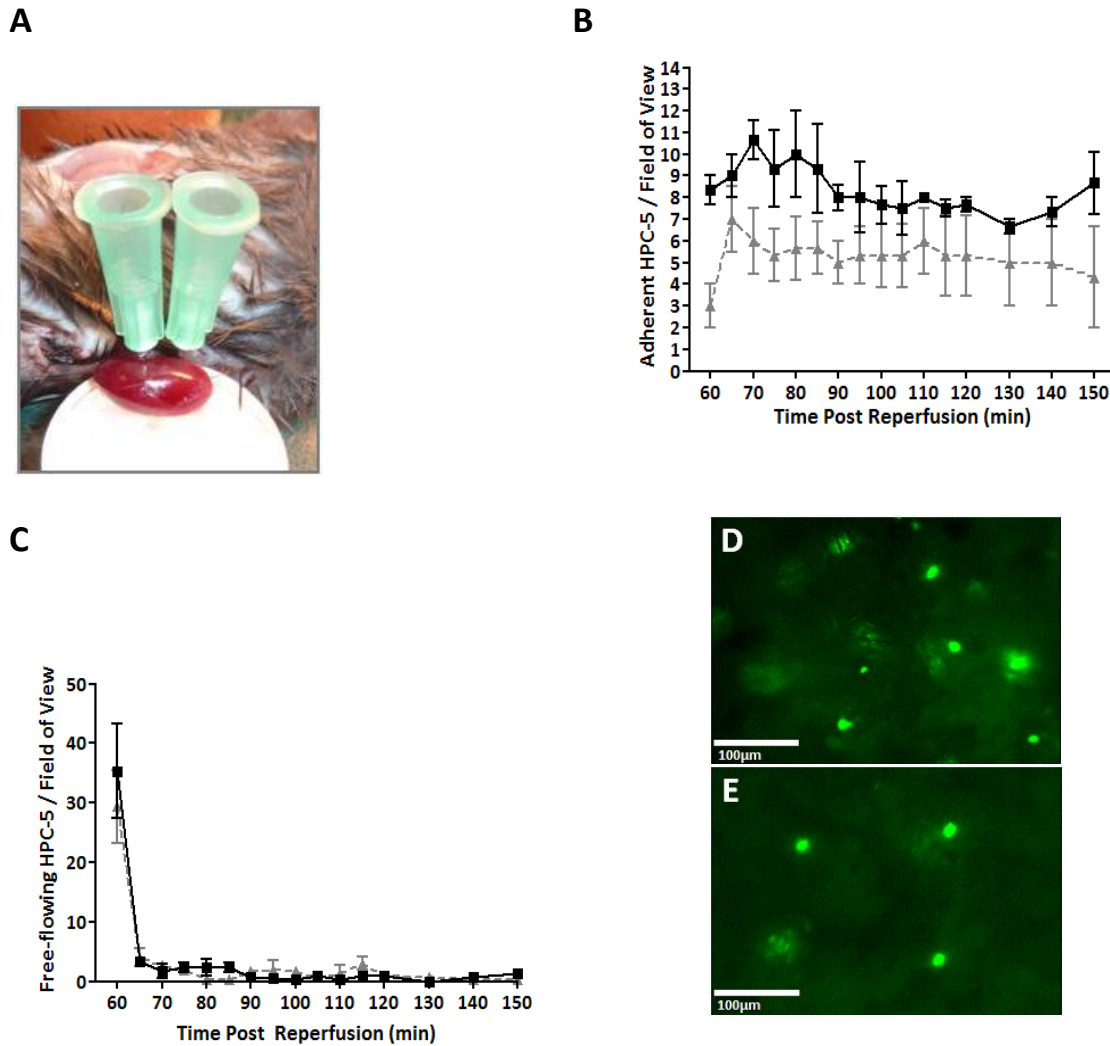


Figure 3.3. Renal IR injury does not promote changes in HPC-5 adhesion and the number of free-flowing HPC-5. Adhesion of HPC-5 to the renal peritubular capillaries was examined using intravital microscopy. Animals were subjected to 45 minutes ischaemia and 1 hour reperfusion prior to receiving an intra-arterial bolus of 2×10^6 CFSE-labelled HPC-7. One field of view was selected and 1 minute recordings every 5 minutes starting from the point of infusion (60 minutes post-reperfusion). After 2 hours reperfusion, recordings were taken for 1 minute every 10 minutes for the remaining 30 minutes. Using the upright intravital microscope and the corresponding prep (**panel A**), HPC-5 adhesion is not significantly altered in animals subjected to renal IR injury when compared to sham treated controls (**panel B**; black line: sham treated animals; grey line: renal IR injured animals). There were no significant changes to the number of HPC-5 circulating through the injured microvasculature compared to the sham controls (**panel C**; black line: sham treated animals; grey line: renal IR injured animals). Representative images of HPC-5 adhesion to sham (**panel D**) and IR injured animals (**panel E**) are shown (in and out of focus cells are counted). Non-adherent free-flowing HPC-5 were also analysed in each 1 minute recording. Plots represent a mean adhesion \pm SEM of at least 4 separate experiments; *** $p < 0.001$. **Panel B**: area under the curve calculations; **panel C**: two-way ANOVA with bonferroni post-tests.

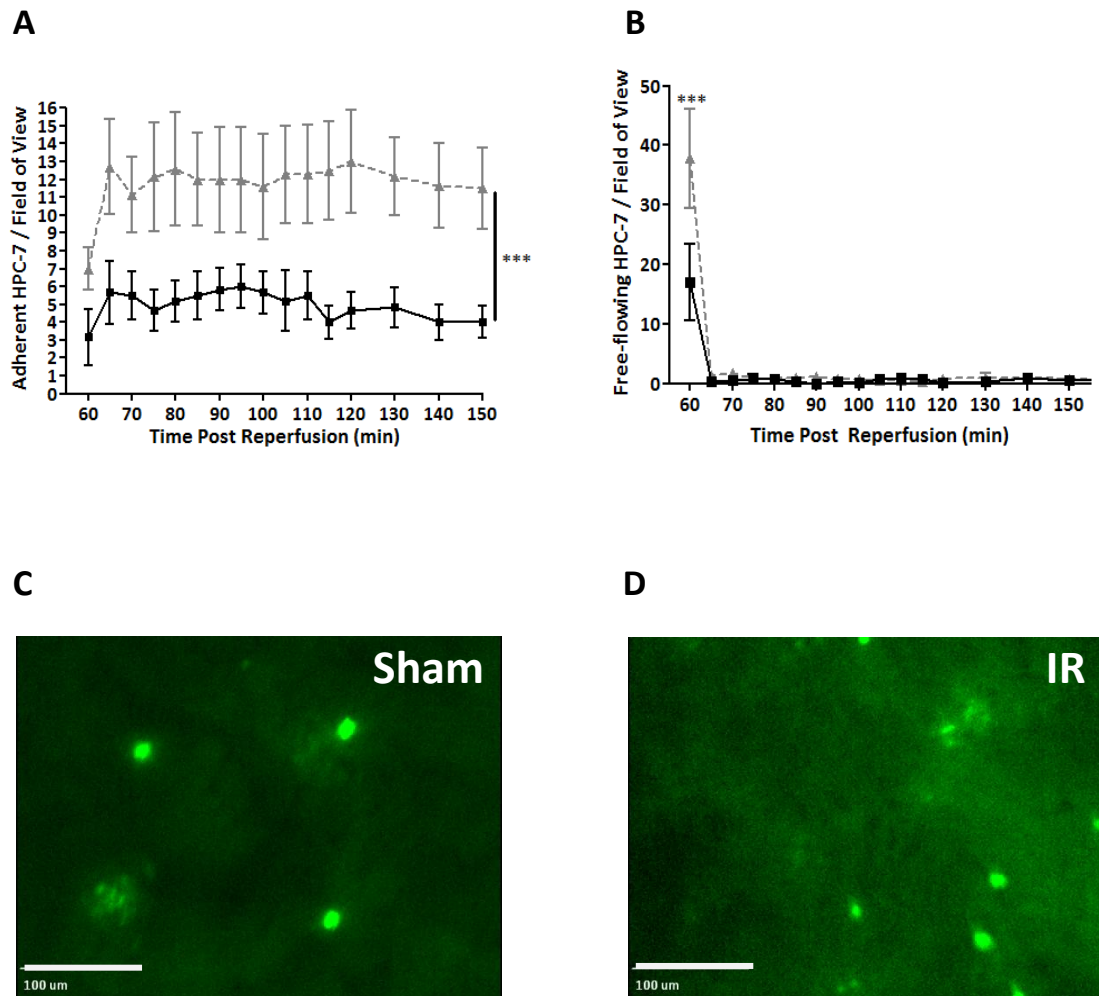


Figure 3.4. Renal IR injury enhances the adhesion of HPC-7 to the injured microvasculature in vivo. Adhesion of HPC-7 to the renal peritubular capillaries was examined using intravital microscopy. Animals were subjected to 45 minutes ischaemia and 1 hour reperfusion prior to receiving an intra-arterial bolus of 2×10^6 CFSE-labelled HPC-7. One field of view was selected and 1 minute recordings every 5 minutes starting from the point of infusion (60 minutes post-reperfusion). After 2 hours reperfusion, recordings were taken for 1 minute every 10 minutes for the remaining 30 minutes. Using the upright intravital microscope and the corresponding prep; HPC-7 adhesion is significantly raised in animals subjected to renal IR injury when compared to sham treated controls (**panel A**; black line: sham treated animals; grey line: renal IR injured animals). Non-adherent free-flowing HPC-7 were also analysed in each 1 minute recording. There were significantly more HPC-7 circulating through the injured microvasculature compared to the sham controls but only at the point of infusion (**panel B**; black line: sham treated animals; grey line: renal IR injured animals). Representative images of HPC-7 adhesion to sham (**panel C**) and IR injured animals (**panel D**) are shown (in and out of focus cells are counted). Plots represent a mean adhesion \pm SEM of at least 5 separate experiments; *** $p < 0.001$. **Panel A**: area under the curve calculations; **panel B**: two-way ANOVA with bonferroni post-tests respectively).

3.3.5 The number of adherent HPC-7 *in vivo* is significantly increased to the injured kidney with the new kidney intravital preparation

To improve the quality and reproducibility of intravital images, studies were also conducted on an inverted IVM set-up (**Figure 3.5.A**). Using this new prep, HPC-7 adhesion was again significantly ($p<0.001$) increased within injured kidney compared to the sham control (AUC: Sham: 221.90 ± 20.62 ; IR: 367.30 ± 21.16 ; **Figures 3.5.B-D**). *Ex vivo* analysis demonstrated that the adhesive events observed in the single pre-selected area during IVM were paralleled by those occurring in other randomly selected regions of the same kidney, with significantly ($p<0.05$) increased adhesion in the injured and CL kidney of IR injured mice compared to sham (CPF: Sham kidney: 11.04 ± 1.70 ; IR kidney: 20.75 ± 3.07 ; Sham CL kidney: 11.30 ± 4.03 ; IR CL kidney: 27.20 ± 4.11 ; **Figures 3.5.E**).

3.3.6 Free-flowing HPC-7 numbers *in vivo* are significantly increased at the point of cell infusion

The inverted IVM set-up demonstrated that at the point of HPC-7 infusion (60 minutes post-reperfusion), the number of free-flowing cells were again significantly ($p<0.001$) increased in injured animals compared to sham animals (CPF: IR: 134.40 ± 29.11 ; Sham: 75.80 ± 7.83 ; **Figure 3.6.A**). This effect was not seen at any other time point. Since this may result from increased renal blood flow following IR injury, laser speckle contrast microscopy was used to determine blood flow in sham and injured kidneys. At 60 minutes post-reperfusion, renal blood flow was significantly ($p<0.05$) decreased in injured mice compared to sham mice (Flux: IR kidney: 1719.20 ± 312.97 ; sham kidney:

2739.57±21.97; **Figure 3.6.B-C**). Furthermore, HPC-7 velocity was also measured *in vivo* and was significantly ($p<0.01$) reduced in the injured microcirculation compared to the microcirculation in sham animals (**Figure 3.6.D**).

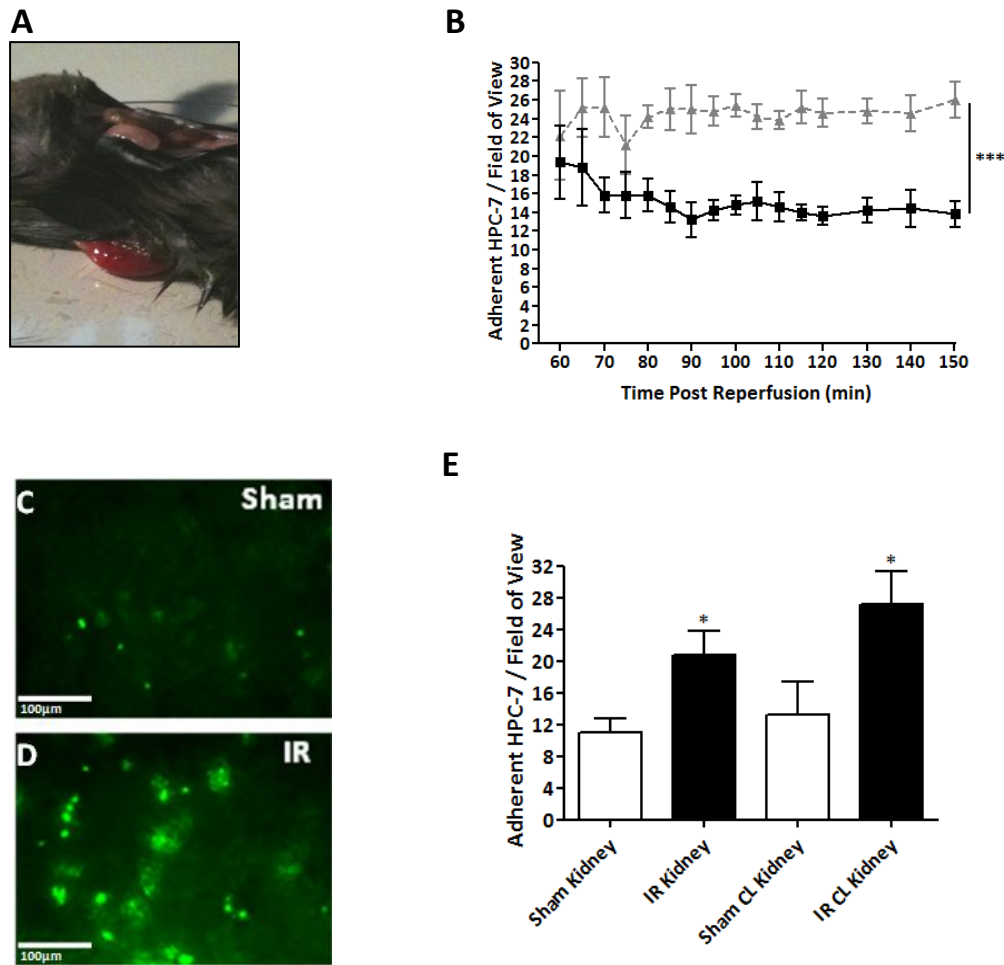


Figure 3.5. Renal IR injury enhances the adhesion of HPC-7 to the injured microvasculature in vivo. HPC-7 adhesion to the renal peritubular capillaries was examined using intravital microscopy. Animals were subjected to 45 minutes ischaemia and 1 hour reperfusion prior to receiving an intra-arterial bolus of 2×10^6 CFSE-labelled HPC-7. One field of view was selected and 1 minute recordings every 5 minutes starting from the point of infusion (60 minutes post-reperfusion). After 2 hours reperfusion, recordings were taken for 1 minute every 10 minutes for the remaining 30 minutes. To get a stiller and crisper prep, the prep was altered and the inverted intravital microscope was used instead (**panel A**); HPC-7 adhesion to the vasculature is significantly increased after renal IR injury compared to non-injured sham control animals (**panel B**; black line: sham treated animals; grey line: renal IR injured animals). Representative images of CFSE-labeled HPC-7 in sham (**panel C**) and IR injured (**panel D**) renal microcirculation are shown (both in focus and out of focus cells are counted). These recorded events were paralleled by those occurring in other randomly selected regions of the injured kidney and there was also a significantly higher number of adherent HPC-7 in the non-injured right contralateral kidney compared to the right sham kidney (**panel E**) compared to the sham control. Plots represents a mean adhesion \pm SEM of at least 4 separate experiments; * $p < 0.05$, ** $p < 0.01$, *** $p < 0.001$. **Panel B:** Area under the curve calculations); **panels E and F:** unpaired t-test.

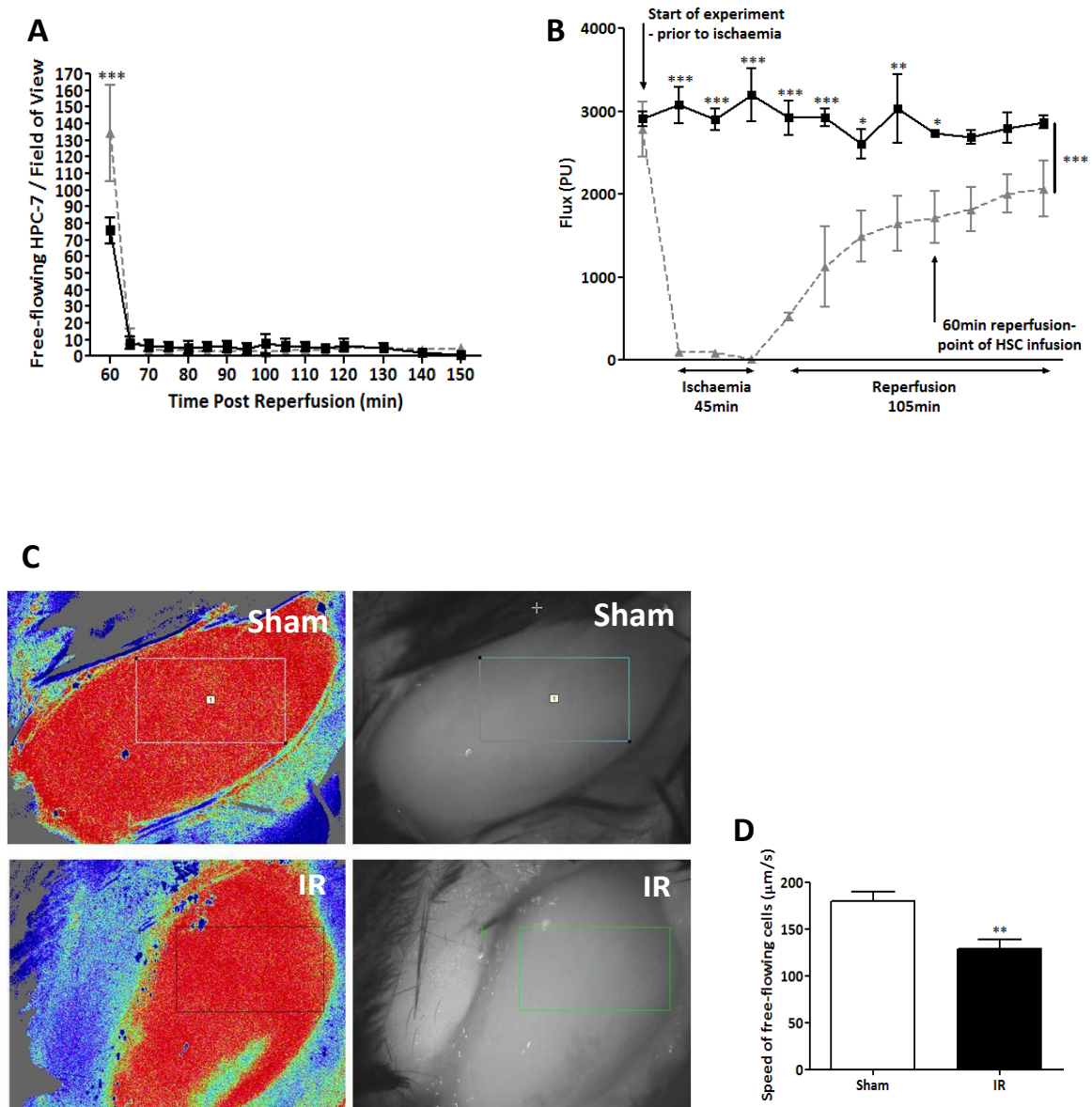


Figure 3.6. More free-flowing HPC-7 are seen in the injured kidney immediately upon HPC-7 infusion. After renal IR injury, the number of free-flowing HPC-7 seen flowing in the injured renal vasculature significantly increases compared to the non-injured sham animal (**panel A**). This effect is limited to the first 1 minute recording only. Blood flow (measured as flux) was significantly reduced in IR injured mice at the time of HPC-7 infusion (**panel B**). Representative images from the laser-speckle microscopy results determining blood flow in sham (**panel C; upper row**) and IR injured kidney (**panel C; lower row**) are shown. HPC-7 velocity *in vivo* was significantly reduced in IR injured renal microcirculation compared to that in sham animals (**panel D**). Plots represent a mean adhesion \pm SEM of at least 4 separate experiments; * $p < 0.05$, ** $p < 0.01$, *** $p < 0.001$. **Panel A and B:** two-way ANOVA with bonferroni post-tests; **panel C:** unpaired t-test.

3.4 Major Findings for Chapter 3

FINDING		HOW?
1	Established murine renal IR injury model	<i>In vivo</i> : Intravital microscopy
2	HPC-5 do not adhere to IR-injured kidney more so than sham	<i>In vitro</i> : Stamper-Woodruff <i>In vivo</i> : Intravital microscopy
3	HPC-7 adhere more to IR-injured kidney than sham	<i>In vitro</i> : Stamper-Woodruff <i>In vivo</i> : Intravital microscopy
4	HPC-7 adhere more to CL kidney than sham	<i>In vitro</i> : Stamper-Woodruff Ex <i>vivo</i> : Intravital microscopy
5	After IR injury, more HPC-7 are seen free-flowing in the kidney in the first minute	<i>In vivo</i> : Intravital microscopy
6	Blood flow continues to be reduced in the IR kidney	<i>In vivo</i> : Laser speckle contrast microscopy

3.5 Discussion

A great deal of excitement surrounds the idea of BM-derived stem/progenitor cells as many studies have shown that they have regenerative potential or therapeutic ability in the kidney. However, following systemic infusion, their recruitment by the renal microcirculation is an essential pre-requisite. Although previous histological studies have demonstrated that HSCs can incorporate into IR injured kidney and confer benefit, no studies have currently used IVM to directly monitor the kinetics of HSC homing immediately upon infusion. Stroo and colleagues (2009) injected BM-derived KSL cells but monitored their presence in mouse renal sections 24 hrs post-infusion. Similarly, Kale *et al.*, (2003) and Lin *et al.*, (2003) monitored KSL cells in IR injured renal sections 7 days and 4-12 weeks post-infusion respectively. Understanding how circulating HSCs traffic through the injured environment is important and may allow us to develop therapeutic strategies to enhance recruitment, thus hopefully improving the efficacy to which they regenerate.

Using IVM, we generated novel data demonstrating that HSC adhesion was increased in IR injured kidneys compared to sham controls. Intravital images are usually acquired from one pre-selected field of view and this same region is imaged throughout the duration of the experiment; this limits the area in which adhesive events are observed. Therefore, the static adhesion assay using frozen tissue sections allows a greater area to be visualised. Both *in vivo* and *in vitro* assays demonstrated that renal IR injury was sufficient to promote the recruitment and adhesion of HPC-7 to the injured microvasculature.

To our knowledge, we are the first lab to use this method to describe the kinetics of SC homing to the kidney. One of the challenges to renal IVM in mice has been the difficulty in exteriorising and stabilising the kidney due to its anatomical location; most renal pathologies often involve damage to structures deeper in the kidney, particularly to the glomerular capillaries. Only the peritubular capillaries can be visualised intravitaly, thus making IVM studies for glomerular diseases near impossible; however, since IR injury also damages the peritubular capillaries (Basile *et al.* 2001), viewing the surface of the kidney has proved invaluable for monitoring injury mediated SC -endothelial interactions *in vivo*. We firstly used an upright Olympus microscope to monitor the surface peritubular capillaries from above. Although we did image SCs trafficking through the kidney with the upright IVM, we further modified this method using an inverted set-up to enable clearer images of the renal microcirculation to be obtained; this resulted in almost double of the adherent CFSE-labelled HPC-7 numbers that we were able to detect. Also, a far greater number of free-flowing HPC-7 were counted.

It is well accepted that performing *in vivo* trafficking studies using primary HSCs is not easy because of the difficulty in isolating large enough numbers so that they can be quantified after their infusion. These cells are extremely rare within the mouse BM (roughly 5000 per animal) so in this thesis, HSC lines were used. Unlike our studies which used HPC-7 cells, previous studies described above have used primary HSCs isolated from donor mouse BM. However, much smaller numbers of cells were injected (eg. 5×10^3 for Kale and colleagues (2003); 2×10^5 for Lin and colleagues (2003)), which are possible to

obtain from donor mice and is sufficient for histological type studies. However, for imaging dynamic cell trafficking intravitaly a much larger dose of cells ($1-2 \times 10^6$) is required, hence the need for a cell line in these studies. HPC-7 are a well-accepted representative cell line of pure HSCs and have been widely used for investigating the control of HSC growth and differentiation at a molecular and cellular level (Pimanda *et al.* 2008; Wilson *et al.* 2009). Furthermore, this cell line can restore haematopoiesis in lethally irradiated mice (Pinto do *et al.* 2002). We have demonstrated that increased numbers of HPC-7 adhere to IR injured kidney microvessels, when compared to sham controls. Our data is in line with the findings of Stroo and colleagues (2009) that HSCs preferentially migrate to the ischaemic kidney. Interestingly, HPC-5 did not show a preference in their adhesion to either IR injured kidney or sham controls in any of our studies. The variation in homing and adhesion of these two HSC cell lines could be due to differences in surface adhesion molecule expression (Pinto do *et al.* 1998; Ivanova *et al.* 2002). Differences in the BM homing capabilities of embryonic and adult HSCs have also been noted (Perlingeiro *et al.* 2001). However, it has been previously shown that HPC-5 can also be recruited to the IR injured liver *in vivo* (Kavanagh *et al.* 2010), therefore showing that HPC-5 cells do have the capability of homing and adhering to an acute ischaemic injury; this shows that there is some tissue specificity with regards to SC trafficking.

Although the findings of Stroo *et al.* (2009) regarding HSC recruitment to the IR kidney are in agreement with our studies, they did not observe a similar increase in HSC adhesion to the CL non-injured kidney. Meldrum *et al.* have shown that unilateral renal

Chapter 3: Recruitment of HSCs Following Renal IR Injury

IR injury causes a significant increase in TNF- α mRNA and protein expression in the IR and CL kidney in similar amounts after 1 hour reperfusion, compared to sham, as assessed by RT-PCR and ELISA assays respectively (Meldrum *et al.* 2002). TNF- α is a pro-inflammatory agent and can enhance neutrophil infiltration and cytokine release, leading to an increased adhesion molecule expression on the endothelium (Devarajan 2006). These results could therefore explain our increases in HSC numbers seen in the CL kidney after renal IR injury, showing that the CL kidney experiences a biologically significant injury after unilateral renal IR injury. In the study by Stroo and colleagues, HSC numbers within the kidneys were quantified after 24 hours, so it is possible that any remote inflammation has already peaked or the HSCs that may have been adherent initially have migrated elsewhere. However, Lin and colleagues (2003) have also noted donor-derived HSCs in the non-injured CL kidney, but after a 2 week reperfusion period. Our results do question the use of the non-clamped CL kidney as an internal control, which it is often used as when assessing renal injury (Stern *et al.* 2004; Melo-Filho *et al.* 2010).

Interestingly, the number of free-flowing HPC-7 cells observed circulating through the kidney was significantly increased but only at the point of infusion in IR injured mice. Some studies have demonstrated that blood flow increases following an inflammatory insult, which may explain the increased numbers of adherent cells (Hopkins and Damewood 1974; Sekizuka *et al.* 1988). Others report that reperfusion of previously ischaemic tissue results in blood velocity decreasing due to vascular congestion as a result of adhesion of activated leukocytes and slowing of red blood cell flow (Cristol *et al.* 1993; Lieberthal 1997). We combined IVM with laser speckle microscopy in order to correlate

the HSC adhesive events with renal blood flow. The Moor FLPI laser speckle camera (Moor Instruments, UK) was used to determine renal surface blood flow within exposed IR injured and sham kidneys. Flow/flux measurements were taken prior, during and after the 45 minute ischaemic period. Using this non-invasive, quick and simple technique, we observed a significant decrease in blood flow within the ischaemic kidney at 60 minutes reperfusion, the point at which HSC infusion takes place, compared to the sham control. The data also confirmed that our IR injury is robust due to the presence of no blood flow within the renal microcirculation during the ischaemic period. Furthermore, our individual cell tracking analysis program demonstrated that HPC-7 flowing through the injured kidney did so at a significantly lower pace.

In conclusion, although there is increasing evidence that HSCs are beneficial following renal injury, the efficacy of such therapies is hypothesis to be proportional to the degree of cell recruitment which can be achieved. Enhancing the effectiveness of regenerative processes may therefore depend on identifying and then modulating the adhesive mechanisms that underpin SC trafficking. In this chapter we present novel data that renal IR injury can mediate active recruitment and subsequent adhesion of HPC-7 and that these events can be reproducibly monitored in real-time using fluorescent IVM. This chapter and other studies from the Kalia lab (Kavanagh *et al.* 2013) demonstrate that the kinetics of HSC recruitment is similar to the well described adhesion cascade for neutrophils (Becker *et al.* 1999; Chan and Watt 2001). The following chapter will examine in depth the adhesive mechanisms governing HSC recruitment to the IR injured mouse kidney.

Chapter 4



Mechanisms that Govern HSC Recruitment to the IR Injured Kidney

4 Mechanisms of Haematopoietic Stem Cell Recruitment to the IR Injured Kidney

4.1 Introduction and Hypotheses

4.1.1 Introduction

Despite emerging clinical evidence that HSCs can improve a variety of inflammatory disorders, benefits are either minor or transitory (Lanzoni *et al.* 2008; Dai and Kloner 2011); this has been partially explained by low numbers of HSCs actually adhering within the local microcirculation of injured organs after injection (Camargo *et al.* 2006). When delivered by the preferred systemic route, SCs exhibit poor homing and a subsequent low efficiency of tissue engraftment occur, showing that these processes are essential for SCs to mediate repair (Karp and Leng Teo 2009). After a myocardial infarction the progenitor cell retention is less than 5% (Aicher *et al.* 2003) and although Lin and colleagues (2003) showed that HSCs could engraft within the IR injured kidney tubules, the number of recruited cells were low, most likely resulting in a sub-maximal therapeutic benefit. Poor homing, combined with the fact that HSCs are rare cells, <0.01% of BM, has likely limited their clinical utility and success. If SC therapy is to be realised for various diseases, a better understanding of the adhesive mechanisms underlying their recruitment to the injured tissue bed would be advantageous.

In the previous chapter, we have shown that our HSC line, HPC-7, preferentially adheres to the IR kidney, as demonstrated using both *in vitro* and *in vivo* assays. However, the

Chapter 4: Mechanisms that Govern HSC Recruitment to the IR Injured Kidney

adult HSC line, HPC-5, did not preferentially bind to the injured kidney. Therefore we continued to use HPC-7 to determine the molecular mechanisms governing their recruitment to sites of renal IR injury.

Currently, our knowledge of the adhesive mechanisms mediating the recruitment of transplanted HSCs to injured kidney is limited. HSCs possess a similar repertoire of surface adhesion molecules to leukocytes; HSCs express β_1 - and β_2 -based integrin heterodimers, which bind to their endothelial counter-receptors, VCAM-1 and ICAM-1 respectively (Turner *et al.* 1995). Recent work from our group has shown the importance of both CD49d (α_4 subunit of $\alpha_4\beta_1$ integrin) and CD18 (β_2 integrin) in mediating HSC recruitment to injured tissues (Kavanagh *et al.* 2010; Kavanagh *et al.* 2013). The role of either of these integrins in HSC recruitment following renal IR injury is unknown. A role for CD18 is likely since ICAM-1 has been shown to be highly expressed on the renal endothelium post-ischaemia and plays an important role in mediating inflammatory leukocyte adhesion. Furthermore, blocking ICAM-1 with monoclonal antibodies *in vivo* protects animals from ischaemic AKI (Kelly *et al.* 1996).

Interestingly, the non-integrin CD44 has shown contrasting results with regards its role in SC trafficking (Khaldoyanidi *et al.* 1996; Vermeulen *et al.* 1998; Oostendorp *et al.* 2000; Avigdor *et al.* 2004). The main ligand for CD44 is HA, which is expressed in the ECM of most tissue beds (Goodison *et al.* 1999). Also, CD44 is highly expressed in the kidney after IR injury (Goransson *et al.* 2004).

Chapter 4: Mechanisms that Govern HSC Recruitment to the IR Injured Kidney

The first part of this chapter initially determined the molecular adhesive mechanisms governing HSC recruitment to IR injured murine renal microcirculation *in vivo*. Expression of CD49d, CD18 and CD44 are expressed on the HPC-7 surface (Kavanagh *et al.* 2010) and due to the expression of their counter-receptors being heightened during renal IR injury, as well as having a role in the leukocyte-adhesion cascade, these receptors and their roles in SC homing to the injured kidney were determined.

In addition to upregulated surface adhesion molecules during injury, chemokines released from the activated endothelium are also essential for activation of circulating cells, such as leukocytes (Granger and Senchenkova 2010). The chemokines IL-8 and SDF-1 α are heavily implicated within this process, and the latter has been noted to be essential in SC trafficking. It has also been shown that IL-8 or its murine homologue, KC, is heavily increased during the very early stages of ischaemic AKI (Molls *et al.* 2006). The roles of these inflammatory chemokines in promoting HSC homing to a healthy kidney were investigated in the second part of this chapter, as well as deciphering if their counter-receptors aid in HSC recruitment to the injured kidney.

4.1.2 Aims and Hypotheses

The main aims and hypotheses of this chapter are:

Chapter 4: Mechanisms that Govern HSC Recruitment to the IR Injured Kidney

1. Hypothesis: Individual blockade of adhesion receptors (CD18, CD44, CD49d) can significantly decrease HPC-7 adhesion to the IR injured kidney *in vivo*
2. Hypothesis: Blocking endothelial counter-receptors via an intra-arterial injection will reduce HPC-7 adhesion to the IR injured kidney *in vivo*
3. Aims: Establish a murine prep that enables the healthy kidney to be immersed by the chemokine in question
4. Hypothesis: KC and SDF-1 α act as guidance cues to enhance HPC-7 homing
5. Hypothesis: CXCR2 and CXCR4 have a major role in HPC-7 trafficking to the injured kidney

4.2 Methods

The methods used in this chapter are described in detail in chapter 2. Briefly, to assess which HSC surface adhesion molecules have a role in trafficking to the injured kidney *in vivo*, our viable HSC cell line, HPC-7, were incubated with 80 μ g/ml function-blocking monoclonal antibodies (CD18, CD49d, CD44) against the specific adhesion molecule in question prior to injection into the carotid artery. After this, the recruitment of these cells to the injured kidney was monitored intravitaly. To understand which counter-ligands the HPC-7 receptors are interacting with, an *in vivo* monoclonal antibody (anti-VCAM-1 or anti-CD44) or enzyme (hyaluronidase) was injected at 1 minute reperfusion. 2 x 10⁶ CFSE-stained HPC-7 were then injected at 60 minutes post-reperfusion and recruitment of these cells to the injured kidney was monitored intravitaly.

Chapter 4: Mechanisms that Govern HSC Recruitment to the IR Injured Kidney

As both KC and SDF-1 α are released from the injured kidney, their role in regulating HPC-7 homing to the kidney was determined. To initially decipher if they could be having a role, the expression of their receptors, CXCR2 and CXCR4 respectively, on the HSC cell surface was determined using flow cytometry. A novel preparation was designed in which the healthy non-injured kidney was continuously bathed in either chemokine for 4 hours prior to SC administration and the number of adherent and free-flowing cells were subsequently quantified intravitaly. Blood flow was also monitored in this set of experiments using laser-speckle microscopy.

After each intravital experiment, the animal was sacrificed and the left (sham/IR/treated) and right (non-injured CL) kidney were removed and adherent CFSE-labelled HPC-7 were quantified in five fields of view to obtain an average adherent cell count: this was used to make sure the HPC-7 events monitored in the one pre-selected field of view during intravital experiments was a true representation of events taking place in other regions of the kidney.

4.3 Results

4.3.1 Blocking HSC surface expression of CD18 does not have a role in HPC-7 adhesion to the injured kidney

Using flow cytometry, we have previously demonstrated that HPC-7 express CD18, CD49d and CD44 (Kavanagh *et al.* 2010). Blocking CD18 on HPC-7 did not significantly decrease the number of adherent HPC-7 to the injured kidney (AUC: Anti-CD18: 268.3 \pm 10.65; IgG:

Chapter 4: Mechanisms that Govern HSC Recruitment to the IR Injured Kidney

282.3±20.69; **Figure 4.1.A**). Also, free-flowing HPC-7 numbers in the IR kidney after blocking CD18 were not significantly different compared to cells treated with an IgG control (**Figure 4.1.B**). *Ex vivo* analysis of both IR injured and CL non-injured kidneys also confirms that CD18 does not have a role in HSC recruitment to the kidney (**Figure 4.1.C-D**).

4.3.2 CD49d has an important role in HPC-7 adhesion to the injured kidney

Blocking CD49d significantly ($p<0.01$) decreased HPC-7 adhesion to the injured kidney (AUC: anti-CD49d: 164.9±36.68; IgG: 282.3±20.69; **Figure 4.2.A**). After CD49d blockade, there was a significant ($p<0.001$) decrease in the numbers of free-flowing HPC-7 seen in the IR kidney, this effect is only seen during the first intravital recording when HPC-7 are infused (CPF: anti-CD49d IR kidney: 52.80±12.02; IgG IR kidney: 73.00±11.36; **Figure 4.2.B**). *Ex vivo* analysis shows there is a significant decrease in HPC-7 adhesion to IR injured ($p<0.05$) and CL non-injured ($p<0.01$) kidney (CPF: anti-CD49d IR kidney: 10.44±1.076; IgG IR kidney: 15.50±1.895; **Figure 4.2.C**; anti-CD49d CL kidney: 12.00±1.388; IgG CL kidney: 20.60±2.145; **Figure 4.2.D**).

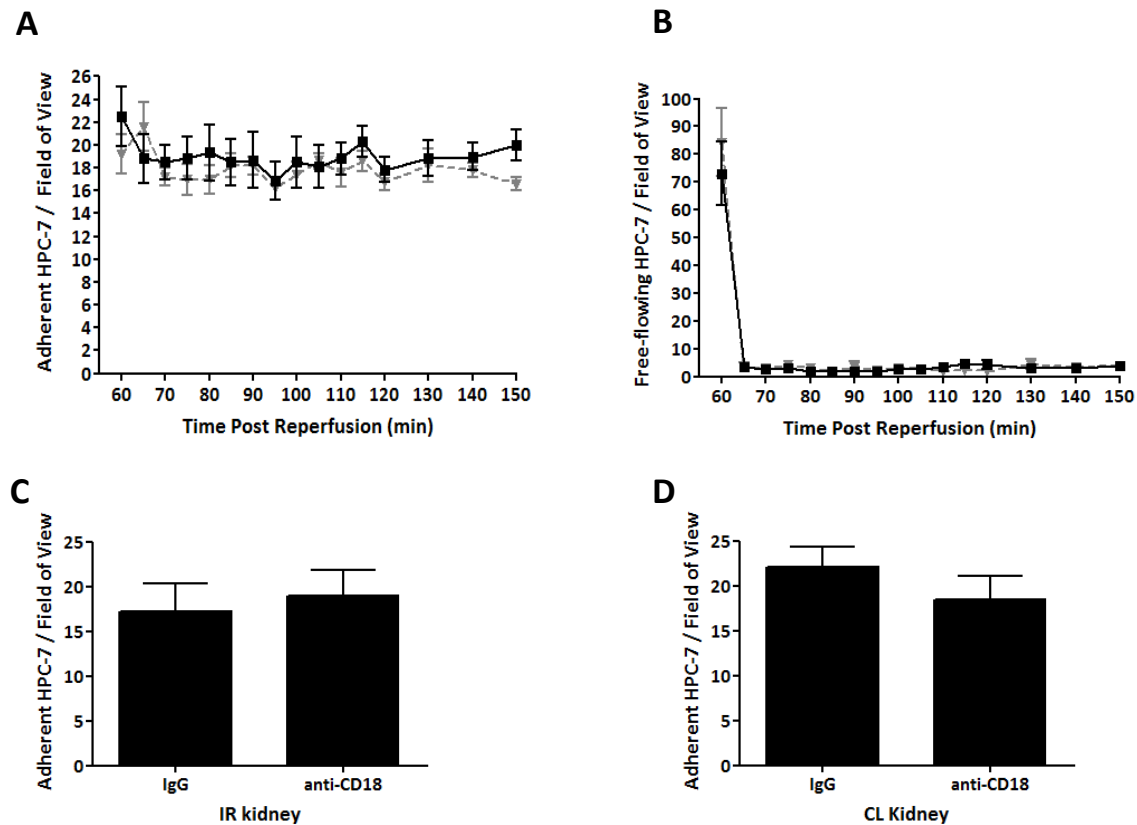


Figure 4.1. Adhesion of HPC-7 to renal IR injury does not require CD18. Surface HPC-7 expression was blocked by incubating cells with 80 μ g/ml of a CD18 function-blocking monoclonal antibody for 30 minutes prior to administration into the animal model of renal IR injury. Animals were subjected to 45 minutes ischaemia and 1 hour reperfusion, and then received an intra-arterial bolus of 2×10^6 CFSE-labelled CD18-blocked HPC-7. One field of view was selected and 1 minute recordings every 5 minutes started from the point of infusion (60 minutes post-reperfusion). After 2 hours reperfusion, recordings were taken for 1 minute every 10 minutes for the remaining 30 minutes. HPC-7 adhesion to the renal peritubular capillaries was examined using intravital microscopy. HPC-7 adhesion to the injured vasculature is not significantly altered after blocking HPC-7 surface expression of CD18 compared to IgG controls (**panel A**; black line: IgG treated HPC-7; grey line: anti-CD18 treated HPC-7). The number of free-flowing cells was also quantified and there were no significant differences at any time points (**panel B**). *Ex vivo* analysis confirms that there is no difference in HPC-7 adhesion to the IR injured kidney (**panel C**) and also in the non-injured right contralateral kidney (**panel D**). Plots represent a mean adhesion \pm SEM of at least 4 separate experiments. **Panel A**: area under the curve calculation; **panel B**: two-way ANOVA with bonferroni post-tests; **panels C and D**: unpaired t-test.

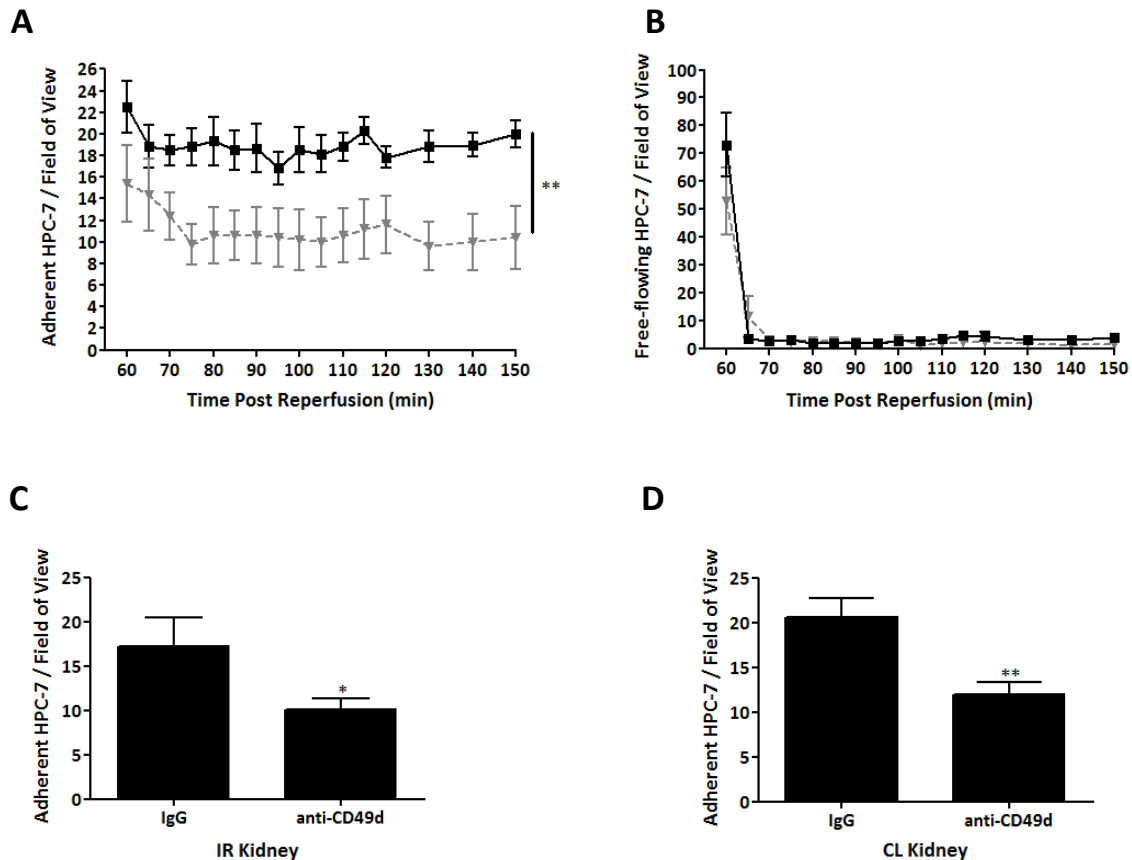


Figure 4.2. Adhesion of HPC-7 to renal IR injury requires CD49d. Surface HPC-7 expression was blocked by incubating cells with 80µg/ml of a CD49d function-blocking monoclonal antibody for 30 minutes prior to administration into the animal model of renal IR injury. HPC-7 adhesion to the renal peritubular capillaries was examined using intravital microscopy. HPC-7 adhesion to the injured vasculature is significantly decreased after blocking HPC-7 surface expression of CD49d compared to IgG controls (**panel A**; black line: IgG treated HPC-7; grey line: anti-CD49d treated HPC-7). The number of free-flowing cells was also quantified and there was a significant decrease in free-flowing HPC-7 at the point of infusion only (**panel B**). *Ex vivo* analysis of the IR kidney confirms there is an overall decrease in the number of adherent HPC-7 after anti-CD49d treatment (**panel C**) and also in the non-injured right contralateral kidney (**panel D**). IgG controls were the same cohort as used in Figure 4.1 to reduce the number of animals used. Plots represent a mean adhesion \pm SEM of at least 5 separate experiments; * $p < 0.05$; ** $p < 0.01$; *** $p < 0.001$. **Panel A**: area under the curve calculation; **panel B**: two-way ANOVA with bonferroni post-tests; **panels C and D**: unpaired t-test.

4.3.3 HPC-7 adhesion is significantly reduced by *in vivo* blockade of VCAM-1

Administration of an anti-VCAM-1 antibody, one of the counter-ligands to CD49d, intra-arterially significantly ($p < 0.001$) reduced HPC-7 adhesion when compared to intra-arterial administration of an IgG control (AUC: anti-VCAM-1: 209.9 ± 16.06 ; IgG: 312.6 ± 15.79 ; **Figure 4.3.A**). VCAM-1 appears to also have a role in HPC-7 trafficking to the injured renal microvasculature (CPF: anti-VCAM1: 99.80 ± 16.50 ; IgG: 134.3 ± 15.01 ; **Figure 4.3.B**). *Ex vivo* analysis of the IR injured and CL non-injured kidney again confirms that blocking VCAM-1 significantly ($p < 0.01$) decreases IR kidney adhesion (CPF: anti-VCAM-1 IR kidney: 11.40 ± 1.200 ; IgG IR kidney: 16.99 ± 1.174 ; **Figure 4.3.C**). VCAM-1 did not have a role in HPC-7 adhesion to the non-injured CL kidney (**Figure 4.3.D**).

4.3.4 CD44 also has an important role in HPC-7 adhesion to the injured kidney

Blocking HPC-7 surface expression of CD44 significantly ($p < 0.05$) decreased HPC-7 adhesion to the injured kidney (AUC: anti-CD44: 178.0 ± 35.00 ; IgG: 282.3 ± 20.69 ; **Figure 4.4.A**). There was no change in the number of HPC-7 trafficking through the injured microvasculature after anti-CD44 treatment (**Figure 4.4.B**). *Ex vivo* analysis demonstrated a significant ($p < 0.05$) decrease in HPC-7 adhesion to IR injured kidney only (CPF: anti-CD44 IR kidney: 10.08 ± 1.728 ; IgG IR kidney: 15.50 ± 1.895 ; **Figure 4.4.C**). HPC-7 adhesion to the non-injured CL kidney did not significantly change after blocking CD44 (CPF: anti-CD44 CL kidney: 16.81 ± 1.959 ; IgG CL kidney: 20.60 ± 2.145 ; **Figure 4.4.D**).

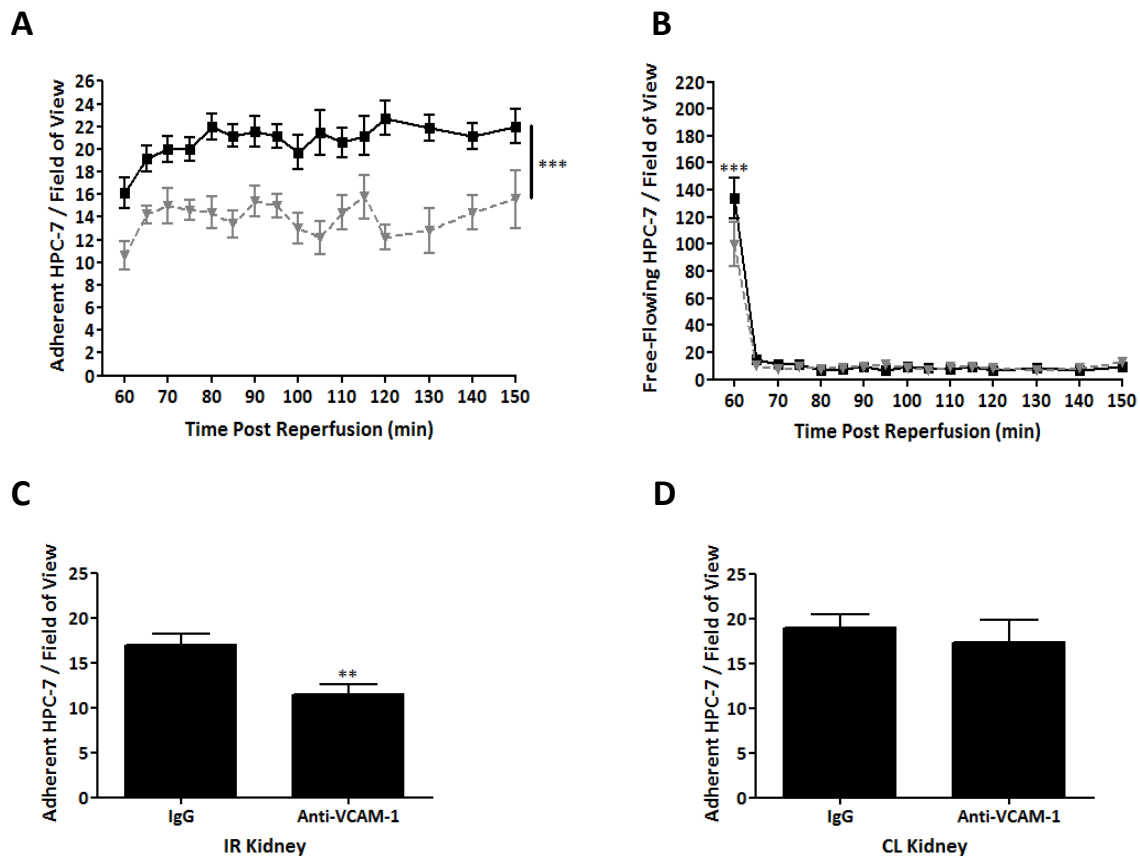


Figure 4.3. Recruitment and subsequent adhesion of HPC-7 to renal IR injury requires VCAM-1. An anti-VCAM-1 antibody was infused into the animal at 1 minute post-reperfusion. After 60 min post-reperfusion 2×10^6 naïve HPC-7 were introduced and their adhesion to the renal peritubular capillaries was examined using intravital microscopy. HPC-7 adhesion to the injured vasculature is significantly decreased after blocking VCAM-1 compared to IgG controls (**panel A**; black line: IgG treated HPC-7; grey line: anti-VCAM-1). The number of free-flowing cells was also quantified and there was a significant decrease in free-flowing HPC-7 at the point of infusion only (**panel B**). *Ex vivo* analysis of the IR kidney confirms there is an overall decrease in the number of adherent HPC-7 after *in vivo* anti-VCAM-1 treatment (**panel C**) but no differences were seen in the non-injured right contralateral kidney (**panel D**). Plots represent a mean adhesion \pm SEM of at least 5 separate experiments; * $p < 0.05$; ** $p < 0.01$; *** $p < 0.001$. **Panel A**: area under the curve calculation; **panel B**: two-way ANOVA with bonferroni post-tests; **panels C and D**: unpaired t-test.

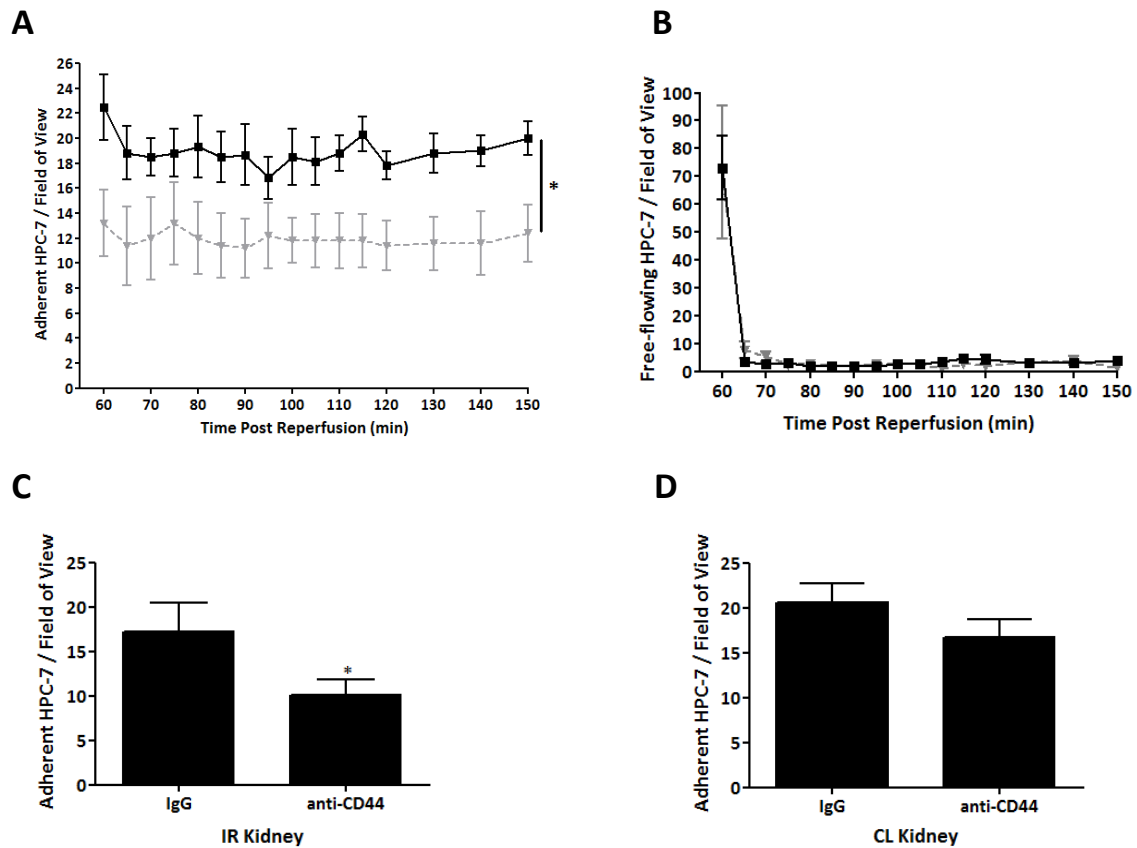


Figure 4.4. Adhesion of HPC-7 to renal IR injury requires CD44. Surface HPC-7 expression was blocked by incubating cells with 80 μ g/ml of a CD44 function-blocking monoclonal antibody for 30 minutes prior to administration into the animal model of renal IR injury. HPC-7 adhesion to the renal peritubular capillaries was examined using intravital microscopy. HPC-7 adhesion to the injured vasculature is significantly decreased after blocking HPC-7 surface expression of CD44 compared to IgG controls (**panel A**; black line: IgG treated HPC-7; grey line: anti-CD44 treated HPC-7). There were no differences in the number of free-flowing HPC-7 (**panel B**). *Ex vivo* analysis of the IR kidney confirms there is an overall decrease in the number of adherent HPC-7 after anti-CD44 treatment (**panel C**) but not in the non-injured right contralateral kidney (**panel D**). IgG controls were the same cohort as used in Figure 4.1 to reduce the number of animals used. Plots represent a mean adhesion \pm SEM of at least 5 separate experiments; * $p < 0.05$. **Panel A:** area under the curve calculation; **panel B:** two-way ANOVA with bonferroni post-tests; **panels C and D:** unpaired t-test.

4.3.5 HA is the counter-ligand for CD44 and helps HPC-7 adhere to the injured kidney

The main endothelial counter-ligands to CD44 include HA and CD44 itself. To decipher which counter-ligand is interacting with CD44 on the SC, an *in vivo* injection of either hyaluronidase, which breaks down HA, or a function blocking CD44 antibody was administered intra-arterially during reperfusion. The major endothelial counter-ligand for CD44 on HPC-7 appeared to be HA, as digestion with hyaluronidase *in vivo* was associated with a significant ($p<0.01$) decrease in HPC-7 adhesion (AUC: PBS: 353.0 ± 49.67 ; hyaluronidase: 190.9 ± 24.53 ; **Figure 4.5.A**). Blocking endothelial CD44 *in vivo* did not alter HPC-7 adhesion (**Figure 4.5.B**). Removing either HA ($p<0.001$) or CD44 ($p<0.001$) activity causes a significant decrease in the number of free-flowing HPC-7 compared to the PBS and IgG controls respectively (CPF: hyaluronidase: 132.0 ± 28.60 ; PBS: 197.5 ± 18.62 ; anti-CD44: 81.67 ± 12.75 ; IgG: 134.29 ± 15.00 ; **Figure 4.5.C-D**); this effect is only seen at the point of infusion. Both *in vivo* HPC-7 adhesion results were confirmed during *ex vivo* analysis: hyaluronidase treatment significantly reduces HPC-7 adhesion in both the IR injured kidney and the non-injured CL kidney (CPF: hyaluronidase IR kidney: 8.714 ± 1.206 ; PBS IR kidney: 22.33 ± 0.7333 ; $p<0.001$; **Figure 4.5.E**; hyaluronidase CL kidney: 12.37 ± 1.601 ; PBS: 21.07 ± 1.618 ; $p<0.01$; **Figure 4.5.F**); CD44 did not reduce HPC-7 adhesion in either IR or CL kidneys (**Figure 4.5.G-H**).

Chapter 4: Mechanisms that Govern HSC Recruitment to the Injured Kidney

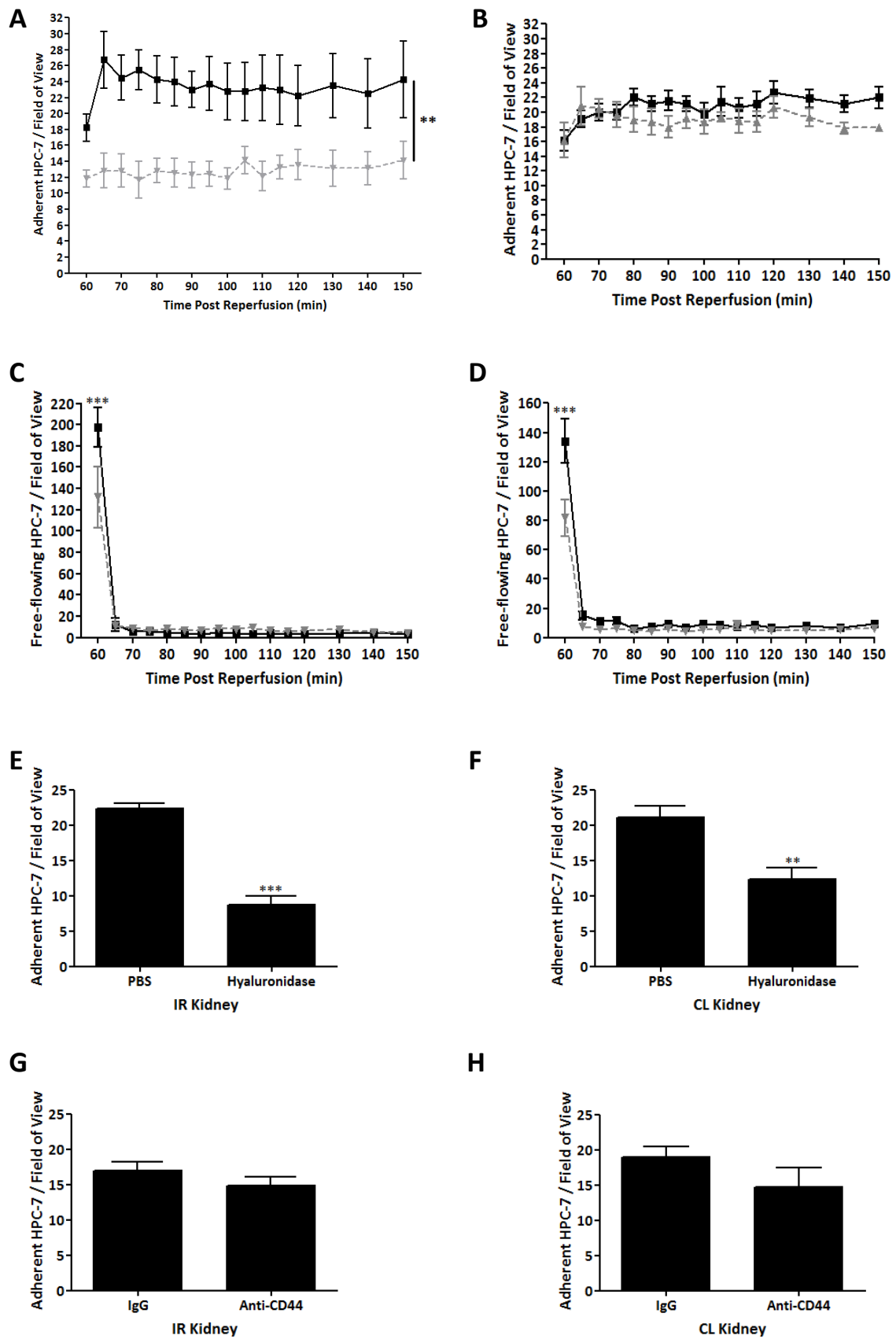


Figure 4.5. Recruitment and subsequent adhesion of HPC-7 to renal IR injury requires HA but not CD44. An *in vivo* injection of hyaluronidase or anti-CD44 was infused into the animal at 1 minute post-reperfusion. After 60 min post-reperfusion 2×10^6 naive HPC-7 were introduced and their adhesion to the renal peritubular capillaries was examined using intravital microscopy. HPC-7 adhesion to the injured vasculature is significantly decreased after digesting HA compared to IgG controls (**panel A**; black line: IgG treated HPC-7; grey line: hyaluronidase). There was no difference in HPC-7 adhesion after anti-CD44 *in vivo* treatment (**panel B**). The number of free-flowing cells was also quantified and there was a significant decrease in free-flowing HPC-7 after hyaluronidase (**panel C**) and anti-CD44 (**panel D**) treatment, but only at the point of infusion only. *Ex vivo* analysis of the IR and CL kidney confirms there is an overall decrease in the number of adherent HPC-7 after *in vivo* hyaluronidase treatment (**panel E and F**). After anti-CD44 treatment *ex vivo* analysis confirms intravital results and no difference in HPC-7 adhesion to IR and CL kidneys are seen (**panel G and H**). IgG controls were the same cohort as used in Figure 4.3 to reduce the number of animals used. Plots represent a mean adhesion \pm SEM of at least 5 separate experiments; * $p < 0.05$; ** $p < 0.01$; *** $p < 0.001$. **Panel A**: area under the curve calculation; **panel B**: two-way ANOVA with bonferroni post-tests; **panels D and E**: unpaired t-test.

4.3.6 The chemokines receptors CXCR2 and CXCR4 are expressed on HPC-7

As KC is one of the first biomarkers of acute renal injury (Molls *et al.* 2006) and SDF-1 α is known to be involved in BMSC homing (Togel *et al.* 2005), we decided to investigate if these chemokines had a role in HPC-7 recruitment to the IR injured kidney. Flow cytometry was firstly conducted to detect if the main receptors for KC and SDF-1 α , CXCR2 and CXCR4 respectively, were present on HPC-7. Both receptors were present on the HPC-7 surface (**Figure 4.6.A-B**).

4.3.7 The chemokines KC and SDF-1 α are involved in HPC-7 homing to the kidney

To understand the specific roles of the chemokines KC and SDF-1 α in HPC-7 trafficking to the kidney, the healthy kidney was bathed in either chemokine for 4 hours and then naïve HPC-7 were injected into the animal intra-arterially. Renal HPC-7 recruitment was significantly increased when a healthy kidney was topically exposed to KC ($p < 0.05$; **Figure 4.7.A**) or SDF-1 α ($p < 0.01$; **Figure 4.7.B**) when compared to PBS controls (AUC: KC: 457.2 ± 79.55 ; SDF-1 α : 393.5 ± 26.87 ; PBS: 299.7 ± 16.59). When imaged at 4 hours post KC exposure, increased HPC-7 adhesion was observed. However, this was not the case with exposure to SDF-1 α , where the adhesion was a more gradual process peaking at around 4½ hours post-SDF-1 α exposure. *Ex vivo* analysis confirmed the increases that are seen in one field of view after topical KC and SDF-1 α treatment during the intravital studies are universal in different areas of the kidney (CPF: KC kidney: 32.85 ± 4.118 ; $p < 0.05$; **Figure 4.7.D**; SDF-1 α kidney: 26.73 ± 2.536 ; $p < 0.05$; **Figure 4.7.E**; PBS: 17.20 ± 3.200). No difference in HPC-7 adhesion was observed in the CL kidney (**Figure 4.7.D-E**).

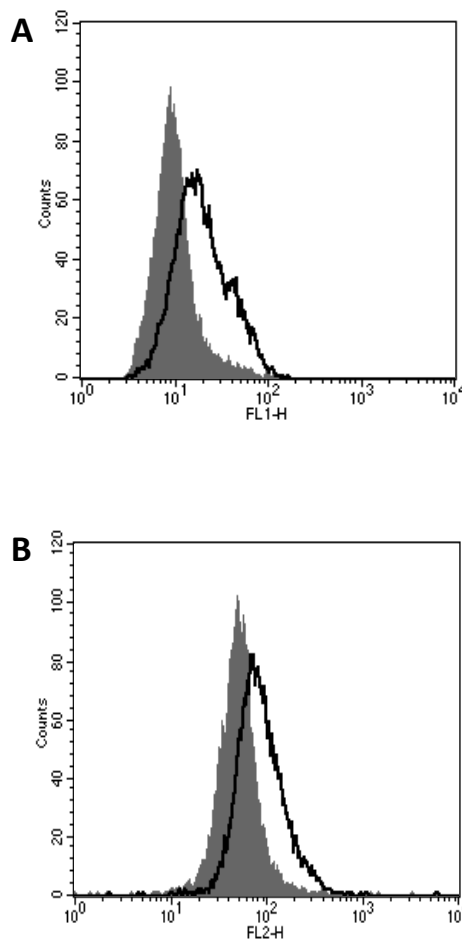


Figure 4.6. HPC-7 express chemokine receptors, CXCR2 and CXCR4, on their surface. Flow cytometry was used to determine if HPC-7 express the receptors to the chemokines KC and SDF-1 α , CXCR2 and CXCR4 respectively. Both CXCR2 (**panel A**; grey line and fill: IgG treated HPC-7; black line: CXCR2) and CXCR4 (**panel B**; grey line and fill: IgG treated HPC-7; black line: CXCR4) are expressed on HPC-7.

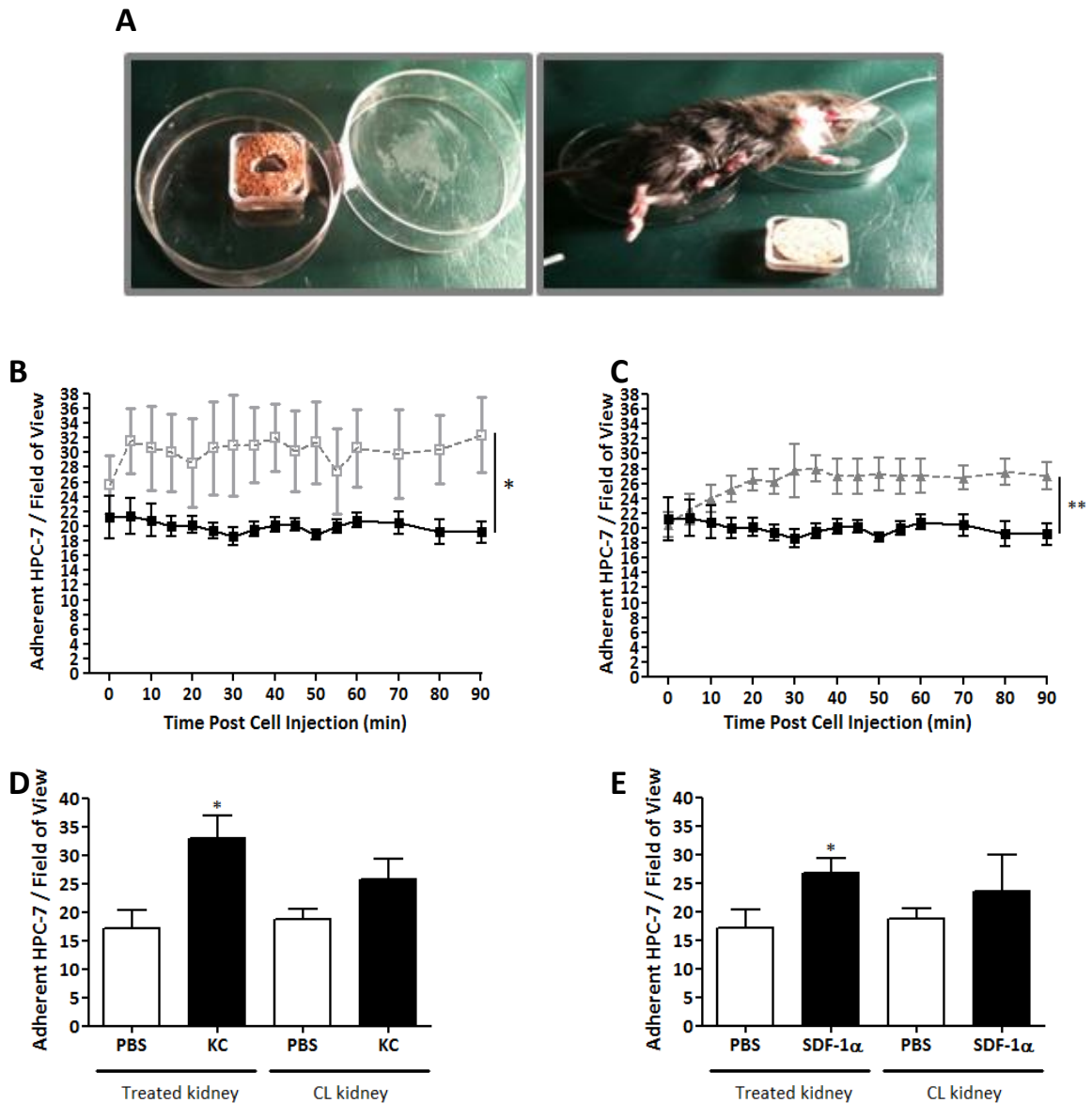


Figure 4.7. Chemokines KC and SDF-1 α both help to recruit HPC-7 to the kidney. Healthy kidneys were exteriorised and immersed in a bath containing KC [200ng/ml] or SDF-1 α [200ng/ml] for 4 hours (**panel A**). Topical chemokine baths were removed and 2×10^6 HPC-7 were injected intra-arterially into the animal and subsequent HPC-7 adhesion was monitored intravitaly. There was a significant increase in HPC-7 recruitment compared to the PBS control after both KC (**panel B**: black line: PBS treated kidney; grey line: KC treated kidney) and SDF-1 α (**panel C**: black line: PBS treated kidney; grey line: SDF-1 α treated kidney) topical treatments. *Ex vivo* analysis of the kidneys post KC and SDF-1 α topical treatment confirms there is an overall increase in the number of adherent HPC-7 after both treatments (**panel D and E**) but not in the non-treated right contralateral kidney. PBS controls are of the same cohort in both KC and SDF-1 α topical experiments. Plots represent a mean adhesion \pm SEM of at least 4 separate experiments; * $p < 0.05$; ** $p < 0.01$. **Panels B and C**: area under the curve calculation; **panels D and E**: unpaired t-test.

4.3.8 Both KC and SDF-1 α topical treatments cause decreases in free-flowing HPC-7

Interestingly, a significant decrease in the number of free-flowing HPC-7 after KC and SDF-1 α topical treatments compared to the PBS-treated kidneys was observed (CPF: KC: 123.5 ± 31.26 ; $p < 0.001$; **Figure 4.8.A**; SDF-1 α : 49.75 ± 7.878 ; $p < 0.001$; **Figure 4.8.B**; PBS: 174.4 ± 22.72). To decipher if these chemokines were having an effect on renal blood flow, perhaps through vaso-regulation, we utilised laser-speckle microscopy to monitor any changes in blood flow throughout the four hour topical exposure period and the following 45 minutes after HPC-7 were injected. There was no change in blood flow in the kidney after SDF-1 α treatment at any time point when compared to corresponding time point in the PBS control kidney (**Figure 4.8.C**). However, blood flow does decrease in PBS ($p < 0.05$) and SDF-1 α (0.001) after 4 hour topical treatments when compared to the blood flow prior to PBS or SDF-1 α treatment. There was not a change in blood flow after exposure to KC compared to the blood flow prior to KC treatment. In fact, blood flow was significantly sustained in the healthy kidney that received KC topical treatment when compared to the PBS control at 4 hours topical treatments, 5 min (the point of HPC-7 infusion), 10 min and 15 min post-topical treatment (**Figure 4.8.C**). The speed of the free-flowing cells within the first 1 minute recording was also calculated in each of the treated kidneys: after SDF-1 α topical treatment, HPC-7 moved slower in the first 1 minute recording, although this did not reach significance. However, there was no difference in HPC-7 speed within the KC-treated kidney compared to the PBS control (**Figure 4.8.D**). Free flowing cells were defined as the total number of cells observed flowing through the field of view in a 1 minute time-frame of continuous observation; the blood circulation time for a mouse is approximately 4-6 seconds, thus meaning blood circulates

Chapter 4: Mechanisms that Govern HSC Recruitment to the Injured Kidney

approximately 10 times during a 1 minute observation period. To determine whether HPC-7 only passed once through the kidney or if they were re-circulated, numbers of freely flowing cells at 6 second intervals were determined for the first observation minute. Less freely circulating HPC-7 were observed at each 6 second time point for the first minute following KC or SDF-1 α topical treatment, suggesting more were lost to extra-renal sites (**Figure 4.8.E**).

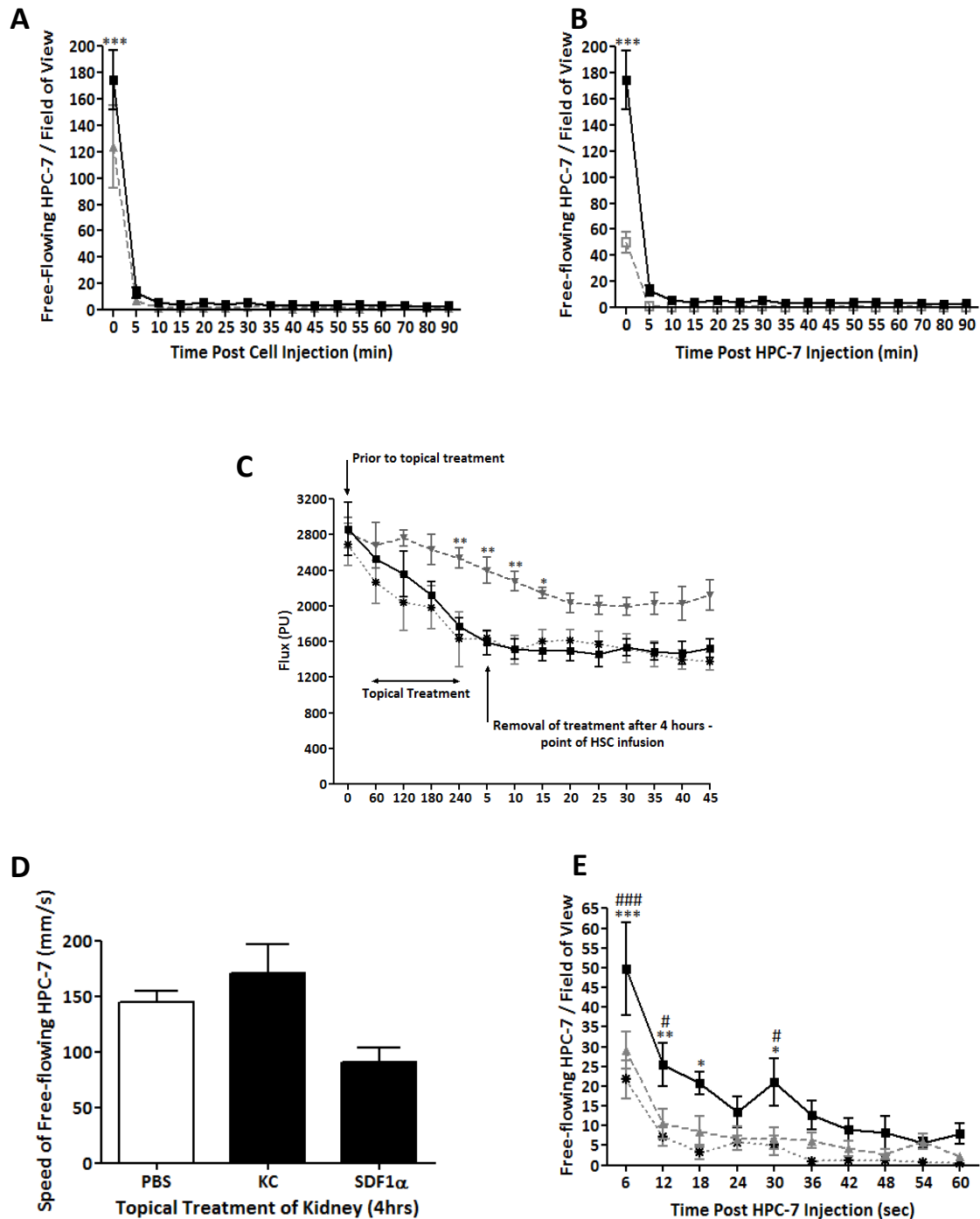


Figure 4.8. Topical kidney treatment with KC and SDF-1α [200ng/ml] decreases free-flowing HPC-7 to the kidney. The number of free-flowing HPC-7 after topical treatments was quantified: KC (**panel A**) and SDF-1α (**panel B**) topical treatment of a healthy kidney significantly reduced the number of free-flowing HPC-7 (Black line: PBS treated kidney; grey line: chemokine treated kidney). This effect only occurred at the point of infusion. There was no difference in blood flow at any time points when comparing SDF-1α and PBS treated kidneys (**panel C**; square black line: PBS treated kidney; black star grey line: SDF-1α treated kidney). There was a decrease in blood flow after SDF-1α and PBS 4 hour topical treatments when compared to their blood flow prior to treatment. KC

Chapter 4: Mechanisms that Govern HSC Recruitment to the Injured Kidney

significantly stabilised blood flow at 4 hours treatments and 5 min, 10 min and 15 min after KC treatment time points, compared to the same time points in the PBS treated kidney (**panel C**; square black line: PBS treated kidney; triangle grey line: KC-treated kidney). There were no changes in HPC-7 speed in the first 1 minute recording after chemokine treatments (**panel D**). Number of free-flowing HPC-7 within topically treated kidneys were analysed for each circulatory pass: significantly less HPC-7 were seen upon each circulatory pass after KC and SDF-1 α topical treatments (**panel E**; square black line: PBS treated kidney; triangle grey line: KC-treated kidney; # $p < 0.05$, ### $p < 0.001$; black star grey line: SDF-1 α treated kidney; * $p < 0.05$; ** $p < 0.01$, *** $p < 0.001$). Plots represent a mean adhesion \pm SEM of at least 4 separate experiments; * $p < 0.05$, ** $p < 0.01$, *** $p < 0.001$. **Panels A, B, C and E**: two-way ANOVA with bonferroni post-tests; **panel D**: one-way ANOVA with Dunnett's post-tests.

4.3.9 A direct role of CXCR2 and CXCR4 in HPC-7 recruitment was confirmed *in vivo*

A role for KC and SDF-1 α in mediating HPC-7 recruitment to injured kidney was also demonstrated, as functionally blocking CXCR2 ($p<0.05$) or CXCR4 ($p<0.01$) on HPC-7 significantly decreased adhesion within injured kidney *in vivo* compared to IgG control (AUC: anti-CXCR2: 212.3 ± 20.94 ; anti-CXCR4: 150.0 ± 22.96 ; IgG: 288.3 ± 20.69 ; **Figure 4.9.A-B**); this decrease was more pronounced when blocking CXCR4. The results seen *in vivo* in the one field of view were again consistent to what was seen throughout the kidney, as demonstrated by our *ex vivo* data (CPF: anti-CXCR2 IR: 10.80 ± 1.273 ; anti-CXCR4 IR: 9.750 ± 0.5439 ; IgG: 18.52 ± 3.533 ; **Figure 4.9.C-D**). HPC-7 adhesion to the non-injured CL kidney was also quantified; there were significantly less HPC-7 adherent to the CL kidney after blocking surface expression of CXCR2 and CXCR4 (CPF: anti-CXCR2 CL: 11.87 ± 1.225 ; $p<0.001$; anti-CXCR4 CL: 11.60 ± 1.995 ; $p<0.01$; IgG: 23.52 ± 2.290 ; **Figure 4.9.E-F**). There was also a significant ($p<0.001$) increase in the number of free-flowing HPC-7 after blocking CXCR2 and CXCR4 (CPF: anti-CXCR2: 89.00 ± 3.571 ; anti-CXCR4: 103.3 ± 15.39 ; IgG: 73.00 ± 10.37 ; **Figure 4.9.G-H**). This effect occurred at the point of infusion only.

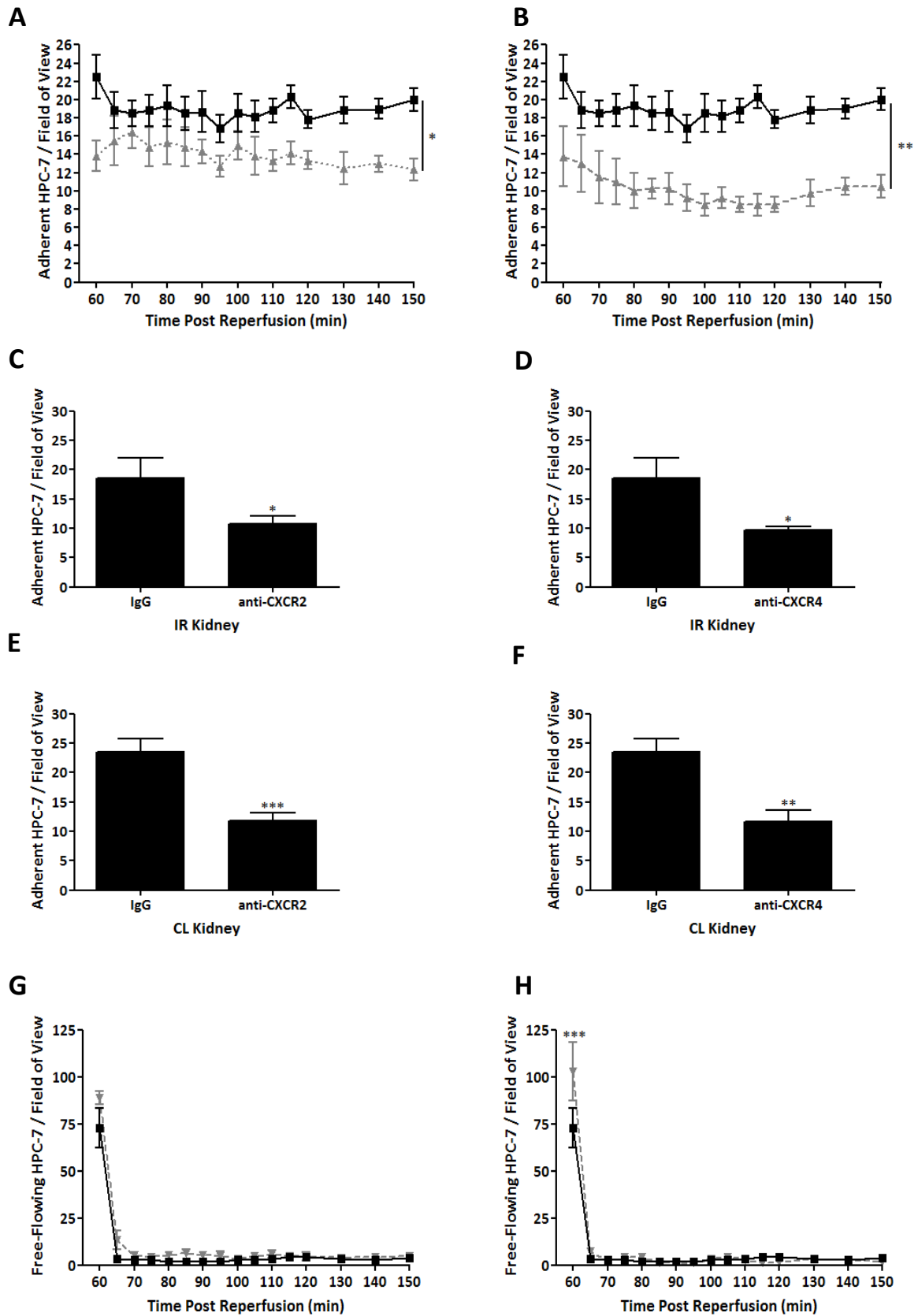


Figure 4.9. Both CXCR2 and CXCR4 chemokine receptors are required for the adhesion of HPC-7 to renal IR injury. HPC-7 surface expression of CXCR2 and CXCR4 was blocked by

incubating cells with 50µg/ml and 40µg/ml of function-blocking monoclonal antibodies respectively, for 30 minutes prior to administration into the animal model of renal IR injury. Animals were subjected to 45 minutes ischaemia and 1 hour reperfusion, prior to receiving an intra-arterial bolus of 2×10^6 CFSE-labelled CXCR2/CXCR4-blocked HPC-7. One field of view was selected and 1 minute recordings every 5 minutes started from the point of infusion (60 minutes post-reperfusion). After 2 hours reperfusion, recordings were taken for 1 minute every 10 minutes for the remaining 30 minutes. HPC-7 adhesion to the renal peritubular capillaries was examined using intravital microscopy. HPC-7 adhesion to the injured vasculature is significantly decreased after blocking HPC-7 surface expression of CXCR2 (**panel A**) and CXCR4 (**panel B**) compared to IgG controls (black line: IgG treated HPC-7; grey line: anti-CXCR2/CXCR4 treated HPC-7). *Ex vivo* analysis of the IR kidney confirms there is an overall decrease in the number of adherent HPC-7 after anti-CXCR2 (**panel C**) and anti-CXCR4 treatment (**panel D**). Similar decreases are also seen in the contralateral kidney after anti-CXCR2 (**panel E**) and anti-CXCR4 treatment (**panel F**). There were also decreases in the number of free-flowing HPC-7 when blocking CXCR2 (**panel G**) and CXCR4 (**panel H**) on the HPC-7 surface. IgG controls are from the same cohort as Figure 4.1 to reduce the number of animals used. Plots represent a mean adhesion \pm SEM of at least 5 separate experiments; * $p < 0.05$. **Panels A and B**: area under the curve calculation; **panels C, D, E and F**: unpaired t-test; **panels G-H**: two-way ANOVA with bonferroni post-tests.

4.4 Major Findings of Chapter 4

FINDING		HOW?
1	CD18 on HPC-7 surface is not needed for their recruitment to the IR-injured kidney	<i>In vivo</i> and <i>ex vivo</i> : Intravital microscopy HPC-7 pre-treated with function blocking antibodies
2	CD49d and CD44 on HPC-7 surface is required for their adhesion to the IR-injured kidney	<i>In vivo</i> and <i>ex vivo</i> : Intravital microscopy HPC-7 pre-treated with function blocking antibodies
3	Endothelial VCAM-1 is required for HPC-7 adhesion to the IR-injured kidney	<i>In vivo</i> and <i>ex vivo</i> : Intravital microscopy Intra-arterial injection of function blocking antibodies
4	Endothelial hyaluronan is required for HPC-7 adhesion to the IR-injured kidney	<i>In vivo</i> and <i>ex vivo</i> : Intravital microscopy Intra-arterial injection of function blocking antibodies
5	Endothelial CD44 is not required for HPC-7 adhesion to the IR-injured kidney	<i>In vivo</i> and <i>ex vivo</i> : Intravital microscopy Intra-arterial injection of function blocking antibodies
6	CD49d on HPC-7 and endothelial hyaluronidase govern HPC-7 adhesion to the CL kidney after renal IR injury	<i>Ex vivo</i> : Intravital microscopy
7	Topical KC and SDF-1α can cause HPC-7 adhesion to a healthy kidney	<i>In vivo</i> and <i>ex vivo</i> : Intravital microscopy
8	KC helps stabilise blood flow after topical treatment	<i>In vivo</i> : Laser speckle contrast microscopy
9	CXCR2 and CXCR4 on HPC-7 govern HPC-7 adhesion to the IR-injured kidney	<i>In vivo</i> and <i>ex vivo</i> : Intravital microscopy
10	CXCR2 and CXCR4 on HPC-7 govern HPC-7 adhesion to the CL kidney after renal IR injury	<i>In vivo</i> and <i>ex vivo</i> : Intravital microscopy

4.5 Discussion

Despite the general excitement about SC clinical trials, a major lack of understanding of how SCs home to injured tissues quite likely hinders their overall success. To improve the potential regenerative efficiency of these rare cells, an increased understanding of homing mechanisms and in particular site-specific recruitment, would be of benefit. HSCs are ultimately involved in generating blood cells and so their adhesion to injured vasculature might be similar to that of leukocyte adhesion. Therefore, CD18, CD49d and CD44, which are well-established in playing critical roles in leukocyte adhesion, were investigated using our intravital model of renal IR injury. We have shown that HPC-7 adhesion within the injured kidney *in vivo* is dependent upon CD44 and CD49d interactions with endothelial HA and VCAM-1 respectively. Both of these endothelial ligands are known to be up-regulated in IR injured kidney (Johnsson *et al.* 1996; Burne *et al.* 2001; Akhtar *et al.* 2010). Interestingly, blocking these adhesion molecules or their endothelial counter-ligands only inhibited HPC-7 adhesion in the IR injured but not the CL non-injured kidney; it is possible that critical endothelial counter-ligands were only upregulated during high levels of oxidative stress and endothelial cell destruction, which would have occurred to a greater degree in the actual injured rather than CL kidney.

A role for these particular adhesion pathways in a wide variety of other scenarios is well described. The VLA-4 integrin ($\alpha_4\beta_1$; CD49d/CD29) is also responsible for mediating tethering, rolling and firm adhesion of leukocytes to VCAM-1 (Springer 1994; Ley and Tedder 1995) and this pathway is used in homing exogenous HSCs to the BM in a lethally irradiated host. We have previously shown a critical role for CD49d/VCAM-1 interactions

Chapter 4: Mechanisms that Govern HSC Recruitment to the Injured Kidney

in mediating HSC recruitment to the liver and the cremaster muscle post IR injury (Kavanagh *et al.* 2010). Furthermore, treating progenitor cells with a VLA-4 mAb causes less homing to the BM thus increasing the number of circulating cells (Papayannopoulou *et al.* 1995). The VLA-4/VCAM-1 and CD44/HA pathways are also implicated in causing the adhesion of metastatic B-cells to endothelium (Okada *et al.* 1999).

CD44 is also used by MSCs to migrate on and towards HA (Zhu *et al.* 2006; Herrera *et al.* 2007). With respect to endothelial counter-ligands, HA isn't the sole partner for CD44, as it has been shown to interact homotypically with CD44 expressed on endothelial cells (Termeer *et al.* 2001). However, while CD44 is up-regulated on renal capillary ECs after IR injury (Lewington *et al.* 2000), we found that CD44 homotypic interactions did not govern HSC adhesion in our renal IR injury model. Although blocking endothelial CD44 *in vivo* did not affect adherent HSC numbers in our injury model, it may have other benefits as CD44^{-/-} mice have a reduced influx of neutrophils and improved kidney function after IR injury compared to WT mice (Rouschop *et al.* 2005). Interestingly, studies suggest the CD44/HA pathway also governs MSC recruitment in the glycerol-induced model of AKI (Herrera *et al.* 2007). This study utilised immunohistochemistry and electron microscopy to demonstrate that only CD44^{+/+} and not CD44^{-/-} MSCs could be located within the renal cortex. More importantly, it demonstrated that MSCs lacking CD44 could not be recruited to the kidney and that this directly resulted in a loss of therapeutic renal benefit, clearly demonstrating that the active local recruitment of SCs using surface adhesion molecules, such as CD44, is an essential pre-requisite for their beneficial effect.

Chapter 4: Mechanisms that Govern HSC Recruitment to the Injured Kidney

The β_2 integrin sub-unit CD18 was not involved in mediating HPC-7 recruitment to our IR injured kidney model. Interestingly, CD18 has been implicated in governing HSC recruitment to injured gut and to IR injured cremaster muscle venules (Kavanagh *et al.* 2013), which further supports previous data illustrating that the β_2 integrin is important during HSC and progenitor cell adhesion to endothelial cells and their subsequent transmigration (Imai *et al.* 1999; Peled *et al.* 2000). In contrast, studies by Papayannopoulou and colleagues have shown that HSC homing to the bone marrow is not dependant on CD18; although, the CD18-deficient mice in this study do have altered HSC homing when CD49d/CD29 functions are inhibited, suggesting that CD18 can contribute to BM recruitment but in a redundant fashion (Papayannopoulou *et al.* 2001). As it stands, the role of the β_2 integrin in HSC recruitment to different sites is not clear-cut, suggesting that there may be a degree of site specificity with regards to the adhesive mechanisms involved. This further shows that understanding site-specificity is vital when developing strategies to target SC adhesion within specific organs.

In the second part of this chapter we investigated whether chemokines, such as SDF-1 α and KC, could also influence HPC-7 recruitment. For chemokines to elicit chemotaxis *in vivo* these basic proteins are secreted by the endothelium and are bound and immobilised by particular glycoaminoglycans (GAGs) within the ECM or at the surface of vascular endothelium (Kuschert *et al.* 1999). Chemokine presentation via GAGs forms chemokine gradients that can influence and interact with corresponding GAGs on passing leukocytes that express the chemokine counter-receptor. Using a novel preparation that immerses the exteriorised kidney in chemokine, we demonstrated that both SDF-1 α and

Chapter 4: Mechanisms that Govern HSC Recruitment to the Injured Kidney

KC could both promote HSC adhesion within a healthy kidney. In agreement with our studies, Togel *et al.* (2005) observed that SDF-1 α plays an important role in mediating the homing of CXCR4⁺ BM-derived cells in IR injured kidney. Also, in the heart, SDF-1 α expressing plasmids were transplanting into various ischaemic myocardial zones and this caused an increase recruitment of primary HSCs to the site of damage. Conversely, Stroo *et al.* (2009) showed that manipulating the SDF-1 α /CXCR4 axis, either by increasing local SDF-1 α concentrations in the injured kidney or by blocking CXCR4 on HSCs, did not affect their migration; however, they injected recombinant SDF-1 α into just one focal point in the kidney, which may explain this discrepancy. Although SDF-1 α is currently considered one of the most potent chemokines mediating SC homing both to the BM and to extramedullary tissues (Peled *et al.* 1999; Wright *et al.* 2002; Schulz *et al.* 2009), it was interesting to observe that HSC adhesion to the KC-exposed healthy kidney was more rapid than SDF-1 α treatment. This is the first time a novel role for this classical neutrophil chemoattractant has been directly demonstrated in mediating SC recruitment in a tissue bed.

Topical exposure of SDF-1 α to the healthy kidney did not elicit a change in blood flow compared to the PBS treated control; however after 4 hours topical exposure to both SDF-1 α and PBS, there was a decrease in renal blood flow compared to the initial blood flow measurement prior to topical treatments. During topical treatments, 1ml of fluid had to be replaced every hour and this could be due to the kidney absorbing the solution; this potentially could be leading to tissue swelling, which could influence blood flow by physically constricting or compressing the blood vessels. It is well known that oedema,

Chapter 4: Mechanisms that Govern HSC Recruitment to the Injured Kidney

which results from fluid loss from vessels into the interstitium, can compress capillaries; therefore what we may have inadvertently caused with these topical experiments is a kind of outside-in oedema. A point to also make is that we have removed the tough fibrous kidney capsule to improve vascular imaging; one of its functions is to limit the expansion of the tissue spaces in response to oedemagenic stress. What is important to note is that despite the reduced renal blood flow at the point of cell infusion after 4 hours topical treatment, increased adhesion of HPC-7 was still observed in SDF-1 α treated kidneys and since this was not demonstrated in PBS treated kidneys, it suggests SDF-1 α can actively prime circulating SCs to adhere. It is also possible that the increased adhesion is because they are flowing through the kidney at a lower velocity and so the potential for adhesive interactions to take place is increased.

After 4 hours of KC topical treatment, there was not a reduction in renal blood flow to such a great degree from resting starting blood flow, as seen in SDF-1 α or PBS topical treatments. Fluid was still lost from the bath during KC topical treatments, so it is likely that the kidney still absorbed the treatment but somehow topical KC treatment may have stabilised any changes in blood flow. KC has been shown to stimulate mesangial cells of the kidney to release prostaglandin E2 (Tsai *et al.* 2004), which is an effective vasodilator at low concentrations and can increase blood flow to the kidney and other areas (Haylor and Towers 1982; Purdy and Arendshorst 2000; Nakatsuka *et al.* 2005; Rincon-Sanchez *et al.* 2005); this could likely explain the sustained blood flow seen in the KC topical treated kidneys.

Chapter 4: Mechanisms that Govern HSC Recruitment to the Injured Kidney

The exposure of the healthy kidney to chemokines does highlight that they can induce SC adhesion, despite changes in renal blood flow. Furthermore, both chemokines played a significant role in modulating adhesion in the injured kidney, as blocking CXCR2 and CXCR4 inhibited their recruitment. Although the SDF-1 α /CXCR4 pathway is well established regarding SC trafficking, this is the first time that KC and its main receptor CXCR2 have been shown to be involved in SC recruitment and was published this year (White *et al.* 2013). KC can also interact with murine CXCR1 (Fan *et al.* 2007), but the role of this receptor in HSC recruitment was not investigated in this study. CXCR2 has however been showed to be involved in other types of cellular recruitment: Morgan *et al.* (1997) used intravital microscopy to demonstrate that CXCR2-deficient mice exhibited a decrease in the adhesion of activated leukocytes (mainly neutrophils) and an increase in rolling leukocytes velocity in the cremaster venules: this demonstrates that this receptor may be involved in slowing down leukocytes so that then β_2 integrins can cause full arrest. We have shown that blocking CD18 does not affect adhesion of HSCs in renal IR injury, therefore it is unlikely that CXCR2 and CD18 are working cooperatively within our model. CXCR4 and CXCR2 regulate neutrophil extravasation into the peripheral circulation by working antagonistically to each other (Eash *et al.* 2010). The relationship between CXCR4 and HSCs is well characterised and a genetic deletion of CXCR4 in murine haematopoietic cells or an injection of AMD3100 (CXCR4 antagonist) actually increases their mobilisation into the circulation from the BM (Broxmeyer *et al.* 2005; Eash *et al.* 2009). Also, neutralising CXCR4 abrogated the migration of CD34⁺ cells towards injured kidney cells *in vitro* and *in vivo* (Togel *et al.* 2005). CXCR4 is also involved in mediating cellular migration during development, homeostasis, inflammation and regeneration.

A better understanding of the basic biology underlying SC adhesion is needed if SC therapy is to be utilized to its optimum. We have identified that KC/CXCR2 and SDF-1 α /CXCR4 pathways can regulate HSC adhesion to the kidney. However, the clinical applicability of such topical chemokine techniques is debatable and may be associated with aggravated tissue injury due to the detrimental effects SDF-1 α had on blood flow in our model and also SDF-1 α -dependent lymphocyte recruitment (Liekens *et al.* 2010). Adhesion pathways governing HSC recruitment to sites of renal injury were previously scarce but we now know that the CD49d/VCAM-1 and CD44/HA adhesion pathways are essential for HSC adhesion to the IR injured kidney. Understanding these recruitment mechanisms may enable the development of strategies that can further enhance this trafficking; one way could be to modulate the important adhesion molecules on the HSC surface, which could potentially lead to more rapid, efficient and longer lasting tissue repair. Therefore, the following chapter will focus on ways of improving renal retention of HPC-7.

Chapter 5



Methods of Enhancing HSC Recruitment to the Injured Kidney

5 Methods of Enhancing Haematopoietic Stem Cell Adhesion to the IR Injured Kidney

5.1 Introduction and Hypotheses

5.1.1 Introduction

A variety of chemical mediators are released from inflamed kidney, including cytokines and ROS: these can activate adhesion molecules on trafficking HSCs in a similar manner to leukocytes and subsequently initiate their adhesion to microvessels (Seegerer *et al.* 2000). Hydrogen peroxide (H_2O_2) is known to be released by ischaemically injured tissues and sources include the damaged endothelium or the accumulating neutrophils upon reperfusion (Ardanaz and Pagano 2006). Our group have recently examined the effects of pre-treating HPC-7 with H_2O for 1 hour on HPC-7 adhesion to the IR injured gut (Kavanagh *et al.* 2012). *In vitro* and *in vivo* experiments demonstrated that H_2O_2 could increase HPC-7 adhesion to the injured gut tissue and this was mediated through enhancing the ability of HPC-7 adhesion receptors to bind to their endothelial counter-ligands. This suggests HSC homing is not maximal and that enhancement of HSC recruitment may be possible.

In Chapter 3, HPC-7 adhesion to injured kidney was increased compared to sham and this is most likely due to the injured kidney releasing factors that activate both the endothelium and the trafficking HPC-7. Cytokines are well-known inflammatory mediators that are robustly activated during IR injury (Luster 1998) and is well

documented that they provide a powerful stimulus for neutrophil recruitment to the injured tissue (Mulligan *et al.* 1998; Burne *et al.* 2001). However, how and if inflammatory cytokines/chemokines can cause HSC recruitment is less clear. Local production of IL-1 β , KC, TNF- α and SDF-1 α has been shown to be increased soon after renal IR injury and many other tissues post IR injury (Furuichi *et al.* 2002): this can provide chemoattractant cues or activate cells to enhance neutrophil recruitment and their subsequent adhesion. SDF-1 α has been extensively studied with regards to SC homing, but the roles of other signalling molecules in SC recruitment are less well known.

This chapter firstly investigates whether pre-treating SCs with media conditioned by an injured kidney can enhance HPC-7 adhesion compared to the adhesion seen without pre-treatment. We further investigated which specific cytokines/chemokines could be involved in causing enhanced adhesion to the IR kidney. The effects of HPC-7 pre-treatment with H₂O₂ were also explored, as it has been previously shown by us to be effective at modifying adhesion in the similarly injured gut (Kavanagh *et al.* 2012). Mechanistic studies were conducted to determine how the cytokine/chemokine pre-treatments could be enhancing SC adhesion; this involved looking at receptor expression and their localisation on the surface, as well as the deformability of SCs.

5.1.2 Aims and Hypotheses

The main aims and hypotheses of this chapter are:

1. Hypotheses: Pre-treatment of HPC-7 with ICM enhances their adhesion.

2. Hypotheses: Cyto/chemokines, including IL-1 β , TNF- α , KC and SDF-1 α , are responsible for any increased HPC-7 adhesion.
3. Hypotheses: Cyto/chemokines mediate HPC-7 adhesion by: increasing adhesion ligand expression; enhancing HPC-7 adhesion molecule affinity for its endothelial counter-ligand; increasing receptor clustering on the HPC-7 surface; and/or changing the deformability of HPC-7.
4. Aims: Investigate the effects of ICM and cyto/chemokine pre-treatment of HPC-7 both *in vitro* and *in vivo* and use flow cytometry, static adhesion assays and confocal microscopy to determine the mechanisms of their action.

5.2 Methods

The methods used in this chapter are described in detail in Chapter 2. Briefly, ICM and SCM were prepared from homogenised kidney subjected to 45 minutes ischaemia and 1 hour reperfusion or sham surgery respectively. HPC-7 were pre-treated with an ICM, SCM, SDF-1 α , KC, IL-1 β , TNF- α or H₂O₂, for various durations, prior to determining their adhesion to renal sections or mouse renal endothelial cells *in vitro* or to the injured kidney *in vivo*. For *in vitro* studies, 1 x 10⁵ CFSE-labelled HPC-7 were added to each section/well and the average number of adherent cells within 5 fields of view was determined. For *in vivo* studies, 2 x 10⁶ CFSE-labelled HPC-7 were introduced via the carotid artery and one field of view was continually analysed for 90 minutes post-HPC-7 administration.

Chapter 5: Methods of Enhancing HSC Recruitment to the Injured Kidney

For mechanistic studies, HPC-7 were analysed for changes in expression of adhesion molecules following pre-treatment with KC and SDF-1 α for 5 minutes. FACS analysis was conducted using fluorescently conjugated antibodies against CD49d and CD44; these were the important adhesion molecules for governing HPC-7 adhesion to the IR injured kidney, as shown in Chapter 4. To investigate whether these chemokines enhanced the ability of HPC-7 to bind to the important endothelial ligands, pre-treated cells were added to VCAM-1 and HA, which were immobilised to plastic culture plates. To visualise adhesion molecule distribution on the surface of HPC-7, pre-treated cells were fixed to preserve any changes in receptor localisation and then CD49d and CD44 were labelled with the corresponding primary antibody followed with a fluorescent secondary antibody prior to confocal imaging. In order to understand any changes in the number of free-flowing HPC-7 after pre-treatment, a micropipette assay was carried out to assess cell deformability; this involved applying suction pressure to pre-treated cells and recording the time taken for the cell to be fully aspirated into a glass pipette of a similar diameter to a capillary.

5.3 Results

5.3.1 Media conditioned by the injured kidney can enhance HPC-7 recruitment *in vitro*

Incubating HPC-7 with ICM for 5 and 10 minutes did not enhance their adhesion to frozen IR injured renal sections compared to SCM treated controls (**Figure 5.1.A**). However, pre-treating HPC-7 for 30 minutes with ICM caused a significant ($p<0.001$) increase in adhesion compared to SCM (CPF: 30 min ICM: 113.5 ± 11.21 ; 30 min SCM: 26.67 ± 6.741 ; **Figure 5.1.A**). After 21 hours incubation, this effect was lost. Interestingly, pre-treating HPC-7 with ICM also significantly ($p<0.01$) increased their adhesion to non-injured sham frozen kidney sections after 5 minutes incubation with ICM when compared to SCM treated cells (CPF: 5 min ICM: 18.14 ± 3.04 ; 5 min SCM: 7.43 ± 2.33 ; **Figure 5.1.B**). After longer HPC-7 pre-treatments this increased adhesion was lost. Also, HPC-7 adhesion to sham sections was to a lesser extent in comparison to what is observed with ICM on IR tissue sections.

Immortalised renal endothelium was given to our lab as a kind gift from Dr. J. Steven Alexander, LSU-HSC, USA. Pre-treating HPC-7 with ICM for 30 minutes also enhances their adhesion to PBS and TNF- α treated renal endothelium (CPF: 30 min ICM + PBS endo: 27.08 ± 2.313 ; 30 min SCM + PBS endo: 9.843 ± 0.6639 ; 30 min ICM + TNF- α endo: 17.54 ± 4.714 ; 30 min SCM + TNF- α endo: 9.843 ± 0.6639 ; **Figure 5.1.C-D**).

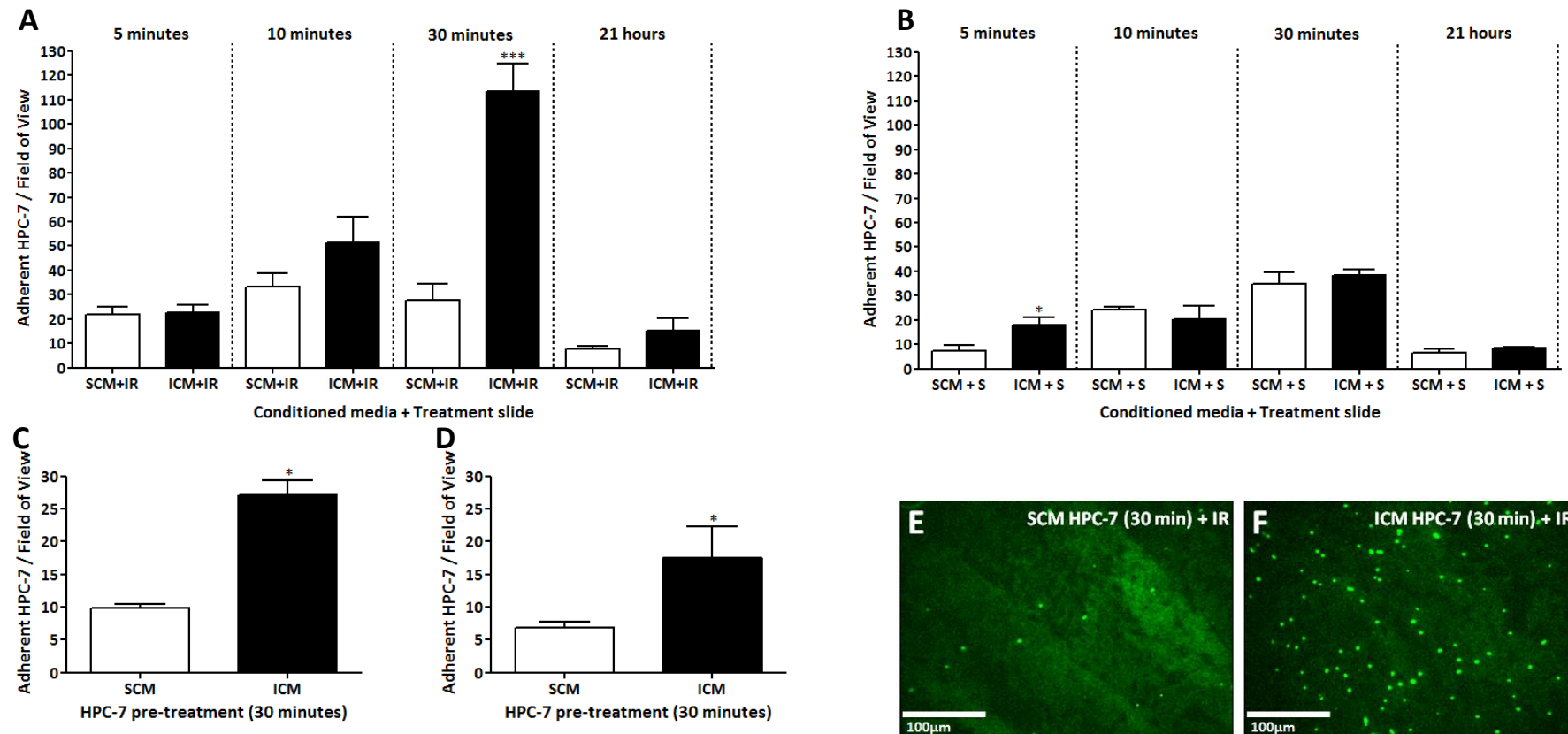


Figure 5.1. Pre-treatment of HPC-7 with injured conditioned media (ICM) for 30 minutes significantly increases HPC-7 adhesion in vitro. A significant increase in HPC-7 adhesion to frozen kidney IR injured sections compared to SCM pre-treated HPC-7 controls was only observed after 30 minutes pre-treatment with an ICM (**panel A**). ICM pre-treatment for 5 minutes only enhanced HPC-7 adhesion to sham frozen kidney sections (**panel B**). 1×10^5 CFSE-labelled HPC-7 were pre-treated with ICM and SCM for 30 minutes and applied to PBS and TNF- α treated endothelium: pre-treating HPC-7 with ICM caused enhanced HPC-7 adhesion to both PBS (**panel C**) and TNF- α (**panel D**) treated murine renal endothelium. Representative images of HPC-7 adhesion to IR kidney sections with SCM (**panel E**) and ICM (**panel F**) are shown. Plots represent a mean adhesion \pm SEM of at least 4 separate experiments; * $p < 0.05$; *** $p < 0.001$. **Panels A and B**: one-way ANOVA with bonferroni post-tests; **panels C and D**: unpaired t-test.

5.3.2 Increased levels of small molecular weight proteins are within the IR injured kidneys

Samples of the SCM and ICM were denatured, run through a 10% SDS polyacrylamide gel and subsequently stained with Coomassie: this demonstrated that there were differences in protein expression levels between ICM and SCM (**Figure 3.5.A**). However, as this 10% gel does not show the expression of smaller molecular weight proteins, a 15% polyacrylamide SDS gel was also prepared, as this denser gel allowed smaller proteins to be resolved. Differences in proteins bands were again seen between the ICM and SCM: most notably there was a larger band between 7-19 kDa in the ICM compared to the SCM (**Figure 3.5.B**). The amount of protein loaded into each ladder was not quantified but an equal volume of each kidney conditioned media was applied to each lane.

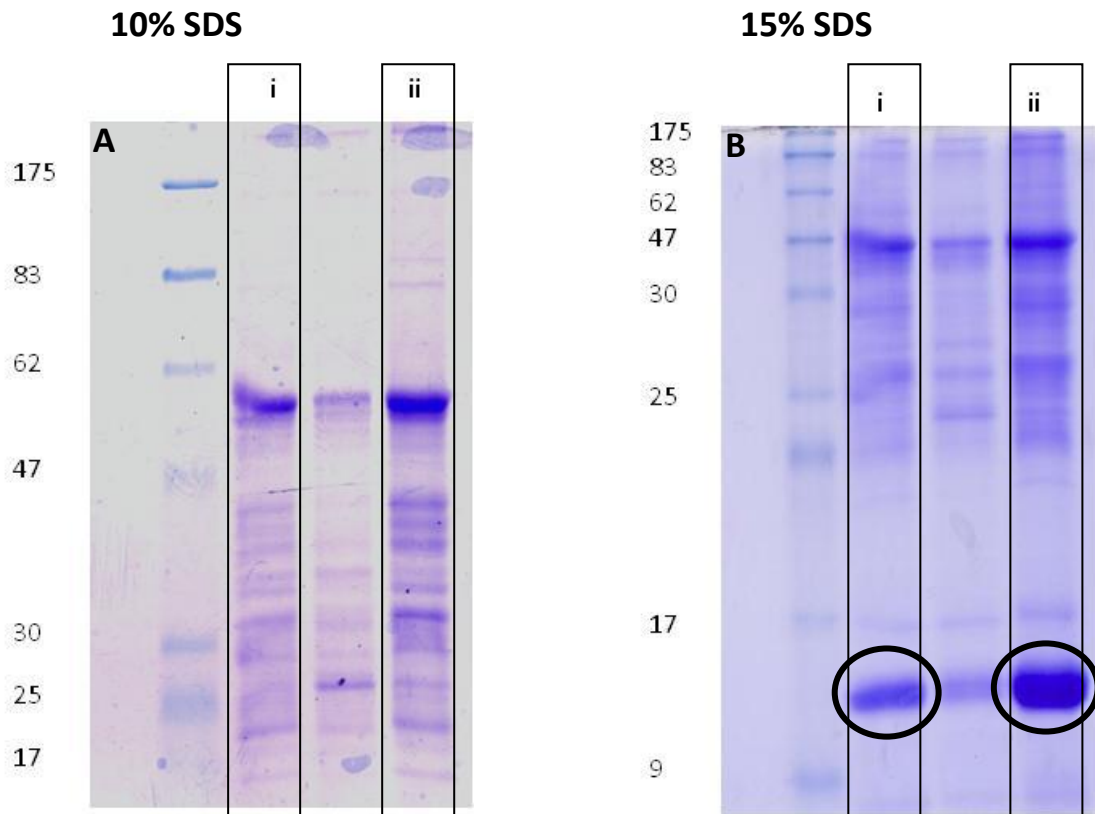


Figure 5.2. *There is a greater presence of small molecular weight proteins in the injured kidney conditioned media.* After injury, the kidney is known to release multiple soluble and pro-inflammatory factors that can activate both the endothelium and trafficking SCs resulting in increased HPC-7 adhesion. Therefore, kidney homogenates from injured and sham kidneys were prepared and the same volume was applied to a SDS polyacrylamide gel to separate the proteins. A protein ladder of known weights was also run down the left-hand side as a reference. Initially a 10% SDS gel was used and there was a clear difference in the bands between the SCM (**row i**) and ICM (**row ii**). The ICM showed thicker bands, containing a higher amount of smaller proteins, when compared to SCM (**panel A**). To resolve differences in smaller proteins than 19 kDa, such as cytokines, we increased the concentration of SDS to 15%, as this denser gel allows smaller proteins to resolve through more slowly. There is a distinctly thicker band in the ICM column (**row ii**) in the 7-19 kDa weight range compared to SCM (**row i**; **panel B**).

5.3.3 Pre-treating HPC-7 with low doses of SDF-1 α enhances HPC-7 adhesion *in vitro*

Most murine inflammatory cytokines have a molecular weight between 7-19 kDa. It is therefore likely that a cyto/chemokine with a molecular weight in this range is mediating the pro-adhesive effects observed with the ICM. SDF-1 α is a chemokine that is well known to be increased after renal IR injury (Togel *et al.* 2005) and has a molecular weight of 8 kDa. Therefore, HPC-7 were pre-treated with different concentrations of SDF-1 α for 5 minutes to determine any effective pro-adhesive concentrations.

Pre-treating HPC-7 with 25ng/ml SDF-1 α for 5 minutes significantly ($p<0.05$) increased adhesion to the injured kidney section compared to the PBS control (CPF: 25ng/ml: 110.8 ± 18.15 ; PBS: 19.00 ± 5.132 ; **Figure 5.4.A**). HPC-7 adhesion was not significantly different after 50ng/ml SDF-1 α or 125ng/ml SDF-1 α pre-treatments. HPC-7 that were pre-treated with these three different concentrations of SDF-1 α were also applied to TNF- α treated endothelium and again, 25ng/ml was the only pre-treatment to cause a significant increase in HPC-7 adhesion (CPF: 25ng/ml: 33.80 ± 6.129 ; PBS: 7.560 ± 3.438 ; **Figure 5.1.B**).

5.3.4 SDF-1 α pre-treatment is the only cytokine to enhance HPC-7 adhesion using the Stamper-Woodruff assay

HPC-7 were also pre-treated with other well-known inflammatory mediators, such as IL-1 β , KC and TNF- α at 25ng/ml for 5 minutes before applying to renal IR injured tissue sections. These cyto/chemokines are all within the 7-19 kDa range (IL-1 β : 17 kDa; KC: 8

Chapter 5: Methods and Mechanisms of Enhancing HSC Recruitment to the Injured Kidney

kDa; TNF- α : 17.4 kDa) and might well be contributing to the enhanced adhesion seen in the IR kidney and could be within the ICM. The results were compared to a control pre-treatment with PBS. However, only SDF-1 α induced a significant ($p < 0.01$) increase in HPC-7 adhesion to injured kidney tissue (CPF: SDF-1 α : 110.8 ± 18.15 ; PBS: 19.00 ± 5.132 ; **Figure 5.5.A**). Pre-treated HPC-7 were also applied to sham renal tissue sections but no significant differences could be seen (**Figure 5.5.B**).

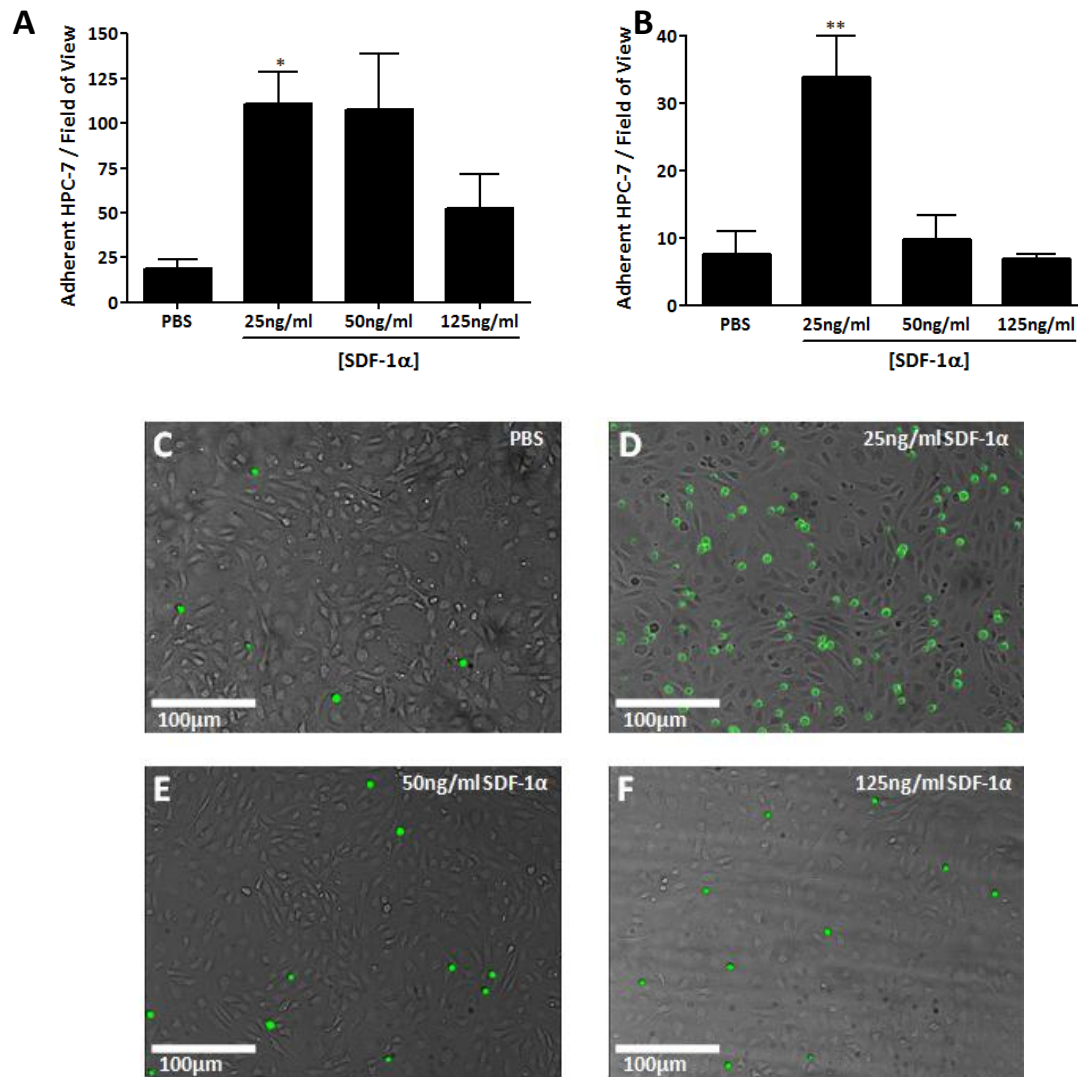


Figure 5.3. Pre-treatment of HPC-7 with varying concentrations of SDF-1α for 5 minutes produces differences in HPC-7 adhesion in vitro. Pre-treating 1×10^5 CFSE-labelled HPC-7 with 25ng/ml of SDF-1α for 5 minutes significantly enhanced HPC-7 adhesion to frozen kidney IR injured sections, using the Stamper-Woodruff assay (**panel A**). However, 50ng/ml and 125ng/ml SDF-1α pre-treatments did not cause any significant differences in HPC-7 adhesion to frozen kidney IR injured sections compared to PBS pre-treated HPC-7 controls (**panel A**). 1×10^5 CFSE-labelled HPC-7 were again pre-treated with 25ng/ml, 50ng/ml and 125ng/ml of SDF-1α for 5 minutes and applied to TNF-α treated renal endothelium: pre-treating HPC-7 with the lowest dose of SDF-1α, 25ng/ml, caused enhanced HPC-7 adhesion to TNF-α activated endothelium (**panel B**). Representative images of HPC-7 adhesion to TNF-α activated renal endothelium after PBS (**panel C**), 25ng/ml SDF-1α (**panel D**), 50ng/ml SDF-1α (**panel E**) and 125ng/ml SDF-1α (**panel F**) HPC-7 pre-treatments. Plots represent a mean adhesion \pm SEM of at least 4 separate experiments; * $p < 0.05$; ** $p < 0.01$. **Panels A and B:** one-way ANOVA with Dunnett's post-tests.

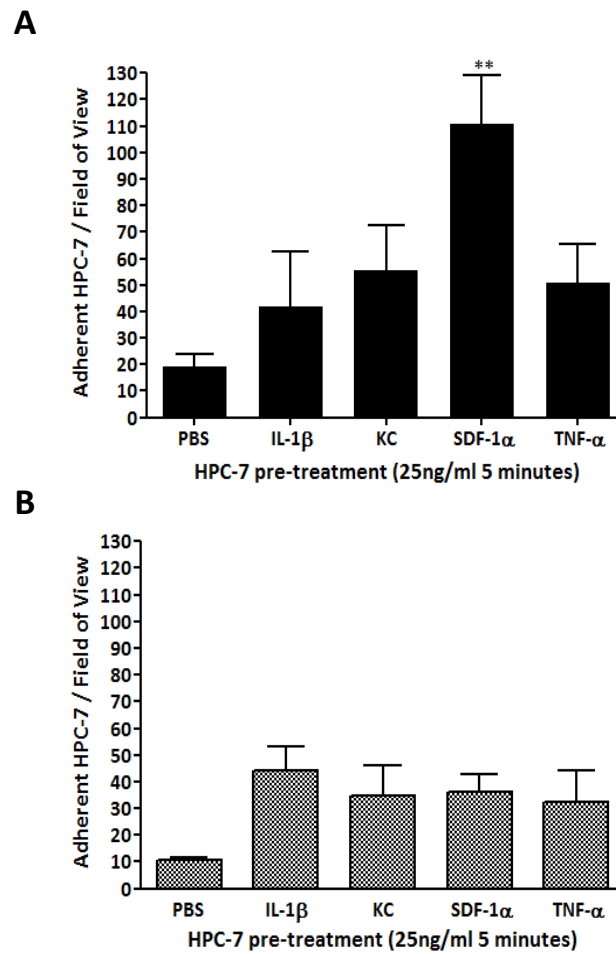


Figure 5.4. Pre-treatment of HPC-7 with 25ng/ml of IL-1 β , KC, SDF-1 α and TNF- α for 5 minutes produces differences in HPC-7 adhesion to IR injured renal sections. Pre-treating 1×10^5 CFSE-labelled HPC-7 with 25ng/ml of SDF-1 α for 5 minutes significantly enhanced HPC-7 adhesion to frozen kidney IR injured sections, using the Stamper-Woodruff assay. However, IL-1 β , KC and TNF- α HPC-7 pre-treatments did not cause any significant differences in HPC-7 adhesion to frozen kidney IR injured sections compared to PBS pre-treated HPC-7 controls (**panel A**; black fill: IR injured frozen renal sections). 1×10^5 CFSE-labelled HPC-7 were again pre-treated with 25ng/ml of all cytokines for 5 minutes and applied to sham renal sections: there were no significant differences with any cytokine pre-treatment compared to the PBS treated HPC-7 (**panel B**; grey fill: sham frozen renal sections). Plots represent a mean adhesion \pm SEM of at least 4 separate experiments; ** $p < 0.01$. **Panels A and B:** one-way ANOVA with Dunnett's post-tests.

5.3.5 KC and SDF-1 α HPC-7 pre-treatments enhance adhesion to TNF- α treated renal endothelium

HPC-7 were pre-treated at 25ng/ml for 5 minutes as before and were then applied to TNF- α treated immortalised renal endothelium. After IL-1 β and TNF- α pre-treatments, there was a slight increase in HPC-7 adhesion, but this did not reach significance. However, unlike on frozen section, this time both KC and SDF-1 α pre-treatments caused a significant ($p < 0.01$) increase to TNF- α treated endothelium (CPF: IL-1 β : 20.80 ± 3.208 ; KC: 39.16 ± 4.281 ; SDF-1 α : 33.80 ± 6.128 ; TNF- α : 20.64 ± 5.221 ; PBS: 7.560 ± 3.438 ; **Figure 5.5.A**). Pre-treated HPC-7 were also applied to PBS treated endothelium and similar results were seen as with TNF- α treated endothelium. HPC-7 adhesion increased after IL-1 β or TNF- α but the values did not attain statistical significance. However, following KC and SDF-1 α pre-treatments there were significant ($p < 0.05$ and $p < 0.01$ respectively) increases in HPC-7 adhesion compared to the PBS control (CPF: IL-1 β : 18.74 ± 2.960 ; KC: 25.96 ± 3.687 ; SDF-1 α : 39.75 ± 8.371 ; TNF- α : 22.03 ± 2.947 ; PBS: 8.600 ± 2.128 ; **Figure 5.5.B**).

5.3.6 IL-1 β pre-treatment does not enhance HPC-7 adhesion to the IR injured kidney *in vivo*

The role of various cytokines in directly mediating HPC-7 adhesion was determined *in vivo* by pre-treating HPC-7 for 5 minutes with each cytokine, starting with 25ng/ml of IL-1 β . 2×10^6 CFSE-labelled IL-1 β pre-treated HPC-7 were injected intra-arterially into a murine model of renal IR injury and the numbers of adherent and free-flowing cells were quantified. There was no significant difference in the number of adherent HPC-7 after IL-

1 β pre-treatment compared to the PBS treated HPC-7 control (AUC: IL-1 β : 300.3 \pm 25.62; PBS: 280.8 \pm 35.54; **Figure 5.6.A**). Although there was no difference in adherent HPC-7 after IL-1 β pre-treatment, there was a significant ($p < 0.001$) increase in the number of cells free-flowing in the injured mouse after IL-1 β pre-treatment (**Figure 5.6.B**).

5.3.7 KC pre-treatment enhances HPC-7 adhesion to the IR injured kidney *in vivo*

There was a significant ($p < 0.01$) increase in the number of adherent HPC-7 after KC pre-treatment compared to the PBS-treated control (AUC: KC: 449.3 \pm 30.69; PBS: 300.3 \pm 25.62; **Figure 5.7.A**). There were no significant differences in the number of free-flowing HPC-7 after KC pre-treatment compared to PBS control (**Figure 5.7.B**).

5.3.8 SDF-1 α pre-treatment enhances HPC-7 adhesion to the IR injured kidney *in vivo*

There was a significant ($p < 0.01$) increase in the number of adherent HPC-7 after SDF-1 α pre-treatment compared to the PBS treatment control (AUC: SDF-1 α : 409.3 \pm 16.67; PBS: 300.3 \pm 25.62; **Figure 5.8.A**). There was also a significant ($p < 0.001$) difference in the number of free-flowing HPC-7 after SDF-1 α pre-treatment at the point of infusion only (60 minutes reperfusion) compared to PBS control (**Figure 5.8.B**).

5.3.9 TNF- α pre-treatment enhances HPC-7 adhesion to the IR injured kidney *in vivo*

There was a significant ($p < 0.05$) increase in the number of adherent HPC-7 after TNF- α pre-treatment compared to the PBS treatment control (AUC: SDF-1 α : 409.3 \pm 16.67; PBS:

300.3±25.62; **Figure 5.9.A**). There was also a significant ($p<0.001$) difference in the number of free-flowing HPC-7 after TNF- α pre-treatment compared to PBS control (**Figure 5.9.B**).

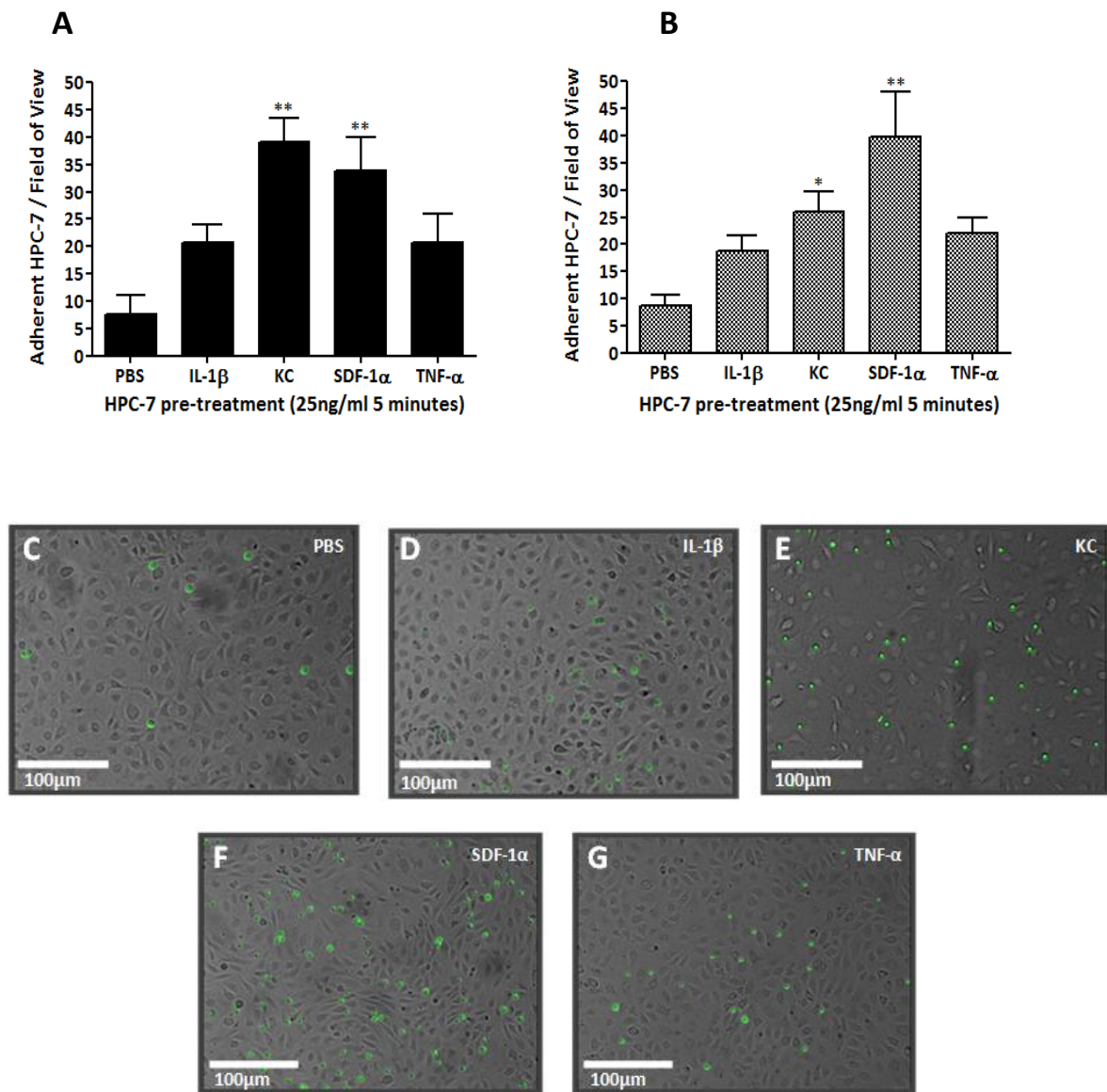


Figure 5.5. Pre-treatment of HPC-7 with 25ng/ml of IL-1β, KC, SDF-1α and TNF-α for 5 minutes produces differences in HPC-7 adhesion to immortalised renal endothelium. Pre-treating 1×10^5 CFSE-labelled HPC-7 with 25ng/ml of KC or SDF-1α for 5 minutes significantly enhanced HPC-7 adhesion to TNF-α activated renal endothelium in vitro. However, IL-1β and TNF-α HPC-7 pre-treatments did not cause any significant differences in HPC-7 adhesion to the activated endothelium compared to PBS pre-treated HPC-7 controls (**panel A**; black fill: TNF-α activated renal endothelium). 1×10^5 CFSE-labelled HPC-7 were again pre-treated with 25ng/ml of all cytokines for 5 minutes and applied to PBS treated renal endothelium: again, KC and SDF-1α were the only cytokine pre-treatments to cause a significant increase in HPC-7 adhesion (**panel B**; grey fill: PBS treated endothelium). Representative images of HPC-7 adhesion to TNF-α activated renal endothelium after PBS (**panel C**), IL-1β (**panel D**), KC (**panel E**) SDF-1α (**panel F**), TNF-α (**panel G**) HPC-7 pre-treatments. Plots represent a mean adhesion \pm SEM of at least 4 separate experiments; * $p < 0.05$; ** $p < 0.01$. **Panels A and B:** one-way ANOVA with Dunnett's post-tests.

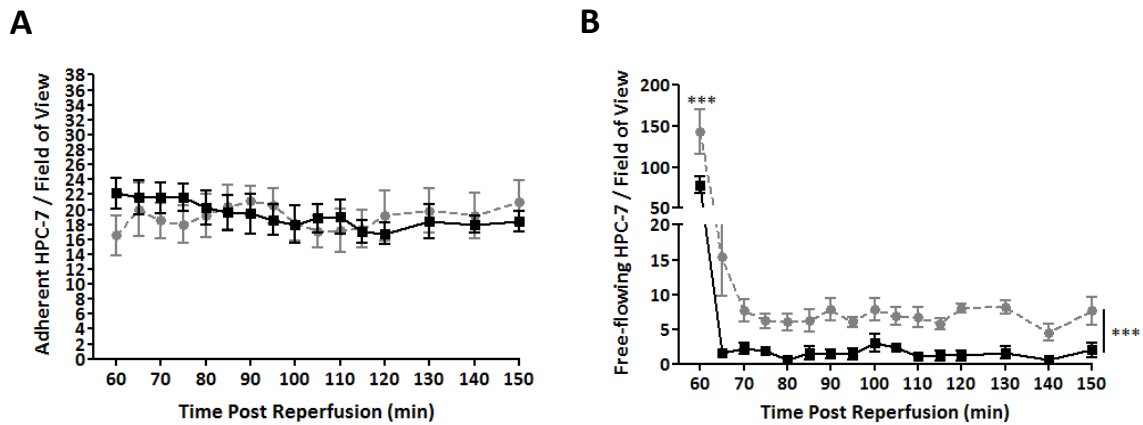


Figure 5.6. HPC-7 pre-treatment with IL-1 β does not increase adhesion but enhances the number of free-flowing HPC-7 in the injured kidney vasculature. Kidneys were clamped for 45 minutes and allowed to reperfuse for 60 minutes prior to HPC-7 administration. 2×10^6 HPC-7 were pre-treated with 25ng/ml of IL-1 β for 5 minutes, washed and then injected intra-arterially into the IR injured animal. Subsequent HPC-7 adhesion and free-flowing numbers in the IR kidney were monitored intravitaly. There was no significant increase in HPC-7 adhesion compared to the PBS control after IL-1 β treatment (**panel A**: black solid line: PBS treated HPC-7; grey dotted line: IL-1 β treated HPC-7). However the number of free-flowing cells at the point of infusion was significantly higher after cell IL-1 β treatment (**panel B**: black solid line: PBS treated HPC-7; grey dotted line: IL-1 β treated HPC-7). Plots represent a mean adhesion \pm SEM of at least 4 separate experiments; *** $p < 0.001$. **Panel A**: area under the curve calculation; **panel B**: two-way ANOVA with bonferroni post-tests.

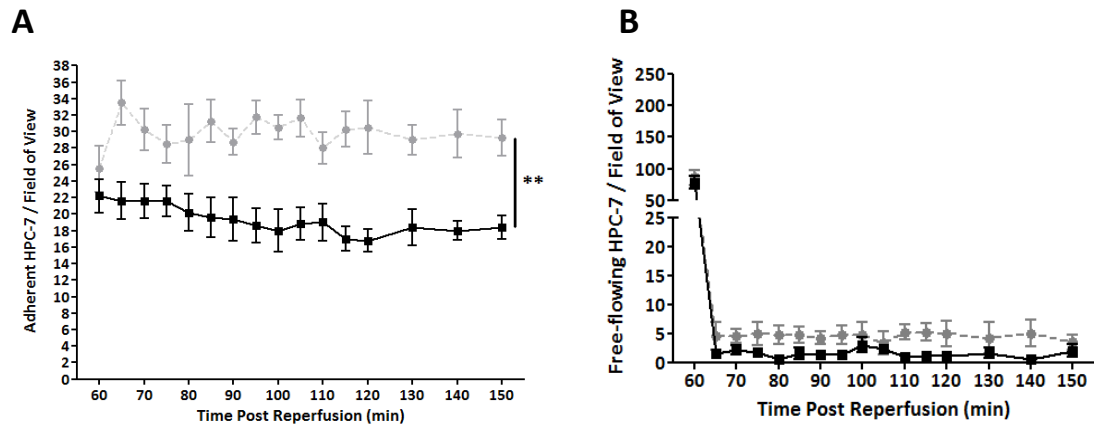


Figure 5.7. HPC-7 pre-treatment with KC increases HPC-7 adhesion but do not enhance the number of free-flowing HPC-7 in the injured kidney vasculature. Kidneys were clamped for 45 minutes and allowed to reperfuse for 60 minutes prior to HPC-7 administration. 2×10^6 HPC-7 were pre-treated with 25ng/ml of KC for 5 minutes, washed and then injected intra-arterially into the IR injured animal. Subsequent HPC-7 adhesion and free-flowing numbers in the IR kidney were monitored intravitaly. There was an increase in HPC-7 adhesion compared to the PBS control after KC treatment (**panel A**: black line: PBS treated HPC-7; grey line: KC treated HPC-7). No changes in the number of free-flowing HPC-7 were seen after KC treatment (**panel B**: black solid line: PBS treated HPC-7; grey dotted line: KC treated HPC-7). PBS controls are from the same cohort as Figure 5.6; this was to reduce the number of animals used. Plots represent a mean adhesion \pm SEM of at least 4 separate experiments; ** $p < 0.01$. **Panel A**: area under the curve calculation; **panel B**: two-way ANOVA with bonferroni post-tests.

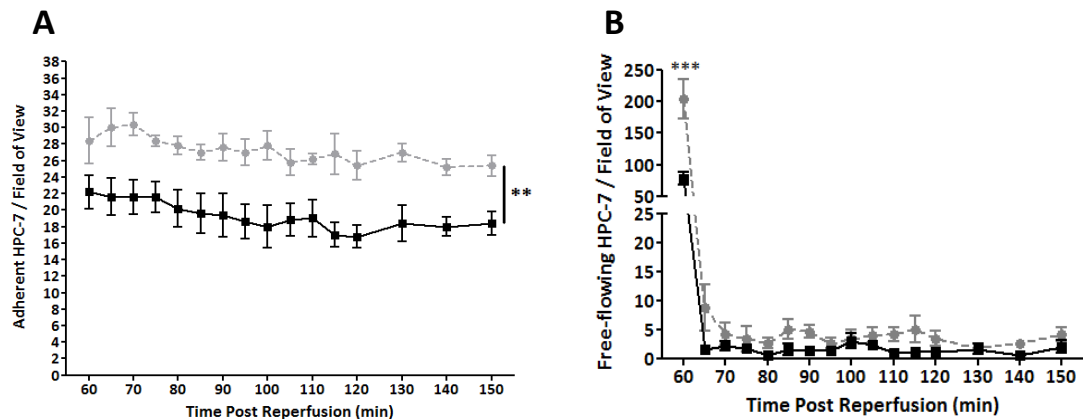


Figure 5.8. HPC-7 pre-treatment with SDF-1 α increases HPC-7 adhesion and the number of free-flowing HPC-7 in the injured kidney vasculature. Kidneys were clamped for 45 minutes and allowed to reperfuse for 60 minutes prior to HPC-7 administration. 2×10^6 HPC-7 were pre-treated with 25ng/ml of SDF-1 α for 5 minutes, washed and then injected intra-arterially into the IR injured animal. Subsequent HPC-7 adhesion and free-flowing numbers in the IR kidney were monitored intravitaly. There was an increase in HPC-7 adhesion and free-flowing cell numbers compared to the PBS control after SDF-1 α treatment (**panel A and B**: black solid line: PBS treated HPC-7; grey dotted line: SDF-1 α treated HPC-7). PBS controls are from the same cohort as Figure 5.6; this was to reduce the number of animals used. Plots represent a mean adhesion \pm SEM of at least 4 separate experiments; ** $p < 0.01$; *** $p < 0.001$. **Panel A**: area under the curve calculation; **panel B**: two-way ANOVA with bonferroni post-tests.

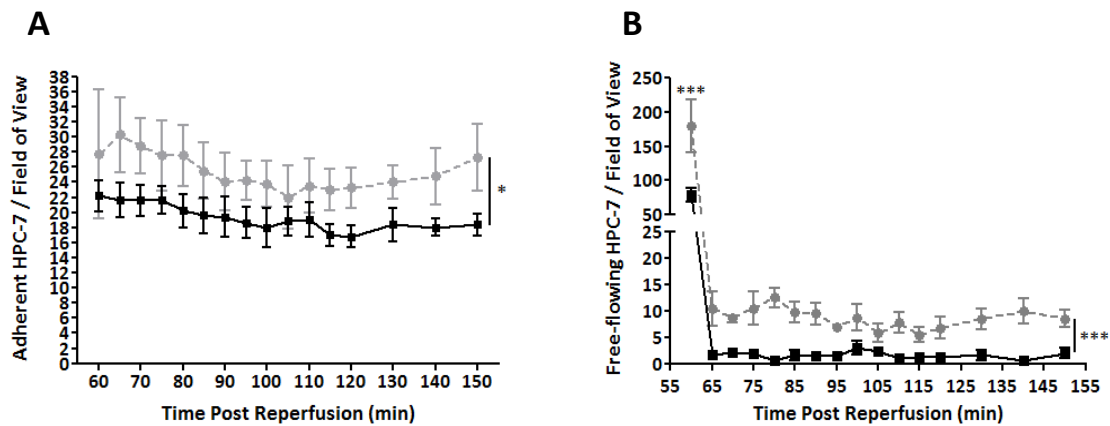


Figure 5.9. HPC-7 pre-treatment with TNF- α increases HPC-7 adhesion and the number of free-flowing HPC-7 in the injured kidney vasculature. Kidneys were clamped for 45 minutes and allowed to reperfuse for 60 minutes prior to HPC-7 administration. 2×10^6 HPC-7 were pre-treated with 25ng/ml of TNF- α for 5 minutes, washed and then injected intra-arterially into the IR injured animal. Subsequent HPC-7 adhesion and free-flowing numbers in the IR kidney were monitored intravitaly. There was an increase in HPC-7 adhesion compared to the PBS control after TNF- α treatment (**panel A**: black line: PBS treated HPC-7; grey line: TNF- α treated HPC-7). There was also an increase in the number of free-flowing cells at the point of infusion after TNF- α treatment compared to PBS-treated HPC-7 (**panel B**: black solid line: PBS treated HPC-7; grey dotted line: TNF- α treated HPC-7). PBS controls are from the same cohort as Figure 5.6; this was to reduce the number of animals used. Plots represent a mean adhesion \pm SEM of at least 4 separate experiments; * $p < 0.05$; *** $p < 0.001$. **Panel A**: area under the curve calculation; **panel B**: two-way ANOVA with bonferroni post-tests.

**5.3.10 Dual HPC-7 pre-treatment with KC and SDF-1 α does not further enhance HPC-7
adhesion**

2 x 10⁶ CFSE-labelled HPC-7 were pre-treated with 25ng/ml of KC and SDF-1 α together for 5 minutes and injected intra-arterially. There was a significant ($p < 0.01$) difference in the number of adherent HPC-7 after KC+SDF-1 α pre-treatment compared to the PBS treatment control (AUC: KC+SDF-1 α : 427.3 \pm 27.92; PBS: 300.30 \pm 25.62; **Figure 5.10.A**). However this increase in adherent HPC-7 was not significantly different from KC or SDF-1 α treatment alone. There was also a significant ($p < 0.01$) difference in the number of free-flowing HPC-7 after SDF-1 α pre-treatment at the point of infusion only (60 minutes reperfusion) compared to PBS control (**Figure 5.10.B**).

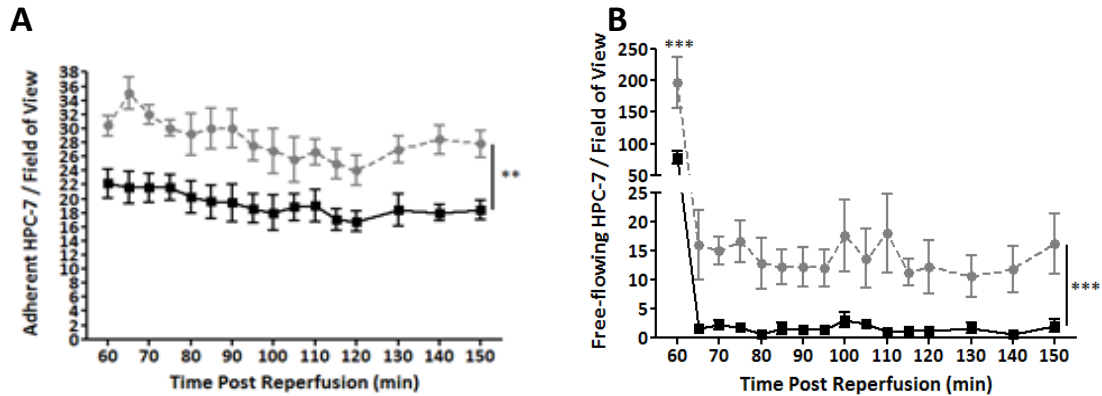


Figure 5.10. HPC-7 pre-treatment with KC+SDF-1 α increases HPC-7 adhesion and the number of free-flowing HPC-7 in the injured kidney vasculature. Kidneys were clamped for 45 minutes and allowed to reperfuse for 60 minutes prior to HPC-7 administration. 2×10^6 HPC-7 were pre-treated with 25ng/ml of KC+SDF-1 α for 5 minutes, washed and then injected intra-arterially into the IR injured animal. Subsequent HPC-7 adhesion and free-flowing numbers in the IR kidney were monitored intravitaly. There was an increase in HPC-7 adhesion compared to the PBS control after dual chemokine treatment (**panel A and B**: black solid line: PBS treated HPC-7; grey dotted line: KC+SDF-1 α treated HPC-7). PBS controls are from the same cohort as Figure 5.6; this was to reduce the number of animals used. Plots represent a mean adhesion \pm SEM of at least 4 separate experiments; * $p < 0.05$; *** $p < 0.001$. **Panel A**: area under the curve calculation; **panel B**: two-way ANOVA with bonferroni post-tests.

**5.3.11 Hydrogen peroxide increases HPC-7 adhesion to activated renal endothelium
only**

HPC-7 were pre-treated with 100 μ M for 5 or 60 minutes and then applied to TNF- α activated renal endothelium. After both H₂O₂ treatments, there was an increase in HPC-7 adhesion to the activated endothelium compared to the PBS treated control (CPF: H₂O₂ 1 hour: 29.32 \pm 4.611; H₂O₂ 5 minutes: 29.27 \pm 2.373; PBS: 7.560 \pm 3.438; **Figure 5.11.A**). Pre-treated HPC-7 were also applied to PBS treated endothelium and similar results were seen as with TNF- α treated endothelium.

Since no differences in adhesion were observed with a 5 or 60 minute incubation period, we decided to keep treatment time to a minimum and so incubated HPC-7 for 5 minutes with H₂O₂ for the *in vivo* experiments. H₂O₂ HPC-7 pre-treatment does not increase HPC-7 adhesion or the number of free-flowing cells in a renal IR injured model (AUC: H₂O₂: 228.7 \pm 33.05; PBS: 300.3 \pm 25.62; **Figure 5.11.B-C**).

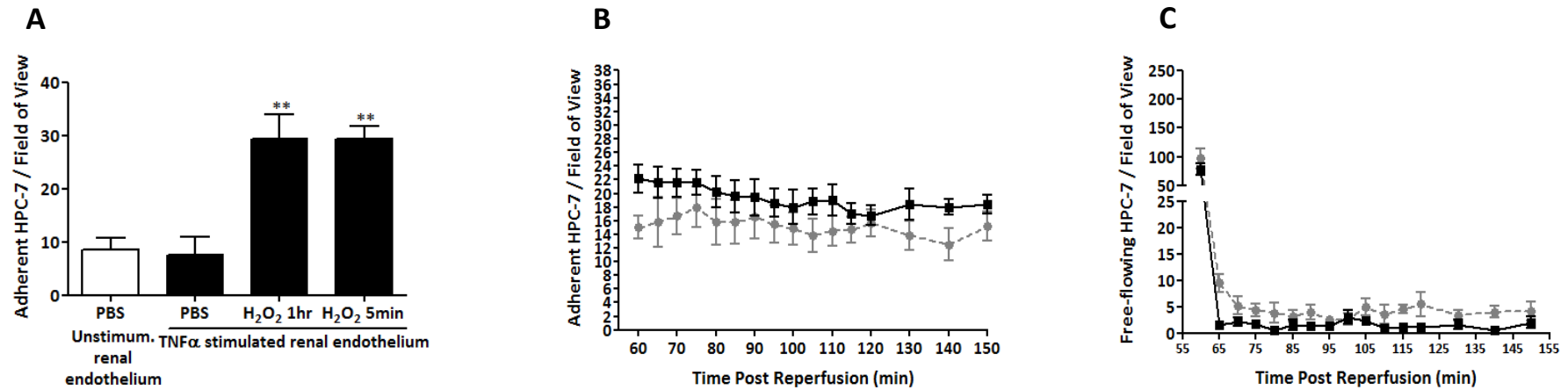


Figure 5.11. HPC-7 pre-treatment with H₂O₂ increases HPC-7 adhesion to activated renal endothelium in in-vitro experiments only. Pre-treating 1×10^5 CFSE-labelled HPC-7 with 100 μ M of H₂O₂ for 1 hour or 5 minutes significantly enhanced HPC-7 adhesion to TNF- α activated renal endothelium in vitro (**panel A**). Kidneys were clamped for 45 minutes and allowed to reperfuse for 60 minutes prior to HPC-7 administration. 2×10^6 HPC-7 were pre-treated with 100mM of H₂O₂ for 5 minutes, washed and then injected intra-arterially into the IR injured animal. Subsequent HPC-7 adhesion and free-flowing numbers in the IR kidney were monitored intravitaly. There were no increases in the number of adherent or free-flowing HPC-7 numbers after H₂O₂ treatment compared to the PBS controls (**panel B and C**: black line: PBS treated HPC-7; grey dashed line: H₂O₂ treated HPC-7). PBS controls are from the same cohort as Figure 5.6; this was to reduce the number of animals used. Plots represent a mean adhesion \pm SEM of at least 4 separate experiments; ** $p < 0.01$. **Panel A**: one-way ANOVA with Dunnett's post-tests; **panel B**: area under the curve calculation; **panel C**: two-way ANOVA with bonferroni post-tests.

5.3.12 Cytokines, especially SDF-1 α , significantly increase HPC-7 deformability

As outlined above, pre-treating HPC-7 with some of the cyto/chemokines tested increased the number of free-flowing cells observed within the injured renal microcirculation immediately upon infusion. Interestingly, this effect was not observed at any other time point. Free-flowing cells were defined as the total number of cells observed flowing through the field of view in a 1 minute time-frame of continuous monitoring. The blood circulation time for a mouse is approximately 4-6 seconds, meaning blood circulates approximately 10 times during a 1 minute observation period. To determine whether pre-treated HPC-7 only passed once through the kidney or if they were re-circulated, numbers of freely flowing cells at 6 second intervals were determined for the first observation minute. More freely circulating HPC-7 were observed at each 6 second time point for the first minute following IL-1 β , SDF-1 α , TNF- α and KC+SDF-1 α pre-treatments, suggesting more were continually re-circulated, with less being lost to extra-renal sites (**Figure 5.12.A-D** respectively).

No significant change in HPC-7 size was observed as a result of cytokine pre-treatment, as assessed by using a coulter counter (**Figure 5.12.F**). The phalloidin levels within pre-treated HPC-7 and the velocity of these free-flowing pre-treated cells in microvessels was also calculated using flow cytometry and the Slidebook analysis program respectively, but no significant changes were noted (**Figure 5.12.G-H**). IL-1 β ($p < 0.01$), SDF-1 α ($p < 0.01$) and KC+SDF-1 α ($p < 0.05$) treated cells were significantly more deformable, as determined by a reduction in the time taken for cells to be fully aspirated into a glass micropipette, which

was of a diameter that was comparable to blood capillaries. (*Figure 5.12.I-J*). SDF-1 α alone caused a 61% reduction in entry time.

Chapter 5: Methods and Mechanisms of Enhancing HSC Recruitment to the Injured Kidney

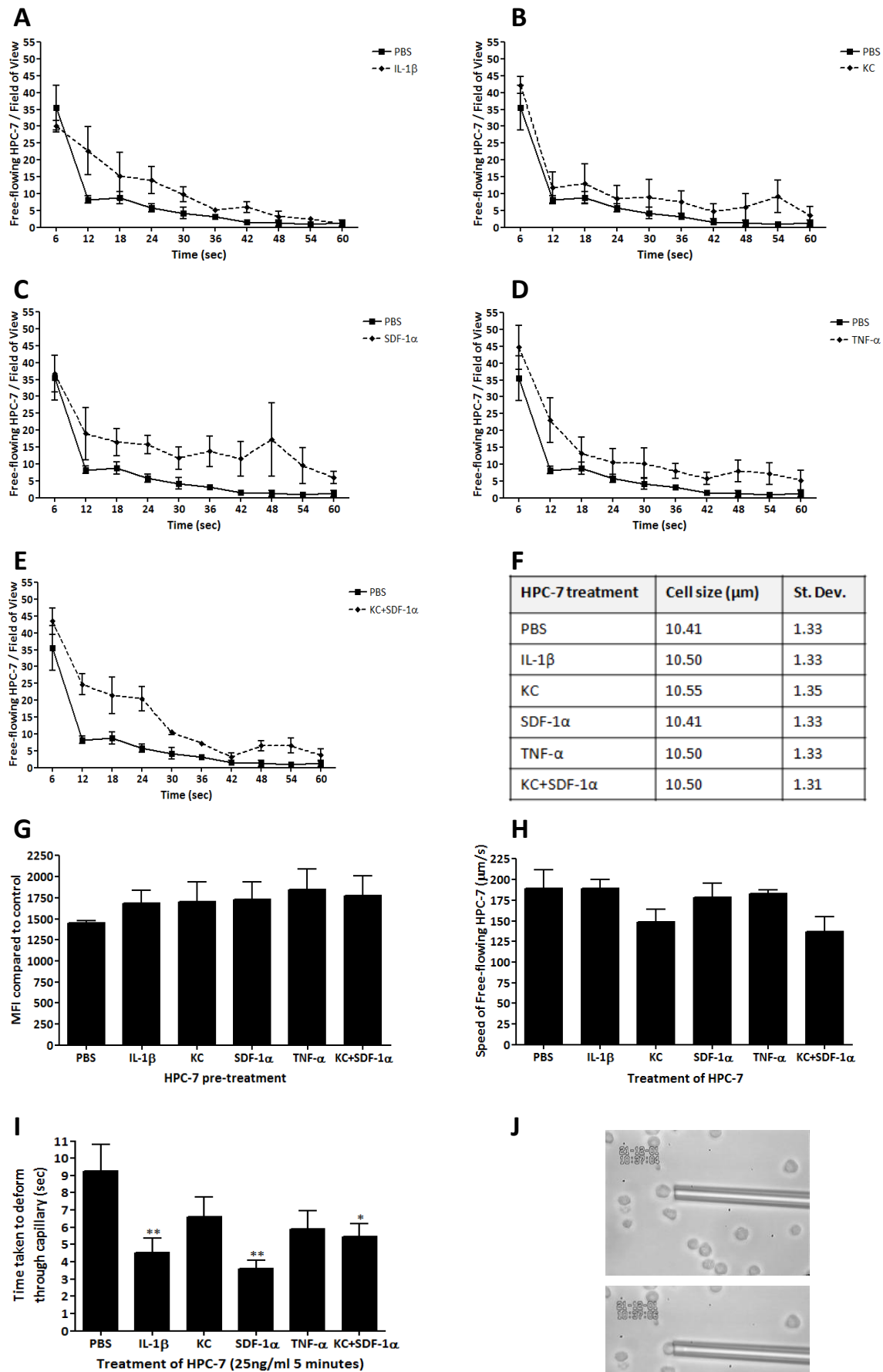


Figure 5.12. *The increased free-flowing HPC-7 numbers seen in the injured kidney vasculature after cytokine treatment due to changes in deformability.* The first one minute recording was broken down into 6 second intervals to illustrate each full circulatory pass. With IL-1 β , SDF-1 α , TNF- α and KC+SDF-1 α pre-treatments, more HPC-7 continue to flow between 6-24 seconds suggesting less are lost to the circulation (**panels A,C-E**). KC pre-treatment did not cause any increases in HPC-7 free-flowing cells (**panel B**). There were no changes in HPC-7 size after pre-treatments (**panel F**). The amount of phalloidin within HPC-7 and HPC-7 velocity *in vivo* was not affected by any pre-treatment (**panel G-H**). HPC-7 became significantly more deformable with SDF-1 α and KC+SDF-1 α pre-treatment as demonstrated by reduced time taken to aspirate into a glass capillary (**panel I**). Photographs illustrating the method is shown and 50 cells were tested / group (**panel H**). For all line graphs; black line: PBS treated HPC-7; grey dashed line: cytokine treated HPC-7. Plots represent a mean adhesion \pm SEM of at least 4 separate experiments; * $p < 0.05$, ** $p < 0.01$. **Panels G-I:** one-way ANOVA with Dunnett's post-tests.

5.3.13 KC or SDF-1 α HPC-7 pre-treatments do not alter adhesion molecule expression

As KC and SDF-1 α pre-treatments were most effective at increasing HPC-7 adhesion across the various assays, we further investigated the mechanisms mediating increased adhesion for these pre-treatments. One way in which these chemokine pre-treatments could be causing an effect is by upregulating the number of important adhesion molecules on the HPC-7 surface. To examine this, flow cytometry was utilised: 1×10^6 HPC-7 were pre-treated with 25ng/ml of KC or SDF-1 α for 5 minutes and were subsequently labelled for CD49d and CD44. No significant upregulation of CD49d or CD44 occurred after KC or SDF-1 α (**Figure 5.13.A-B**).

5.3.14 KC and SDF-1 α pre-treatments enhances HPC-7 adhesion to both VCAM-1 and HA *in vitro*

As we have shown CD49d and CD44, and their counter-ligands VCAM-1 and HA, are important in governing HPC-7 adhesion to the IR injured kidney we examined whether our chemokine pre-treatments could improve the ability of HPC-7 surface molecules to bind to their endothelial counter-ligands. 1×10^6 HPC-7 were pre-treated with 25ng/ml of KC or SDF-1 α for 5 minutes and then applied to immobilised VCAM-1 and HA, adherent HPC-7 were then quantified. Both KC ($p < 0.05$) and SDF-1 α ($p < 0.01$) pre-treatments caused an enhanced adhesion of HPC-7 to both VCAM-1 and HA substrates compared to PBS-treated controls (CPF: VCAM: KC: 6.386 ± 0.986 ; SDF-1 α : 7.912 ± 1.227 ; PBS: 2.610 ± 0.6038 ; **Figure 5.14.A**; HA: KC: 9.753 ± 1.352 ; SDF-1 α : 13.39 ± 4.310 ; PBS: 1.819 ± 0.2791 ; **Figure 5.14.B**).

**5.3.15 KC and SDF-1 α pre-treatments alter CD44 and CD49d adhesion molecule
distribution on the HPC-7 cell surface**

HPC-7 were pre-treated with 25ng/ml of KC or SDF-1 α for 5 minutes and were then fixed. Treated cells were then exposed to fluorescent antibodies against CD44 and CD49d and any changes in adhesion molecule distribution were imaged using a confocal microscope. After pre-treating HPC-7 with SDF-1 α , there was an increase ($p < 0.05$) in the number of CD49d microclusters on the surface of the HPC-7 (**Figure 5.15.A-B**). There were no changes in the number of CD44 clusters after SDF-1 α treatment. Conversely, after KC treatment there was an increase ($p < 0.05$) in CD44 microclusters but no changes were seen to CD49d (**Figure 5.15.C-D**).

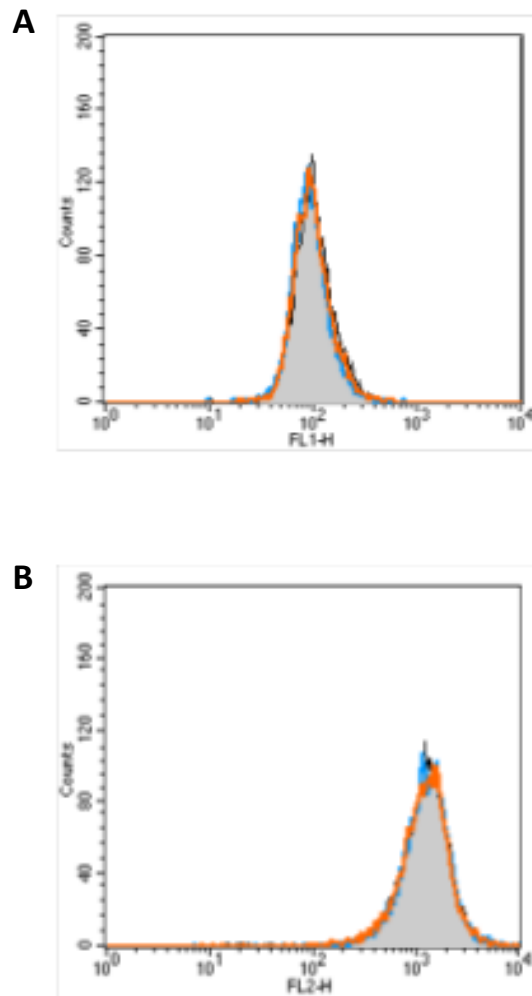


Figure 5.13. *The increased HPC-7 adhesion after KC and SDF-1 α pre-treatments is not because of an increase in surface CD49d (A) or CD44 (B) expression.* 1×10^6 HPC-7 were pre-treated with 25ng/ml of KC and SDF-1 α for 5 minutes and any changes in adhesion molecules were examined using flow cytometry. There wasn't any upregulation of either CD49d (**panel A**) or CD44 (**panel B**) after KC and SDF-1 α pre-treatments (grey fill: PBS control; blue line: KC pre-treated; orange line: SDF-1 α pre-treated HPC-7).

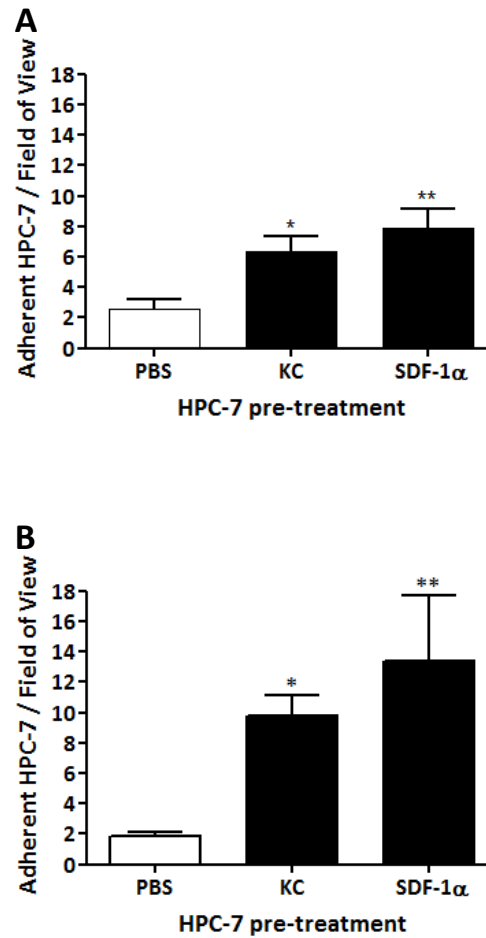


Figure 5.14. *KC and SDF-1α pre-treatments enhance the ability of HPC-7 to adhere to 10μg/ml VCAM-1 (A) and 0.5mg/ml HA respectively (B).* 1×10^5 HPC-7 were pre-treated with 25ng/ml of KC and SDF-1α for 5 minutes and applied to 10μg/ml of immobilised VCAM-1 and 0.5mg/ml of immobilised HA in a 96-well plate. Both KC and SDF-1α pre-treatments caused an increase in HPC-7 adhesion to both VCAM-1 (**panel A**) and HA (**panel B**). Plots represent a mean adhesion \pm SEM of at least 4 separate experiments; * $p < 0.05$; ** $p < 0.01$. **Panel A and B:** one-way ANOVA with Dunnett's post-tests.

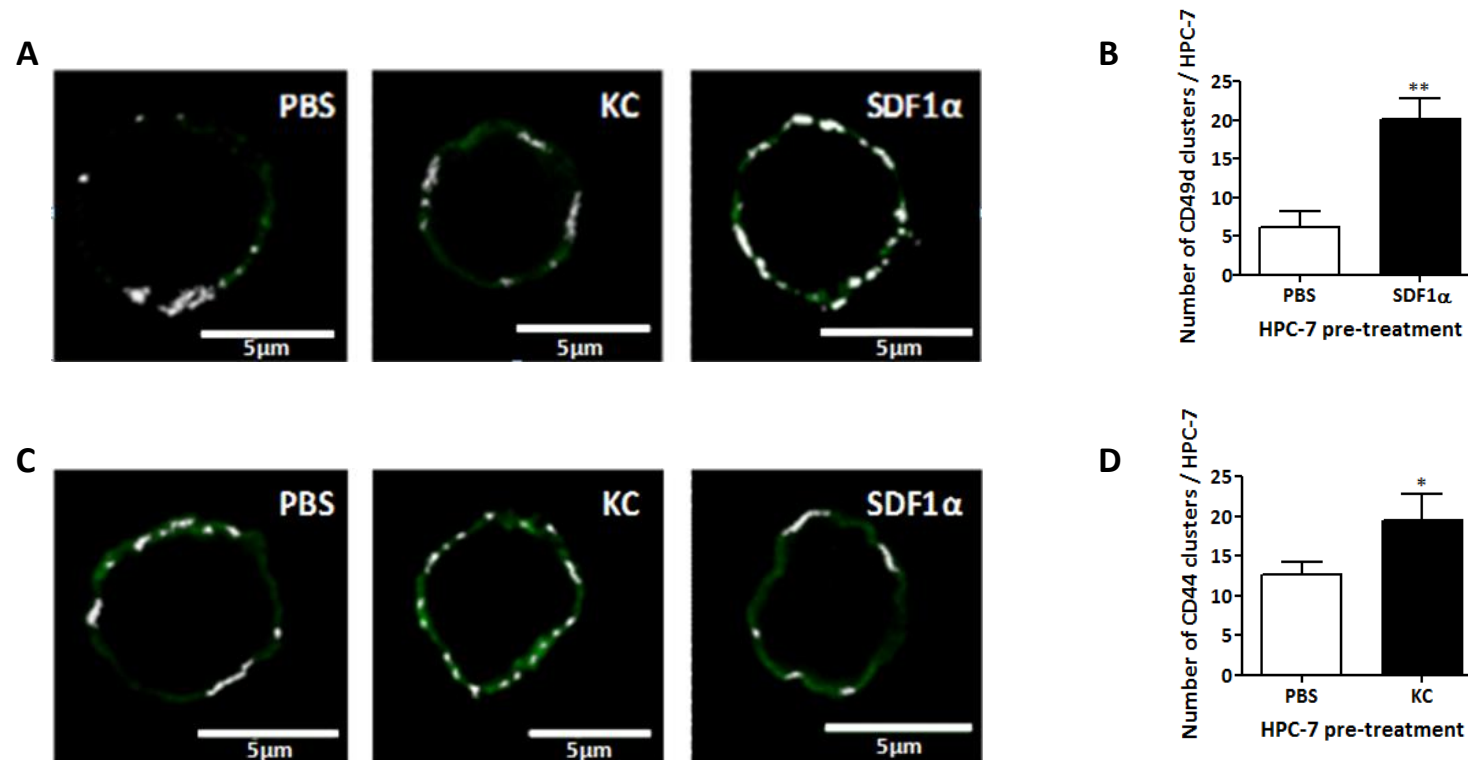


Figure 5.15. KC and SDF-1α pre-treatments alter the distribution of CD49d (A-B) and CD44 (C-D) on the HPC-7 surface. 1×10^6 HPC-7 were pre-treated with 25ng/ml of KC and SDF-1α for 5 minutes, fixed and then labelled with antibodies against CD49d and CD44. Cells were imaged using scanning confocal microscopy and areas of clustering were identified using the “Find Maxima” plugin in ImageJ. Maxima plots were produced by identifying regions of maximal intensity within control determined tolerance level to separate clusters from background. CD49d adhesion molecule distribution is altered only after SDF-1α pre-treatment, there is no change with KC treatment (**panel A**; points of maximal intensity are highlighted in white). SDF-1α increases the number of CD49d microclusters on the HPC-7 surface (**panel B**). An increase in CD44 microclusters is seen after KC treatment only (**panel C and D**; points of maximal intensity are highlighted in white). Plots represent a mean number of microclusters \pm SEM per cells of at least 50 HPC-7; * $p < 0.05$. **Panel B and D**: unpaired t-tests.

5.4 Major Findings of Chapter 5

FINDING		HOW?
1	30 minute HPC-7 pre-treatment with ICM enhanced HPC-7 adhesion to the IR-injured kidney compared to SCM	<i>In vitro</i> : Stamper-Woodruff and renal endothelial assays
2	HPC-7 pre-treatment with 25ng/ml of SDF-1α for 5 minutes, increased HPC-7 adhesion to the IR-injured kidney	<i>In vitro</i> : Stamper-Woodruff and renal endothelial assays <i>In vivo</i> and <i>ex vivo</i> : Intravital microscopy
3	HPC-7 pre-treatment with 25ng/ml of KC for 5 minutes, increased HPC-7 adhesion to the IR-injured kidney	<i>In vitro</i> : Renal endothelial assays <i>In vivo</i> and <i>ex vivo</i> : Intravital microscopy
4	HPC-7 pre-treatment with 25ng/ml of TNF-α for 5 minutes, increased HPC-7 adhesion to the IR-injured kidney	<i>In vivo</i> and <i>ex vivo</i> : Intravital microscopy
5	HPC-7 pre-treatment with 25ng/ml of KC + SDF-1α for 5 minutes, increased HPC-7 adhesion and number of free-flowing to the IR-injured kidney but not more so than using either chemokine alone	<i>In vivo</i> and <i>ex vivo</i> : Intravital microscopy
6	HPC-7 pre-treatment with 25ng/ml of IL-1β , SDF-1α or TNF-α for 5 minutes, increased the number of HPC-7 free-flowing through the IR-injured kidney at the point of infusion	<i>In vivo</i> : Intravital microscopy
7	HPC-7 pre-treatment with 25ng/ml of IL-1β , SDF-1α or TNF-α for 5 minutes caused an increase in HPC-7 deformability	<i>In vitro</i> : Micropipette analysis
8	HPC-7 pre-treatment with 25ng/ml of KC causes an increase in the number of CD44 micro-clusters on the HPC-7 surface	<i>In vitro</i> : Clustering protocol using confocal microscopy
9	HPC-7 pre-treatment with 25ng/ml of SDF-1α caused an increase in the number of CD44 micro-clusters on the HPC-7 surface	<i>In vitro</i> : Clustering protocol using confocal microscopy

5.5 Discussion

Identifying the molecular adhesive mechanisms governing HSC adhesion to a damaged tissue bed is the first step to understanding how to enhance these rare but potentially clinically therapeutic cells to sites of injury. The previous chapter identified CD49d and CD44, and their respective counter-ligands VCAM-1 and HA, as critical modulators governing HSC recruitment to the IR injured renal microcirculation. Modulating the expression and/or binding ability of these specific adhesion molecules for endothelial counter-ligands might be an important approach to improving renal HSC homing. In this chapter, we show a quick and effective pre-treatment strategy can increase HSC adhesion within the ischaemically injured kidney. This novel data demonstrated that HSC recruitment to the kidney was an event that could be enhanced and that the adhesion brought about by the presence of an injury was not maximal.

The use of an ICM demonstrated that soluble factors released by the injured kidney had the ability to modulate SC adhesion. However, these were simply proof of principle experiments, as generating an ICM is not a likely therapeutic option. Our Coomassie-stained gels demonstrated that ICM did contain proteins that were not present or were present at a lower concentration in healthy kidneys (SCM). IL-1 β , SDF1 α , IL-8 and other pro-inflammatory cyto/chemokines are within the region of 7-19 kDa, which reflects the region of the proteins bands that were increased in ICM. These cyto/chemokines are known to be secreted in abundance following renal IR injury and have a key role in mediating leukocyte recruitment (Olson and Ley 2002; Anders *et al.* 2003; Stroo *et al.*

2010). Interestingly, inflammatory cytokines TNF- α and IL-1 β have been shown to stimulate MSCs and enhance their migration *in vitro* (Ries *et al.* 2007). It is likely that SC activation and subsequent adhesion is also mediated by similar soluble proteins. We present data in this chapter that chemokine pre-treatment can significantly modulate the adhesion of HPC-7 cells within the renal microcirculation *in vivo*.

This chapter identified HPC-7 pre-treatment with the chemokines SDF-1 α and KC can substantially increase their adhesion to the IR injured kidney. Interestingly, the inflammatory cytokine TNF- α also significantly increased HSC homing to the IR injured kidney. The greatest amount of HPC-7 adhesion was seen with KC pre-treatment, whereas SDF-1 α caused a greater number of freely circulating cells within the kidney. The importance of these particular chemokines is given further significance by the results from the previous chapter, in which topical exposure to SDF-1 α and KC can also mediate homing to the healthy kidney. We have provided additional data in a publication arising from the work in this chapter which demonstrates that these pre-treatment strategies could also enhance the adhesion of primary BM-derived Lin⁻ cells *in vitro* (White *et al.* 2013). This importantly shows that chemokine pre-treatment modulates the HPC-7 cell line in a similar manner to primary stem/progenitor cells.

SDF-1 α is a well-known and thoroughly investigated chemoattractant with regards to SC homing (Peled *et al.* 1999; Wright *et al.* 2002; Togel *et al.* 2005); even platelet-released SDF-1 α has been shown to aid in the recruitment of progenitor cells (Massberg *et al.*

2006; Stellos and Gawaz 2007). Interestingly, Stroo *et al.* showed that manipulating the SDF-1 α /CXCR4 axis, either by increasing local SDF-1 α concentrations in the injured kidney or by blocking CXCR4 on HSCs, did not affect their migration (Stroo *et al.* 2009). However, in these studies, they injected recombinant SDF-1 α into just one focal point in the kidney, which may explain this discrepancy. In this chapter, we demonstrated that only SDF-1 α enhanced HPC-7 adhesion in all of the assays utilised: frozen tissue sections, renal endothelium and *in vivo*. Although intravital microscopy only images the cortical peritubular capillaries of the kidney, the frozen tissue section S-W assay allowed adhesion to the deeper medullary regions to also be quantitated. It is well-documented that the cortico-medullary areas are the most injured during renal IR injury (Sutton 2009) and SDF-1 α enhanced HPC-7 adhesion in these regions too. Therefore, this particular chemokine would be a good molecule to use to target SCs to the most damaged regions of the kidney. However, it is also important to note that the *in vivo* studies showed that KC produced the most HPC-7 adhesion to the peritubular capillaries. This is the first time that KC has been implicated in HSC homing to any injured tissue.

H₂O₂ is also increased during renal IR injury (Kim, 2009). Recent studies in our lab have demonstrated that pre-treatment with this ROS could increase HPC-7 adhesion to IR injured gut through enhancing surface integrin clustering (Kavanagh *et al.* 2012). This study demonstrated that a 1 hour incubation with 100 μ M H₂O₂ did not induce any cytotoxic effects on HPC-7 cells. For the renal studies presented in this chapter, we tested the same concentration but pre-treated for 5 minutes and 1 hour so as to keep incubation durations consistent with previous cyto/chemokine pre-treatment strategies.

Since significant increases in HPC-7 adhesion to TNF- α activated renal endothelium were observed after both pre-treatment durations, intravital studies were conducted using a 5 minute protocol. However, unlike our previous studies in the gut, no significant increases in HPC-7 adhesion to IR injured kidney were observed. It is unclear why the same pre-treatment would not universally improve SC adhesion in all injured organs, but may be related to the fact that site specific adhesion molecules govern SC homing. For example, we presented in Chapter 4 the importance of CD44 and CD49d in mediating renal homing. However, in the gut CD18 appears to be more critical (Kavanagh *et al.* 2012). It is possible therefore, that H₂O₂ affects the affinity of these surface adhesion molecules differently and the modulation of those involved in renal homing is less efficient; this would require further detailed investigation. Furthermore, HPC-7 are exposed to shear stress during *in vivo* experiments: The blood flow rate is a lot higher in the mouse kidney compared to that of the gut - 7.88mL/min/g vs. 2.79mL/min/g - so it is possible that H₂O₂ does not facilitate changes in adhesion molecules that are strong enough to withstand the high shear in kidneys (Milia *et al.* 2001; Garrelds *et al.* 2002). In agreement with these studies, Peled and colleagues demonstrated using *in vitro* studies that SDF-1 α could rapidly activate the firm shear-resistant adhesion of human CD34⁺ cells to immobilized ICAM-1 and VCAM-1 (Peled *et al.*, 2000).

The second part of this chapter investigated whether KC and SDF-1 α mediated increased adhesion through effects on CD49d and CD44 expression. Others have shown, for example, that MSC homing to bone could be increased using cells genetically engineered to express higher surface levels of CD49d (Kumar and Ponnazhagan 2007). However,

despite showing that both CD49d and CD44 governed HPC-7 adhesion to the IR injured kidney *in vivo*, neither KC nor SDF-1 α pre-treatments enhanced CD49d or CD44 expression on the HPC-7 surface: this could be due to HPC-7 not having intracellular stores of each receptor that can be quickly transported to the cell surface; or perhaps 5 minutes stimulation is not long enough for receptor cycling to occur. Montecucco and colleagues observed that neutrophils produced significant increases in both CD11b and CD18 subunits after a longer period (30 minutes) of TNF- α treatment (Montecucco *et al.* 2008). Primary human HSCs have been shown to contain CD44 intracellular stores; however, it has been noted that their adhesion is not dependant on the upregulation of CD44 numbers but actually due to altering the avidity of β_1 integrins that work in conjunction with CD44 (Lundell *et al.* 1997; Pilarski *et al.* 1999).

Another way of enhancing adhesion is through altering the receptor localisation on the cell surface. Although conformational changes in adhesion molecules from an inactive to an active state are important for mediating cell adhesion, the dynamic reorganisation of adhesion molecules into clusters is also a major mechanism that regulates their binding capacity, acting to strengthen cell-cell adhesion (van Kooyk and Figdor 2000). KC and SDF-1 α induced an increase in the number of surface clusters of CD44 and CD49d respectively: this most likely contributed to the increased binding capacity that these adhesion molecules had for their counter-ligands HA and VCAM-1 respectively, as was demonstrated *in vitro* using immobilised substrates. Various studies have actually stated that adherence of leukocytes post-chemokine treatment is not due to increases in VLA-4 receptor numbers, but of alterations in both affinity and avidity of said receptor (DiVietro

et al. 2007), which is in agreement with our HPC-7 studies. Grabovsky and colleagues (2000) demonstrated that the close proximity between chemokine receptors and surface integrins facilitates inside-out signalling events into rapid integrin clustering in leukocytes, which may also explain why the 5 minute incubation period was all that was required for adhesive events to be modulated.

Using the micropipette aspiration technique, we have provided the first evidence that cytokines could also alter HSC deformability. It is possible that this decreased resistance to deformation prevented circulating cells from becoming entrapped within non-renal sites and maintained their presence within peripheral blood. Non-specific entrapment is a major obstacle for systemic SC delivery for regenerative purposes both experimentally and clinically (Fischer *et al.* 2009) and significantly reduces the pool of circulating transplanted HSCs available for recruitment. At the time of infusion only, SDF-1 α pre-treated HSCs were observed to repeatedly circulate, unlike PBS pre-treated cells which were rapidly lost from the peripheral circulation. IL-1 β , TNF- α pre-treatments and KC+SDF-1 α dual pre-treated cells continuously trafficked through the kidney throughout the duration of the experiment, with approximately 10-15 cells observed at each time point: this phenomenon may increase the chance of trafficking cells becoming adherent within injured renal microvessels and also contribute to the enhanced adhesion observed. Interestingly, it is well accepted that cytokines, such as TNF- α and IL-1 β , generally reduce the deformability of circulating cells: for instance, leukocytes usually adopt a flatter and more rigid cellular structure post-cytokine exposure, which decreases their deformability (Skoutelis *et al.* 2000).

In conclusion, despite huge advances in the field of cellular therapy, a major limitation is their poor retention within target tissues on systemic delivery. Modulation of HSC homing mechanisms may be used as a therapeutic strategy to improve the efficacy of potential SC therapy. We provide a simple, quick and effective method for enhancing HSC adhesion into injured kidney using SDF-1 α or KC. These chemokines most likely mediate increased recruitment either through the modulation of CD49d and/or CD44, or by reducing HSCs clearance from the circulation. Previous studies have enhanced SC recruitment by introducing genes encoding for SDF-1 α within cardiac tissue (Tang *et al.* 2005). However, the clinical applicability of such techniques is debatable and may be associated with aggravated tissue injury due to side effects such as SDF-1 α -dependent lymphocyte recruitment (Liekens *et al.* 2010). The current study benefits from identifying a strategy that increases recruitment without genetically manipulating the HSCs or the host tissue and thus has the potential to be used clinically. Our data may therefore help in the design of future cellular therapies using HSCs for renal repair. It is anticipated that enhancing HSC recruitment to injured kidney may expedite the recovery process and encourage greater therapeutic success clinically. The vasculo-protective effects of these recruited HSCs forms the focus of the next chapter.

Chapter 6



Beneficial Effects of HSCs upon the Injured Renal Microvasculature

6 Beneficial Effects of Haematopoietic Stem Cells within the Injured Renal Microvasculature

6.1 Introduction and Hypotheses

6.1.1 Introduction

In the previous chapters, the adhesion receptors governing HSC recruitment to the injured kidney and strategies to enhance this renal homing have been elucidated. However two pertinent questions remain - do these specific SCs confer any beneficial effects once within the injured kidney and does enhancing their local presence improve their therapeutic efficacy? Inflammation is thought to play a major role in acute kidney injury (Bonventre and Zuk 2004; Friedewald and Rabb 2004). Following an ischaemic insult, both the renal endothelial and proximal tubular cells produce cytokines and chemokines that lead to inflammatory cell infiltration. The pathophysiology of AKI, particularly renal IR injury which is the major and most serious cause of AKI, is defined predominantly by inflammation and marked microcirculatory dysfunction (Bonventre and Yang 2011). It is therefore reasonable to suggest that improvements in renal structure and function can be achieved if the marked inflammation and microcirculatory disturbances within the kidney can be resolved.

The mechanisms by which HSCs could potentially produce beneficial effects may be through differentiation into functional resident renal cells or by stem, cell fusion with

Chapter 6: Beneficial Effects of HSCs upon the Injured Renal Microvasculature

local cells. Early studies in the kidney focussed on the idea of differentiation; however the level of SC differentiation and fusion, and the number of newly generated cells, has been too low to explain the degree of improvement observed following SC transplantation (Poulsom *et al.* 2001). Recent studies have implicated a transient paracrine effect, whereby SCs secrete potent combinations of trophic factors and anti-inflammatory factors that modulate the molecular composition of the environment to evoke responses from resident cells (Burdon *et al.* 2011). This paracrine effect has been demonstrated for a variety of bone marrow-derived progenitor cells with most studies focussing on MSCs. However, investigations into HSC paracrine activity remain limited although our group previously demonstrated a beneficial role for HSCs in reducing leukocyte accumulation in the IR injured gut.

In this chapter we focussed on the vasculoprotective benefits that HSCs could confer within the injured kidney. Improvements in the efficacy of these benefits following enhanced homing, and thus local renal presence of HSCs, were also assessed. More importantly, we were able to quantitate for the first time the actual microvascular disturbances that took place in the IR injured mouse kidney. The specific events monitored were neutrophil adhesion, microthrombus formation, vascular albumin leakage and overall renal blood flow. High resolution intravital images were obtained using the spinning Nipkow based confocal microscope and by labelling endogenous cells using specific antibodies tagged with fluorescent dyes. As explained earlier, direct intravital imaging of the mouse kidney *in vivo* has been challenging and therefore, in

Chapter 6: Beneficial Effects of HSCs upon the Injured Renal Microvasculature

comparison to other organs such as the liver and gut, there is no published study that has fully described these events.

6.1.2 Aims and Hypotheses

The main aims and hypotheses of this chapter are:

1. Aim: Describe the microcirculatory disturbances associated with renal IR injury using Spinning Nipkow based confocal intravital microscopy
2. Aim: Label endogenous platelets and neutrophils for confocal intravital imaging
3. Hypotheses: Renal IR injury increases the presence of neutrophils and platelet within peritubular capillaries, the adhesion of which can be reduced using HSCs
4. Hypotheses: HSCs improve renal structure and function

6.2 Methods

The methods used in this chapter are described in detail in chapter 2. To image the kidney using an upright confocal intravital microscope, the renal preparation was designed which was slightly more stationary. Again, the ischaemia was induced for 45 minutes and the tissue reperfused for up to 6 hours to induce substantial injury. Fluorescently conjugated antibodies to label endogenous platelets and neutrophils or FITC-BSA were via the carotid artery. There were 4 treatment groups for these experiments: sham animals, IR injury alone; IR injury plus naïve HPC-7 injection introduced at 1 hour reperfusion; IR injury plus KC+SDF-1 α treated HPC-7 injection

introduced at 1 hour reperfusion. 5 fields of view were taken at 1 hour, 4 hour and 6 hour reperfusion time points and neutrophil and platelet microthrombi numbers were quantified. At the end of the experiments, CL kidneys and lungs were removed to analyse platelet microthrombi and neutrophil infiltration immunohistochemically. Serum was also removed for analysis of the renal injury markers, urea and creatinine. IR kidneys and corresponding sham kidneys were snap frozen or fixed in formalin and then sectioned ready for histological analysis. Additional experiments were conducted using Chandler loops, used to assess the weight of platelet thrombi in whole blood in the presence or absence of HPC-7 cells.

6.3 Results

6.3.1 HPC-7 reduce neutrophil numbers in a murine model of renal IR injury *in vivo*

After renal IR injury, neutrophil numbers significantly ($p < 0.001$) increased at 6 hours reperfusion compared to non-injured sham controls (CPF: IR only: 72.15 ± 24.38 ; Sham: 12.50 ± 1.256 ; **Figure 6.1.A-C**). These increases in neutrophil adhesion were not observed at 1 or 4 hours reperfusion. As far as we can tell, the neutrophils were adherent within the peritubular capillaries. Interestingly, infusion of either naïve HPC-7 ($p < 0.001$) or KC+SDF-1 α ($p < 0.001$) pre-treated HPC-7 significantly reduced neutrophil accumulation within the IR injured kidney compared to IR injury without HPC-7 (CPF: IR + naïve HPC-7: 21.48 ± 9.053 ; IR + KC+SDF-1 α HPC-7: 34.10 ± 4.740 ; IR only: 72.15 ± 24.38 ; **Figure 6.1.A,C-E**). There was significant difference in neutrophil adhesion at 6 hours between the two groups receiving HSCs.

6.3.2 HPC-7 also reduce the number of platelet microthrombi in the IR injured microvasculature *in vivo*

After renal IR injury, platelet microthrombi numbers significantly ($p<0.001$) increased at 6 hours reperfusion compared to non-injured sham controls (CPF: IR only: 63.80 ± 14.93 ; Sham: 18.50 ± 6.900 ; **Figure 6.2.A-C**). Similarly to neutrophils, these increases were not observed at 1 or 4 hours reperfusion. The aggregates of platelets were observed adherent within the renal peritubular vessels and were sometimes large enough to impair the blood flow in that region. Infusion of either naïve ($p<0.001$) or KC+SDF-1 α ($p<0.001$) pre-treated HPC-7 significantly reduced platelet microthrombi accumulation within the IR injured kidney compared to IR injury without HPC-7 (CPF: IR + naïve HPC-7: 22.40 ± 10.33 ; IR + KC+SDF-1 α HPC-7: 17.10 ± 9.948 ; IR only: 63.80 ± 14.93 ; **Figure 6.2.A,C-E**). There was significant difference in platelet microthrombi numbers at 6 hours between the two groups receiving HSCs.

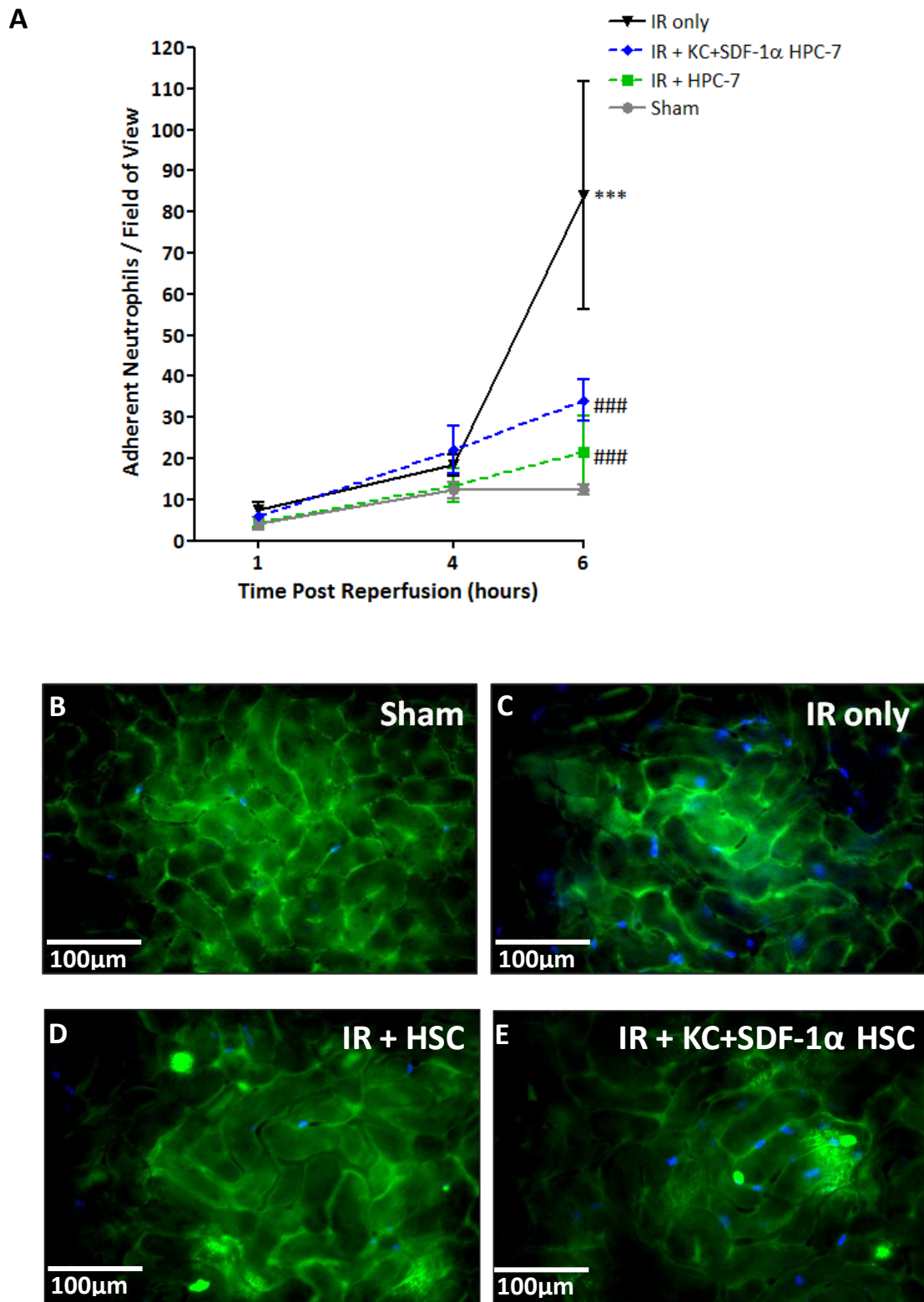


Figure 6.1. Naïve and KC+ SDF-1α pre-treated HPC-7 reduce neutrophil adhesion to an IR injured kidney at 6 hours reperfusion. Neck surgery was performed and eFluor 660 anti-Gr1 antibody was injected intra-arterially. Kidneys were then clamped for 45

Chapter 6: Beneficial Effects of HSCs upon the Injured Renal Microvasculature

minutes and allowed to reperfuse for 60 minutes prior to HPC-7 administration. Five fields of view were taken of the kidney at 1 hour, 4 hours and 6 hours reperfusion and neutrophil numbers were quantified. There was a significant increase in the number of neutrophils at 6 hours reperfusion in the IR injured kidney compared to that of the sham (**panel A**: black line: IR injured; grey line: sham). When injecting naïve and KC+SDF-1 α treated cells at 1 hour reperfusion, there was a significant decrease in the number of adherent neutrophils compared to the IR injured kidney (**panel A**; green line: naïve HPC-7; blue line: KC+SDF-1 α treated HPC-7; black line: IR only). Representative images showing neutrophil numbers in: sham (**panel B**); IR only (**panel C**); naïve HPC-7 + IR (**panel D**); KC+SDF-1 α HPC-7 (**panel E**; **neutrophils: blue; HPC-7: green**). Plots represent a mean adhesion \pm SEM of at least 5 separate experiments; *** $p < 0.001$. **Panel A**: two-way ANOVA with bonferroni post-tests.

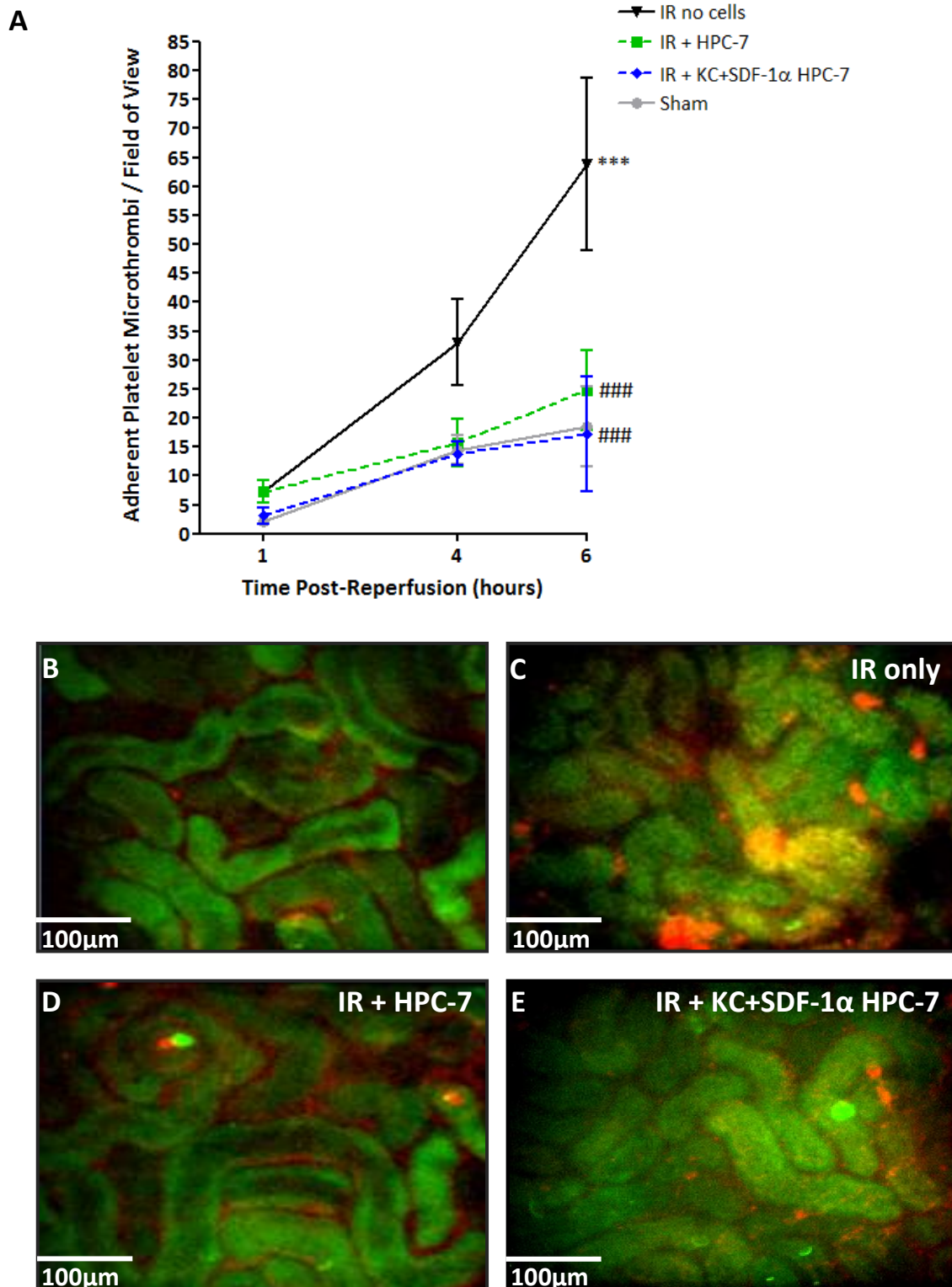


Figure 6.2. *Naïve and KC+ SDF-1α pre-treated HPC-7 reduce platelet microthrombi adhesion to an IR injured kidney at 6 hours reperfusion.* Neck surgery was performed and Alexa 568 and anti-CD41 antibody was injected intra-arterially. Kidneys were then clamped for 45 minutes and allowed to reperfuse for 60 minutes prior to HPC-7

Chapter 6: Beneficial Effects of HSCs upon the Injured Renal Microvasculature

administration. Five fields of view were taken of the kidney at 1 hour, 4 hours and 6 hours reperfusion and platelet numbers were quantified. There was a significant increase in the number of platelet microthrombi at 6 hours reperfusion in the IR injured kidney compared to that of the sham (**panel A**: black line: IR injured; grey line: sham). When injecting naïve and KC+SDF-1 α treated cells at 1 hour reperfusion, there was a significant decrease in the number of adherent platelet microthrombi compared to the IR injured kidney (**panel A**; green line: naïve HPC-7; blue line: KC+SDF-1 α treated HPC-7; black line: IR only). Representative images showing platelet numbers in: sham (**panel B**); IR only (**panel C**); naïve HPC-7 + IR (**panel D**); KC+SDF-1 α HPC-7 (**panel E**; **platelets: red; HPC-7: green**). Plots represent a mean adhesion \pm SEM of at least 5 separate experiments; *** $p < 0.001$. **Panel A**: two-way ANOVA with bonferroni post-tests.

6.3.3 Platelet microthrombi decrease in size after HPC-7 administration *in vivo*

As well as the number of platelet microthrombi, the average size and fluorescent intensity of each microthrombi at 6 hours reperfusion was also analysed. There was a significant ($p<0.001$) increase in the size of the platelet microthrombi after IR injury compared to sham (Average Platelet Microthrombi Size (APMS): IR only: 43.88 ± 10.23 ; Sham: 8.840 ± 1.821 ; **Figure 6.3.A**). Both naïve HPC-7 or KC+SDF-1 α pre-treated HPC-7 cells significantly ($p<0.001$) reduced platelet microthrombi size within the IR injured kidney compared to IR injury without HPC-7 (APMS: IR + naïve HPC-7: 12.61 ± 3.673 ; IR + KC+SDF-1 α HPC-7: 19.64 ± 5.20 ; IR only: 43.88 ± 10.23 ; **Figure 6.3.A**). The overall fluorescent intensity of the microthrombus, indicative of the density of platelets present, did not change between treatments (**Figure 6.3.B**).

6.3.4 Fluorescent immunohistochemistry of frozen renal sections further confirms the *in vivo* observations that HPC-7 can reduce platelet microthrombi after IR injury

Following intravital experiments, kidneys were removed, frozen in liquid nitrogen and sectioned to quantitate platelet numbers using histological techniques with an anti-CD42b primary antibody and an Alexa 488 secondary antibody. A significant ($p<0.05$) increase in platelet numbers was observed following renal IR injury compared to sham tissue sections (CPF: IR only: 47.84 ± 14.59 ; Sham: 13.34 ± 2.815 ; **Figure 6.4.A-C**). The presence of naïve HPC-7 or KC+SDF-1 α pre-treated HPC-7 significantly ($p<0.05$) reduced platelet accumulation within the IR injured kidney compared to IR injury without HPC-7

Chapter 6: Beneficial Effects of HSCs upon the Injured Renal Microvasculature

(CPF: IR + naïve HPC-7: 16.61 ± 3.821 ; IR + KC+SDF-1 α HPC-7: 17.10 ± 9.948 ; IR only: 47.84 ± 14.59 ; **Figure 6.4.A,C-E**). Again, there was no significant difference in platelet numbers between the two groups receiving HSCs.

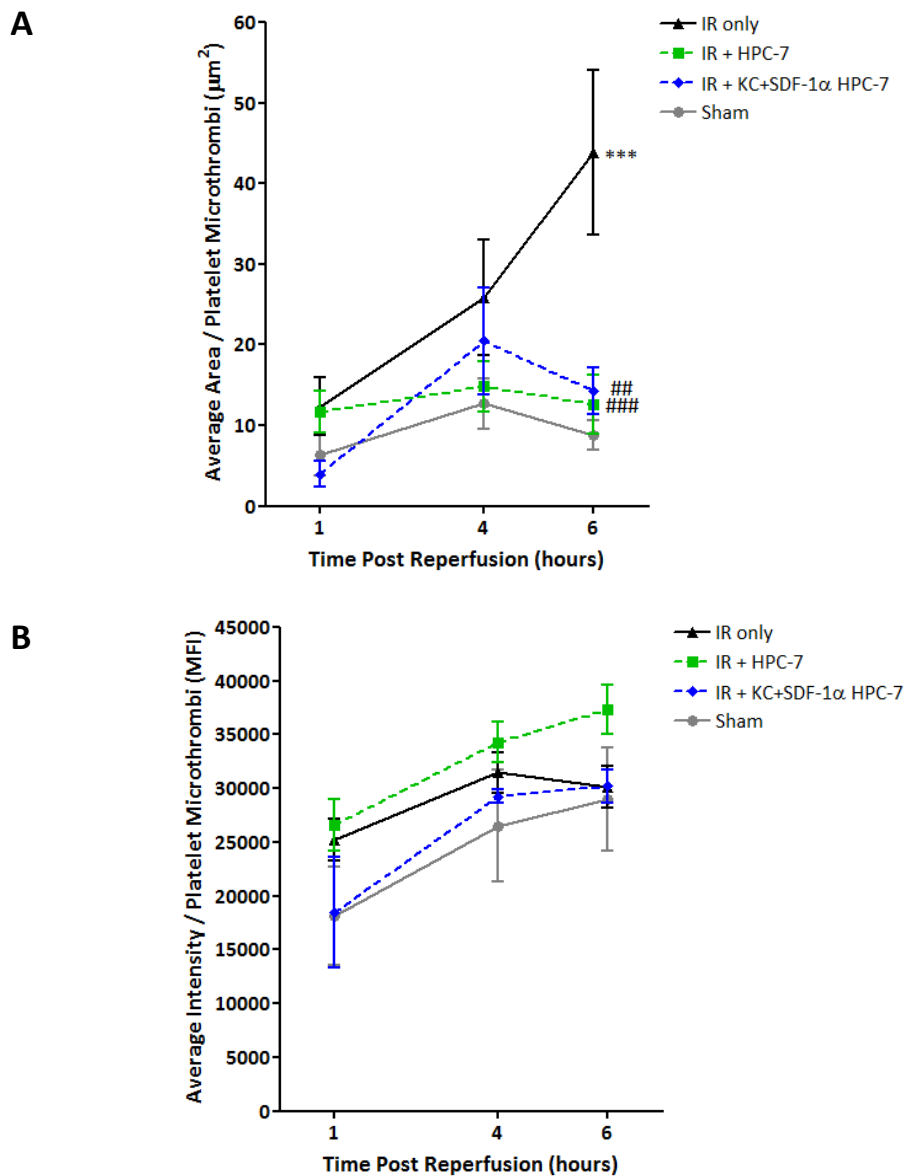


Figure 6.3. *The size of platelet microthrombi is reduced in IR injured animals at 6 hours reperfusion when animals receive 2×10^6 naïve and/or KC+ SDF-1 α pre-treated HPC-7.* Five fields of view were taken of the kidney at 1 hour, 4 hours and 6 hours reperfusion and each microthrombus size and fluorescent intensity was quantified using Slidebook's offline analysis program and the mean quantitated. A significant increase in the size of microthrombi at 6 hours reperfusion in the IR injured kidney was observed compared to sham (**panel A**: black line: IR injured; grey line: sham). Injecting naïve or KC+SDF-1 α treated cells at 1 hour reperfusion, significantly decreased the size of each adherent platelet microthrombi (**panel A**; green line: naïve HPC-7; blue line: KC+SDF-1 α treated HPC-7; black line: IR only). There were no changes in the microthrombus fluorescent intensity (arbitrary units) between any of the treatments (**panel B**). Plots represent a mean adhesion \pm SEM of at least 5 separate experiments; ** $p < 0.01$, *** $p < 0.001$. **Panel A and B**: two-way ANOVA with bonferroni post-tests.

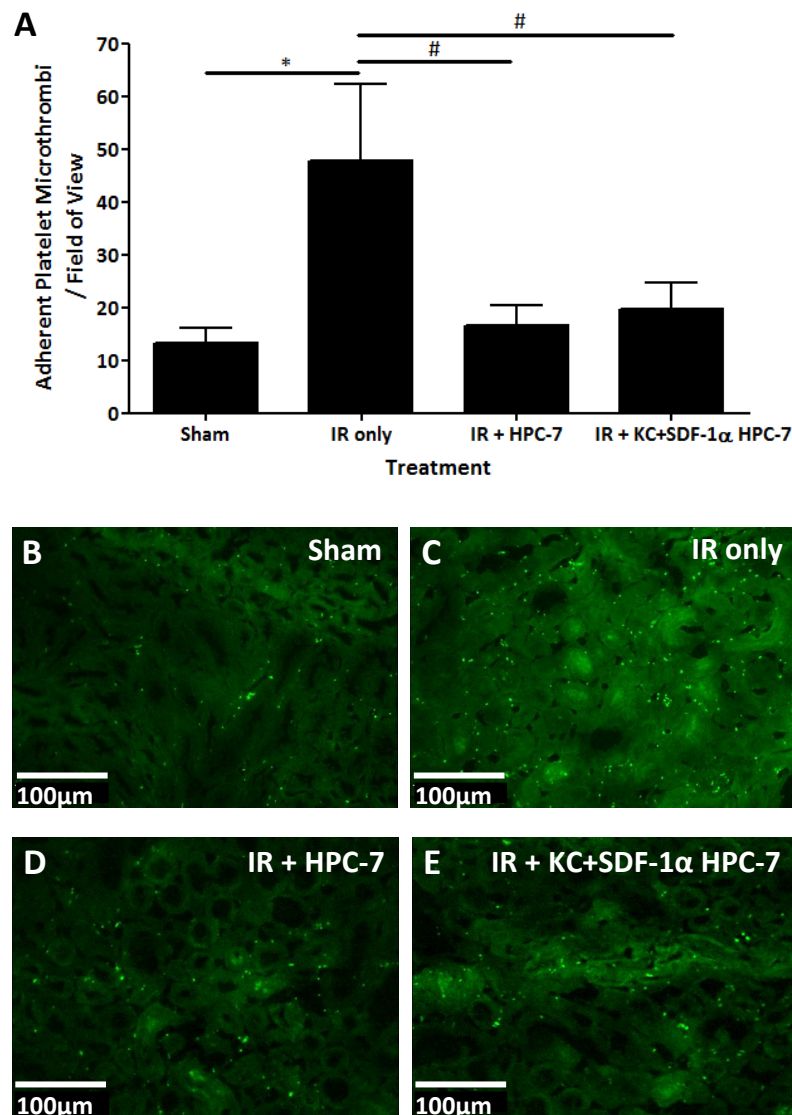


Figure 6.4. Fluorescent immunohistochemistry shows that naïve and KC+ SDF-1α pre-treated HPC-7 reduce platelet microthrombi adhesion to an IR injured kidney at 6 hours reperfusion. After intravital surgery, mice were sacrificed at 6 hours reperfusion and kidneys were snap frozen in liquid nitrogen ready for sectioning. 10µm sections were cut and fixed to glass slides ready for fluorescent immunohistochemistry. Platelet microthrombi numbers were proven by using a primary anti-CD42b platelet marker and a fluorescent Alexa 448 secondary antibody. Five fields of view were taken from each different kidney and the numbers of platelets were quantified. There was a significant increase in the number of platelet microthrombi in the IR injured kidney compared to that of the sham (**panel A**). Kidney that had received naïve and/or KC+SDF-1α treated cells at 1 hour reperfusion showed a significant decrease in the number of adherent platelet microthrombi compared to the IR injured kidney (**panel A**). Representative images showing platelet numbers in: sham (**panel B**); IR only (**panel C**); naïve HPC-7 + IR (**panel D**); KC+SDF-1α HPC-7 (**panel E**). Plots represent a mean adhesion ±SEM of at least 4 separate experiments; * p<0.05. **Panel A:** one-way ANOVA with Dunnett's post-tests.

6.3.5 Vascular albumin leakage is improved after HPC-7 administration

Following systemic injection, FITC-BSA is normally contained within the microvessels, which appear white (false colour green) against a black background. However, when the integrity of the vasculature is disturbed, FITC-BSA leaks out and appears as a flare in the interstitium. Following renal IR injury, a substantial increase in the macromolecular leakage of FITC-BSA at 6 hours reperfusion was observed when compared to the sham controls at 6 hours reperfusion (**Figure 6.5.A-B**). However, macromolecular leakage decreased in mice receiving naïve or KC+SDF-1 α treated HPC-7 when compared to IR injured kidneys without HPC-7 (**Figure 6.5.C-D**).

6.3.6 Using the Chandler loop, administration of HPC-7 reduces blood clot weigh

Preliminary Chandler loop studies were conducted to determine whether the reduction in microthrombus formation was due to a direct effect of HPC-7 on the platelets themselves. Whole blood, isolated from the mouse descending aorta, was introduced into a Chandler loop in the presence or absence of 5×10^5 HPC-7 or just a vehicle (saline) control. There was no significant change in the weight of blood clots at 4 hours although there was a trend for weight to decrease slightly in the presence of HPC-7 (Average weight (AW): Saline control: 115.8mg \pm 36.08mg; HPC-7: 92.02mg \pm 12.96mg; **Figure 6.6.A**). After 24 hours, there was a significant decrease in clot weight when treated with HPC-7 (AW: 144.9mg \pm 30.45mg; HPC-7: 75.67mg \pm 19.58mg; **Figure 6.6.B**).

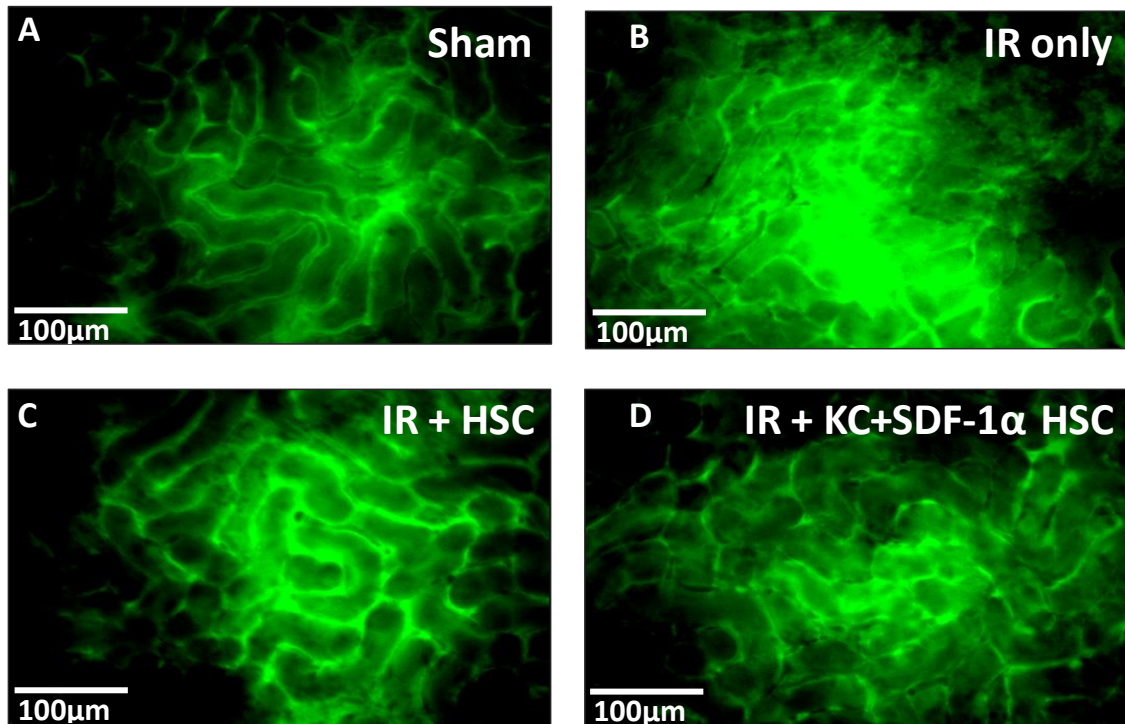


Figure 6.5. Vascular macromolecular leakage of labelled albumin is decreased in an IR injured kidney when HPC-7 are injected. Kidneys were clamped for 45 minutes and allowed to reperfuse for 6 hours prior to a 200μl intra-arterial bolus of FITC-BSA. Five fields of view were taken of the kidney at 6 hours reperfusion. There was a significant increase in the leakage of a macromolecule at 6 hours reperfusion in the IR injured kidney (**panel B**) compared to that of the sham (**panel A**). Naïve and KC+SDF-1α treated HPC-7 were injected at 1 hour reperfusion: there appears to be a visible decrease in the amount of vascular leakage in the IR injured kidneys after naïve (**panel C**) and KC+SDF-1α treated HPC-7 (**panel D**) administration, compared to IR injury alone.

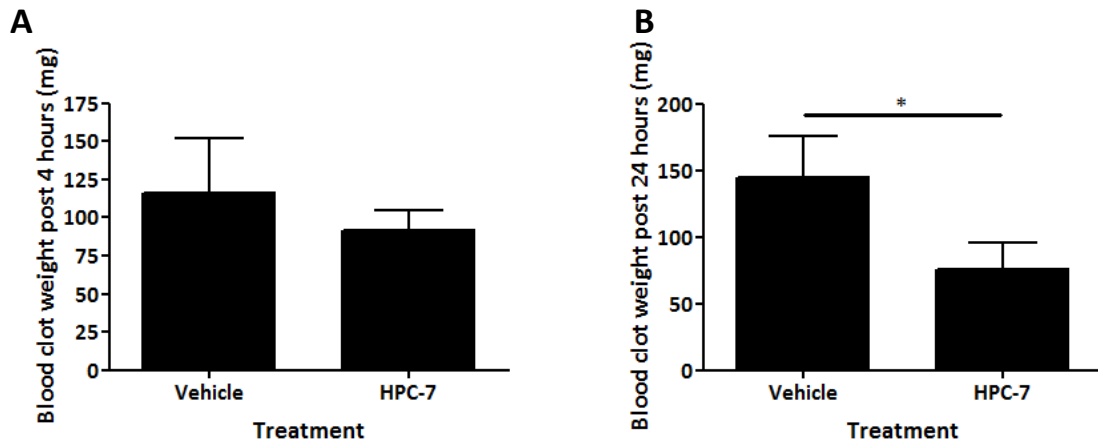


Figure 6.6. The mass of a thrombus is reduced when HPC-7 are present. Blood was removed from murine donors into citrate coated tubes and then introduced into the Chandler loop, along with calcium chloride and then this was allowed to rotate for 4 hours in the presence of HPC-7 or a saline control. After 4 hours, there was a decline in the weight of the blood clot with the presence of HPC-7, but this did not reach significance (**panel A**). Clots were then put into HBSS and incubated for 24 hours and clot weights were measured again: There was a significant decrease in the weight of the thrombus when 5×10^5 HPC-7 were present (**panel B**). Plots represent a mean adhesion \pm SEM of at least 3 separate experiments; * $p < 0.05$. **Panel A and B:** unpaired t-test.

6.3.7 Blood flow in IR injured kidneys is improved after HPC-7 administration

Blood flow decreased in IR injured kidneys compared to sham, as determined by laser Doppler flux imaging (**Figure 6.7**). When naïve or KC+SDF-1 α pre-treated HPC-7 were injected, a significant improvement in blood flow was observed compared to IR injury alone at 6 hours reperfusion (**Figure 6.7**).

6.3.8 Urea and creatinine levels are reduced, thereby function improves, after HPC-7 administration

Blood was removed from mice after 6 hours reperfusion from the descending aorta and serum was analysed for urea and creatinine. After renal IR injury there was a significant ($p<0.01$) increase in the urea and creatinine compared to healthy shams (Urea: Sham: 8.325 ± 0.3250 ; IR only: 11.35 ± 0.6739 ; **Figure 6.8.A**; Creatinine: Sham: 18.25 ± 0.8539 ; IR only: 31.50 ± 1.658 ; **Figure 6.8.B**). IR injured mice receiving naïve HPC-7 had a significantly lower urea and creatinine level ($p<0.001$ and $p<0.01$ respectively) compared to non-treated mice (Urea: IR + naïve HPC-7; 7.280 ± 0.2990 ; **Figure 6.8.A**; Creatinine: IR + naïve HPC-7: 20.00 ± 0.6325 ; **Figure 6.8.B**). KC+SDF-1 α HPC-7 treated IR injured animals also had a significantly lower urea and creatinine levels ($p<0.001$ and $p<0.05$ respectively) compared to non-treated IR only (Urea: IR + KC+SDF-1 α HPC-7; 8.260 ± 0.4739 ; **Figure 6.8.A**; Creatinine: IR + KC+SDF-1 α HPC-7: 24.80 ± 2.417 ; **Figure 6.7.B**). However there were no differences in urea and creatinine serum levels between naïve and KC+SDF-1 α treated HPC-7.

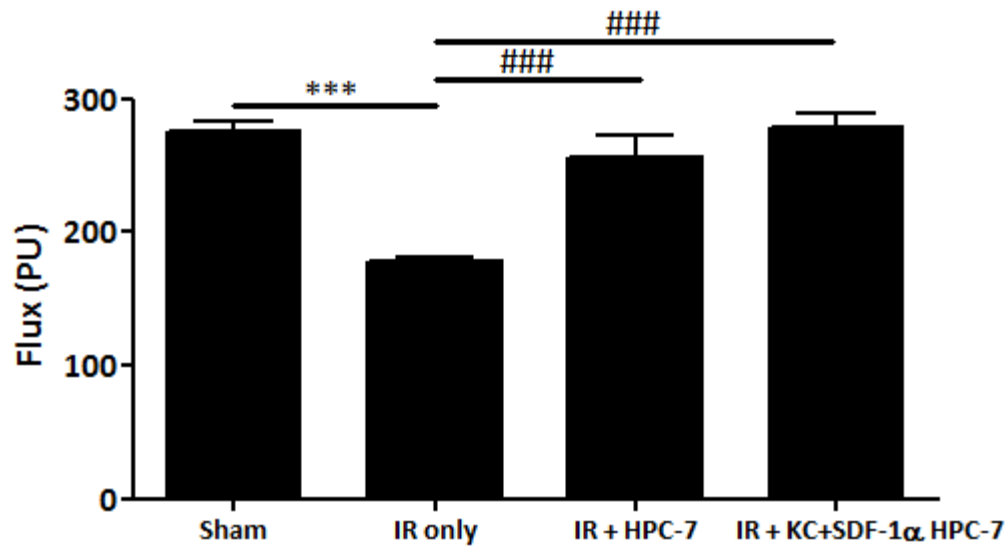


Figure 6.7. Blood flow is improved in IR injured kidneys when HPC-7 are injected. Kidneys were then clamped for 45 minutes and allowed to reperfuse for 6 hours prior to blood flow measurements. Five fields of view were taken of the kidney at 6 hours reperfusion with the laser Doppler equipment. There was a significant decrease in the flux at 6 hours reperfusion in the IR injured kidney compared to that of the sham. Naïve and KC+SDF-1 α treated HPC-7 were injected at 1 hour reperfusion: there is a significant increase in blood flow in the IR injured kidneys after naïve and KC+SDF-1 α treated HPC-7 administration, compared to IR injury alone.

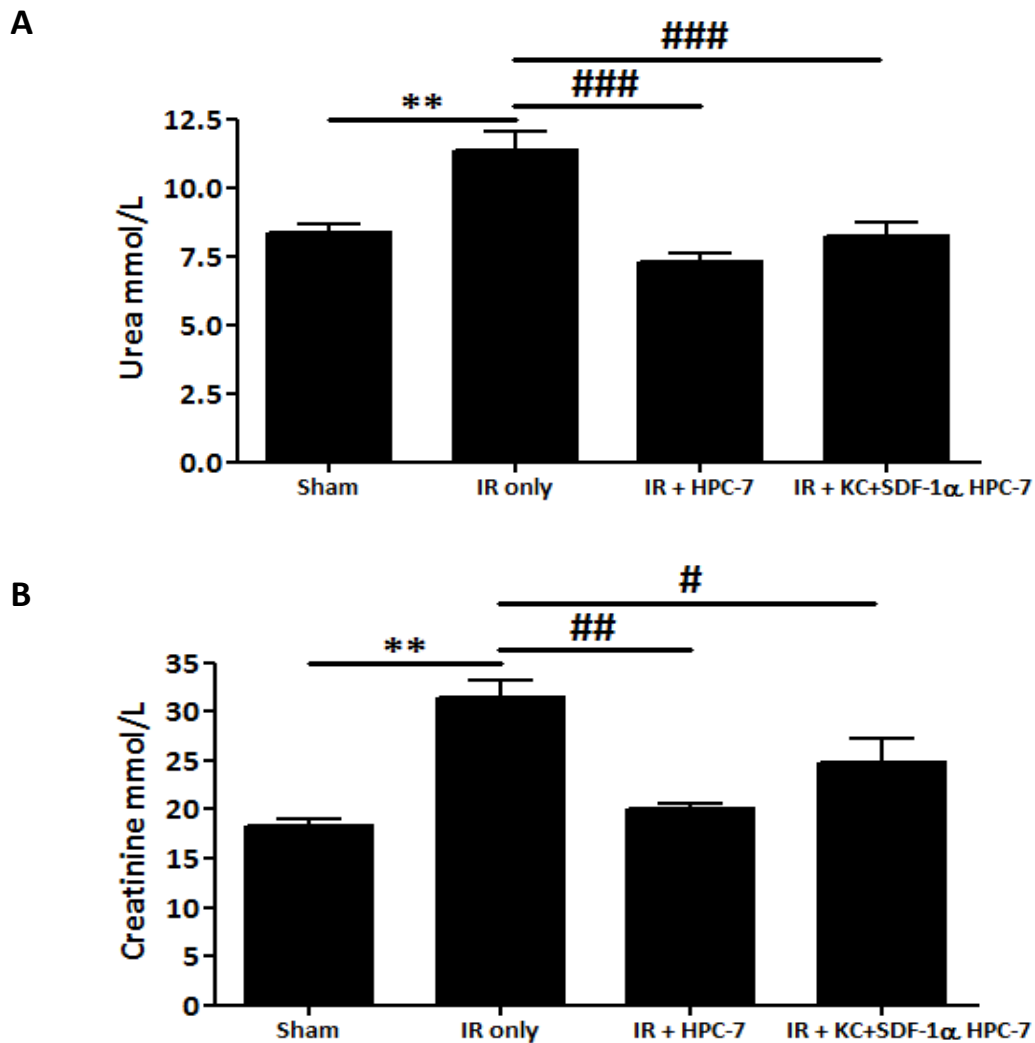


Figure 6.8. Urea and creatinine serum concentrations were reduced with the presence of HPC-7. Blood was removed from the murine models of renal IR injury after intravital monitoring and then centrifuged at 1000g for 10 minutes at 4°C. The serum was removed from the pellet and frozen at -80°C ready for analysis by the Pathology department, Queen Elizabeth Hospital, Birmingham, UK. There was a significant increase in the urea (**panel A**) and creatinine (**panel B**) serum concentrations after 45 minutes ischaemia and 6 hours reperfusion, compared to a sham animal. When naïve or KC+SDF-1α pre-treated HPC-7 were injected into an IR injured animal at 1 hour reperfusion, urea (**panel A**) and creatinine (**panel B**) serum concentrations were decreased, compared to IR injured animals without HPC-7. Plots represent a mean adhesion \pm SEM of at least 3 separate experiments; * $p < 0.05$, ** $p < 0.01$. **Panel A and B:** one-way ANOVA with bonferroni post-tests.

6.4 Major Findings for Chapter 6

FINDING		HOW?
1	Establish 6 hour reperfusion IR injury model to image inflammatory cell recruitment	<i>In vivo</i> : Confocal intravital microscopy
2	After renal IR injury , increased neutrophil numbers were observed at 6 hours reperfusion compared to a sham animal	<i>In vivo</i> : Confocal intravital microscopy
3	When HPC-7 are injected into an IR-injured animal, they decreased the number of neutrophils at 6 hours reperfusion, compared to an untreated IR control	<i>In vivo</i> : Confocal intravital microscopy
4	After renal IR injury , increased platelet microthrombi numbers were observed at 6 hours reperfusion compared to a sham animal	<i>In vitro</i> : Fluorescent immunohistochemistry <i>In vivo</i> : Confocal intravital microscopy
5	When HPC-7 are injected into an IR-injured animal, they decreased the number of platelet microthrombi at 6 hours reperfusion, compared to an untreated IR control	<i>In vivo</i> : Confocal intravital microscopy
6	HPC-7 improved blood flow and vascular leakage in the IR-injured animal compared to a no cell IR-injured control	<i>In vivo</i> : Confocal intravital microscopy and laser Doppler microscopy
7	There is increased urea and creatinine injury markers after 6 hours reperfusion in a renal IR-injured model compared to a sham control	<i>In vitro</i> : Blood serum analysis
8	HPC-7 reduced injury markers at 6 hours reperfusion in the IR-injured animal compared to a no cell IR-injured control	<i>In vitro</i> : Blood serum analysis
9	HPC-7 pre-treatment with 25ng/ml of KC + SDF-1α for 5 minutes does not appear to confer any greater benefit to inflammatory cell numbers or injury	<i>In vitro</i> : Fluorescent immunohistochemistry and blood serum analysis <i>In vivo</i> : Confocal intravital microscopy and laser Doppler microscopy

6.5 Discussion

This chapter presents novel data obtained using confocal IVM demonstrating that significant neutrophil and platelet adhesion occurs following mouse renal IR injury *in vivo*, and that these events are key contributors to microcirculatory and tissue damage. Adherent platelet microthrombi could subsequently block blood flow, further exacerbating the injury. Additional microcirculatory disorders included marked albumin leakage, an indicator that vascular integrity had been disturbed, and an overall decrease in renal blood flow. Considering these observations, it is essential therefore, that the development of new strategies to treat AKI must involve approaches that improve renal microcirculatory haemodynamics. This study demonstrated that HSCs could confer quite remarkable vasculoprotective effects within the injured kidney, which is incredibly remarkable. Novel labelling methodologies for imaging within the kidney were utilised for these studies, generating images of renal microcirculatory disturbances not previously seen.

Numerous studies have previously demonstrated infiltration of neutrophils into IR injured tissues. Increased renal distribution of leukocytes has also been shown histochemically, often as early as two hours post-reperfusion (Willinger *et al.* 1992). Our intravital data is consistent with these findings. Clearly blocking neutrophil adhesion is beneficial as antibodies against renal ICAM-1 prevented neutrophil adhesion, which subsequently protected from AKI (Kelly *et al.* 1996). Although an anti-inflammatory role for MSCs is well described, the ability of HSCs to modulate neutrophil presence in inflamed tissue has received little attention (Schwartz *et al.* 2008). However, our novel intravital data

Chapter 6: Beneficial Effects of HSCs upon the Injured Renal Microvasculature

indicates HSCs can indeed reduce neutrophil adhesion in mice undergoing renal IR injury. The role of platelets in the mouse kidney following IR injury has not previously been investigated directly. In an early study in rats, radio-labelled donor platelets accumulated in the kidney 30 minutes post-reperfusion (Chintala *et al.* 1994). Similarly, within the IR injured gut, platelet adhesion increases at 30 minutes post-reperfusion (Holyer 2010). These pro-thrombotic events take place much earlier than what we have observed in the current study in which the number of microthrombi increased most significantly at 6 hours post-reperfusion. In intestinal IR injury, platelet rich microthrombi predisposes the animal model to organ failure (Kalia *et al.* 2001; Salter *et al.* 2001); therefore reducing platelet microthrombi would be extremely advantageous. Our novel imaging methodology has allowed us to generate exciting data that shows HSCs also markedly modulate platelet adhesion.

Although potent anti-platelet drugs are available for clinical use, there are advantages in using SCs to potentially inhibit platelets. Although the anti-thrombotic / anti-aggregatory effects of well known drugs (eg. aspirin, GPIIb/IIIa antagonists) are described, there is little direct evidence from *in vivo* studies that these drugs also prevent platelet-endothelial (P-E) interactions. Indeed, Schulz and colleagues demonstrated intravitaly, that although aspirin, in combination with clopidogrel, reduced platelet thrombus formation following rupture of an atherosclerotic plaque *in vivo*, they did not prevent adhesion of platelets to dysfunctional endothelial cells (Schulz *et al.* 2008).

Chapter 6: Beneficial Effects of HSCs upon the Injured Renal Microvasculature

Although a role for neutrophils is recognised in ischaemic disorders, there is increasing evidence that implicates a pathological role for adherent platelets on activated endothelium in IR injury. Platelets have been shown to recruit inflammatory leukocytes to sites of IR injury and further aggravate endothelial damage. Studies in the heart (Kupatt *et al.* 2002; Gawaz 2004), kidney (Singbartl *et al.* 2001) and liver (Khandoga *et al.* 2002; Khandoga *et al.* 2003) have all shown that platelets mediate leukocyte adhesion during the reperfusion stage. In our intravital studies, the microthrombi are generally observed earlier, and therefore they may be promoting the neutrophil recruitment in our model. Furthermore, activated platelets can support the rolling and adhesion of leukocytes to the injured endothelium (Buttrum *et al.* 1993; Yeo *et al.* 1994) but also bind leukocytes via P-selectin-PSGL interactions (Palabrica *et al.* 1992). Indeed, several studies, including our own research, have demonstrated that targeting leukocytes is not sufficient and preventing platelet-endothelial interactions is also needed. Since adherent platelets on activated endothelium can recruit inflammatory cells (neutrophils, monocytes) and further exacerbate pathology, any strategy that *simultaneously* inhibits platelet and leukocyte adhesion will be desirable, particularly in IR injured tissue. In addition, since SCs become adherent within the injured tissue microcirculation, their beneficial paracrine effects are localised within the immediate vicinity in which they are present i.e. in the disturbed microvessels. This prevents any systemic effects being mediated and as such avoids unwanted side effects associated with pharmacological anti-platelet agents e.g. bleeding complications.

Chapter 6: Beneficial Effects of HSCs upon the Injured Renal Microvasculature

It is unclear how HSCs mediate anti-platelet and anti-neutrophil effects and this will need to be investigated further. They could have direct effects on platelets and neutrophils themselves and/or on other cells, such as the endothelium, in the surrounding environment. Indeed, many functions have been postulated that HSCs can act beyond their role in haematopoiesis. Circulating HSCs have been shown to fight against bacterial infection by releasing cytotoxic cytokines, such as $\text{TNF-}\alpha$, act as readily available precursors of mature blood leukocytes, or release anti-inflammatory and pro-growth factors at sites of inflammation (Granick *et al.* 2012). Evidence does suggest that commonly used anti-platelet drugs may not just work on the various actions on platelets, but also influence endothelial function (Zhao *et al.* 2006).

Our preliminary data obtained using the Chandler loops suggests HSCs may directly modify platelet aggregation, as no endothelium was present in these assays; this effect was only significant after 24 hours. The thrombi were stringy and brittle and were even more so when HPC-7 were present. The appearance of these thrombi were different to how we expected, even though the shear rates were calculated to be similar to those experienced within a mouse renal arteriole, yet the clots resembled were more so of venous structure. These are however very early studies and we cannot speculate further as to any potential protective mechanism.

Interestingly, Abou-Saleh (2009) has shown that endothelial progenitor cells (EPC) and their supernatant can also inhibit platelet activation and aggregation through releasing

Chapter 6: Beneficial Effects of HSCs upon the Injured Renal Microvasculature

PGI₂ and upregulating COX-2 production, thereby promoting an anti-thrombotic phenotype. This effect was abolished when treated with a COX inhibitor, indomethacin. Using an *in vivo* model of arterial injury, Saleh and colleagues also showed that when EPCs or their supernatant was introduced intra-arterially 15 minutes before a FeCl₃-induced injury, it could effectively reduced thrombus mass by 33% and subsequently improved blood flow.

It was originally hypothesised that any vasculoprotective effects would be proportional to the degree of HSC recruitment. However, quite surprisingly, we demonstrated that HSCs recruited simply by injury alone were capable of reducing inflammation to levels observed in sham animals. This is the opposite to what was observed by Kavanagh and colleagues (2013), as HPC-7 only reduced leukocyte adhesion in the IR injured gut when pre-treated with SDF-1 α to enhance their recruitment. This may be explained by the fact that physiologically, the renal blood flow (RBF), or the volume of blood delivered to the kidneys, is higher than in other organs. Approximately 34% of the cardiac output in mice is delivered to the kidneys and 19% to the gut; calculated from the following published data in mice: CO=14.9ml/min ; RBF=5.1ml/min; Small intestinal BF= 2.79ml/min (Broulik *et al.* 1973; Garrelds *et al.* 2002). This would mean that in 'first passes', more HSCs are delivered to the kidneys compared to other organs. Hence the degree of HSC recruitment within gut may not be sufficient to confer a therapeutic effect. Also, the intestinal mucosa is incredibly susceptible to ischaemic injury, which possibly does not affect the renal cortex (region viewed) to the same degree. Therefore, more SCs may be required to aid in the repair of a severely damaged intestinal environment.

An increase in vascular permeability to albumin was also observed in renal IR injured microcirculation as shown by macromolecular leakage of FITC-BSA. Leakage from vessels can occur as a result of direct injury to endothelium but has been demonstrated to be highly correlated with the number and location of adherent and emigrated leukocytes (Kurose *et al.* 1993). Blockage of microvessels with microthrombi, adherent leukocytes and/or platelet-leukocyte aggregates can reduce blood flow in the IR injured tissue (Frenette *et al.* 1998). The additional advantages of inhibiting leukocyte and platelet adhesion using HSCs are therefore the reduction in macromolecular leakage and also the restoration of blood flow. Several studies have shown that treatments aimed at reducing the trapping of RBC, leukocytes and also promoting the anticoagulant state significantly improved kidney morphology and function (Hellberg *et al.* 1990; Rabb *et al.* 1994; Kelly *et al.* 1996; Druid *et al.* 1998).

Data presented in this chapter also showed improvements in renal function. During renal injury, the glomerular capillaries are unable to filter blood efficiently due to a reduction in blood flow – this results in an increase in both urea and creatinine. Serum urea and creatinine concentrations were elevated in renal IR injured mice compared to sham, indicating a malfunction in kidney function. Even small increases in creatinine result in worsened long-term outcomes and an associated greater mortality risk (Coca *et al.* 2007). However, improvements in these parameters were observed in HSC-treated mice indicating this cellular therapy can also improve renal function. This is in contrast to data presented recently by Burst and colleagues (2013) who demonstrated that rat-derived

Chapter 6: Beneficial Effects of HSCs upon the Injured Renal Microvasculature

HSCs, characterised as being Lin⁻ CD90⁺, could not ameliorate renal function or structure after damage to their IR injury model; however, this study was conducted in rats in which fewer cells were injected than in this work.

Future studies would need to determine the long term benefits of HSCs in the kidney, as this study only observed a relatively short period of reperfusion in the acutely injured kidney. Although no therapeutic advantage was demonstrated in enhancing SC presence in this injury mode, it may be that increased SC presence becomes essential in more chronic models of renal injury. Thus strategies that enhance renal HSC adhesion may be necessary for their vasculoprotective benefits to be apparent and is thus a worthwhile pursuit.

Chapter 7



General Discussion

7 General Discussion

7.1 Summary of Main Findings

Although HSCs are potentially beneficial for a variety of renal disorders, their efficacy may depend on successful local recruitment (Lin *et al.* 2003; Li *et al.* 2010; Li *et al.* 2011; Li *et al.* 2012). HSCs are rare cells constituting <0.05% of the BM and this scarcity has hindered their clinical use. Improving their therapeutic efficacy may therefore depend on identifying adhesive mechanisms that underpin SC trafficking. However, no studies have previously described the molecular adhesive mechanisms governing renal HSC recruitment. Therefore, one of the primary aims of this thesis was to understand the adhesion mechanisms involved in HSC recruitment to the IR injured kidney and to utilise the information to develop strategies to improve renal homing. We developed an intravital imaging methodology to obtain valuable insights into the kinetics of SC homing within the mouse renal microcirculation *in vivo* immediately following their infusion. This study not only generated data on renal SC homing, but also provided novel data on some of the microcirculatory disturbances that are associated with renal IR injury. The major findings from this study include the following:

- HSCs are recruited to injured and non-injured CL kidney post-renal IR injury, with increased free-flowing HSCs numbers observed in injured kidneys at the point of infusion. This increased adhesion is despite the fact that blood flow is reduced in the injured kidney upon reperfusion.

- Topical application of chemokines KC or SDF-1 α can recruit HSCs to a healthy kidney and their receptors, CXCR2 and CXCR4, are expressed on the HSC surface.
- Blocking studies have shown CD49d, CD44, CXCR2 and CXCR4 are responsible for governing HSC adhesion to the injured peritubular capillaries *in vivo*. VCAM-1 and HA are the endothelial counter-receptors for CD49d and CD44 and are important in mediating recruitment following renal ischaemic damage.
- HSC pre-treatment with KC or SDF-1 α enhanced adhesion to renal endothelium *in vitro*, whereas IL-1 β or TNF- α did not. However, all tested cytokine pre-treatments enhanced HSC adhesion to IR injured kidney *in vivo*. IL-1 β , SDF-1 α , TNF- α or KC+SDF-1 α treatments also increased the number of free-flowing HSCs.
- Enhanced adhesion can be explained by various mechanisms: these included that after IL-1 β , SDF-1 α and KC+SDF-1 α pre-treatments HSCs were more deformable when moving through (glass) capillaries. Also, KC or SDF-1 α increased HSC adhesion to both VCAM-1 and HA, indicating an increased binding capacity of HSCs adhesion molecules for their respective counter-ligands. Furthermore, an increase in the number of CD49d and CD44 micro-clusters after SDF-1 α or KC pre-treatment was observed, most likely explaining the increases in adhesion to their immobilised counter-receptors *in vitro*.
- A longer perfusion model of renal IR injury showed an increase in platelet microthrombi and neutrophils at 6 hours reperfusion in injured peritubular capillaries compared to sham. Additional microcirculatory disturbances include increases in vascular permeability and decreased blood flow within the kidney. Most strikingly, HSC injection at 1 hour reperfusion reduced both platelet and neutrophil numbers at 6 hours reperfusion in an IR injured kidney *in vivo*, as well

as reducing renal vascular permeability and increasing renal blood flow; this resulted in an overall improvement in kidney function at 6 hours reperfusion.

Intravital studies monitoring HSC trafficking *in vivo* to sites of injury have been limited due to difficulties in isolating sufficient numbers for detection following systemic infusion. We and others have found that approximately 5000 primary murine HSCs (KSL cells) can be obtained from one adult mouse (Orlic *et al.* 2001); this is too low for intravital or even *in vitro* adhesion assays and pooling cells from mice would require an unacceptable number of donor mice to be culled for individual intravital experiments. A murine HSC line, HPC-7, was therefore used. Many studies have used these HPC-7 to model primary HSCs in detailed molecular, cellular signalling and homing studies (Pinto do *et al.* 1998; Pinto do *et al.* 2001; Pinto do *et al.* 2002; Kavanagh *et al.* 2010; Kavanagh and Kalia 2011; Kavanagh *et al.* 2012). However, it is essential to point out that our pre-treatment strategies also enhanced the adhesion of primary SCs in a similar manner when using an activated renal endothelium adhesion assay (White *et al.* 2013). This repertoire of information validates the use of HPC-7 as a HSC alternative.

The body of work contained in this thesis firstly presented data showing that acute inflammation of the kidney results in increased adhesion of exogenously administered HPC-7 cells. Both *in vitro* and *in vivo* data demonstrates that renal IR injury acts as a stimulus to promote the recruitment and adhesion of HPC-7 to the injured microvasculature. This stimulus could be in the form of small molecular weight proteins,

which were identified in a greater concentration within the ICM compared to the SCM. We initially demonstrated that pre-treating cells with this ICM resulted in increased HPC-7 adhesion *in vitro*; these proof-of-concept experiments clearly demonstrated that HSC adhesion can be modified and this is the first time this has been demonstrated within an injured kidney. However, this strategy does not have the potential to be applied clinically, and so more translational approaches were identified.

Although we speculated and identified a critical role for SDF-1 α and other cyto/chemokines such as KC, we would need to perform detailed analysis of the ICM to identify any additional chemical and biological factors within the ICM. There may be more potent modulators of SC behaviour than those identified in this study; powerful cellular activators such as leukotrienes and complement factors are also known to be released in abundance following IR injury and can influence circulating blood cell adhesion. Furthermore, these molecules may be unique to tissue or injury type and may offer the potential to further refine the targeting process to specific sites. This is particularly important since not all studies have identified SDF-1 α as a critical homing molecule: Ip and colleagues (2007) have shown that blockade of CXCR4 on MSCs did not reduce their recruitment to the ischaemic myocardium; this could be due to a lower expression of CXCR4 on MSCs compared to HSCs. Although many studies have highlighted a key role for SDF-1 α in mediating HSC recruitment and homing (Lapidot 2001; De Falco *et al.* 2004; Porecha *et al.* 2006), we present novel data that KC is equally as potent at enhancing HSC adhesion. Identifying more than one effective strategy is

important, as it is not clear which pre-treatment, if any, will be effective when used in translational studies in humans.

The VLA-4/VCAM-1 pathway has previously been implicated in SC homing to different tissues (Mazo *et al.* 1998; Zhang *et al.* 2007; Kavanagh *et al.* 2010). This is not surprising as the trafficking of leukocytes is also somewhat dependant on this pathway (Woodside *et al.* 2006). The α_4 but not β_1 , on MSCs has been showed to be essential for MSC recruitment and engraftment to the heart after myocardial infarction (Ip *et al.* 2007). We have shown the α_4 subunit is essential for HSC recruitment to the IR-injured kidney but whether the β_1 subunit is also responsible for this adhesion is yet to be investigated. As well as being important in acute injuries, the VLA-4/VCAM pathway has been proposed to be of importance in chronic disease states (Yusuf-Makagiansar *et al.* 2002); this suggests strategies that modify the interactions of this pathway may also improve their homing in more chronic renal diseases. The molecular adhesive mechanisms' governing HSC homing to experimental models of CKD have yet to be determined and is certainly important area to pursue in future studies.

The final part of this work focussed on the inflammatory environment during renal IR injury. Neutrophil infiltration is heightened at 6 hours reperfusion: CD18 on their surface is the primary adhesion molecule responsible for their adhesion and its endothelial counter-ligand ICAM-1 is heavily upregulated after 24 hours of renal IR injury (Burne *et al.* 2001). Therefore, as AKI is split into several stages, it is conceivable that CD18 could

become predominant in HSC trafficking in the later stages of kidney injury. This could also be true of endothelial CD44: we have shown HPC-7 require their CD44 expression to adhere to injured renal endothelium and although CD44 can interact with itself (Isacke 1994) and is expressed on capillary endothelial cells after renal IR injury (Rouschop *et al.* 2005), in our model of renal IR injury HSC adhesion to the peritubular endothelium was not governed by endothelial CD44. After renal IR injury, CD44 expression on capillary vasculature has been shown to peak at 24 hours (Lewington *et al.* 2000), whereas HSC adhesion in our model was examined at 1-2 hours reperfusion. We have shown that HA was the endothelial counter-ligand for CD44 on HSCs and is required for HSC homing to the injured renal microvasculature. This reiterates that another important pathway for HSC adhesion has a role in leukocyte rolling and firm adhesion to endothelium (DeGrendele *et al.* 1997; Gal *et al.* 2003). Collectively this data provides sufficient evidence that the kinetics of HSC adhesion follows a similar process to that of the leukocyte-endothelial cascade. From a clinical perspective, one of the major areas of debate for cellular therapy is which would be the best and most effective route for delivery: intra-arterial injection of SCs is the preferred method of delivery of cellular therapy in patients; this current study (and others from our group) demonstrates that these cells can be delivered systemically, that they are capable of circulating in the bloodstream and can home to and be captured by inflamed renal vasculature.

Peled and colleagues (2000) suggested that HSC receptor activation could be modulated by the inflammatory environment the cells are exposed to within an injured organ and this activation can happen within minutes. They showed that more CD34⁺ cells adhered

to ICAM-1 and VCAM-1 after 1 minute stimulation with SDF-1 α , compared to untreated control; therefore a 5 minute HSC treatment with individual cytokines was used to pre-activate HSCs to enhance adhesion. KC and SDF-1 α are known to be released by the injured kidney (Togel *et al.* 2005; Molls *et al.* 2006) and both of these chemokines cause an increase in the number of CD44 and CD49d receptor micro-clusters and subsequently enhance their binding to their endothelial counter-ligands, HA and VCAM-1. Wards and colleagues (1994) have shown that the cooperative effects of more receptor clusters actually increases the resistance of the bond breaking, thereby enhancing firm adhesion. Other studies have shown that small patches of adhesion receptors, known as point contacts, contribute to cell attachment and spreading on ligand-coated substrates (Streeter and Rees 1987; Tawil *et al.* 1993). These studies support our hypothesis that HSC pre-treatments enhance adhesion through modulating receptor localisation. Overall, our data suggests that modulating the binding capacity and/or cluster number of surface adhesion molecules provides a relatively easy and effective means by which to modify SC recruitment and that such strategies are a worthwhile pursuit.

The final part of this work focussed on characterising the inflammatory environment during renal IR injury. Although neutrophil infiltration has been demonstrated following renal IR injury, no previous studies have directly reported increased platelet thrombus presence within peritubular capillaries *in vivo*, noted at 6 hours reperfusion. These can contribute to microvascular congestion, poor blood flow and exacerbation of the inflammatory injury. There are currently few treatments specifically aimed at inhibiting the root cause of IR injury, which has been hypothesised to be the reduction in blood

flow due to reduced NOS activity and microvascular congestion. These have been hypothesised to be the main cause of sustained AKI (Regner and Roman 2012). Increased platelet and neutrophil presence has also been implicated in the pathophysiology of a number of other kidney conditions. Studies have suggested that platelet activation and leukocyte-endothelial interactions may be important in early post-transplantation renal failure and rejection in humans and clinical trials using PAF antagonists have shown to be beneficial in ischaemic AKI (Haug *et al.* 1993; Grino 1994). In the glomeruli of transplanted human kidneys, increased platelet and neutrophil deposition has been correlated with higher serum creatinine levels (Koo *et al.* 1998) and their presence immediately after transplantation of a renal allograft is indicative of a non specific, inflammatory event that is potentially detrimental to long-term graft function. Therefore, methods such as targeted HSC delivery to the kidney, which can effectively reduce both platelet and neutrophil infiltration would be extremely important long-term and in may confer therapeutic benefit in many other renal disorders in which platelets and neutrophils contribute to the pathology.

Sutton and colleagues (2002) stated that in ischaemic AKI, there is a short therapeutic window in which administered treatments will be useful for prevention of tissue injury. Studies have shown this window of opportunity to be a real phenomena, as angiogenic therapy following CKD is only useful in reducing injury when administered at certain time points (Long *et al.* 2012). In our studies, we have shown in our longer perfusion model of renal IR injury that HSC infusion at 1 hour reperfusion can reduce platelet microthrombi and neutrophil infiltration and also improved blood flow. We speculate that this

improvement in blood flow and reduced inflammatory cell number underlies the observation of decreased urea and creatinine levels are decreased, thus improving GFR and the kidneys capability to filter nitrogenous substances. Urea and creatinine levels are brought down to similar levels to those seen in a non-injured sham-operated animal. This is the first study to show that HSCs can confer vasculoprotective and functional benefits within such a short period of time. Ratajczak and colleagues (2012) suggest that paracrine signals from a variety of SCs results in similar therapeutic benefits: Ren *et al.* (2008) and Abou-Saleh *et al.* (2009) have shown that MSCs and EPCs release NO after exposure to pro-inflammatory molecule and additional studies involving MSCs, HSCs or EPCs administration after myocardial injury have shown similar therapeutic effects on ventricular function (Orlic *et al.* 2001; Kucia *et al.* 2004; Quevedo *et al.* 2009). We hypothesise that once HSCs are within the injury site, they are exposed to many inflammatory factors and could be acting in a paracrine action, similar to MSCs and EPCs in the above studies by releasing immunosuppressive factors and NO, which would explain decreases in neutrophil and platelet adhesion, altering the injured environment from a pro-inflammatory phenotype to a more anti-inflammatory one (**Figure 7.1**).

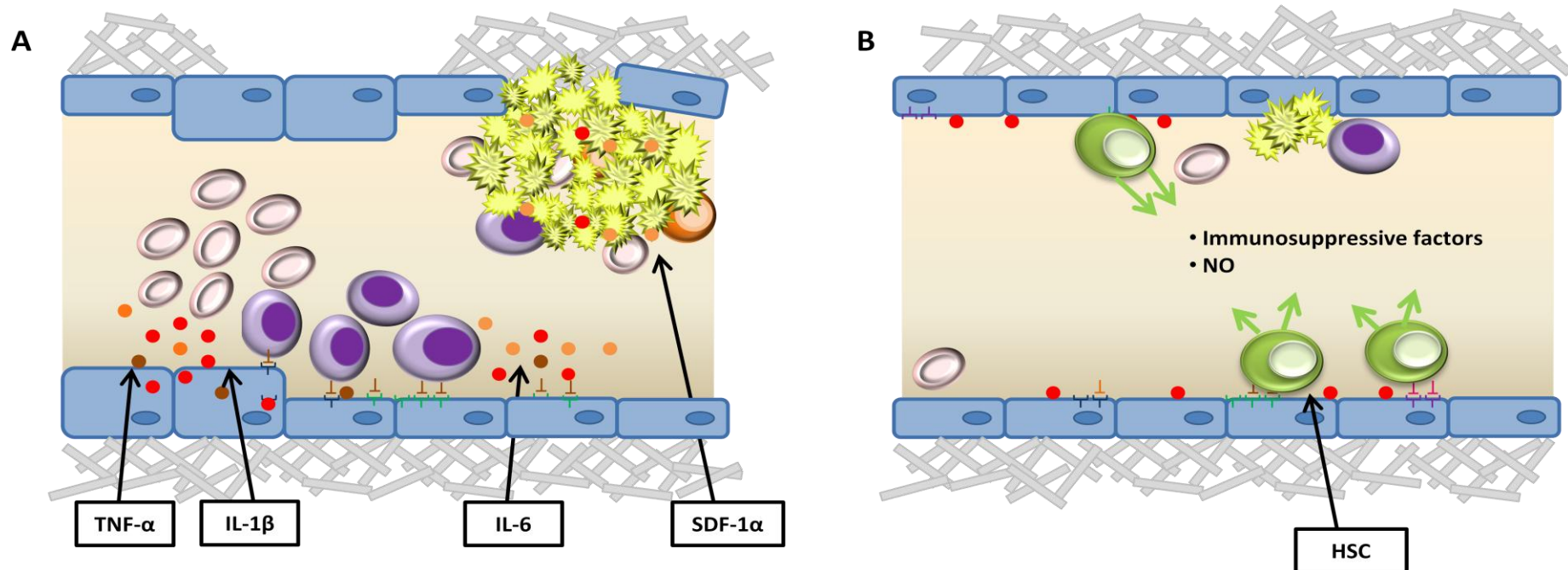


Figure 7.1. HSC anti-inflammatory hypothesis. Renal IR injury causes an upregulation in adhesion molecules. This promotes subsequent adhesion of leukocytes and platelets, which reduces blood flow. Blood flow is worsened due to endothelial cell swelling because of altered eNOS activity (**panel A**). We hypothesise that HSCs adhere to the injured environment and release a concoction of anti-inflammatory factors, which would act to reduce cytokine and leukotriene secretion. In addition, we believe HSCs could be releasing NO, which is an important protective molecule, as it can also reduce platelet and leukocyte activation and adhesion (**panel B**).

7.2 Future Work

Even though the literature on HSC recruitment to injured or diseased tissues is expanding, there are still questions which remain to be answered. Therefore there are several ways in which the work detailed in this thesis could be expanded. If we anticipate taking our pre-treatment strategies into the clinic, we would need to conduct studies using human HSCs to determine whether similar modifications in human HSC homing can be made. Furthermore, the vasculoprotective effects of human cells would also need to be investigated in similar *in vivo* experimental studies.

The paracrine factors released from the HPC-7 that are responsible for the vasculoprotective effects clearly need to be identified. Cytokines are heavily upregulated in IR injury and their production can worsen IR injury and several anti-cytokine agents have been tested to determine whether they ameliorate AKI (Eason *et al.* 1996). Neutrophils predominate in IR injuries and it has been shown that reducing CXC chemokines can reduce neutrophil infiltration. It is possible that HSCs create an anti-inflammatory environment by reducing the release of such chemokines, which may explain the decrease in neutrophils we have observed after HSC administration. Therefore detailed analysis of the releasate from HSCs when exposed to an inflammatory environment needs to be determined. We have collected serum from IR injured animals that received HPC-7 which will be compared using ELISAs with serum from injured mice without cells and will compare their cytokine profiles. Schwarting and colleagues demonstrated that Lin⁻ HSCs reduced infarct size and reduce inflammation in a mouse model of stroke; they analysed gene transcript levels of a variety of trophic factors

including brain-derived neurotrophic factor, glial-derived neurotrophic factor, VEGF and TGF- β . However, although no changes in the presence of growth factors were observed, RT-PCR analysis of pro-inflammatory cytokines in spleens 24 hours after HSC injection demonstrated decreased gene transcripts of pro-inflammatory cytokines TNF- α and IL-1 β (Schwartz *et al.* 2008). This study is the first to demonstrate that HSCs are capable of modulating gene expression of inflammatory markers.

The body of literature studying paracrine-mediated effects of SCs is quickly increasing, especially regarding their anti-inflammatory properties. MSCs have been shown to express high levels of iNOS and release various chemokines such as CXCL9 and CXCL10 after IFN- γ and TNF- α pre-treatment (Ren *et al.* 2008). These leukocyte-recruiting chemokines can enhance inflammatory cell homing towards MSCs, but instead of exacerbating the damage, pro-inflammatory cytokine treated MSCs release large quantities of NO, which acts to locally suppress the adhesion of immune cells. This NO elevation is continued days after the treatment is removed; this could also be of use in later stages of regeneration as NO is known to propagate new blood vessel growth. Ratajczak and colleagues (2012) hypothesised that different types of SCs may have similar anti-inflammatory paracrine effects to each other, therefore studies would need to be conducted to understand if our HSCs released similar compounds.

In addition to HSCs, accumulating evidence now suggests that MSCs may be protective in animal models of IR injury including following renal IR injury (Wise and Ricardo 2012).

Current interest has focussed heavily on using MSCs primarily because of their ability to avoid rejection and their relative ease of expansion in culture. Interestingly, a recent study has shown that MSCs can improve kidney function after renal IR injury by enhancing regulatory T cell infiltration and provided beneficial effects at 72 hours (Hu *et al.* 2013). It is unknown whether MSCs share the potential to elicit reductions in platelet and neutrophil numbers post IR injury and would be worthy of experimentation. Within the previous study, MSCs did not need to home to the injury site to confer beneficial effects; currently, the molecular mechanisms that govern the recruitment of MSCs to the kidney post IR injury are also unknown but if these were understood, would increasing their homing to sites of injury enhance their regenerative capacity?

Although we have shown that HSCs were vasculoprotective at 6 hours post-injury, it is not known whether these beneficial effects would be sustained if animals were allowed to recover. Crockett and colleagues (2006) reduced liver IR injury in the early stages of reperfusion by administering acetylcholine receptor (AChR) agonists prior to ischaemia as acetylcholine is known to bind to macrophages and inhibit their cytokine release. Although these agonists reduced the early elevation in plasma cytokines and injury markers, after 6 hours reperfusion these beneficial effects slowly diminished and by 24 hours the results were negligible. In our lab, experiments are underway to understand if HPC-7 can reduce pro-inflammatory cytokine plasma concentrations. However we have yet to determine to determine whether HPC-7 are also protective in the later stages of reperfusion.

7.3 Concluding Remarks

In conclusion, despite huge advances in the field of cellular therapy, a major impediment remains their poor retention within target tissues on systemic delivery. This is the first time that the main adhesive and cytokine pathways governing HSC recruitment to an IR-injured kidney have been detailed. Manipulating such mechanisms that target these cells to the site of injury is essential to realising their full potential. We provide a simple, quick and effective method for increasing HSC adhesion into injured kidney using cytokine pre-treatments, with KC and SDF-1 α eliciting maximal enhancement. Previous studies have enhanced SC recruitment by introducing genes encoding for SDF-1 α within cardiac tissue (Tang *et al.* 2005); however, the clinical applicability of such techniques is debatable and may be associated with aggravated tissue injury due to side effects, such as SDF-1 α -dependent lymphocyte recruitment (Liekens *et al.* 2010). The current study benefits from identifying a strategy that increases recruitment without genetically manipulating the HSCs or the host tissue and thus has the potential to be used clinically. It is anticipated that enhancing HSC recruitment to injured kidney may expedite the recovery process and encourage greater therapeutic success clinically. There are currently no clinical trials using HSCs in AKI; our data may therefore help in the design of future clinical studies that use HSCs for renal repair. HSCs have been shown to improve kidney function within a short period of time and the study of these beneficial effects using naïve/pre-treated HSCs in recovery models will need to be carried out.

Chapter 8



References

8 References

- Abbate, M., D. Brown and J. V. Bonventre** (1999). "Expression of NCAM recapitulates tubulogenic development in kidneys recovering from acute ischemia." Am J Physiol **277**(3 Pt 2): F454-463.
- Abou-Saleh, H., D. Yacoub, J. F. Theoret, M. A. Gillis, P. E. Neagoe, B. Labarthe, P. Theroux, M. G. Sirois, M. Tabrizian, E. Thorin and Y. Merhi** (2009). "Endothelial progenitor cells bind and inhibit platelet function and thrombus formation." Circulation **120**(22): 2230-2239.
- Agmon, Y. and M. Brezis** (1993). "Acute renal failure: a multifactorial syndrome. Pathogenesis and prevention strategies." Contrib Nephrol **102**: 23-36.
- Aicher, A., W. Brenner, M. Zuhayra, C. Badorff, S. Massoudi, B. Assmus, T. Eckey, E. Henze, A. M. Zeiher and S. Dimmeler** (2003). "Assessment of the tissue distribution of transplanted human endothelial progenitor cells by radioactive labeling." Circulation **107**(16): 2134-2139.
- Akashi, K., X. He, J. Chen, H. Iwasaki, C. Niu, B. Steenhard, J. Zhang, J. Haug and L. Li** (2003). "Transcriptional accessibility for genes of multiple tissues and hematopoietic lineages is hierarchically controlled during early hematopoiesis." Blood **101**(2): 383-389.
- Akcay, A., Q. Nguyen and C. L. Edelstein** (2009). "Mediators of inflammation in acute kidney injury." Mediators Inflamm **2009**: 137072.
- Akhtar, A. M., J. E. Schneider, S. J. Chapman, A. Jefferson, J. E. Digby, K. Mankia, Y. Chen, M. A. McAteer, K. J. Wood and R. P. Choudhury** (2010). "In vivo quantification of VCAM-1 expression in renal ischemia reperfusion injury using non-invasive magnetic resonance molecular imaging." PLoS One **5**(9): e12800.

- Akira, S., S. Uematsu and O. Takeuchi** (2006). "Pathogen recognition and innate immunity." Cell **124**(4): 783-801.
- Ali, Z. A., C. J. Callaghan, E. Lim, A. A. Ali, S. A. Nouraei, A. M. Akthar, J. R. Boyle, K. Varty, R. K. Kharbanda, D. P. Dutka and M. E. Gaunt** (2007). "Remote ischemic preconditioning reduces myocardial and renal injury after elective abdominal aortic aneurysm repair: a randomized controlled trial." Circulation **116**(11 Suppl): I98-105.
- Alison, M. R., R. Poulsom, R. Jeffery, A. P. Dhillon, A. Quaglia, J. Jacob, M. Novelli, G. Prentice, J. Williamson and N. A. Wright** (2000). "Hepatocytes from non-hepatic adult stem cells." Nature **406**(6793): 257.
- Alon, R. and K. Ley** (2008). "Cells on the run: shear-regulated integrin activation in leukocyte rolling and arrest on endothelial cells." Curr Opin Cell Biol **20**(5): 525-532.
- Anders, H. J., V. Vielhauer and D. Schlondorff** (2003). "Chemokines and chemokine receptors are involved in the resolution or progression of renal disease." Kidney Int **63**(2): 401-415.
- Ardanaz, N. and P. J. Pagano** (2006). "Hydrogen peroxide as a paracrine vascular mediator: regulation and signaling leading to dysfunction." Exp Biol Med (Maywood) **231**(3): 237-251.
- Au, P., J. Tam, D. Fukumura and R. K. Jain** (2008). "Bone marrow-derived mesenchymal stem cells facilitate engineering of long-lasting functional vasculature." Blood **111**(9): 4551-4558.
- Avigdor, A., P. Goichberg, S. Shivtiel, A. Dar, A. Peled, S. Samira, O. Kollet, R. HersHKoviz, R. Alon, I. Hardan, H. Ben-Hur, D. Naor, A. Nagler and T. Lapidot** (2004). "CD44 and hyaluronic acid cooperate with SDF-1 in the trafficking of human CD34+ stem/progenitor cells to bone marrow." Blood **103**(8): 2981-2989.
- Badr, K. F. and I. Ichikawa** (1988). "Prerenal failure: a deleterious shift from renal compensation to decompensation." N Engl J Med **319**(10): 623-629.
- Bailey, A. S., S. Jiang, M. Afentoulis, C. I. Baumann, D. A. Schroeder, S. B. Olson, M. H. Wong and W. H. Fleming** (2004). "Transplanted adult hematopoietic stems cells differentiate into functional endothelial cells." Blood **103**(1): 13-19.

- Balakrishnan, V. S., D. Guo, M. Rao, B. L. Jaber, H. Tighiouart, R. L. Freeman, C. Huang, A. J. King and B. J. Pereira** (2004). "Cytokine gene polymorphisms in hemodialysis patients: association with comorbidity, functionality, and serum albumin." Kidney Int **65**(4): 1449-1460.
- Basile, D. P.** (2007). "The endothelial cell in ischemic acute kidney injury: implications for acute and chronic function." Kidney Int **72**(2): 151-156.
- Basile, D. P., D. Donohoe, K. Roethe and J. L. Osborn** (2001). "Renal ischemic injury results in permanent damage to peritubular capillaries and influences long-term function." Am J Physiol Renal Physiol **281**(5): F887-899.
- Becker, P. S., S. K. Nilsson, Z. Li, V. M. Berrios, M. S. Dooner, C. L. Cooper, C. C. Hsieh and P. J. Quesenberry** (1999). "Adhesion receptor expression by hematopoietic cell lines and murine progenitors: modulation by cytokines and cell cycle status." Exp Hematol **27**(3): 533-541.
- Belcher, J. D., H. Mahaseth, T. E. Welch, A. E. Vilback, K. M. Sonbol, V. S. Kalambur, P. R. Bowlin, J. C. Bischof, R. P. Hebbel and G. M. Vercellotti** (2005). "Critical role of endothelial cell activation in hypoxia-induced vasoocclusion in transgenic sickle mice." Am J Physiol Heart Circ Physiol **288**(6): H2715-2725.
- Bellomo, R., J. A. Kellum and C. Ronco** (2004). "Defining acute renal failure: physiological principles." Intensive Care Med **30**(1): 33-37.
- Bensidhoum, M., A. Chapel, S. Francois, C. Demarquay, C. Mazurier, L. Fouillard, S. Bouchet, J. M. Bertho, P. Gourmelon, J. Aigueperse, P. Charbord, N. C. Gorin, D. Thierry and M. Lopez** (2004). "Homing of in vitro expanded Stro-1- or Stro-1+ human mesenchymal stem cells into the NOD/SCID mouse and their role in supporting human CD34 cell engraftment." Blood **103**(9): 3313-3319.
- Biziuleviciene, G., G. Puidokaite, A. Siaurys and M. Mauricas** (2007). "An anti-inflammatory effect of murine fetal liver cells in BALB/c mouse contact hypersensitivity model." Int Immunopharmacol **7**(6): 744-749.

- Bonventre, J. V. and J. M. Weinberg** (2003). "Recent advances in the pathophysiology of ischemic acute renal failure." J Am Soc Nephrol **14**(8): 2199-2210.
- Bonventre, J. V. and L. Yang** (2011). "Cellular pathophysiology of ischemic acute kidney injury." J Clin Invest **121**(11): 4210-4221.
- Bonventre, J. V. and A. Zuk** (2004). "Ischemic acute renal failure: an inflammatory disease?" Kidney Int **66**(2): 480-485.
- Brezis, M. and S. Rosen** (1995). "Hypoxia of the renal medulla--its implications for disease." N Engl J Med **332**(10): 647-655.
- Broulik, P. D., C. D. Kochakian and J. Dubovsky** (1973). "Influence of castration and testosterone propionate on cardiac output, renal blood flow, and blood volume in mice." Proc Soc Exp Biol Med **144**(2): 671-673.
- Broxmeyer, H. E., C. M. Orschell, D. W. Clapp, G. Hangoc, S. Cooper, P. A. Plett, W. C. Liles, X. Li, B. Graham-Evans, T. B. Campbell, G. Calandra, G. Bridger, D. C. Dale and E. F. Srouf** (2005). "Rapid mobilization of murine and human hematopoietic stem and progenitor cells with AMD3100, a CXCR4 antagonist." J Exp Med **201**(8): 1307-1318.
- Buras, J. A. and W. R. Reenstra** (2007). "Endothelial-neutrophil interactions during ischemia and reperfusion injury: basic mechanisms of hyperbaric oxygen." Neurol Res **29**(2): 127-131.
- Burdon, T. J., A. Paul, N. Noiseux, S. Prakash and D. Shum-Tim** (2011). "Bone marrow stem cell derived paracrine factors for regenerative medicine: current perspectives and therapeutic potential." Bone Marrow Res **2011**: 207326.
- Burne, M. J., A. Elghandour, M. Haq, S. R. Saba, J. Norman, T. Condon, F. Bennett and H. Rabb** (2001). "IL-1 and TNF independent pathways mediate ICAM-1/VCAM-1 up-regulation in ischemia reperfusion injury." J Leukoc Biol **70**(2): 192-198.
- Burst, V., F. Putsch, T. Kubacki, L. A. Volker, M. P. Bartram, R. U. Muller, M. Gillis, C. E. Kurschat, F. Grundmann, J. Muller-Ehmsen, T. Benzing and S. Teschner** (2013). "Survival and

- distribution of injected haematopoietic stem cells in acute kidney injury." Nephrol Dial Transplant **28**(5): 1131-1139.
- Bussolati, B., P. V. Hauser, R. Carvalhosa and G. Camussi** (2009). "Contribution of stem cells to kidney repair." Curr Stem Cell Res Ther **4**(1): 2-8.
- Butcher, E. C.** (1991). "Leukocyte-endothelial cell recognition: three (or more) steps to specificity and diversity." Cell **67**(6): 1033-1036.
- Buttrum, S. M., R. Hatton and G. B. Nash** (1993). "Selectin-mediated rolling of neutrophils on immobilized platelets." Blood **82**(4): 1165-1174.
- Camargo, F. D., S. M. Chambers, E. Drew, K. M. McNagny and M. A. Goodell** (2006). "Hematopoietic stem cells do not engraft with absolute efficiencies." Blood **107**(2): 501-507.
- Caplan, A. I.** (1991). "Mesenchymal stem cells." J Orthop Res **9**(5): 641-650.
- Carvalho, A. C., R. W. Colman and R. S. Lees** (1974). "Platelet function in hyperlipoproteinemia." N Engl J Med **290**(8): 434-438.
- Ceradini, D. J., A. R. Kulkarni, M. J. Callaghan, O. M. Tepper, N. Bastidas, M. E. Kleinman, J. M. Capla, R. D. Galiano, J. P. Levine and G. C. Gurtner** (2004). "Progenitor cell trafficking is regulated by hypoxic gradients through HIF-1 induction of SDF-1." Nat Med **10**(8): 858-864.
- Chakravorty, S. J., A. J. Howie, P. Cockwell, D. Adu and C. O. Savage** (1999). "T lymphocyte adhesion mechanisms within inflamed human kidney: studies with a Stamper-Woodruff assay." Am J Pathol **154**(2): 503-514.
- Chan, J. Y. and S. M. Watt** (2001). "Adhesion receptors on haematopoietic progenitor cells." Br J Haematol **112**(3): 541-557.
- Charles, K. A., H. Kulbe, R. Soper, M. Escorcio-Correia, T. Lawrence, A. Schultheis, P. Chakravarty, R. G. Thompson, G. Kollias, J. F. Smyth, F. R. Balkwill and T. Hagemann** (2009). "The tumor-promoting actions of TNF-alpha involve TNFR1 and IL-17 in ovarian cancer in mice and humans." J Clin Invest **119**(10): 3011-3023.

- Chertow, G. M., E. Burdick, M. Honour, J. V. Bonventre and D. W. Bates** (2005). "Acute kidney injury, mortality, length of stay, and costs in hospitalized patients." J Am Soc Nephrol **16**(11): 3365-3370.
- Chertow, G. M., E. Burdick, M. Honour, J. V. Bonventre and D. W. Bates** (2005). "Acute kidney injury, mortality, length of stay, and costs in hospitalized patients." Journal of the American Society of Nephrology **16**(11): 3365-3370.
- Chintala, M. S., V. Bernardino and P. J. Chiu** (1994). "Cyclic GMP but not cyclic AMP prevents renal platelet accumulation after ischemia-reperfusion in anesthetized rats." J Pharmacol Exp Ther **271**(3): 1203-1208.
- Christensen, J. L., D. E. Wright, A. J. Wagers and I. L. Weissman** (2004). "Circulation and chemotaxis of fetal hematopoietic stem cells." PLoS Biol **2**(3): E75.
- Civin, C. I., L. C. Strauss, C. Brovall, M. J. Fackler, J. F. Schwartz and J. H. Shaper** (1984). "Antigenic analysis of hematopoiesis. III. A hematopoietic progenitor cell surface antigen defined by a monoclonal antibody raised against KG-1a cells." J Immunol **133**(1): 157-165.
- Clemetson, K. J. and J. M. Clemetson** (2008). "Platelet GPIb complex as a target for anti-thrombotic drug development." Thromb Haemost **99**(3): 473-479.
- Coca, S. G., A. J. Peixoto, A. X. Garg, H. M. Krumholz and C. R. Parikh** (2007). "The prognostic importance of a small acute decrement in kidney function in hospitalized patients: a systematic review and meta-analysis." Am J Kidney Dis **50**(5): 712-720.
- Cohnheim, J.** (1877). Vorlesungen über Allgemeine Pathologie. Berlin, August Hirschwald.
- Cristol, J. P., C. Thiernemann, J. A. Mitchell, C. Walder and J. R. Vane** (1993). "Support of renal blood flow after ischaemic-reperfusion injury by endogenous formation of nitric oxide and of cyclo-oxygenase vasodilator metabolites." Br J Pharmacol **109**(1): 188-194.
- Crockett, E. T., J. J. Galligan, B. D. Uhal, J. Harkema, R. Roth and K. Pandya** (2006). "Protection of early phase hepatic ischemia-reperfusion injury by cholinergic agonists." BMC Clin Pathol **6**: 3.

- Cugini, D., N. Azzollini, E. Gagliardini, P. Cassis, R. Bertini, F. Colotta, M. Noris, G. Remuzzi and A. Benigni** (2005). "Inhibition of the chemokine receptor CXCR2 prevents kidney graft function deterioration due to ischemia/reperfusion." Kidney Int **67**(5): 1753-1761.
- Dai, W. and R. A. Kloner** (2011). "Bone marrow-derived cell transplantation therapy for myocardial infarction: lessons learned and future questions." Am J Transplant **11**(11): 2297-2301.
- Danese, S., C. de la Motte and C. Fiocchi** (2004). "Platelets in inflammatory bowel disease: Clinical, pathogenic, and therapeutic implications." American Journal of Gastroenterology **99**(5): 938-945.
- De Falco, E., D. Porcelli, A. R. Torella, S. Straino, M. G. Iachininoto, A. Orlandi, S. Truffa, P. Biglioli, M. Napolitano, M. C. Capogrossi and M. Pesce** (2004). "SDF-1 involvement in endothelial phenotype and ischemia-induced recruitment of bone marrow progenitor cells." Blood **104**(12): 3472-3482.
- De Greef, K. E., D. K. Ysebaert, S. Dauwe, V. Persy, S. R. Vercauteren, D. Mey and M. E. De Broe** (2001). "Anti-B7-1 blocks mononuclear cell adherence in vasa recta after ischemia." Kidney International **60**(4): 1415-1427.
- DeGrendele, H. C., P. Estess and M. H. Siegelman** (1997). "Requirement for CD44 in activated T cell extravasation into an inflammatory site." Science **278**(5338): 672-675.
- Deng, W., Q. Han, L. Liao, C. Li, W. Ge, Z. Zhao, S. You, H. Deng, F. Murad and R. C. Zhao** (2005). "Engrafted bone marrow-derived flk-(1+) mesenchymal stem cells regenerate skin tissue." Tissue Eng **11**(1-2): 110-119.
- Detmers, P. A., S. K. Lo, E. Olsen-Egbert, A. Walz, M. Baggiolini and Z. A. Cohn** (1990). "Neutrophil-activating protein 1/interleukin 8 stimulates the binding activity of the leukocyte adhesion receptor CD11b/CD18 on human neutrophils." J Exp Med **171**(4): 1155-1162.

- Devarajan, P.** (2006). "Update on mechanisms of ischemic acute kidney injury." J Am Soc Nephrol **17**(6): 1503-1520.
- Dimitroff, C. J., J. Y. Lee, S. Rafii, R. C. Fuhlbrigge and R. Sackstein** (2001). "CD44 is a major E-selectin ligand on human hematopoietic progenitor cells." J Cell Biol **153**(6): 1277-1286.
- DiVietro, J. A., D. C. Brown, L. A. Sklar, R. S. Larson and M. B. Lawrence** (2007). "Immobilized stromal cell-derived factor-1alpha triggers rapid VLA-4 affinity increases to stabilize lymphocyte tethers on VCAM-1 and subsequently initiate firm adhesion." J Immunol **178**(6): 3903-3911.
- Druid, H., S. Enestrom and L. Rammer** (1998). "Effect of anticoagulation upon nephron obstruction in experimental acute ischaemic renal failure. A morphological study." Int J Exp Pathol **79**(1): 55-66.
- Duffield, J. S., K. M. Park, L. L. Hsiao, V. R. Kelley, D. T. Scadden, T. Ichimura and J. V. Bonventre** (2005). "Restoration of tubular epithelial cells during repair of the postischemic kidney occurs independently of bone marrow-derived stem cells." J Clin Invest **115**(7): 1743-1755.
- Eash, K. J., A. M. Greenbaum, P. K. Gopalan and D. C. Link** (2010). "CXCR2 and CXCR4 antagonistically regulate neutrophil trafficking from murine bone marrow." J Clin Invest **120**(7): 2423-2431.
- Eash, K. J., J. M. Means, D. W. White and D. C. Link** (2009). "CXCR4 is a key regulator of neutrophil release from the bone marrow under basal and stress granulopoiesis conditions." Blood **113**(19): 4711-4719.
- Eason, J. D., M. Pascual, S. Wee, M. Farrell, J. Phelan, S. Boskovic, C. Blosch, K. M. Mohler and A. B. Cosimi** (1996). "Evaluation of recombinant human soluble dimeric tumor necrosis factor receptor for prevention of OKT3-associated acute clinical syndrome." Transplantation **61**(2): 224-228.

- Elices, M. J., L. Osborn, Y. Takada, C. Crouse, S. Luhowskyj, M. E. Hemler and R. R. Lobb** (1990). "VCAM-1 on activated endothelium interacts with the leukocyte integrin VLA-4 at a site distinct from the VLA-4/fibronectin binding site." Cell **60**(4): 577-584.
- Eltzschig, H. K. and C. D. Collard** (2004). "Vascular ischaemia and reperfusion injury." Br Med Bull **70**: 71-86.
- Enestrom, S., H. Druid and L. Rammer** (1988). "Fibrin deposition in the kidney in post-ischaemic renal damage." Br J Exp Pathol **69**(3): 387-394.
- Eppihimer, M. J., J. Russell, D. C. Anderson, C. J. Epstein, S. Laroux and D. N. Granger** (1997). "Modulation of P-selectin expression in the postischemic intestinal microvasculature." Am J Physiol **273**(6 Pt 1): G1326-1332.
- Fan, X. D., A. C. Patera, A. Pong-Kennedy, G. Deno, W. Gonsiorek, D. J. Manfra, G. Vassileva, M. Zeng, C. Jackson, L. Sullivan, W. Sharif-Rodriguez, G. Opdenakker, J. Van Damme, J. A. Hedrick, D. Lundell, S. A. Lira and R. W. Hipkin** (2007). "Murine CXCR1 is a functional receptor for GCP-2/CXCL6 and interleukin-8/CXCL8." Journal of Biological Chemistry **282**(16): 11658-11666.
- Fang, T. C., M. R. Alison, H. T. Cook, R. Jeffery, N. A. Wright and R. Poulsom** (2005). "Proliferation of bone marrow-derived cells contributes to regeneration after folic acid-induced acute tubular injury." J Am Soc Nephrol **16**(6): 1723-1732.
- Faubel, S., E. C. Lewis, L. Reznikov, D. Ljubanovic, T. S. Hoke, H. Somerset, D. J. Oh, L. Lu, C. L. Klein, C. A. Dinarello and C. L. Edelstein** (2007). "Cisplatin-induced acute renal failure is associated with an increase in the cytokines interleukin (IL)-1beta, IL-18, IL-6, and neutrophil infiltration in the kidney." J Pharmacol Exp Ther **322**(1): 8-15.
- Feng, D., J. A. Nagy, K. Pyne, H. F. Dvorak and A. M. Dvorak** (1998). "Neutrophils emigrate from venules by a transendothelial cell pathway in response to FMLP." J Exp Med **187**(6): 903-915.

- Ficek, R., F. Kokot, J. Chudek, M. Adamczak, J. Ficek and A. Wiecek** (2006). "Plasma concentrations of tumor necrosis factor alpha may predict the outcome of patients with acute renal failure." Kidney Blood Press Res **29**(4): 203-209.
- Fischer, U. M., M. T. Harting, F. Jimenez, W. O. Monzon-Posadas, H. Xue, S. I. Savitz, G. A. Laine and C. S. Cox, Jr.** (2009). "Pulmonary passage is a major obstacle for intravenous stem cell delivery: the pulmonary first-pass effect." Stem Cells Dev **18**(5): 683-692.
- Flores, J., D. R. DiBona, C. H. Beck and A. Leaf** (1972). "The role of cell swelling in ischemic renal damage and the protective effect of hypertonic solute." J Clin Invest **51**(1): 118-126.
- Forbes, J. M., T. D. Hewitson, G. J. Becker and C. L. Jones** (2000). "Ischemic acute renal failure: long-term histology of cell and matrix changes in the rat." Kidney Int **57**(6): 2375-2385.
- Franca, M. S., S. S. Lima, C. N. Duclou, E. M. Goulart and R. M. de Castro Romanelli** (2013). "Antimicrobials and renal failure in neutropenic patients." Braz J Infect Dis **17**(4): 487-490.
- Frangogiannis, N. G.** (2007). "Chemokines in ischemia and reperfusion." Thromb Haemost **97**(5): 738-747.
- Frenette, P. S., C. Moyna, D. W. Hartwell, J. B. Lowe, R. O. Hynes and D. D. Wagner** (1998). "Platelet-endothelial interactions in inflamed mesenteric venules." Blood **91**(4): 1318-1324.
- Frenette, P. S., S. Subbarao, I. B. Mazo, U. H. von Andrian and D. D. Wagner** (1998). "Endothelial selectins and vascular cell adhesion molecule-1 promote hematopoietic progenitor homing to bone marrow." Proc Natl Acad Sci U S A **95**(24): 14423-14428.
- Friedewald, J. J. and H. Rabb** (2004). "Inflammatory cells in ischemic acute renal failure." Kidney Int **66**(2): 486-491.
- Furlani, D., M. Ugurlucan, L. Ong, K. Bieback, E. Pittermann, I. Westien, W. Wang, C. Yerebakan, W. Li, R. Gaebel, R. K. Li, B. Vollmar, G. Steinhoff and N. Ma** (2009). "Is the intravascular administration of mesenchymal stem cells safe? Mesenchymal stem cells and intravital microscopy." Microvasc Res **77**(3): 370-376.

- Furuichi, K., T. Wada, H. Yokoyama and K. I. Kobayashi** (2002). "Role of Cytokines and Chemokines in Renal Ischemia-Reperfusion Injury." Drug News Perspect **15**(8): 477-482.
- Gal, I., J. Lesley, W. Ko, A. Gonda, R. Stoop, R. Hyman and K. Mikecz** (2003). "Role of the extracellular and cytoplasmic domains of CD44 in the rolling interaction of lymphoid cells with hyaluronan under physiologic flow." J Biol Chem **278**(13): 11150-11158.
- Gallatin, W. M., I. L. Weissman and E. C. Butcher** (1983). "A cell-surface molecule involved in organ-specific homing of lymphocytes." Nature **304**(5921): 30-34.
- Garrelds, I. M., J. P. Heiligers, M. E. Van Meeteren, D. J. Duncker, P. R. Saxena, M. A. Meijssen and F. J. Zijlstra** (2002). "Intestinal blood flow in murine colitis induced with dextran sulfate sodium." Dig Dis Sci **47**(10): 2231-2236.
- Gawaz, M.** (2004). "Role of platelets in coronary thrombosis and reperfusion of ischemic myocardium." Cardiovasc Res **61**(3): 498-511.
- Gnecchi, M., H. He, O. D. Liang, L. G. Melo, F. Morello, H. Mu, N. Noiseux, L. Zhang, R. E. Pratt, J. S. Ingwall and V. J. Dzau** (2005). "Paracrine action accounts for marked protection of ischemic heart by Akt-modified mesenchymal stem cells." Nat Med **11**(4): 367-368.
- Gnecchi, M., H. He, N. Noiseux, O. D. Liang, L. Zhang, F. Morello, H. Mu, L. G. Melo, R. E. Pratt, J. S. Ingwall and V. J. Dzau** (2006). "Evidence supporting paracrine hypothesis for Akt-modified mesenchymal stem cell-mediated cardiac protection and functional improvement." FASEB J **20**(6): 661-669.
- Golino, P., P. R. Maroko and T. E. Carew** (1987). "Efficacy of platelet depletion in counteracting the detrimental effect of acute hypercholesterolemia on infarct size and the no-reflow phenomenon in rabbits undergoing coronary artery occlusion-reperfusion." Circulation **76**(1): 173-180.
- Goodison, S., V. Urquidi and D. Tarin** (1999). "CD44 cell adhesion molecules." Mol Pathol **52**(4): 189-196.

- Goransson, V., C. Johnsson, A. Jacobson, P. Heldin, R. Hallgren and P. Hansell** (2004). "Renal hyaluronan accumulation and hyaluronan synthase expression after ischaemia-reperfusion injury in the rat." Nephrol Dial Transplant **19**(4): 823-830.
- Grabovsky, V., S. Feigelson, C. Chen, D. A. Bleijs, A. Peled, G. Cinamon, F. Baleux, F. Arenzana-Seisdedos, T. Lapidot, Y. van Kooyk, R. R. Lobb and R. Alon** (2000). "Subsecond induction of alpha4 integrin clustering by immobilized chemokines stimulates leukocyte tethering and rolling on endothelial vascular cell adhesion molecule 1 under flow conditions." J Exp Med **192**(4): 495-506.
- Graf, T.** (2002). "Differentiation plasticity of hematopoietic cells." Blood **99**(9): 3089-3101.
- Granger, D. N. and P. Kubes** (1994). "The microcirculation and inflammation: modulation of leukocyte-endothelial cell adhesion." J Leukoc Biol **55**(5): 662-675.
- Granger, D. N. and E. Senchenkova** (2010).
- Granick, J. L., S. I. Simon and D. L. Borjesson** (2012). "Hematopoietic stem and progenitor cells as effectors in innate immunity." Bone Marrow Res **2012**: 165107.
- Grino, J. M.** (1994). "BN 52021: a platelet activating factor antagonist for preventing post-transplant renal failure. A double-blind, randomized study. The BN 52021 Study Group in Renal Transplantation." Ann Intern Med **121**(5): 345-347.
- Gupta, S., C. Verfaillie, D. Chmielewski, Y. Kim and M. E. Rosenberg** (2002). "A role for extrarenal cells in the regeneration following acute renal failure." Kidney Int **62**(4): 1285-1290.
- Haq, M., J. Norman, S. R. Saba, G. Ramirez and H. Rabb** (1998). "Role of IL-1 in renal ischemic reperfusion injury." J Am Soc Nephrol **9**(4): 614-619.
- Hattori, K., B. Heissig, K. Tashiro, T. Honjo, M. Tateno, J. H. Shieh, N. R. Hackett, M. S. Quitariano, R. G. Crystal, S. Rafii and M. A. Moore** (2001). "Plasma elevation of stromal cell-derived factor-1 induces mobilization of mature and immature hematopoietic progenitor and stem cells." Blood **97**(11): 3354-3360.

- Haug, C. E., R. B. Colvin, F. L. Delmonico, H. Auchincloss, Jr., N. Tolkoﬀ-Rubin, F. I. Preﬀer, R. Rothlein, S. Norris, L. Scharschmidt and A. B. Cosimi (1993). "A phase I trial of immunosuppression with anti-ICAM-1 (CD54) mAb in renal allograft recipients." Transplantation **55**(4): 766-772; discussion 772-763.
- Haylor, J. and J. Towers (1982). "Renal vasodilator activity of prostaglandin E2 in the rat anaesthetized with pentobarbitone." Br J Pharmacol **76**(1): 131-137.
- Held, P. K., M. Al-Dhalimy, H. Willenbring, Y. Akkari, S. Jiang, Y. Torimaru, S. Olson, W. H. Fleming, M. Finegold and M. Grompe (2006). "In vivo genetic selection of renal proximal tubules." Mol Ther **13**(1): 49-58.
- Hellberg, P. O., O. T. Kallskog, G. Ojteg and M. Wolgast (1990). "Peritubular capillary permeability and intravascular RBC aggregation after ischemia: effects of neutrophils." Am J Physiol **258**(4 Pt 2): F1018-1025.
- Herrera, M. B., B. Bussolati, S. Bruno, L. Morando, G. Mauriello-Romanazzi, F. Sanavio, I. Stamenkovic, L. Biancone and G. Camussi (2007). "Exogenous mesenchymal stem cells localize to the kidney by means of CD44 following acute tubular injury." Kidney Int **72**(4): 430-441.
- Hirsch, E., A. Iglesias, A. J. Potocnik, U. Hartmann and R. Fassler (1996). "Impaired migration but not differentiation of haematopoietic stem cells in the absence of beta1 integrins." Nature **380**(6570): 171-175.
- Holstein-Rathlou, N. H., O. V. Sosnovtseva, A. N. Pavlov, W. A. Cupples, C. M. Sorensen and D. J. Marsh (2011). "Nephron blood flow dynamics measured by laser speckle contrast imaging." Am J Physiol Renal Physiol **300**(2): F319-329.
- Holyer, I. (2010). The role of platelets and their associated recruitment mechanisms in intestinal ischaemia reperfusion injury. Institute of Biomedical Research, University of Birmingham. PhD.

- Hopkins, R. W. and C. A. Damewood** (1974). "Septic shock: hemodynamics of endotoxin and inflammation." Am J Surg **127**(4): 476-483.
- Hu, J., L. Zhang, N. Wang, R. Ding, S. Cui, F. Zhu, Y. Xie, X. Sun, D. Wu, Q. Hong, Q. Li, S. Shi, X. Liu and X. Chen** (2013). "Mesenchymal stem cells attenuate ischemic acute kidney injury by inducing regulatory T cells through splenocyte interactions." Kidney Int.
- Huo, Y., C. Weber, S. B. Forlow, M. Sperandio, J. Thatte, M. Mack, S. Jung, D. R. Littman and K. Ley** (2001). "The chemokine KC, but not monocyte chemoattractant protein-1, triggers monocyte arrest on early atherosclerotic endothelium." J Clin Invest **108**(9): 1307-1314.
- Hynes, R. O.** (2002). "Integrins: bidirectional, allosteric signaling machines." Cell **110**(6): 673-687.
- Ichikawa, H., S. Flores, P. R. Kvietys, R. E. Wolf, T. Yoshikawa, D. N. Granger and T. Y. Aw** (1997). "Molecular mechanisms of anoxia/reoxygenation-induced neutrophil adherence to cultured endothelial cells." Circ Res **81**(6): 922-931.
- Imai, K., M. Kobayashi, J. Wang, Y. Ohiro, J. Hamada, Y. Cho, M. Imamura, M. Musashi, T. Kondo, M. Hosokawa and M. Asaka** (1999). "Selective transendothelial migration of hematopoietic progenitor cells: a role in homing of progenitor cells." Blood **93**(1): 149-156.
- Ip, J. E., Y. Wu, J. Huang, L. Zhang, R. E. Pratt and V. J. Dzau** (2007). "Mesenchymal stem cells use integrin beta1 not CXC chemokine receptor 4 for myocardial migration and engraftment." Mol Biol Cell **18**(8): 2873-2882.
- Isacke, C. M.** (1994). "The role of the cytoplasmic domain in regulating CD44 function." J Cell Sci **107 (Pt 9)**: 2353-2359.
- Ivanova, N. B., J. T. Dimos, C. Schaniel, J. A. Hackney, K. A. Moore and I. R. Lemischka** (2002). "A stem cell molecular signature." Science **298**(5593): 601-604.
- Iwatani, H. and E. Imai** (2010). "Kidney repair using stem cells: myth or reality as a therapeutic option?" J Nephrol **23**(2): 143-146.

- Jackson, K. A., S. M. Majka, H. Wang, J. Pocius, C. J. Hartley, M. W. Majesky, M. L. Entman, L. H. Michael, K. K. Hirschi and M. A. Goodell (2001). "Regeneration of ischemic cardiac muscle and vascular endothelium by adult stem cells." J Clin Invest **107**(11): 1395-1402.
- Jia, X., X. Xie, G. Feng, H. Lu, Q. Zhao, Y. Che, Y. Zheng, Z. Han, Y. Xu, Z. Li and D. Kong (2012). "Bone marrow-derived cells can acquire renal stem cells properties and ameliorate ischemia-reperfusion induced acute renal injury." BMC Nephrol **13**: 105.
- Jin, H., A. Aiyer, J. Su, P. Borgstrom, D. Stupack, M. Friedlander and J. Varner (2006). "A homing mechanism for bone marrow-derived progenitor cell recruitment to the neovasculature." J Clin Invest **116**(3): 652-662.
- Jo, S. K., S. A. Sung, W. Y. Cho, K. J. Go and H. K. Kim (2006). "Macrophages contribute to the initiation of ischaemic acute renal failure in rats." Nephrology Dialysis Transplantation **21**(5): 1231-1239.
- Jo, S. K., S. A. Sung, W. Y. Cho, K. J. Go and H. K. Kim (2006). "Macrophages contribute to the initiation of ischaemic acute renal failure in rats." Nephrol Dial Transplant **21**(5): 1231-1239.
- John, B. and I. N. Crispe (2004). "Passive and active mechanisms trap activated CD8+ T cells in the liver." J Immunol **172**(9): 5222-5229.
- Johnsson, C., G. Tufveson, J. Wahlberg and R. Hallgren (1996). "Experimentally-induced warm renal ischemia induces cortical accumulation of hyaluronan in the kidney." Kidney Int **50**(4): 1224-1229.
- Jung, Y., J. Wang, A. Schneider, Y. X. Sun, A. J. Koh-Paige, N. I. Osman, L. K. McCauley and R. S. Taichman (2006). "Regulation of SDF-1 (CXCL12) production by osteoblasts; a possible mechanism for stem cell homing." Bone **38**(4): 497-508.
- Kale, S., A. Karihaloo, P. R. Clark, M. Kashgarian, D. S. Krause and L. G. Cantley (2003). "Bone marrow stem cells contribute to repair of the ischemically injured renal tubule." J Clin Invest **112**(1): 42-49.

- Kalia, N., A. G. Pockley, R. F. Wood and N. J. Brown** (2001). "Effects of FK409 on intestinal ischemia-reperfusion injury and ischemia-induced changes in the rat mucosal villus microcirculation." Transplantation **72**(12): 1875-1880.
- Kalia, N., A. G. Pockley, R. F. Wood and N. J. Brown** (2002). "Effects of hypothermia and rewarming on the mucosal villus microcirculation and survival after rat intestinal ischemia-reperfusion injury." Ann Surg **236**(1): 67-74.
- Karp, J. M. and G. S. Leng Teo** (2009). "Mesenchymal stem cell homing: the devil is in the details." Cell Stem Cell **4**(3): 206-216.
- Karsou, S. A., B. L. Jaber and B. J. Pereira** (2000). "Impact of intermittent hemodialysis variables on clinical outcomes in acute renal failure." Am J Kidney Dis **35**(5): 980-991.
- Katayama, Y., A. Hidalgo, B. C. Furie, D. Vestweber, B. Furie and P. S. Frenette** (2003). "PSGL-1 participates in E-selectin-mediated progenitor homing to bone marrow: evidence for cooperation between E-selectin ligands and alpha4 integrin." Blood **102**(6): 2060-2067.
- Kavanagh, D.** (2009). Molecular Events Governing Haematopoietic Stem Cell Recruitment *in vivo* in Murine Liver Following Ischaemia-Reperfusion Injury. School of Clinical and Experimental Medicine. Birmingham, University of Birmingham. **PhD**.
- Kavanagh, D. P., L. E. Durant, H. A. Crosby, P. F. Lalor, J. Frampton, D. H. Adams and N. Kalia** (2010). "Haematopoietic stem cell recruitment to injured murine liver sinusoids depends on (alpha)4(beta)1 integrin/VCAM-1 interactions." Gut **59**(1): 79-87.
- Kavanagh, D. P. and N. Kalia** (2011). "Hematopoietic Stem Cell Homing to Injured Tissues." Stem Cell Rev.
- Kavanagh, D. P., A. I. Yemm, J. S. Alexander, J. Frampton and N. Kalia** (2012). "Enhancing the adhesion of haematopoietic precursor cell integrins with hydrogen peroxide increases recruitment within murine gut." Cell Transplant.

- Kavanagh, D. P., A. I. Yemm, Y. Zhao, J. Frampton and N. Kalia** (2013). "Mechanisms of Adhesion and Subsequent Actions of a Haematopoietic Stem Cell Line, HPC-7, in the Injured Murine Intestinal Microcirculation In Vivo." PLoS One **8**(3): e59150.
- Kelly, K. J., N. E. Tolkoff-Rubin, R. H. Rubin, W. W. Williams, Jr., S. M. Meehan, C. L. Meschter, J. G. Christenson and J. V. Bonventre** (1996). "An oral platelet-activating factor antagonist, Ro-24-4736, protects the rat kidney from ischemic injury." Am J Physiol **271**(5 Pt 2): F1061-1067.
- Kelly, K. J., W. W. Williams, Jr., R. B. Colvin and J. V. Bonventre** (1994). "Antibody to intercellular adhesion molecule 1 protects the kidney against ischemic injury." Proc Natl Acad Sci U S A **91**(2): 812-816.
- Kelly, K. J., W. W. Williams, Jr., R. B. Colvin, S. M. Meehan, T. A. Springer, J. C. Gutierrez-Ramos and J. V. Bonventre** (1996). "Intercellular adhesion molecule-1-deficient mice are protected against ischemic renal injury." J Clin Invest **97**(4): 1056-1063.
- Khaldoyanidi, S., A. Denzel and M. Zoller** (1996). "Requirement for CD44 in proliferation and homing of hematopoietic precursor cells." J Leukoc Biol **60**(5): 579-592.
- Khandoga, A., P. Biberthaler, G. Enders, D. Teupser, S. Axmann, B. Luchting, J. Hutter, K. Messmer and F. Krombach** (2002). "P-selectin mediates platelet-endothelial cell interactions and reperfusion injury in the mouse liver in vivo." Shock **18**(6): 529-535.
- Khandoga, A., P. Biberthaler, K. Messmer and F. Krombach** (2003). "Platelet-endothelial cell interactions during hepatic ischemia-reperfusion in vivo: a systematic analysis." Microvasc Res **65**(2): 71-77.
- Kinashi, T. and T. A. Springer** (1994). "Steel factor and c-kit regulate cell-matrix adhesion." Blood **83**(4): 1033-1038.
- Kinsey, G. R., L. Huang, A. L. Vergis, L. Li and M. D. Okusa** (2010). "Regulatory T cells contribute to the protective effect of ischemic preconditioning in the kidney." Kidney Int **77**(9): 771-780.

- Klausner, J. M., I. S. Paterson, G. Goldman, L. Kobzik, C. Rodzen, R. Lawrence, C. R. Valeri, D. Shepro and H. B. Hechtman (1989). "Postischemic renal injury is mediated by neutrophils and leukotrienes." Am J Physiol **256**(5 Pt 2): F794-802.
- Koizumi, K., V. Poulaki, S. Doehmen, G. Welsandt, S. Radetzky, A. Lappas, N. Kociok, B. Kirchhof and A. M. Jousen (2003). "Contribution of TNF-alpha to leukocyte adhesion, vascular leakage, and apoptotic cell death in endotoxin-induced uveitis in vivo." Invest Ophthalmol Vis Sci **44**(5): 2184-2191.
- Koo, D. D., K. I. Welsh, J. A. Roake, P. J. Morris and S. V. Fuggle (1998). "Ischemia/reperfusion injury in human kidney transplantation: an immunohistochemical analysis of changes after reperfusion." Am J Pathol **153**(2): 557-566.
- Krause, D. S., T. Ito, M. J. Fackler, O. M. Smith, M. I. Collector, S. J. Sharkis and W. S. May (1994). "Characterization of murine CD34, a marker for hematopoietic progenitor and stem cells." Blood **84**(3): 691-701.
- Kucia, M., B. Dawn, G. Hunt, Y. Guo, M. Wysoczynski, M. Majka, J. Ratajczak, F. Rezzoug, S. T. Ildstad, R. Bolli and M. Z. Ratajczak (2004). "Cells expressing early cardiac markers reside in the bone marrow and are mobilized into the peripheral blood after myocardial infarction." Circ Res **95**(12): 1191-1199.
- Kumar, S. and S. Ponnazhagan (2007). "Bone homing of mesenchymal stem cells by ectopic alpha 4 integrin expression." FASEB J **21**(14): 3917-3927.
- Kupatt, C., R. Wichels, J. Horstkotte, F. Krombach, H. Habazettl and P. Boekstegers (2002). "Molecular mechanisms of platelet-mediated leukocyte recruitment during myocardial reperfusion." J Leukoc Biol **72**(3): 455-461.
- Kurose, I., P. Kubes, R. Wolf, D. C. Anderson, J. Paulson, M. Miyasaka and D. N. Granger (1993). "Inhibition of nitric oxide production. Mechanisms of vascular albumin leakage." Circ Res **73**(1): 164-171.

Kuschert, G. S., F. Coulin, C. A. Power, A. E. Proudfoot, R. E. Hubbard, A. J. Hoogewerf and T. N.

Wells (1999). "Glycosaminoglycans interact selectively with chemokines and modulate receptor binding and cellular responses." Biochemistry **38**(39): 12959-12968.

Lagasse, E., H. Connors, M. Al-Dhalimy, M. Reitsma, M. Dohse, L. Osborne, X. Wang, M.

Finegold, I. L. Weissman and M. Grompe (2000). "Purified hematopoietic stem cells can differentiate into hepatocytes in vivo." Nat Med **6**(11): 1229-1234.

Lanzoni, G., G. Roda, A. Belluzzi, E. Roda and G. P. Bagnara (2008). "Inflammatory bowel disease:

Moving toward a stem cell-based therapy." World J Gastroenterol **14**(29): 4616-4626.

Lapidot, T. (2001). "Mechanism of human stem cell migration and repopulation of NOD/SCID and

B2mnull NOD/SCID mice. The role of SDF-1/CXCR4 interactions." Ann N Y Acad Sci **938**: 83-95.

Lapidot, T. and I. Petit (2002). "Current understanding of stem cell mobilization: the roles of

chemokines, proteolytic enzymes, adhesion molecules, cytokines, and stromal cells." Exp Hematol **30**(9): 973-981.

Lawrence, M. B., D. F. Bainton and T. A. Springer (1994). "Neutrophil tethering to and rolling on

E-selectin are separable by requirement for L-selectin." Immunity **1**(2): 137-145.

Laws, K. H., J. A. Clanton, V. A. Starnes, F. M. Lupinetti, J. C. Collins, J. A. Oates and J. W.

Hammon, Jr. (1983). "Kinetics and imaging of indium-11-labeled autologous platelets in experimental myocardial infarction." Circulation **67**(1): 110-116.

Lewington, A. J., B. J. Padanilam, D. R. Martin and M. R. Hammerman (2000). "Expression of

CD44 in kidney after acute ischemic injury in rats." Am J Physiol Regul Integr Comp Physiol **278**(1): R247-254.

Ley, K., C. Laudanna, M. I. Cybulsky and S. Nourshargh (2007). "Getting to the site of

inflammation: the leukocyte adhesion cascade updated." Nat Rev Immunol **7**(9): 678-689.

Ley, K. and T. F. Tedder (1995). "Leukocyte interactions with vascular endothelium. New insights

into selectin-mediated attachment and rolling." J Immunol **155**(2): 525-528.

- Li, B., A. Cohen, T. E. Hudson, D. Motlagh, D. L. Amrani and J. S. Duffield** (2010). "Mobilized human hematopoietic stem/progenitor cells promote kidney repair after ischemia/reperfusion injury." Circulation **121**(20): 2211-2220.
- Li, L., R. Black, Z. Ma, Q. Yang, A. Wang and F. Lin** (2011). "Use of Mouse Hematopoietic Stem and Progenitor Cells to Treat Acute Kidney Injury." Am J Physiol Renal Physiol.
- Li, L., R. Black, Z. Ma, Q. Yang, A. Wang and F. Lin** (2012). "Use of mouse hematopoietic stem and progenitor cells to treat acute kidney injury." Am J Physiol Renal Physiol **302**(1): F9-F19.
- Li, L., P. Truong, P. Igarashi and F. Lin** (2007). "Renal and bone marrow cells fuse after renal ischemic injury." J Am Soc Nephrol **18**(12): 3067-3077.
- Lieberthal, W.** (1997). "Biology of acute renal failure: therapeutic implications." Kidney Int **52**(4): 1102-1115.
- Liekens, S., D. Schols and S. Hatse** (2010). "CXCL12-CXCR4 axis in angiogenesis, metastasis and stem cell mobilization." Curr Pharm Des **16**(35): 3903-3920.
- Lim, L. H., B. S. Bochner and E. M. Wagner** (2002). "Leukocyte recruitment in the airways: an intravital microscopic study of rat tracheal microcirculation." Am J Physiol Lung Cell Mol Physiol **282**(5): L959-967.
- Lin, F., K. Cordes, L. Li, L. Hood, W. G. Couser, S. J. Shankland and P. Igarashi** (2003). "Hematopoietic stem cells contribute to the regeneration of renal tubules after renal ischemia-reperfusion injury in mice." J Am Soc Nephrol **14**(5): 1188-1199.
- Lin, F., A. Moran and P. Igarashi** (2005). "Intrarenal cells, not bone marrow-derived cells, are the major source for regeneration in postischemic kidney." J Clin Invest **115**(7): 1756-1764.
- Linas, S. L., P. F. Shanley, D. Whittenburg, E. Berger and J. E. Repine** (1988). "Neutrophils accentuate ischemia-reperfusion injury in isolated perfused rat kidneys." Am J Physiol **255**(4 Pt 2): F728-735.

- Linass, S. L., D. Whitenburg, P. E. Parsons and J. E. Repine** (1995). "Ischemia Increases Neutrophil Retention and Worsens Acute-Renal-Failure - Role of Oxygen Metabolites and Icam-1." Kidney International **48**(5): 1584-1591.
- Liu, M. C., C. C. Chien, M. Burne-Taney, R. R. Molls, L. C. Racusen, R. B. Colvin and H. Rabb** (2006). "A pathophysiologic role for T lymphocytes in murine acute cisplatin nephrotoxicity." Journal of the American Society of Nephrology **17**(3): 765-774.
- Lo Celso, C., C. P. Lin and D. T. Scadden** (2011). "In vivo imaging of transplanted hematopoietic stem and progenitor cells in mouse calvarium bone marrow." Nat Protoc **6**(1): 1-14.
- Long, D. A., J. T. Norman and L. G. Fine** (2012). "Restoring the renal microvasculature to treat chronic kidney disease." Nat Rev Nephrol **8**(4): 244-250.
- Lundell, B. I., J. B. McCarthy, N. L. Kovach and C. M. Verfaillie** (1997). "Activation of beta1 integrins on CML progenitors reveals cooperation between beta1 integrins and CD44 in the regulation of adhesion and proliferation." Leukemia **11**(6): 822-829.
- Luster, A. D.** (1998). "Chemokines--chemotactic cytokines that mediate inflammation." N Engl J Med **338**(7): 436-445.
- Marelli-Berg, F. M., E. Peek, E. A. Lidington, H. J. Stauss and R. I. Lechler** (2000). "Isolation of endothelial cells from murine tissue." J Immunol Methods **244**(1-2): 205-215.
- Mashiach, E., S. Sela, J. Winaver, S. M. Shasha and B. Kristal** (1998). "Renal ischemia-reperfusion injury: contribution of nitric oxide and renal blood flow." Nephron **80**(4): 458-467.
- Massberg, S., K. Brand, S. Gruner, S. Page, E. Muller, I. Muller, W. Bergmeier, T. Richter, M. Lorenz, I. Konrad, B. Nieswandt and M. Gawaz** (2002). "A critical role of platelet adhesion in the initiation of atherosclerotic lesion formation." Journal of Experimental Medicine **196**(7): 887-896.
- Massberg, S., G. Enders, R. Leiderer, S. Eisenmenger, D. Vestweber, F. Krombach and K. Messmer** (1998). "Platelet-endothelial cell interactions during ischemia/reperfusion: The role of P-selectin." Blood **92**(2): 507-515.

- Massberg, S., I. Konrad, K. Schurzinger, M. Lorenz, S. Schneider, D. Zohlnhoefer, K. Hoppe, M. Schiemann, E. Kennerknecht, S. Sauer, C. Schulz, S. Kerstan, M. Rudelius, S. Seidl, F. Sorge, H. Langer, M. Peluso, P. Goyal, D. Vestweber, N. R. Emambokus, D. H. Busch, J. Frampton and M. Gawaz** (2006). "Platelets secrete stromal cell-derived factor 1alpha and recruit bone marrow-derived progenitor cells to arterial thrombi in vivo." J Exp Med **203**(5): 1221-1233.
- Massberg, S., P. Schaerli, I. Knezevic-Maramica, M. Kollnberger, N. Tubo, E. A. Moseman, I. V. Huff, T. Junt, A. J. Wagers, I. B. Mazo and U. H. von Andrian** (2007). "Immunosurveillance by hematopoietic progenitor cells trafficking through blood, lymph, and peripheral tissues." Cell **131**(5): 994-1008.
- Mazo, I. B., J. C. Gutierrez-Ramos, P. S. Frenette, R. O. Hynes, D. D. Wagner and U. H. von Andrian** (1998). "Hematopoietic progenitor cell rolling in bone marrow microvessels: parallel contributions by endothelial selectins and vascular cell adhesion molecule 1." J Exp Med **188**(3): 465-474.
- McEver, R. P.** (1991). "Selectins: novel receptors that mediate leukocyte adhesion during inflammation." Thromb Haemost **65**(3): 223-228.
- Meirelles Lda, S., A. M. Fontes, D. T. Covas and A. I. Caplan** (2009). "Mechanisms involved in the therapeutic properties of mesenchymal stem cells." Cytokine Growth Factor Rev **20**(5-6): 419-427.
- Meldrum, K. K., D. R. Meldrum, X. H. Meng, L. H. Ao and A. H. Harken** (2002). "TNF-alpha-dependent bilateral renal injury is induced by unilateral renal ischemia-reperfusion." American Journal of Physiology-Heart and Circulatory Physiology **282**(2): H540-H546.
- Melo-Filho, N. M., C. L. Belmiro, R. G. Goncalves, C. M. Takiya, M. Leite, Jr., M. S. Pavao and P. A. Mourao** (2010). "Fucosylated chondroitin sulfate attenuates renal fibrosis in animals submitted to unilateral ureteral obstruction: a P-selectin-mediated event?" Am J Physiol Renal Physiol **299**(6): F1299-1307.

- Milia, A. F., V. Gross, R. Plehm, J. A. De Silva, Jr., M. Bader and F. C. Luft** (2001). "Normal blood pressure and renal function in mice lacking the bradykinin B(2) receptor." Hypertension **37**(6): 1473-1479.
- Molitoris, B. A. and J. Marrs** (1999). "The role of cell adhesion molecules in ischemic acute renal failure." Am J Med **106**(5): 583-592.
- Molitoris, B. A. and T. A. Sutton** (2004). "Endothelial injury and dysfunction: role in the extension phase of acute renal failure." Kidney Int **66**(2): 496-499.
- Molls, R. R., V. Savransky, M. Liu, S. Bevans, T. Mehta, R. M. Tuder, L. S. King and H. Rabb** (2006). "Keratinocyte-derived chemokine is an early biomarker of ischemic acute kidney injury." Am J Physiol Renal Physiol **290**(5): F1187-1193.
- Montecucco, F., S. Steffens, F. Burger, A. Da Costa, G. Bianchi, M. Bertolotto, F. Mach, F. Dallegri and L. Ottonello** (2008). "Tumor necrosis factor-alpha (TNF-alpha) induces integrin CD11b/CD18 (Mac-1) up-regulation and migration to the CC chemokine CCL3 (MIP-1alpha) on human neutrophils through defined signalling pathways." Cell Signal **20**(3): 557-568.
- Morgan, S. J., M. W. Moore, G. Cacalano and K. Ley** (1997). "Reduced leukocyte adhesion response and absence of slow leukocyte rolling in interleukin-8 receptor-deficient mice." Microvasc Res **54**(2): 188-191.
- Mulligan, M. S., A. B. Lentsch and P. A. Ward** (1998). "In vivo recruitment of neutrophils: consistent requirements for L-arginine and variable requirements for complement and adhesion molecules." Inflammation **22**(3): 327-339.
- Nadar, S. K., G. Y. Lip, K. W. Lee and A. D. Blann** (2005). "Circulating endothelial cells in acute ischaemic stroke." Thromb Haemost **94**(4): 707-712.
- Nakatsuka, A., R. Mizuno, N. Ono, J. Nakayama and T. Ohhashi** (2005). "Arachidonic Acid-Induced COX-1 and COX-2-Mediated Vasodilation in Rat Gingival Arterioles In Vivo." Jpn J Physiol **55**(5): 293-302.

- Nikolic-Paterson, D. J. and R. C. Atkins** (2001). "The role of macrophages in glomerulonephritis." Nephrol Dial Transplant **16 Suppl 5**: 3-7.
- Norman, K. E., K. L. Moore, R. P. McEver and K. Ley** (1995). "Leukocyte rolling in vivo is mediated by P-selectin glycoprotein ligand-1." Blood **86**(12): 4417-4421.
- Okada, T., R. G. Hawley, M. Kodaka and H. Okuno** (1999). "Significance of VLA-4-VCAM-1 interaction and CD44 for transendothelial invasion in a bone marrow metastatic myeloma model." Clin Exp Metastasis **17**(7): 623-629.
- Oken, D. E.** (1984). "Hemodynamic basis for human acute renal failure (vasomotor nephropathy)." Am J Med **76**(4): 702-710.
- Olson, T. S. and K. Ley** (2002). "Chemokines and chemokine receptors in leukocyte trafficking." Am J Physiol Regul Integr Comp Physiol **283**(1): R7-28.
- Oostendorp, R. A., S. Ghaffari and C. J. Eaves** (2000). "Kinetics of in vivo homing and recruitment into cycle of hematopoietic cells are organ-specific but CD44-independent." Bone Marrow Transplant **26**(5): 559-566.
- Orito, H., M. Fujimoto, N. Ishiura, K. Yanaba, T. Matsushita, M. Hasegawa, F. Ogawa, K. Takehara and S. Sato** (2007). "Intercellular adhesion molecule-1 and vascular cell adhesion molecule-1 cooperatively contribute to the cutaneous Arthus reaction." J Leukoc Biol **81**(5): 1197-1204.
- Orlic, D., J. Kajstura, S. Chimenti, I. Jakoniuk, S. M. Anderson, B. Li, J. Pickel, R. McKay, B. Nadal-Ginard, D. M. Bodine, A. Leri and P. Anversa** (2001). "Bone marrow cells regenerate infarcted myocardium." Nature **410**(6829): 701-705.
- Osawa, M., K. Hanada, H. Hamada and H. Nakauchi** (1996). "Long-term lymphohematopoietic reconstitution by a single CD34-low/negative hematopoietic stem cell." Science **273**(5272): 242-245.
- Ostermann, M., R. Chang and R. I. P. U. Grp** (2008). "Correlation between the AKI classification and outcome." Critical Care **12**(6).

- Owen, W. F., Jr., N. L. Lew, Y. Liu, E. G. Lowrie and J. M. Lazarus (1993). "The urea reduction ratio and serum albumin concentration as predictors of mortality in patients undergoing hemodialysis." N Engl J Med **329**(14): 1001-1006.
- Palabrica, T., R. Lobb, B. C. Furie, M. Aronovitz, C. Benjamin, Y. M. Hsu, S. A. Sajer and B. Furie (1992). "Leukocyte accumulation promoting fibrin deposition is mediated in vivo by P-selectin on adherent platelets." Nature **359**(6398): 848-851.
- Paller, M. S. (1989). "Effect of neutrophil depletion on ischemic renal injury in the rat." J Lab Clin Med **113**(3): 379-386.
- Papayannopoulou, T., C. Craddock, B. Nakamoto, G. V. Priestley and N. S. Wolf (1995). "The VLA4/VCAM-1 adhesion pathway defines contrasting mechanisms of lodgement of transplanted murine hemopoietic progenitors between bone marrow and spleen." Proc Natl Acad Sci U S A **92**(21): 9647-9651.
- Papayannopoulou, T., G. V. Priestley, B. Nakamoto, V. Zafiropoulos and L. M. Scott (2001). "Molecular pathways in bone marrow homing: dominant role of alpha(4)beta(1) over beta(2)-integrins and selectins." Blood **98**(8): 2403-2411.
- Park, I. K., Y. He, F. Lin, O. D. Laerum, Q. Tian, R. Bumgarner, C. A. Klug, K. Li, C. Kuhr, M. J. Doyle, T. Xie, M. Schummer, Y. Sun, A. Goldsmith, M. F. Clarke, I. L. Weissman, L. Hood and L. Li (2002). "Differential gene expression profiling of adult murine hematopoietic stem cells." Blood **99**(2): 488-498.
- Patel, A. R., J. T. Kuvin, N. G. Pandian, J. J. Smith, J. E. Udelson, M. E. Mendelsohn, M. A. Konstam and R. H. Karas (2001). "Heart failure etiology affects peripheral vascular endothelial function after cardiac transplantation." J Am Coll Cardiol **37**(1): 195-200.
- Peled, A., V. Grabovsky, L. Habler, J. Sandbank, F. Arenzana-Seisdedos, I. Petit, H. Ben-Hur, T. Lapidot and R. Alon (1999). "The chemokine SDF-1 stimulates integrin-mediated arrest of CD34(+) cells on vascular endothelium under shear flow." J Clin Invest **104**(9): 1199-1211.

- Peled, A., O. Kollet, T. Ponomaryov, I. Petit, S. Franitza, V. Grabovsky, M. M. Slav, A. Nagler, O. Lider, R. Alon, D. Zipori and T. Lapidot** (2000). "The chemokine SDF-1 activates the integrins LFA-1, VLA-4, and VLA-5 on immature human CD34(+) cells: role in transendothelial/stromal migration and engraftment of NOD/SCID mice." Blood **95**(11): 3289-3296.
- Perlingeiro, R. C., M. Kyba and G. Q. Daley** (2001). "Clonal analysis of differentiating embryonic stem cells reveals a hematopoietic progenitor with primitive erythroid and adult lymphoid-myeloid potential." Development **128**(22): 4597-4604.
- Petty, J. M., C. C. Lenox, D. J. Weiss, M. E. Poynter and B. T. Suratt** (2009). "Crosstalk between CXCR4/stromal derived factor-1 and VLA-4/VCAM-1 pathways regulates neutrophil retention in the bone marrow." J Immunol **182**(1): 604-612.
- Pilarski, L. M., E. Pruski, J. Wizniak, D. Paine, K. Seeberger, M. J. Mant, C. B. Brown and A. R. Belch** (1999). "Potential role for hyaluronan and the hyaluronan receptor RHAMM in mobilization and trafficking of hematopoietic progenitor cells." Blood **93**(9): 2918-2927.
- Pimanda, J. E., W. Y. Chan, N. K. Wilson, A. M. Smith, S. Kinston, K. Knezevic, M. E. Janes, J. R. Landry, A. Kolb-Kokocinski, J. Frampton, D. Tannahill, K. Ottersbach, G. A. Follows, G. Lacaud, V. Kouskoff and B. Gottgens** (2008). "Endoglin expression in blood and endothelium is differentially regulated by modular assembly of the Ets/Gata hemangioblast code." Blood **112**(12): 4512-4522.
- Pinto do, O. P., A. Kolterud and L. Carlsson** (1998). "Expression of the LIM-homeobox gene LH2 generates immortalized steel factor-dependent multipotent hematopoietic precursors." EMBO J **17**(19): 5744-5756.
- Pinto do, O. P., K. Richter and L. Carlsson** (2002). "Hematopoietic progenitor/stem cells immortalized by Lhx2 generate functional hematopoietic cells in vivo." Blood **99**(11): 3939-3946.

- Pinto do, O. P., E. Wandzioch, A. Kolterud and L. Carlsson** (2001). "Multipotent hematopoietic progenitor cells immortalized by Lhx2 self-renew by a cell nonautonomous mechanism." Exp Hematol **29**(8): 1019-1028.
- Porecha, N. K., K. English, G. Hangoc, H. E. Broxmeyer and K. W. Christopherson, 2nd** (2006). "Enhanced functional response to CXCL12/SDF-1 through retroviral overexpression of CXCR4 on M07e cells: implications for hematopoietic stem cell transplantation." Stem Cells Dev **15**(3): 325-333.
- Poulsom, R., S. J. Forbes, K. Hodivala-Dilke, E. Ryan, S. Wyles, S. Navaratnasah, R. Jeffery, T. Hunt, M. Alison, T. Cook, C. Pusey and N. A. Wright** (2001). "Bone marrow contributes to renal parenchymal turnover and regeneration." J Pathol **195**(2): 229-235.
- Purdy, K. E. and W. J. Arendshorst** (2000). "EP(1) and EP(4) receptors mediate prostaglandin E(2) actions in the microcirculation of rat kidney." Am J Physiol Renal Physiol **279**(4): F755-764.
- Quevedo, H. C., K. E. Hatzistergos, B. N. Oskouei, G. S. Feigenbaum, J. E. Rodriguez, D. Valdes, P. M. Pattany, J. P. Zambrano, Q. Hu, I. McNiece, A. W. Heldman and J. M. Hare** (2009). "Allogeneic mesenchymal stem cells restore cardiac function in chronic ischemic cardiomyopathy via trilineage differentiating capacity." Proc Natl Acad Sci U S A **106**(33): 14022-14027.
- Rabb, H., F. Daniels, M. O'Donnell, M. Haq, S. R. Saba, W. Keane and W. W. Tang** (2000). "Pathophysiological role of T lymphocytes in renal ischemia-reperfusion injury in mice." Am J Physiol Renal Physiol **279**(3): F525-531.
- Rabb, H., C. C. Mendiola, J. Dietz, S. R. Saba, T. B. Issekutz, F. Abanilla, J. V. Bonventre and G. Ramirez** (1994). "Role of CD11a and CD11b in ischemic acute renal failure in rats." Am J Physiol **267**(6 Pt 2): F1052-1058.
- Rabb, H., C. C. Mendiola, S. R. Saba, J. R. Dietz, C. W. Smith, J. V. Bonventre and G. Ramirez** (1995). "Antibodies to ICAM-1 protect kidneys in severe ischemic reperfusion injury." Biochem Biophys Res Commun **211**(1): 67-73.

- Rabb, H., G. Ramirez, S. R. Saba, D. Reynolds, J. Xu, R. Flavell and S. Antonia** (1996). "Renal ischemic-reperfusion injury in L-selectin-deficient mice." Am J Physiol **271**(2 Pt 2): F408-413.
- Ratajczak, M. Z., M. Kucia, T. Jadczyk, N. J. Greco, W. Wojakowski, M. Tendera and J. Ratajczak** (2012). "Pivotal role of paracrine effects in stem cell therapies in regenerative medicine: can we translate stem cell-secreted paracrine factors and microvesicles into better therapeutic strategies?" Leukemia **26**(6): 1166-1173.
- Ratajczak, M. Z., E. Zuba-Surma, M. Kucia, R. Reca, W. Wojakowski and J. Ratajczak** (2006). "The pleiotropic effects of the SDF-1-CXCR4 axis in organogenesis, regeneration and tumorigenesis." Leukemia **20**(11): 1915-1924.
- Regner, K. R. and R. J. Roman** (2012). "Role of medullary blood flow in the pathogenesis of renal ischemia-reperfusion injury." Curr Opin Nephrol Hypertens **21**(1): 33-38.
- Ren, G., L. Zhang, X. Zhao, G. Xu, Y. Zhang, A. I. Roberts, R. C. Zhao and Y. Shi** (2008). "Mesenchymal stem cell-mediated immunosuppression occurs via concerted action of chemokines and nitric oxide." Cell Stem Cell **2**(2): 141-150.
- Rice, G. E. and M. P. Bevilacqua** (1989). "An inducible endothelial cell surface glycoprotein mediates melanoma adhesion." Science **246**(4935): 1303-1306.
- Ries, C., V. Egea, M. Karow, H. Kolb, M. Jochum and P. Neth** (2007). "MMP-2, MT1-MMP, and TIMP-2 are essential for the invasive capacity of human mesenchymal stem cells: differential regulation by inflammatory cytokines." Blood **109**(9): 4055-4063.
- Rincon-Sanchez, A. R., A. Covarrubias, A. M. Rivas-Estilla, J. Pedraza-Chaverri, C. Cruz, M. C. Islas-Carbajal, A. Panduro, A. Estanes and J. Armendariz-Borunda** (2005). "PGE2 alleviates kidney and liver damage, decreases plasma renin activity and acute phase response in cirrhotic rats with acute liver damage." Exp Toxicol Pathol **56**(4-5): 291-303.
- Rosen, S. D. and C. R. Bertozzi** (1996). "Two selectins converge on sulphate. Leukocyte adhesion." Curr Biol **6**(3): 261-264.

- Rouschop, K. M., J. J. Roelofs, N. Claessen, P. da Costa Martins, J. J. Zwaginga, S. T. Pals, J. J. Weening and S. Florquin** (2005). "Protection against renal ischemia reperfusion injury by CD44 disruption." J Am Soc Nephrol **16**(7): 2034-2043.
- Sackstein, R.** (1997). "Expression of an L-selectin ligand on hematopoietic progenitor cells." Acta Haematol **97**(1-2): 22-28.
- Salter, J. W., C. F. Krieglstein, A. C. Issekutz and D. N. Granger** (2001). "Platelets modulate ischemia/reperfusion-induced leukocyte recruitment in the mesenteric circulation." Am J Physiol Gastrointest Liver Physiol **281**(6): G1432-1439.
- Sata, M., A. Saiura, A. Kunisato, A. Tojo, S. Okada, T. Tokuhsa, H. Hirai, M. Makuuchi, Y. Hirata and R. Nagai** (2002). "Hematopoietic stem cells differentiate into vascular cells that participate in the pathogenesis of atherosclerosis." Nat Med **8**(4): 403-409.
- Schroder, J. M. and E. Christophers** (1989). "Secretion of novel and homologous neutrophil-activating peptides by LPS-stimulated human endothelial cells." J Immunol **142**(1): 244-251.
- Schulz, C., I. Konrad, S. Sauer, L. Orschielt, M. Koellnberger, R. Lorenz, U. Walter and S. Massberg** (2008). "Effect of chronic treatment with acetylsalicylic acid and clopidogrel on atheroprogession and atherothrombosis in ApoE-deficient mice in vivo." Thromb Haemost **99**(1): 190-195.
- Schulz, C., U. H. Von Andrian and S. Massberg** (2009). "Trafficking of murine hematopoietic stem and progenitor cells in health and vascular disease." Microcirculation **16**(6): 497-507.
- Schwarting, S., S. Litwak, W. Hao, M. Bahr, J. Weise and H. Neumann** (2008). "Hematopoietic stem cells reduce postischemic inflammation and ameliorate ischemic brain injury." Stroke **39**(10): 2867-2875.
- Segerer, S., P. J. Nelson and D. Schlondorff** (2000). "Chemokines, chemokine receptors, and renal disease: from basic science to pathophysiologic and therapeutic studies." J Am Soc Nephrol **11**(1): 152-176.

- Sekizuka, E., M. B. Grisham, M. A. Li, E. A. Deitch and D. N. Granger** (1988). "Inflammation-induced intestinal hyperemia in the rat: role of neutrophils." Gastroenterology **95**(6): 1528-1534.
- Shamri, R., V. Grabovsky, J. M. Gauguet, S. Feigelson, E. Manevich, W. Kolanus, M. K. Robinson, D. E. Staunton, U. H. von Andrian and R. Alon** (2005). "Lymphocyte arrest requires instantaneous induction of an extended LFA-1 conformation mediated by endothelium-bound chemokines." Nat Immunol **6**(5): 497-506.
- Si, Y., C. L. Tsou, K. Croft and I. F. Charo** (2010). "CCR2 mediates hematopoietic stem and progenitor cell trafficking to sites of inflammation in mice." J Clin Invest **120**(4): 1192-1203.
- Sierro, F., C. Biben, L. Martinez-Munoz, M. Mellado, R. M. Ransohoff, M. Li, B. Woehl, H. Leung, J. Groom, M. Batten, R. P. Harvey, A. C. Martinez, C. R. Mackay and F. Mackay** (2007). "Disrupted cardiac development but normal hematopoiesis in mice deficient in the second CXCL12/SDF-1 receptor, CXCR7." Proc Natl Acad Sci U S A **104**(37): 14759-14764.
- Singbartl, K., S. B. Forlow and K. Ley** (2001). "Platelet, but not endothelial, P-selectin is critical for neutrophil-mediated acute postischemic renal failure." FASEB J **15**(13): 2337-2344.
- Singbartl, K., S. A. Green and K. Ley** (2000). "Blocking P-selectin protects from ischemia/reperfusion-induced acute renal failure." FASEB J **14**(1): 48-54.
- Singbartl, K. and K. Ley** (2000). "Protection from ischemia-reperfusion induced severe acute renal failure by blocking E-selectin." Crit Care Med **28**(7): 2507-2514.
- Skoutelis, A. T., V. E. Kaleridis, C. A. Gogos, G. M. Athanassiou, Y. F. Missirlis and H. P. Bassaris** (2000). "Effect of cytokines and colony-stimulating factors on passive polymorphonuclear leukocyte deformability in vitro." Cytokine **12**(11): 1737-1740.
- Song, J. H. and H. D. Humes** (2009). "The bioartificial kidney in the treatment of acute kidney injury." Curr Drug Targets **10**(12): 1227-1234.

- Sperandio, M., M. L. Smith, S. B. Forlow, T. S. Olson, L. Xia, R. P. McEver and K. Ley** (2003). "P-selectin glycoprotein ligand-1 mediates L-selectin-dependent leukocyte rolling in venules." J Exp Med **197**(10): 1355-1363.
- Springer, T. A.** (1994). "Traffic signals for lymphocyte recirculation and leukocyte emigration: the multistep paradigm." Cell **76**(2): 301-314.
- Stamper, H. B., Jr. and J. J. Woodruff** (1976). "Lymphocyte homing into lymph nodes: in vitro demonstration of the selective affinity of recirculating lymphocytes for high-endothelial venules." J Exp Med **144**(3): 828-833.
- Steegmaier, M., A. Levinovitz, S. Isenmann, E. Borges, M. Lenter, H. P. Kocher, B. Kleuser and D. Vestweber** (1995). "The E-selectin-ligand ESL-1 is a variant of a receptor for fibroblast growth factor." Nature **373**(6515): 615-620.
- Stellos, K. and M. Gawaz** (2007). "Platelet interaction with progenitor cells: potential implications for regenerative medicine." Thromb Haemost **98**(5): 922-929.
- Stellos, K., H. Langer, K. Daub, T. Schoenberger, A. Gauss, T. Geisler, B. Bigalke, I. Mueller, M. Schumm, I. Schaefer, P. Seizer, B. F. Kraemer, D. Siegel-Axel, A. E. May, S. Lindemann and M. Gawaz** (2008). "Platelet-derived stromal cell-derived factor-1 regulates adhesion and promotes differentiation of human CD34+ cells to endothelial progenitor cells." Circulation **117**(2): 206-215.
- Stern, J. M., J. Chen, R. B. Silver, D. P. Poppas, E. D. Vaughan, Jr. and D. Felsen** (2004). "Effect of UUO on D1aR expression reveals a link among dopamine, transforming growth factor-beta, and nitric oxide." Am J Physiol Renal Physiol **286**(3): F509-515.
- Streeter, H. B. and D. A. Rees** (1987). "Fibroblast adhesion to RGDS shows novel features compared with fibronectin." J Cell Biol **105**(1): 507-515.
- Stroo, I., G. Stokman, G. J. Teske, S. Florquin and J. C. Leemans** (2009). "Haematopoietic stem cell migration to the ischemic damaged kidney is not altered by manipulating the SDF-1/CXCR4-axis." Nephrol Dial Transplant **24**(7): 2082-2088.

Stroo, I., G. Stokman, G. J. Teske, A. Raven, L. M. Butter, S. Florquin and J. C. Leemans (2010).

"Chemokine expression in renal ischemia/reperfusion injury is most profound during the reparative phase." Int Immunol **22**(6): 433-442.

Suratt, B. T., J. M. Petty, S. K. Young, K. C. Malcolm, J. G. Lieber, J. A. Nick, J. A. Gonzalo, P. M.

Henson and G. S. Worthen (2004). "Role of the CXCR4/SDF-1 chemokine axis in circulating neutrophil homeostasis." Blood **104**(2): 565-571.

Sutton, T. A. (2009). "Alteration of microvascular permeability in acute kidney injury." Microvasc

Res **77**(1): 4-7.

Sutton, T. A., C. J. Fisher and B. A. Molitoris (2002). "Microvascular endothelial injury and

dysfunction during ischemic acute renal failure." Kidney Int **62**(5): 1539-1549.

Sweeney, E. A., H. Lortat-Jacob, G. V. Priestley, B. Nakamoto and T. Papayannopoulou (2002).

"Sulfated polysaccharides increase plasma levels of SDF-1 in monkeys and mice: involvement in mobilization of stem/progenitor cells." Blood **99**(1): 44-51.

Takada, M., K. C. Nadeau, G. D. Shaw and N. L. Tilney (1997). "Prevention of late renal changes

after initial ischemia/reperfusion injury by blocking early selectin binding." Transplantation **64**(11): 1520-1525.

Tang, Y. L., K. Qian, Y. C. Zhang, L. Shen and M. I. Phillips (2005). "Mobilizing of haematopoietic

stem cells to ischemic myocardium by plasmid mediated stromal-cell-derived factor-1alpha (SDF-1alpha) treatment." Regul Pept **125**(1-3): 1-8.

Tapuria, N., Y. Kumar, M. M. Habib, M. Abu Amara, A. M. Seifalian and B. R. Davidson (2008).

"Remote ischemic preconditioning: a novel protective method from ischemia reperfusion injury--a review." J Surg Res **150**(2): 304-330.

Tavassoli, M. and C. L. Hardy (1990). "Molecular basis of homing of intravenously transplanted

stem cells to the marrow." Blood **76**(6): 1059-1070.

- Tawil, N., P. Wilson and S. Carbonetto** (1993). "Integrins in point contacts mediate cell spreading: factors that regulate integrin accumulation in point contacts vs. focal contacts." J Cell Biol **120**(1): 261-271.
- Terada, N., T. Hamazaki, M. Oka, M. Hoki, D. M. Mastalerz, Y. Nakano, E. M. Meyer, L. Morel, B. E. Petersen and E. W. Scott** (2002). "Bone marrow cells adopt the phenotype of other cells by spontaneous cell fusion." Nature **416**(6880): 542-545.
- Termeer, C., H. Johannsen, T. Braun, A. Renkl, T. Ahrens, R. W. Denfeld, M. B. Lappin, J. M. Weiss and J. C. Simon** (2001). "The role of CD44 during CD40 ligand-induced dendritic cell clustering and maturation." J Leukoc Biol **70**(5): 715-722.
- Thadhani, R., M. Pascual and J. V. Bonventre** (1996). "Acute renal failure." N Engl J Med **334**(22): 1448-1460.
- Theilmeier, G., C. Michiels, E. Spaepen, I. Vreys, D. Collen, J. Vermynen and M. F. Hoylaerts** (2002). "Endothelial von Willebrand factor recruits platelets to atherosclerosis-prone sites in response to hypercholesterolemia." Blood **99**(12): 4486-4493.
- Till, J. E., E. A. McCulloch and L. Siminovitch** (1964). "A Stochastic Model of Stem Cell Proliferation, Based on the Growth of Spleen Colony-Forming Cells." Proc Natl Acad Sci U S A **51**: 29-36.
- Toback, F. G.** (1992). "Regeneration after acute tubular necrosis." Kidney Int **41**(1): 226-246.
- Togel, F., J. Isaac, Z. Hu, K. Weiss and C. Westenfelder** (2005). "Renal SDF-1 signals mobilization and homing of CXCR4-positive cells to the kidney after ischemic injury." Kidney Int **67**(5): 1772-1784.
- Togel, F., K. Weiss, Y. Yang, Z. Hu, P. Zhang and C. Westenfelder** (2007). "Vasculotropic, paracrine actions of infused mesenchymal stem cells are important to the recovery from acute kidney injury." Am J Physiol Renal Physiol **292**(5): F1626-1635.

- Togel, F., P. Zhang, Z. Hu and C. Westenfelder** (2009). "VEGF is a mediator of the renoprotective effects of multipotent marrow stromal cells in acute kidney injury." J Cell Mol Med **13**(8B): 2109-2114.
- Tsagalidis, G.** (2011). "Update of acute kidney injury: intensive care nephrology." Hippokratia **15**(Suppl 1): 53-68.
- Tsai, C. Y., C. L. Yu, T. H. Wu, S. C. Hsieh and Y. Y. Tsai** (2004). "Proinflammatory cytokines enhance COX-1 gene expression in cultured rat glomerular mesangial cells." Int Immunopharmacol **4**(1): 47-56.
- Tse, W. Y., G. B. Nash, P. Hewins, C. O. Savage and D. Adu** (2005). "ANCA-induced neutrophil F-actin polymerization: implications for microvascular inflammation." Kidney Int **67**(1): 130-139.
- Turner, M. L., K. McIlwaine, R. S. Anthony and A. C. Parker** (1995). "Differential expression of cell adhesion molecules by human hematopoietic progenitor cells from bone marrow and mobilized adult peripheral blood." Stem Cells **13**(3): 311-316.
- van Kooyk, Y. and C. G. Figdor** (2000). "Avidity regulation of integrins: the driving force in leukocyte adhesion." Curr Opin Cell Biol **12**(5): 542-547.
- Vermeulen, M., F. Le Pesteur, M. C. Gagnerault, J. Y. Mary, F. Sainteny and F. Lepault** (1998). "Role of adhesion molecules in the homing and mobilization of murine hematopoietic stem and progenitor cells." Blood **92**(3): 894-900.
- Ward, M. D., M. Dembo and D. A. Hammer** (1994). "Kinetics of cell detachment: peeling of discrete receptor clusters." Biophys J **67**(6): 2522-2534.
- Weller, A., S. Isenmann and D. Vestweber** (1992). "Cloning of the mouse endothelial selectins. Expression of both E- and P-selectin is inducible by tumor necrosis factor alpha." J Biol Chem **267**(21): 15176-15183.
- Weyrich, A. S., S. Lindemann and G. A. Zimmerman** (2003). "The evolving role of platelets in inflammation." J Thromb Haemost **1**(9): 1897-1905.

- White, R. L., G. Nash, D. P. Kavanagh, C. O. Savage and N. Kalia** (2013). "Modulating the Adhesion of Haematopoietic Stem Cells with Chemokines to Enhance Their Recruitment to the Ischaemically Injured Murine Kidney." PLoS One **8**(6): e66489.
- White, R. L., G. Nash, D. P. J. Kavanagh, C. O. S. Savage and N. Kalia** (2013). "Modulating the Adhesion of Haematopoietic Stem Cells with Chemokines to Enhance Their Recruitment to the Ischaemically Injured Murine Kidney." PLoS One **8**(6): e66489.
- Willinger, C. C., H. Schramek, K. Pfaller and W. Pfaller** (1992). "Tissue distribution of neutrophils in postischemic acute renal failure." Virchows Arch B Cell Pathol Incl Mol Pathol **62**(4): 237-243.
- Wilson, N. K., D. Miranda-Saavedra, S. Kinston, N. Bonadies, S. D. Foster, F. Calero-Nieto, M. A. Dawson, I. J. Donaldson, S. Dumon, J. Frampton, R. Janky, X. H. Sun, S. A. Teichmann, A. J. Bannister and B. Gottgens** (2009). "The transcriptional program controlled by the stem cell leukemia gene Scl/Tal1 during early embryonic hematopoietic development." Blood **113**(22): 5456-5465.
- Winterberg, P. D. and C. Y. Lu** (2012). "Acute kidney injury: the beginning of the end of the dark ages." Am J Med Sci **344**(4): 318-325.
- Wise, A. F. and S. D. Ricardo** (2012). "Mesenchymal stem cells in kidney inflammation and repair." Nephrology (Carlton) **17**(1): 1-10.
- Witzgall, R., E. O'Leary, R. Gessner, A. J. Ouellette and J. V. Bonventre** (1993). "Kid-1, a putative renal transcription factor: regulation during ontogeny and in response to ischemia and toxic injury." Mol Cell Biol **13**(3): 1933-1942.
- Woodside, D. G., R. M. Kram, J. S. Mitchell, T. Belsom, M. J. Billard, B. W. McIntyre and P. Vanderslice** (2006). "Contrasting roles for domain 4 of VCAM-1 in the regulation of cell adhesion and soluble VCAM-1 binding to integrin alpha4beta1." J Immunol **176**(8): 5041-5049.

Wright, D. E., E. P. Bowman, A. J. Wagers, E. C. Butcher and I. L. Weissman (2002).

"Hematopoietic stem cells are uniquely selective in their migratory response to chemokines." J Exp Med **195**(9): 1145-1154.

Wright, D. E., A. J. Wagers, A. P. Gulati, F. L. Johnson and I. L. Weissman (2001). "Physiological migration of hematopoietic stem and progenitor cells." Science **294**(5548): 1933-1936.

Yamamoto, K., D. R. Wilson and R. Bauma (1984). "Outer medullary circulatory defect in ischemic acute renal failure." Am J Pathol **116**(2): 253-261.

Yamasawa, H., S. Shimizu, T. Inoue, M. Takaoka and Y. Matsumura (2005). "Endothelial nitric oxide contributes to the renal protective effects of ischemic preconditioning." J Pharmacol Exp Ther **312**(1): 153-159.

Yeo, E. L., J. A. Sheppard and I. A. Feuerstein (1994). "Role of P-selectin and leukocyte activation in polymorphonuclear cell adhesion to surface adherent activated platelets under physiologic shear conditions (an injury vessel wall model)." Blood **83**(9): 2498-2507.

Yokoo, T., T. Ohashi, J. S. Shen, K. Sakurai, Y. Miyazaki, Y. Utsunomiya, M. Takahashi, Y. Terada, Y. Eto, T. Kawamura, N. Osumi and T. Hosoya (2005). "Human mesenchymal stem cells in rodent whole-embryo culture are reprogrammed to contribute to kidney tissues." Proc Natl Acad Sci U S A **102**(9): 3296-3300.

Yoshimura, T., K. Matsushima, S. Tanaka, E. A. Robinson, E. Appella, J. J. Oppenheim and E. J. Leonard (1987). "Purification of a human monocyte-derived neutrophil chemotactic factor that has peptide sequence similarity to other host defense cytokines." Proc Natl Acad Sci U S A **84**(24): 9233-9237.

Yusuf-Makagiansar, H., M. E. Anderson, T. V. Yakovleva, J. S. Murray and T. J. Siahaan (2002).

"Inhibition of LFA-1/ICAM-1 and VLA-4/VCAM-1 as a therapeutic approach to inflammation and autoimmune diseases." Med Res Rev **22**(2): 146-167.

Zhang, C., X. Xu, B. J. Potter, W. Wang, L. Kuo, L. Michael, G. J. Bagby and W. M. Chilian (2006).

"TNF-alpha contributes to endothelial dysfunction in ischemia/reperfusion injury."

Arterioscler Thromb Vasc Biol **26**(3): 475-480.

Zhang, S., E. Shpall, J. T. Willerson and E. T. Yeh (2007). "Fusion of human hematopoietic

progenitor cells and murine cardiomyocytes is mediated by alpha 4 beta 1 integrin/vascular cell adhesion molecule-1 interaction." Circ Res **100**(5): 693-702.

Zhao, L., L. Gray, J. Leonardi-Bee, C. S. Weaver, S. Heptinstall and P. M. Bath (2006). "Effect of

aspirin, clopidogrel and dipyridamole on soluble markers of vascular function in normal volunteers and patients with prior ischaemic stroke." Platelets **17**(2): 100-104.

Zhou, W., D. Zeng, R. Chen, J. Liu, G. Yang, P. Liu and X. Zhou (2010). "Limb ischemic

preconditioning reduces heart and lung injury after an open heart operation in infants."

Pediatr Cardiol **31**(1): 22-29.

Zhu, H., N. Mitsuhashi, A. Klein, L. W. Barsky, K. Weinberg, M. L. Barr, A. Demetriou and G. D.

Wu (2006). "The role of the hyaluronan receptor CD44 in mesenchymal stem cell migration in the extracellular matrix." Stem Cells **24**(4): 928-935.